

Journal of
Mechanics of
Materials and Structures

Volume 3, N° 6

June 2008

 mathematical sciences publishers

JOURNAL OF MECHANICS OF MATERIALS AND STRUCTURES

<http://www.jomms.org>

EDITOR-IN-CHIEF Charles R. Steele
ASSOCIATE EDITOR Marie-Louise Steele
Division of Mechanics and Computation
Stanford University
Stanford, CA 94305
USA

BOARD OF EDITORS

D. BIGONI University of Trento, Italy
H. D. BUI École Polytechnique, France
J. P. CARTER University of Sydney, Australia
R. M. CHRISTENSEN Stanford University, U.S.A.
G. M. L. GLADWELL University of Waterloo, Canada
D. H. HODGES Georgia Institute of Technology, U.S.A.
J. HUTCHINSON Harvard University, U.S.A.
C. HWU National Cheng Kung University, R.O. China
IWONA JASIUK University of Illinois at Urbana-Champaign
B. L. KARIHALOO University of Wales, U.K.
Y. Y. KIM Seoul National University, Republic of Korea
Z. MROZ Academy of Science, Poland
D. PAMPLONA Universidade Católica do Rio de Janeiro, Brazil
M. B. RUBIN Technion, Haifa, Israel
Y. SHINDO Tohoku University, Japan
A. N. SHUPIKOV Ukrainian Academy of Sciences, Ukraine
T. TARNAI University Budapest, Hungary
F. Y. M. WAN University of California, Irvine, U.S.A.
P. WRIGGERS Universität Hannover, Germany
W. YANG Tsinghua University, P.R. China
F. ZIEGLER Technische Universität Wien, Austria

PRODUCTION

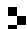
PAULO NEY DE SOUZA Production Manager
SHEILA NEWBERY Senior Production Editor
SILVIO LEVY Scientific Editor

See inside back cover or <http://www.jomms.org> for submission guidelines.

Regular subscription rate: \$500 a year.

Subscriptions, requests for back issues, and changes of address should be sent to Mathematical Sciences Publishers, 798 Evans Hall, Department of Mathematics, University of California, Berkeley, CA 94720-3840.

©Copyright 2008. Journal of Mechanics of Materials and Structures. All rights reserved.

 mathematical sciences publishers

PREFACE

BOGDAN T. MARUSZEWSKI, WOLFGANG MUSCHIK AND KRZYSZTOF W. WOJCIECHOWSKI

The International Symposia on Trends in Continuum Physics have been held every three years since 1998. The first three events took place at the Poznan University of Technology in Poznan, Poland. The fourth and most recent one took place in Lviv, Ukraine, for the first time outside the European Union. All the symposia were jointly planned and organized by B. T. Maruszewski (Poznan University of Technology), W. Muschik (Technische Universität Berlin) and A. Radowicz (Kielce University of Technology).

One of the main aims of those meetings has been to bring together scientists from Eastern Europe working in different fields of continuum physics, widely understood, as well as those from Western and Central European countries, in order to extend their cooperation and to create new connections and acquaintances.

Special emphasis was placed on the representation of various concepts applied to different physical fields interacting with each other. The scope of the Symposia includes fundamentals of continuum physics, new trends in thermodynamics and in electrodynamics, physics of materials (encompassing defective crystals, ferroic crystals, liquid crystals, molecular crystals, high-temperature superconductors, semiconductors, plasma, polymers, amorphous media, smart materials, and anomalous phenomena such as auxetics and negative thermal expansion), biophysics, multiphase systems, and multiscale problems.

The chairs of the Fourth International Symposium on Trends in Continuum Physics (TRECOP'07), where most of the articles in this issue were presented, would like to acknowledge support by the sponsoring institutions who made the meeting possible. They are:

- Institute of Applied Mechanics, Poznan University of Technology
- Pidstryhach Institute for Applied Problems in Mechanics, Ukrainian NAS Centre for Mathematical Modeling, Lviv, Ukraine
- National Academy of Public Administration Office of the President of Ukraine, Lviv Regional Institute of Public Administration, Lviv, Ukraine
- Foundation for Development of Poznan University of Technology

Krzysztof W. Wojciechowski
Chair of the Scientific Committee

Bogdan T. Maruszewski
Wolfgang Muschik
Andrzej Radowicz
Symposium Chairs

Scientific Committee

Krzysztof W. Wojciechowski (Institute of Molecular Physics, Polish Academy of Sciences, Poznan, Poland)

Jan Awrejcewicz (Lodz University of Technology, Lodz, Poland)

Angelo M. Anile (University of Catania, Catania, Italy — deceased)

Vladimir Alshits (Institute of Crystallography, Russian Academy of Sciences, Moscow, Russia)

Arkadi Berezovski (CENS – Institute of Cybernetics, Tallinn, Estonia)

Yaroslav Burak (Institute of Applied Mathematics and Mechanics, Ukrainian National Academy of Sciences, Lviv, Ukraine)

Enzo Ciancio (University of Messina, Messina, Italy)

Yevhen Czaplya (Pidstryhach Institute of Applied Problems of Mechanics and Mathematics, Ukrainian National Academy of Sciences, Lviv, Ukraine)

Juri Engelbrecht (Estonian Academy of Sciences, Tallinn, Estonia)

Karl H. Hoffmann (Chemnitz University of Technology, Chemnitz, Germany)

David Jou (University of Barcelona, Barcelona, Spain)

Jan A. Kołodziej (Institute of Applied Mechanics, Poznan University of Technology, Poznan, Poland)

Józef Kubik (Kazimierz Wielki University, Bydgoszcz, Poland)

Roman Kushnir (Pidstryhach Institute of Applied Problems of Mechanics and Mathematics, Ukrainian National Academy of Sciences, Lviv, Ukraine)

Gerard A. Maugin (University of Paris VI, Paris, France)

Stanisław Matysiak (Warsaw University, Warsaw, Poland)

Henryk Petryk (Institute of Fundamental Technological Research, Polish Academy of Sciences, Warsaw, Poland)

Liliana Restuccia (University of Messina, Messina, Italy)

Jeremiah Rushchitski (Institute of Mechanics, Ukrainian National Academy of Sciences, Kiev, Ukraine)

Czesław Rymarz (Institute of Fundamental Technological Research, Polish Academy of Sciences, Warsaw, Poland)

Jarostaw Rybicki (Gdansk University of Technology, Gdansk, Poland)

Jeremiah Savula (Ivan Franko National University, Lviv, Ukraine)

Igor Selezov (Institute of Hydromechanics, Ukrainian National Academy of Sciences, Kiev, Ukraine)

Stanisław Sieniutycz (Warsaw University of Technology, Warsaw, Poland)

Jarostaw Stefaniak (Poznan University of Technology, Poznan, Poland)

Gwidon Szefer (Cracow University of Technology, Cracow, Poland)

Alfons A. F. van de Ven (Eindhoven University of Technology, Eindhoven, The Netherlands)

Organizing Committee

Chairs:

Bogdan T. Maruszewski (Poznan University of Technology, Institute of Applied Mechanics, Poznan, Poland)

Wolfgang Muschik (Technische Universität Berlin, Institut für Theoretische Physik, Berlin, Germany)

Andrzej Radowicz (Kielce University of Technology, Kielce, Poland)

Secretary:

Anita Uściłowska (Institute of Applied Mechanics, Poznan University of Technology, Poznan, Poland)

Members:

Yevhen Chaplya (Pidstryhach Institute of Applied Problems of Mechanics and Mathematics, Ukrainian National Academy of Sciences, Lviv, Ukraine)

Stepan Mudry (Physics of Metal Department, Ivan Franko National University, Lviv, Ukraine)

Petro Shevchuk (Pidstryhach Institute of Applied Problems of Mechanics and Mathematics, Ukrainian National Academy of Sciences, Lviv, Ukraine)

Tomasz Stręk (Institute of Applied Mechanics, Poznan University of Technology, Poznan, Poland)

Hubert Jopek (Institute of Applied Mechanics, Poznan University of Technology, Poznan, Poland)

Elżbieta Szymkowiak (Institute of Applied Mechanics, Poznan University of Technology, Poznan, Poland)

Organizing Institutions:

Poznan University of Technology, Institute of Applied Mechanics, Poznan, Poland (**Sponsor**)

Polish Academy of Sciences, Institute of Molecular Physics, Poznan, Poland

Pidstryhach Institute of Applied Problems of Mechanics and Mathematics, NAS of Ukraine, Centre of Mathematical Modelling, Lviv, Ukraine (**Sponsor**)

Kazimierz Wielki University, Institute of Environmental Mechanics and Applied Computer Science, Bydgoszcz, Poland

Ivan Franko National University in Lviv, Faculty of Applied Mathematics and Computing Sciences, Lviv, Ukraine

National Academy of Public Administration Office of the President of Ukraine, Lviv Regional Institute of Public Administration, Lviv, Ukraine (**Sponsor**)

Gdansk University of Technology, Gdansk, Poland

Technische Universität Berlin, Institut für Theoretische Physik, Berlin, Germany

Kielce University of Technology, Kielce, Poland

Foundation for Development of Poznan University of Technology, Poznan, Poland (**Sponsor**)

Polish Association of Theoretical and Applied Mechanics, Poznan Division, Poznan, Poland

AN INTRODUCTION OF THE LOCAL DISPLACEMENTS OF MASS AND ELECTRIC CHARGE PHENOMENA INTO THE MODEL OF THE MECHANICS OF POLARIZED ELECTROMAGNETIC SOLIDS

YAROSLAV BURAK, VASYL KONDRAT AND OLHA HRYTSYNA

Using the fundamental principles of thermodynamics of irreversible processes and continuum mechanics and electrodynamics, a complete set of equations of the thermomechanics of an electroconducting polarized medium has been obtained by taking into account the local displacements of mass and electric charge. To determine the thermodynamic state, two additional state parameters, namely the induced mass and the gradient of the energy measure of mass displacement, have been introduced. Two other parameters, the energy measure of mass displacement and the mass displacement vector, have been coupled to the aforementioned parameters. Such an extension of the state parameter space allows one to describe the near-surface inhomogeneity of the stress-strained state and the electric polarization as well as the surface charges and the electromagnetic signals induced by the surface formation.

1. Introduction

The theory of coupled electro-magneto-thermo-mechanical processes in polarized media has been the subject of many investigations, as have the applied problems of electrodynamics and mechanics of polarized structure [de Groot and Mazur 1962; Karnaukhov and Kirichok 1988; Maugin 1988; Nowacki 1983; Sedov 1997; Khoroshun 2006; Burak 1967]. Studying the process of electric polarization (the local displacement of electric charge) authors usually do not take into account the accompanying local displacement of mass, for example, the relative displacement of nuclei and electrons or of hydrogen and oxygen atoms in a water molecule, etc. Note also that the displacement of mass can arise without electric polarization [Hrytsyna and Kondrat 2006], for example, in the case of accelerated motion of a body with mass asymmetric molecules. The process of the mass displacement in thermomechanical systems was reported for the first time in [Burak 1987]. Later the studies in this direction have been concerned mostly with interfacial phenomena including the strength of the surface layers [Burak et al. 1991; Hrytsyna et al. 2006].

The purpose of this paper is the formulation and analysis of a mathematical model for the description of electro-magneto-thermo-mechanical processes in electroconducting polarized solids while taking into account the displacement of electric charges (polarization) and local displacement of mass.

Keywords: coupled electro-magneto-thermo-mechanical processes, electroconducting polarized nonferromagnetic solids, local displacements of mass and electric charges, interfacial phenomena.

2. The model

2A. Investigation object. We consider an isotropic thermoelastic polarized nonferromagnetic solid under the synergistic influence of external stresses, temperature gradients, and electromagnetic fields which induce mechanical, thermal, and electromagnetic processes in the body (domain (V)) enclosed by surface (Σ) . The electromagnetic field causes the ordering of bound electric charges (polarizations) that is described by densities of electric flux \mathbf{J}_{es} and mass flux \mathbf{J}_{ms} . The mass flux is caused by the difference in mass of bounded positive and negative charges.

All fields, which characterize the processes in solids, must satisfy the fundamental physical laws such as the conservation laws of mass, momentum, angular momentum, entropy, and energy.

The initial relations of the proposed model are based on the Euler approach.

2B. Electrodynamics Equations. Maxwell's equations can be written in the local form [Bredov et al. 1985; Landau and Lifshitz 1984; Tamm 1979]

$$\nabla \cdot \mathbf{B} = 0, \quad \nabla \cdot \mathbf{D} = \rho_e, \quad \nabla \times \mathbf{E} = -\frac{\partial \mathbf{B}}{\partial t}, \quad \nabla \times \mathbf{H} = \mathbf{J}_{ef}, \quad (2-1)$$

where \mathbf{E} , \mathbf{H} are the electric and magnetic fields; \mathbf{D} , \mathbf{B} are the vectors of electric and magnetic inductions; for nonferromagnetic mediums $\mathbf{B} = \mu_0 \mathbf{H}$; $\mathbf{D} = \varepsilon_0 \mathbf{E} + \mathbf{\Pi}_e$, where $\mathbf{\Pi}_e \equiv \mathbf{P}$ denotes the local displacement of electric charge (polarization); ε_0 , μ_0 are the electric permittivity and the magnetic permeability of vacuum (electric and magnetic constants); ρ_e is the density of free electric charge; $\mathbf{J}_{ef} = \mathbf{J}_e + \mathbf{J}_{ed} + \mathbf{J}_{es}$ is the density of the total electric current; \mathbf{J}_e is the density of electric current (convection and conduction currents); $\mathbf{J}_{ed} = \varepsilon_0 (\partial \mathbf{E} / \partial t)$; $\mathbf{J}_{es} = \partial \mathbf{\Pi}_e / \partial t$ is the density of current, caused by ordering of a charged system (polarization current), and ∇ is the Hamilton operator.

We introduce the density of induced charge $\rho_{e\pi}$ [Bredov et al. 1985], and require that for an arbitrary solid of finite size (domain (V)) the vector $\mathbf{\Pi}_e$ of the local displacement of the electric charge and the density $\rho_{e\pi}$ satisfy (see also Bredov et al. [1985])

$$\int_{(V)} \mathbf{\Pi}_e dV = \int_{(V)} \rho_{e\pi} \mathbf{r} dV, \quad (2-2)$$

where \mathbf{r} is the position vector. Taking into account the arbitrariness of the domain (V) , the independence of Equation (2-2) from the choice of frame and the identity $\mathbf{a} \cdot \mathbf{\Pi}_e = (\mathbf{\Pi}_e \cdot \nabla) (\mathbf{a} \cdot \mathbf{r})$, where \mathbf{a} is an arbitrary constant vector, from (2-2) we deduce

$$\int_{(V)} \rho_{e\pi} dV = 0, \quad \rho_{e\pi} = -\nabla \cdot \mathbf{\Pi}_e. \quad (2-3)$$

After differentiation by time, the second relation of the set (2-3) and using $\mathbf{J}_{es} = \partial \mathbf{\Pi}_e / \partial t$ we obtain the following equation

$$\frac{\partial \rho_{e\pi}}{\partial t} + \nabla \cdot \mathbf{J}_{es} = 0,$$

which has the form of the conservation law of induced electric charges [Bredov et al. 1985]. From now on instead of $\mathbf{\Pi}_e$ we shall use the standard notation for the polarization vector \mathbf{P} .

2C. The mass balance equation. The mass balance equation in the integral form is given by

$$\frac{d}{dt} \int_{(V)} \rho dV = - \oint_{(\Sigma)} \mathbf{J}_* \cdot \mathbf{n} d\Sigma, \tag{2-4}$$

where ρ is the mass density, \mathbf{J}_* denotes the density of the mass flux, and \mathbf{n} is the outward unit normal to the surface (Σ) . We assume that the density of mass flux \mathbf{J}_* is the sum of the convective component $\mathbf{J}_{mc} = \rho \mathbf{v}_*$, where \mathbf{v}_* is the average velocity of the displaced particles of the body, and the component \mathbf{J}_{ms} related to the ordering of structure of a physically small element of the body. Thus the equation of mass balance (2-4) can be written as follows

$$\frac{d}{dt} \int_{(V)} \rho dV = - \oint_{(\Sigma)} (\rho \mathbf{v}_* + \mathbf{J}_{ms}) \cdot \mathbf{n} d\Sigma.$$

We introduce the local mass displacement vector as $\mathbf{\Pi}_m(t) = \int_0^t \mathbf{J}_{ms}(t') dt'$. Then, for the flux \mathbf{J}_{ms} we obtain

$$\mathbf{J}_{ms} = \partial \mathbf{\Pi}_m / \partial t. \tag{2-5}$$

Thus the velocity \mathbf{v} of the center of mass is $\mathbf{v} = \frac{1}{\rho} \left(\rho \mathbf{v}_* + \frac{\partial \mathbf{\Pi}_m}{\partial t} \right)$, and the equation of mass balance can now be written in the standard form

$$\frac{\partial \rho}{\partial t} + \nabla \cdot (\rho \mathbf{v}) = 0. \tag{2-6}$$

By analogy with the induced charge, we introduce the density of induced mass $\rho_{m\pi}$, which has the dimension of mass density, so that $\rho_{m\pi}$, $\mathbf{\Pi}_m$, \mathbf{r} satisfy (see Equation (2-2))

$$\int_{(V)} \mathbf{\Pi}_m dV = \int_{(V)} \rho_{m\pi} \mathbf{r} dV. \tag{2-7}$$

From Equation (2-7) one deduces the following relations [Bredov et al. 1985]

$$\int_{(V)} \rho_{m\pi} dV = 0, \quad \rho_{m\pi} = -\nabla \cdot \mathbf{\Pi}_m. \tag{2-8}$$

We note that from Equation (2-5) and (2-8) one can obtain the equation

$$\frac{\partial \rho_{m\pi}}{\partial t} + \nabla \cdot \mathbf{J}_{ms} = 0,$$

which has the form of the conservation law of induced mass.

2D. Equation of entropy balance. The general form of the entropy balance equation is [de Groot and Mazur 1962]

$$\frac{d}{dt} \int_{(V)} \rho s dV = - \oint_{(\Sigma)} \mathbf{J}_s \cdot \mathbf{n} d\Sigma - \oint_{(\Sigma)} \rho s \mathbf{v} \cdot \mathbf{n} d\Sigma + \int_{(V)} \sigma_s dV + \int_{(V)} \rho \frac{\mathfrak{R}}{T} dV, \tag{2-9}$$

where s is the specific entropy (entropy per unit mass), \mathbf{J}_s is the density of entropy flux, T is the absolute temperature, σ_s is the strength of the entropy source, or the entropy production per unit volume and unit time, and \mathfrak{R} denotes the distributed thermal sources.

In the local form Equation (2-9) is given by

$$\rho T \frac{ds}{dt} = -\nabla \cdot \mathbf{J}_q + \frac{1}{T} \mathbf{J}_q \cdot \nabla T + T \sigma_s + \rho \mathfrak{R}. \tag{2-10}$$

Here $\mathbf{J}_q = T \mathbf{J}_s$ is the density of heat flux and $d/dt = \partial/\partial t + \mathbf{v} \cdot \nabla$ is the substantive derivative.

2E. Equation of the balance of electromagnetic field energy. From the Maxwell equations (2-1), the equation, which is known as the energy balance equation of the electromagnetic field [Bredov et al. 1985; Landau and Lifshitz 1984; Tamm 1979], follows, namely

$$\frac{\partial U_e}{\partial t} + \nabla \cdot \mathbf{S}_e + \left(\mathbf{J}_e + \frac{\partial \mathbf{P}}{\partial t} \right) \cdot \mathbf{E} = 0, \tag{2-11}$$

where $U_e = (\epsilon_0 \mathbf{E}^2 + \mu_0 \mathbf{H}^2) / 2$ is the energy density of the electromagnetic field and $\mathbf{S}_e = \mathbf{E} \times \mathbf{H}$ is the flux density of its energy.

Let us rewrite the last term in Equation (2-11) in such a way that it contains the specific polarization $\mathbf{p} = \mathbf{P}/\rho$, the vectors \mathbf{E}_* , \mathbf{P}_* , \mathbf{J}_{e*} of the electromagnetic field and density of electric current in the reference frame of the center of mass moving with speed \mathbf{v} relatively to the laboratory reference frame, that is,

$$\mathbf{E}_* = \mathbf{E} + \mathbf{v} \times \mathbf{B}, \quad \mathbf{P}_* = \mathbf{P} + \epsilon_0 \mu_0 \mathbf{v} \times \mathbf{M}, \quad \mathbf{J}_{e*} = \mathbf{J}_e - \rho_e \mathbf{v}.$$

Here \mathbf{M} denotes the magnetization vector (in the nonmagnetic case the magnetization vector is zero) and \mathbf{J}_{e*} is the conduction current density. Using the mass conservation law (2-6), we can rewrite the balance equation of energy of electromagnetic field (2-11) as

$$\begin{aligned} \frac{\partial U_e}{\partial t} + \nabla \cdot \mathbf{S}_e + \mathbf{J}_{e*} \cdot \mathbf{E}_* + \left[\rho_e \mathbf{E}_* + \left(\mathbf{J}_{e*} + \frac{\partial(\rho \mathbf{p})}{\partial t} \right) \times \mathbf{B} + \rho (\nabla \mathbf{E}_*) \cdot \mathbf{p} \right] \cdot \mathbf{v} \\ + \rho \mathbf{E}_* \cdot \frac{d\mathbf{p}}{dt} - \nabla \cdot [\rho (\mathbf{E}_* \cdot \mathbf{p}) \mathbf{I} \cdot \mathbf{v}] = 0. \end{aligned} \tag{2-12}$$

2F. Equation of balance of energy for system body—electromagnetic field. We assume that for an arbitrary moment of time, the total energy of system is the sum of internal energy ρu (u is the specific internal energy), kinetic $\rho \mathbf{v}^2/2$ energy, and the energy of the electromagnetic field U_e . On the other hand, the total energy change is the result of the convective energy transport $\rho (u + \mathbf{v}^2/2)$ through the surface, the work $\hat{\sigma} \cdot \mathbf{v}$ of surface forces; the heat flux \mathbf{J}_q , the electromagnetic energy flux \mathbf{S}_e , the work $\mu \mathbf{J}_m$ connected to the mass transport relative to the center of mass of the body (here $\mathbf{J}_m = \rho (\mathbf{v}_* - \mathbf{v})$); the work $\mu_\pi \partial \mathbf{\Pi}_m / \partial t$ related with structure ordering (local mass displacement), and the action of mass forces \mathbf{F} and distributed thermal sources \mathfrak{R} . One therefore has

$$\begin{aligned} \frac{d}{dt} \int_{(V)} (\rho u + U_e + \frac{1}{2} \rho \mathbf{v}^2) dV = \\ - \oint_{(\Sigma)} \left[\rho (u + \frac{1}{2} \mathbf{v}^2) \mathbf{v} - \hat{\sigma} \cdot \mathbf{v} + \mathbf{S}_e + \mathbf{J}_q + \mu \mathbf{J}_m + \mu_\pi \frac{\partial \mathbf{\Pi}_m}{\partial t} \right] \cdot \mathbf{n} d\Sigma + \int_{(V)} (\rho \mathbf{F} \cdot \mathbf{v} + \rho \mathfrak{R}) dV, \end{aligned} \tag{2-13}$$

where $\hat{\sigma}$ is the Cauchy’s stress tensor, μ is the chemical potential, and μ_π is the energy measure of the influence of the mass displacement on the internal energy.

By the use of the Ostrogradsky–Gauss theorem, the balance equations of mass (2-6), the electromagnetic energy equation (2-12), and the entropy equation (2-10), we obtain from Equation (2-13)

$$\rho \frac{du}{dt} = \rho T \frac{ds}{dt} + \left[\hat{\boldsymbol{\sigma}} - \rho(\mathbf{E}_* \cdot \mathbf{p}) \hat{\mathbf{I}} \right] : \frac{d\hat{\mathbf{e}}}{dt} + \rho \mathbf{E}_* \cdot \frac{d\mathbf{p}}{dt} - \mu'_\pi \frac{\partial \nabla \cdot \boldsymbol{\Pi}_m}{\partial t} - \nabla \mu'_\pi \cdot \frac{\partial \boldsymbol{\Pi}_m}{\partial t} + \rho_e \mathbf{E}_* - \mathbf{J}_{e*} \cdot \mathbf{E}_* - \mathbf{J}_q \cdot \frac{\nabla T}{T} - T \sigma_s + \mathbf{v} \cdot \left\{ -\rho \frac{d\mathbf{v}}{dt} + \nabla \cdot \left[\hat{\boldsymbol{\sigma}} - \rho(\mathbf{E}_* \cdot \mathbf{p}) \hat{\mathbf{I}} \right] + \left(\mathbf{J}_{e*} + \frac{\partial(\rho \mathbf{p})}{\partial t} \right) \times \mathbf{B} + \rho(\nabla \mathbf{E}_*) \cdot \mathbf{p} + \rho \mathbf{F} \right\}, \quad (2-14)$$

where $\mu'_\pi = \mu_\pi - \mu$, $\hat{\mathbf{e}} = [\nabla \mathbf{u} + (\nabla \mathbf{u})^T]/2$ is the strain tensor, \mathbf{u} is the displacement vector, and an upper index T denotes a transposed tensor.

Introducing the specific values $\boldsymbol{\pi}_m = \boldsymbol{\Pi}_m/\rho$ and $\rho_m = \rho_{m\pi}/\rho$ and taking into account the mass balance Equation (2-6), we obtain the following balance equation for the internal energy using Equation (2-14)

$$\rho \frac{du}{dt} = \rho T \frac{ds}{dt} + \hat{\boldsymbol{\sigma}}_* : \frac{d\hat{\mathbf{e}}}{dt} + \rho \mathbf{E}_* \cdot \frac{d\mathbf{p}}{dt} + \rho \mu'_\pi \frac{d\rho_m}{dt} - \rho \nabla \mu'_\pi \cdot \frac{d\boldsymbol{\pi}_m}{dt} + \mathbf{J}_{e*} \cdot \mathbf{E}_* - \mathbf{J}_q \cdot \frac{\nabla T}{T} - T \sigma_s + \mathbf{v} \cdot \left\{ -\rho \frac{d\mathbf{v}}{dt} + \nabla \cdot \hat{\boldsymbol{\sigma}}_* + \rho_e \mathbf{E}_* + \left(\mathbf{J}_{e*} + \frac{\partial(\rho \mathbf{p})}{\partial t} \right) \times \mathbf{B} + \rho(\nabla \mathbf{E}_*) \cdot \mathbf{p} + \rho \mathbf{F}_* \right\}, \quad (2-15)$$

where

$$\hat{\boldsymbol{\sigma}}_* = \hat{\boldsymbol{\sigma}} - \rho(\mathbf{E}_* \cdot \mathbf{p} - \rho_m \mu'_\pi - \boldsymbol{\pi}_m \cdot \nabla \mu'_\pi) \hat{\mathbf{I}}, \quad \mathbf{F}_* = \mathbf{F} + \rho_m \nabla \mu'_\pi - \boldsymbol{\pi}_m \cdot \nabla \nabla \mu'_\pi.$$

Furthermore, when using the new thermodynamical function of the generalized Helmholtz free energy $f = u - Ts - \mathbf{E}_* \cdot \mathbf{p} + \nabla \mu'_\pi \cdot \boldsymbol{\pi}_m$, we obtain from Equation (2-15)

$$\rho \frac{df}{dt} = -\rho s \frac{dT}{dt} + \hat{\boldsymbol{\sigma}}_* : \frac{d\hat{\mathbf{e}}}{dt} - \rho \mathbf{p} \cdot \frac{d\mathbf{E}_*}{dt} + \rho \mu'_\pi \frac{d\rho_m}{dt} + \rho \boldsymbol{\pi}_m \cdot \frac{d\nabla \mu'_\pi}{dt} + \mathbf{J}_{e*} \cdot \mathbf{E}_* - \mathbf{J}_q \cdot \frac{\nabla T}{T} - T \sigma_s + \mathbf{v} \cdot \left\{ -\rho \frac{d\mathbf{v}}{dt} + \nabla \cdot \hat{\boldsymbol{\sigma}}_* + \rho_e \mathbf{E}_* + \left(\mathbf{J}_{e*} + \frac{\partial(\rho \mathbf{p})}{\partial t} \right) \times \mathbf{B} + \rho(\nabla \mathbf{E}_*) \cdot \mathbf{p} + \rho \mathbf{F}_* \right\}. \quad (2-16)$$

From the requirement that Equation (2-16) is invariant with respect to translations and assuming that the free energy f is the function of scalar quantities T , ρ_m , vector quantities \mathbf{E}_* , $\nabla \mu'_\pi$, and tensor quantity $\hat{\mathbf{e}}$ (all of them are independent parameters), we obtain the generalized Gibbs equation

$$df = -sdT + \rho^{-1} \hat{\boldsymbol{\sigma}}_* : d\hat{\mathbf{e}} - \mathbf{p} \cdot d\mathbf{E}_* + \mu'_\pi d\rho_m + \boldsymbol{\pi}_m \cdot d\nabla \mu'_\pi, \quad (2-17)$$

a relation for the entropy production

$$\sigma_s = \mathbf{J}_{e*} \cdot \frac{\mathbf{E}_*}{T} - \mathbf{J}_q \cdot \frac{\nabla T}{T^2}, \quad (2-18)$$

and the momentum equation

$$\rho \frac{d\mathbf{v}}{dt} = \nabla \cdot \hat{\boldsymbol{\sigma}}_* + \mathbf{F}_e + \rho \mathbf{F}_*, \quad (2-19)$$

where $\mathbf{F}_e = \rho_e \mathbf{E}_* + (\mathbf{J}_{e*} + \partial(\rho \mathbf{p})/\partial t) \times \mathbf{B} + \rho(\nabla \mathbf{E}_*) \cdot \mathbf{p}$ is the ponderomotive force.

In this case the free energy depends not only on temperature T , strain tensor $\hat{\mathbf{e}}$ and electric field \mathbf{E}_* , but also on the parameters related to the mass displacement, namely, ρ_m and $\nabla \mu'_\pi$. Note that the introduction of both the local mass displacement and the electric charge displacement leads to additional (ponderomotive) forces in Equation (2-19) and to the redefinition of the stress tensor.

2G. Constitutive relations. Since the parameters T , ρ_m , \mathbf{E}_* , $\nabla\mu'_\pi$, and $\hat{\mathbf{e}}$ are independent, we obtain the following relations from the Gibbs Equation (2-17)

$$s = -\frac{\partial f}{\partial T} \Big|_{\hat{\mathbf{e}}, \rho_m, \nabla\mu'_\pi, \mathbf{E}_*}, \quad \hat{\sigma}_* = \rho \frac{\partial f}{\partial \hat{\mathbf{e}}} \Big|_{T, \rho_m, \nabla\mu'_\pi, \mathbf{E}_*}, \quad \mu'_\pi = \frac{\partial f}{\partial \rho_m} \Big|_{T, \hat{\mathbf{e}}, \nabla\mu'_\pi, \mathbf{E}_*},$$

$$\mathbf{p} = -\frac{\partial f}{\partial \mathbf{E}_*} \Big|_{T, \hat{\mathbf{e}}, \rho_m, \nabla\mu'_\pi}, \quad \boldsymbol{\pi}_m = \frac{\partial f}{\partial (\nabla\mu'_\pi)} \Big|_{T, \hat{\mathbf{e}}, \rho_m, \mathbf{E}_*}. \tag{2-20}$$

Let $\hat{\mathbf{e}} = 0$, $T = T_0$, $\rho_m = 0$, $\mathbf{E}_* = 0$, $\nabla\mu'_\pi = 0$, $s = s_0$, $\hat{\sigma}_* = 0$, $\mu'_\pi = \mu'_{\pi 0}$, $\mathbf{p} = 0$, and $\boldsymbol{\pi}_m = 0$ in the reference state, then in the linear approximation, Equation (2-20) may be written in the form

$$s = s_0 - [a_T^s(T - T_0) + \rho_0^{-1}a_{eT}e + a_{\rho T}\rho_m],$$

$$\hat{\sigma}_* = 2a_2^\sigma \hat{\mathbf{e}} + [a_1^\sigma e + a_{eT}(T - T_0) + a_{e\rho}\rho_m] \hat{\mathbf{I}},$$

$$\mu'_\pi = \mu'_{\pi 0} + a_\rho^\mu \rho_m + \rho_0^{-1}a_{e\rho}e + a_{\rho T}(T - T_0),$$

$$\mathbf{p} = -a_E^p \mathbf{E}_* - a_{E\mu} \nabla\mu'_\pi, \quad \boldsymbol{\pi}_m = a_\mu^\pi \nabla\mu'_\pi + a_{E\mu} \mathbf{E}_*, \tag{2-21}$$

where $e \equiv \hat{\mathbf{e}} : \hat{\mathbf{I}}$ is the first invariant of the strain tensor; a_1^σ , a_2^σ , a_T^s , a_ρ^μ , a_E^p , a_μ^π , a_{eT} , $a_{\rho T}$, $a_{e\rho}$, and $a_{E\mu}$ are the characteristics of material; and s_0 and $\mu'_{\pi 0}$ are the entropy and the reduced potential μ'_π , respectively, in the reference state.

An analysis of the Gibbs equation reveals that our model requires two additional pairs of parameters for enabling us to describe the local thermodynamic state of the body:

- (i) the induced mass $\rho_m = -(\nabla \cdot \boldsymbol{\Pi}_m)/\rho$ and the energy measure μ'_π of the influence of the mass displacement on internal energy;
- (ii) the vector of density of the mass displacement $\boldsymbol{\pi}_m = \boldsymbol{\Pi}_m/\rho$ and the gradient of μ'_π .

These parameters are related to the local displacement of the mass. Such an extension of the state parameters space allows one to describe near-surface inhomogeneity of the stress-strained state and electrical polarization [Hrytsyna and Kondrat 2006; Burak et al. 1991; Hrytsyna et al. 2006]. Indeed, according to the chosen model the electric polarization is caused not solely by the electric field but also by the gradient of μ'_π . In the near-surface region the value of $|\nabla\mu'_\pi|$ can be sufficiently large to induce essential surface polarization. This can be important in studies of electromagnetic emission caused by the formation of a new surface within the body or an electromagnetic response of the body towards external dynamic influence on its surface [Fursa et al. 2003]. The details of such phenomena are considered below where we describe the near-surface inhomogeneity in an infinite polarized layer.

By using the Onsager principle and Equation (2-18) for the entropy production, one finds in the linear approximation [de Groot and Mazur 1962]

$$\mathbf{J}_{e*} = \sigma_e \mathbf{E}_* + \sigma_e \eta \nabla T, \quad \mathbf{J}_q = -\lambda \nabla T + \pi_t \mathbf{J}_{e*},$$

where σ_e and λ are electric and thermal conductivity, respectively. Here coefficients η and π_t characterize thermoelectric phenomena and are related by $T\eta = -\pi_t$, respectively.

The obtained constitutive relations, the conservation laws of momentum, masses, and entropy, the equations of electrodynamics and geometrical relations form a complete set of equations of electro-magneto-thermo-mechanics of the polarized nonferromagnetic solids taking into account the local displacements of the mass and electric charge.

Let us take the displacement vector \mathbf{u} , temperature T , electric field \mathbf{E} , magnetic induction \mathbf{B} , and the induced mass ρ_m as a set of basic functions. Then in the linear approximation we obtain the following equation for ρ_m

$$\Delta\rho_m + \frac{1}{a_{\mu}^{\pi}a_{\rho}^{\mu}}\rho_m = -\frac{1}{a_{\rho}^{\mu}}\left[\frac{a_{e\rho}}{\rho_0}\Delta(\nabla\cdot\mathbf{u}) + a_{\rho T}\Delta T + \frac{a_{E\mu}}{a_{\mu}^{\pi}}\nabla\cdot\mathbf{E}\right].$$

It is possible to show that one may present ρ_m as a functional of functions \mathbf{u} , T , and \mathbf{E} , therefore ρ_m can be eliminated from the basic set of equations and also from the constitutive relations. In this case, the basic set of equations becomes integro-differential equations whereas the constitutive equations (2-21) become spatially nonlocal.

3. Example

We consider an elastic polarized layer of an ideal dielectric in the region $-l \leq x \leq l$. At time $t = 0$ the layer is cut from an infinite medium in such a way that at time $t > 0$ it is in contact with a medium which behaves as vacuum with regards to its electromagnetic properties. The effect of temperature is neglected while the processes of deformation, polarization, and displacement of mass are considered.

In this case the basic functions $\mathbf{f} = \{\mathbf{u}, \mathbf{E}, \mathbf{p}, \mathbf{D}, \pi_m, \mathbf{E}_v\}$ and $g = \{\tilde{\mu}'_{\pi}, \rho_m\}$ are functions of the space coordinate x and time coordinate t such that $\mathbf{f} = (f, 0, 0)$, $f = \{u, E, p, D, \pi_m, E_v\}$, $f = f(x, t)$, and $g = g(x, t)$, where \mathbf{E}_v is the vector of the electric field in vacuum, and $\tilde{\mu}'_{\pi} = \mu'_{\pi} - \mu'_{\pi 0}$.

With this notation our basic set of equations is reduced to the set of equations for the layer $-l \leq x \leq l$

$$\begin{aligned} \rho_0 \frac{\partial^2 u}{\partial t^2} &= \left(a_1^{\sigma} + 2a_2^{\sigma} - \frac{a_{e\rho}^2}{\rho_0 a_{\rho}^{\mu}}\right) \frac{\partial^2 u}{\partial x^2} + \frac{a_{e\rho}}{a_{\rho}^{\mu}} \frac{\partial \tilde{\mu}'_{\pi}}{\partial x}, & \mu_0 \left(\varepsilon_0 - \rho_0 a_E^p\right) \frac{\partial E}{\partial t} - \rho_0 \mu_0 a_{E\mu} \frac{\partial^2 \tilde{\mu}'_{\pi}}{\partial x \partial t} &= 0, \\ \frac{\partial^2 \tilde{\mu}'_{\pi}}{\partial x^2} + \frac{1}{a_{\mu}^{\pi} a_{\rho}^{\mu}} \tilde{\mu}'_{\pi} &= \frac{1}{a_{\mu}^{\pi} a_{\rho}^{\mu}} \frac{a_{e\rho}}{\rho_0} \frac{\partial u}{\partial x} - \frac{a_{E\mu}}{a_{\mu}^{\pi}} \frac{\partial E}{\partial x}, \end{aligned}$$

where $E = -\partial\varphi/\partial x$, φ is the electric potential, and the set of equations for the potential φ_v of the electric field in vacuum ($x < -l, x > l$) is

$$\frac{\partial^2 \varphi_v}{\partial x^2} - \varepsilon_0 \mu_0 \frac{\partial^2 \varphi_v}{\partial t^2} = 0, \quad E_v = -\frac{\partial \varphi_v}{\partial x}.$$

The surfaces of the layer are stress-free and the potential μ'_{π} at $x = \pm l$ is zero. Therefore, taking into account the continuity condition for electric potential, the boundary conditions and radiation conditions become

$$\begin{aligned} \left(a_1^{\sigma} + 2a_2^{\sigma} - \frac{a_{e\rho}^2}{\rho_0 a_{\rho}^{\mu}}\right) \frac{\partial u}{\partial x} + \frac{a_{e\rho}}{a_{\rho}^{\mu}} \tilde{\mu}'_{\pi} &= 0, & \lim_{x \rightarrow \pm\infty} \left(\frac{\partial \varphi_v}{\partial x} \pm \sqrt{\varepsilon_0 \mu_0} \frac{\partial \varphi_v}{\partial t}\right) &= 0, \\ \tilde{\mu}'_{\pi} &= -\mu'_{\pi 0}, & \varphi &= \varphi_v. \end{aligned}$$

We suppose that at $t = 0$ the sought functions are zero. Neglecting the inertial forces, the solution of this boundary problem is given by

$$\begin{aligned} \tilde{\mu}'_{\pi} &= -\mu'_{\pi 0} \frac{\text{ch}(\lambda x)}{\text{ch}(\lambda l)} \theta(t), & E &= -\lambda \mu'_{\pi 0} \frac{\rho_0 a_{E\mu}}{\varepsilon_0 - \rho_0 a_E^p} \frac{\text{sh}(\lambda x)}{\text{ch}(\lambda l)} \theta(t), \\ \varphi &= \mu'_{\pi 0} \frac{\rho_0 a_{E\mu}}{\varepsilon_0 - \rho_0 a_E^p} \frac{\text{ch}(\lambda x)}{\text{ch}(\lambda l)} \theta(t), & p &= \lambda \mu'_{\pi 0} \frac{\varepsilon_0 a_{E\mu}}{\varepsilon_0 - \rho_0 a_E^p} \frac{\text{sh}(\lambda x)}{\text{ch}(\lambda l)} \theta(t), \\ \sigma_{yy} = \sigma_{zz} \equiv \sigma &= -\mu'_{\pi 0} \frac{a_{e\rho}}{a_{\rho}^{\mu}} \left[1 - \frac{a_1^{\sigma}}{a_1^{\sigma} + 2a_2^{\sigma} - a_{e\rho}^2 / (\rho_0 a_{\rho}^{\mu})} \left(1 - \frac{a_{e\rho}^2}{\rho_0 a_{\rho}^{\mu}} \right) \right] \frac{\text{ch}(\lambda x)}{\text{ch}(\lambda l)} \theta(t) \end{aligned}$$

for $-l \leq x \leq l$;

$$\varphi_v = \begin{cases} \mu'_{\pi 0} \frac{\rho_0 a_{E\mu}}{\varepsilon_0 - \rho_0 a_E^p} \theta(t + \sqrt{\varepsilon_0 \mu_0} (x + l)), & \text{if } x < -l, \\ \mu'_{\pi 0} \frac{\rho_0 a_{E\mu}}{\varepsilon_0 - \rho_0 a_E^p} \theta(t - \sqrt{\varepsilon_0 \mu_0} (x - l)), & \text{if } x > l, \end{cases}$$

where

$$\lambda^2 = - \frac{\rho_0 (a_1^{\sigma} + 2a_2^{\sigma}) (\varepsilon_0 - \rho_0 a_E^p)}{[\rho_0 a_{\rho}^{\mu} (a_1^{\sigma} + 2a_2^{\sigma}) - a_{e\rho}^2] [a_{\rho}^{\mu} (\varepsilon_0 - \rho_0 a_E^p) + \rho_0 a_{E\mu}^2]}.$$

For the density of the bound surface charge $\sigma_{se}(\pm l) = \rho_0 p(\pm l)$ at $t > 0$ one has

$$\sigma_{se}(\pm l) = \mu'_{\pi 0} \lambda a_{E\mu} \frac{\varepsilon_0 \rho_0}{\varepsilon_0 - \rho_0 a_E^p} \text{th}(\lambda l). \tag{3-1}$$

The analysis of the solution shows that the distributions of the stresses σ_{yy} , σ_{zz} , the reduced energy measure $\tilde{\mu}'_{\pi}$ and functions E , φ , and p exhibit inhomogeneities close to the surface. Figure 1 displays the distributions of the stresses σ/σ^* , the electric potential φ/φ^* , and electric polarization p/p^* in the layer where

$$\begin{aligned} \varphi^* &= \mu'_{\pi 0} \frac{\rho_0 a_{E\mu}}{\varepsilon_0 - \rho_0 a_E^p}, & p^* &= \mu'_{\pi 0} \frac{\varepsilon_0 \lambda a_{E\mu}}{\varepsilon_0 - \rho_0 a_E^p}, \\ \sigma^* &= -\mu'_{\pi 0} \frac{a_{e\rho}}{a_{\rho}^{\mu}} \left[1 - \frac{a_1^{\sigma}}{a_1^{\sigma} + 2a_2^{\sigma} - a_{e\rho}^2 / (\rho_0 a_{\rho}^{\mu})} \left(1 - \frac{a_{e\rho}^2}{\rho_0 a_{\rho}^{\mu}} \right) \right]. \end{aligned}$$

As one can see, thin layers (curves 1–3 in Figure 1 are characterized by the overlay of the near-surface inhomogeneities while there is a well-defined bulk region characterized by the uniform (constant) profile for thicker layers (curves 4 and 5). This effect manifests itself in the dependence of the surface charge density $\sigma_{se}/\sigma_{se}^*$, where $\sigma_{se}^* = \mu'_{\pi 0} \lambda a_{E\mu} \varepsilon_0 \rho_0 / (\varepsilon_0 - \rho_0 a_E^p)$, on the layer thickness (see Figure 2).

The bounded charge (3-1) is induced at the surfaces of the layer while in the vacuum the momentum of the electric field arises and propagates from $x = \pm l$ to $\pm\infty$. Thus the proposed model allows the description of the interface inhomogeneity of the stress-strained state and the surface polarization in dielectrics, the appearance of electrical charge at surfaces as well as an electromagnetic signal caused by the surface formation.

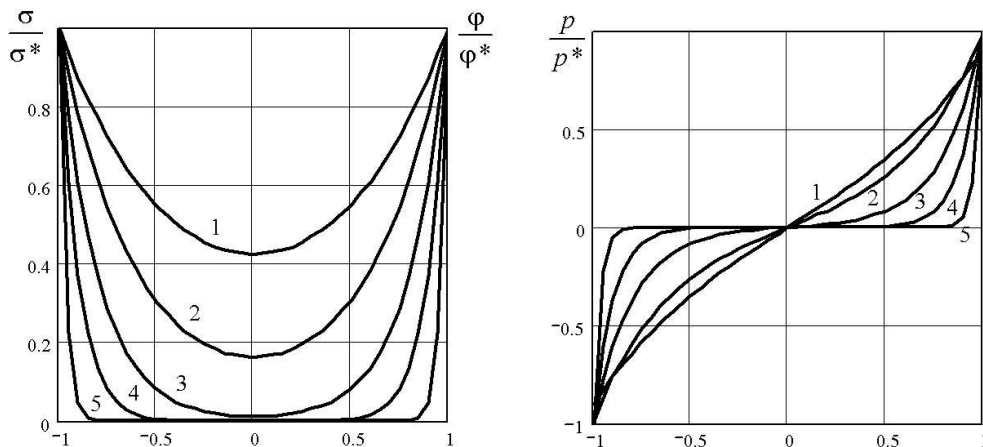


Figure 1. The distributions of the stresses σ/σ^* , the electric potential φ/φ^* , and electric polarization p/p^* in the layer for $\lambda l = 1.5, 2.5, 5, 10, 30$, that is, curves 1–5 respectively.

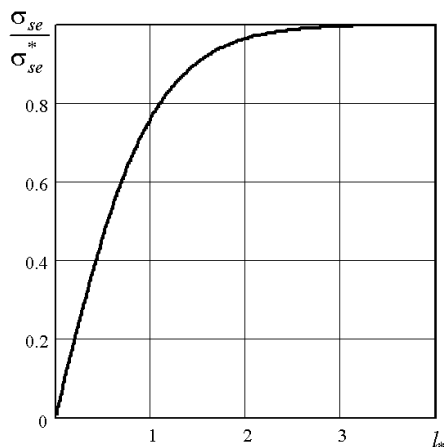


Figure 2. The dependence of the surface charge density $\sigma_{se}/\sigma_{se}^*$ on the layer thickness $l_* = \lambda l$.

References

[Bredov et al. 1985] M. M. Bredov, V. V. Rumjantsev, and I. N. Toptyhin, *Классическая электродинамика*, Nauka, Moscow, 1985.

[Burak 1967] Y. Burak, “Equations of electroelasticity of isotropic dielectrics in electrostatic fields”, *J. Mater. Sci.* **2**:1 (1967), 40–44.

[Burak 1987] Y. Burak, “Constitutive equations of locally gradient thermomechanics”, *Dopovidi Akad. Nauk URSS = Proc. Acad. Sci. Ukrain. SSR* **12** (1987), 19–23. In Ukrainian.

[Burak et al. 1991] Y. Burak, T. Nahirnyj, and O. Hrytsyna, “About one approach to describing the interface nonhomogeneity in thermomechanics of solid solution”, *Dopovidi Akad. Nauk Ukr. = Reports Nat. Acad. Sci. Ukraine* **11** (1991), 47–51. In Ukrainian.

- [Fursa et al. 2003] T. V. Fursa, A. V. Saveljev, and K. Y. Osipov, “The investigation of interaction of electromagnetic response parameters from dielectric materials with characteristic of applied shock”, *Zh. Tekhn. Fiziki = J. Tech. Phys.* **73**:11 (2003), 59–63. In Russian.
- [de Groot and Mazur 1962] S. R. de Groot and P. Mazur, *Non-equilibrium thermodynamics*, Noth-Holland, Amsterdam, 1962.
- [Hrytsyna and Kondrat 2006] O. Hrytsyna and V. Kondrat, “Thermomechanical processes in viscous fluid with respect to the local displacement of mass”, *Fiz.-mat. modelyuvannya ta inform. technologii = Physico-Mathematical Modelling and Informational Technologies* **4** (2006), 39–46. In Ukrainian.
- [Hrytsyna et al. 2006] O. Hrytsyna, T. Nahirnyj, and K. Tchervinka, “Local gradient approach in thermomechanics”, *Fiz.-mat. modelyuvannya ta inform. technologii = Physico-Mathematical Modelling and Informational Technologies* **3** (2006), 72–83. In Ukrainian.
- [Karnaukhov and Kirichok 1988] V. G. Karnaukhov and I. F. Kirichok, *Механика связанных полей в элементах конструкций*, 4: Электротермовязкоупругость, Naukova dumka, Kiev, 1988.
- [Khoroshun 2006] L. Khoroshun, “Constructing the dynamical equations of electromagnetomechanics of dielectrics and piezoelectrics on basis of two-continuum mechanics”, *Fiz.-mat. modelyuvannya ta inform. technologii = Physico-Mathematical Modelling and Informational Technologies* **3** (2006), 177–198. In Russian.
- [Landau and Lifshitz 1984] L. D. Landau and E. M. Lifshitz, *Electrodynamics of continuous media*, Pergamon, Oxford, 1984.
- [Maugin 1988] G. A. Maugin, *Continuum mechanics of electromagnetic solids*, Noth-Holland, Amsterdam, 1988.
- [Nowacki 1983] W. Nowacki, *Efekty elektromagnetyczne w statych ciałach odkształcalnych*, Państwowe Wydawnictwo Naukowe, Warszawa, 1983.
- [Sedov 1997] L. I. Sedov, *Mechanics of continuous media*, vol. 1, World Scientific, Singapore, 1997. In 2 volumes.
- [Tamm 1979] I. E. Tamm, *Fundamentals of the theory of electricity*, Mir, Moscow, 1979.

Received 7 Feb 2008. Revised 1 Jan 2000. Accepted 25 Mar 2008.

YAROSLAV BURAK: burak@cmm.lviv.ua

Center of Mathematical Modeling of the Institute of Applied Mathematics and Mechanics, National Academy of Sciences of Ukraine, Dudajev str. 15, 79005 Lviv, Ukraine

<http://cmm.lviv.ua>

VASYL KONDRAT: kon@cmm.lviv.ua

Center of Mathematical Modeling of the Institute of Applied Mathematics and Mechanics, National Academy of Sciences of Ukraine, Dudajev str. 15, 79005 Lviv, Ukraine

<http://cmm.lviv.ua>

OLHA HRYTSYNA: gryt@cmm.lviv.ua

Center of Mathematical Modeling of the Institute of Applied Mathematics and Mechanics, National Academy of Sciences of Ukraine, Dudajev str. 15, 79005 Lviv, Ukraine

<http://cmm.lviv.ua>

NEW CONCEPTION OF THE FEM BASE FUNCTIONS APPLIED TO SOLVING AN INVERSE HEAT TRANSFER PROBLEM

ANDRZEJ FRĄCKOWIAK, JENS VON WOLFERSDORF AND MICHAŁ CIAŁKOWSKI

The present work shows the modified concept of the finite element method which has been applied to the solution of the inverse problem (of Cauchy type) for heat conduction equation in a circular ring. The main idea of the new concept consists of the application a new type of base function which cause the vanishing of some integrals in the strong formulation. The calculation with the new base functions takes place in the physical space, and there is no need to go to the isoparametric one. Numerical calculations of the inverse problem confirm the good properties of a new set of base functions.

1. Introduction

The complex character of the domain and the equations depicting heat-flow problems in arbitrary bodies impose the need for use of numerical methods such as the finite element method (FEM) for solving them. In order to satisfy continuity of a function between particular finite elements isoparametric elements are typically used, which, in consequence, results in increased computational costs. In order to reduce the computational effort and satisfy continuity of the interpolated function in the entire domain at the same time, interpolation of the solution at the element (the physical space) is proposed with the use of a new type of base functions.

Consideration of the heat conduction equation in discretized form is conducive to some integrals that should be numerically calculated. In order to avoid some of the integrals, test functions are introduced. Their regularity affects accuracy of the temperature field computed this way.

The method proposed in the present paper is a generalization of the finite element methods presented in [Gresho and Sani 2000]. Aspects of such an approach are discussed below.

2. Numerical method for solving the direct and inverse problems

In order to present the new conception let us consider the Laplace equation in the Ω domain, as shown in Figure 1:

$$\Delta T = 0, \quad T \in C^2(\Omega_i). \quad (2-1)$$

First, the neighborhood of the point P_i is considered. The elements including the point P_i form the domain

$$\Omega_i = \bigcup_{\alpha=1}^{n_i} \Omega_{i\alpha}.$$

Keywords: inverse problem, finite element method.

This paper was done with support from a grant from the Ministry of Higher Education (no. 3134/B/T02/2007/33).

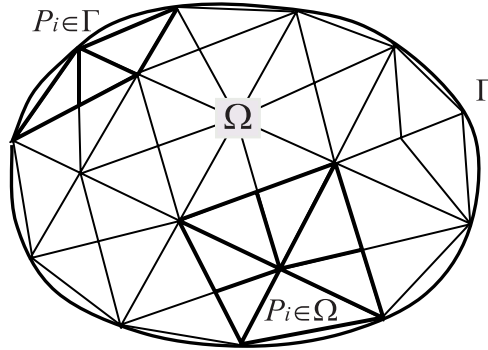


Figure 1. The domain Ω divided into elements.

Let the test function $w \in C^2(\Omega_{i\alpha}) \cap C^1(\Omega_i)$. Multiplication of Equation (2-1) by the w function and integration over the Ω_i domain provides

$$\int_{\Omega_i} \Delta T \cdot w \cdot d\omega = \sum_{\alpha=1}^{n_i} \int_{\Omega_{i\alpha}} \Delta T \cdot w \cdot d\omega = \sum_{\alpha=1}^{n_i} \int_{\partial\Omega_{i\alpha}} [\text{div}(\nabla T \cdot w) - \text{div}(T \cdot \nabla w)] \cdot d\omega + \sum_{\alpha=1}^{n_i} \int_{\Omega_{i\alpha}} T \cdot \Delta w \cdot d\omega = 0.$$

Application of the Gauss–Ostrogradski theorem gives

$$\sum_{\alpha=1}^{n_i} \int_{\partial\Omega_{i\alpha}} \left(w \cdot \frac{\partial T}{\partial n} - T \cdot \frac{\partial w}{\partial n} \right) \cdot ds + \sum_{\alpha=1}^{n_i} \int_{\Omega_{i\alpha}} T \cdot \Delta w \cdot d\omega = 0, \quad i = 1, 2, \dots \tag{2-2}$$

Taking into account continuity of the w function within the element Ω_i and continuity of the derivative $\partial T/\partial n$, the integral of the product $w \cdot \partial T/\partial n$ at common boundaries $\partial\Omega_{i\alpha}$ between the elements vanishes, so that

$$\sum_{\alpha=1}^{n_i} \int_{\partial\Omega_{i\alpha}} w \cdot \frac{\partial T}{\partial n} \cdot ds = \int_{\partial\Omega_i} w \cdot \frac{\partial T}{\partial n} \cdot ds. \tag{2-3}$$

The integral at the right-hand side of Equation (2-3) disappears provided that $w|_{\partial\Omega_i} = 0$. The essence of the present conception consists of the formulation of such a test function that takes zero values at the $\partial\Omega_i$ boundary. In consequence, the number of integrals of (2-2) is reduced. Moreover, if the w function is differentiable in the domain Ω_i , the first sum of (2-2) disappears too. Let us consider the case $w \in C^2(\Omega_{i\alpha}) \cap C^1(\Omega_i) \cap C^0(\partial\Omega_i)$. There, with (2-2), the point $P_i \notin \Gamma$, shown in Figure 2a, takes the form

$$-\sum_{\alpha=1}^{n_i} \int_{\partial\Omega_{i\alpha}} T \cdot \frac{\partial w}{\partial n} \cdot ds + \sum_{\alpha=1}^{n_i} \int_{\Omega_{i\alpha}} T \cdot \Delta w \cdot d\omega = 0, \quad i = 1, 2, \dots \tag{2-4}$$

The condition $P_i \in \Gamma$, shown in Figure 2b, results in $w = 0$ at the boundary $\partial\Omega_i \setminus \Gamma \in \Omega_i$. This gives, for (2-2), the form

$$\int_{\Gamma_i} w \cdot \frac{\partial T}{\partial n} \cdot ds - \sum_{\alpha=1}^{n_i} \int_{\partial\Omega_{i\alpha}} T \cdot \frac{\partial w}{\partial n} \cdot ds + \sum_{\alpha=1}^{n_i} \int_{\Omega_{i\alpha}} T \cdot \Delta w \cdot d\omega = 0, \quad i = 1, 2, \dots \tag{2-5}$$

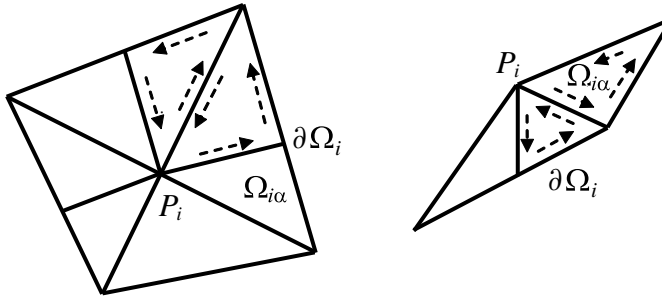


Figure 2. Neighbourhood Ω_i of the P_i points inside (left) and outside (right) of the mesh.

The above equations form a basis for solving the stationary equation of heat conduction with FEM. An important feature of this approach is that only an approximation of temperature function T in the $\Omega_{i\alpha}$ domain is sufficient for solving the equation, without differentiation of the T function approximation or other operations performed on derivatives of the function. The normal derivative of the T function at the boundary of the Ω domain is considered as an independent variable and determined from the boundary conditions. The solution of the Laplace equation in the $\Omega_{i\alpha}$ element is approximated by the function

$$T(P) = \sum_{i=1}^m T_i \cdot \varphi_{i\alpha}(P), \tag{2-6}$$

where the base functions $\varphi_{i\alpha}$ meet the condition

$$\varphi_{i\alpha}(P_j) = \begin{cases} 1, & i = j, \\ 0, & i \neq j. \end{cases} \tag{2-7}$$

The base functions $\varphi_{i\alpha}$ are formulated on the grounds of the observation that

$$\varphi_{PL}(x, y) = \frac{A_L x + B_L y + C_L}{A_L x_p + B_L y_p + C_L}, \tag{2-8}$$

where $A_L x + B_L y + C_L = 0$ is the equation of the straight line L and (x_p, y_p) are the coordinates of the point P (shown in Figure 3), satisfying the condition (2-7) and taking zero values at the line L .

The base functions $\varphi_{i\alpha}$ are products of the functions for various straight lines, (2-8), and the same point P ,

$$\varphi_{i\alpha}(x, y) = \varphi_{ij_1}(x, y) \cdot \varphi_{ij_2}(x, y), \tag{2-9}$$

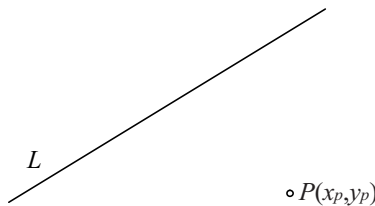


Figure 3. Element line and point for base function considerations.

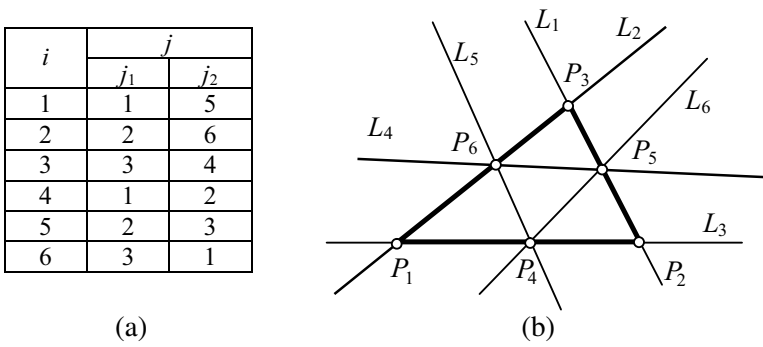


Figure 4. Relationships for base functions.

where the index i is related to the point P , while the indices j_1 and j_2 are related to the straight lines L .

Consideration of the 6-node triangular element of the mesh as shown in Figure 4b enables us to formulate the base function $\varphi_{i\alpha}$ given by Equation (2-9) for each of the nodes $P_i, i = 1, 2, \dots, 6$, where the indices j_1 and j_2 related to the straight lines L are defined in Figure 4. More universal formulation of this type of base functions is described in [Frąckowiak ≥ 2008].

The function $\varphi_{i\alpha}$ defined by (2-9) in the domain $\Omega_{i\alpha}$, apart from having the property (2-7), takes zero values at the sides of the mesh element including no point P . Based on this function let us define another function $\varphi_i(Q)$ continuous in $\Omega_i, \varphi_i(Q) = \varphi_{i\alpha}(Q)$, with $Q \in \Omega_{i\alpha}$ and $\alpha = 1, 2, \dots, n_i$. This definition gives evidence that the function $\varphi_i(Q)$ takes zero values at the boundary $\partial\Omega_i$ of the Ω_i element that bounds the neighborhood of the inner point P_i . When the point P_i is located at the outer boundary Γ , the $\varphi_i(Q)$ function is nonzero at the part of the boundary $\Gamma \cap \partial\Omega_i$.

The above property and the assumption of continuity of the function $\varphi_i(Q)$ in Ω_i provide a basis for solving the problem with FEM.

Substitution of an approximate solution (2-6) into (2-4) and (2-5) and the use of a linear approximation of the normal derivative between the nodes of the Γ boundary allow us to formulate a system of equations in the matrix form

$$\begin{aligned} A_{\Omega\Gamma} T_\Gamma + A_{\Omega\Omega} T_\Omega &= O, \\ A_{\Gamma\Gamma} T_\Gamma + A_{\Gamma\Omega} T_\Omega &= B_\Gamma Q_\Gamma. \end{aligned} \tag{2-10}$$

The number of nodes of the entire field is n . There are inner n_Ω and boundary n_Γ ($n = n_\Gamma + n_\Omega$) nodes. Determining the vector T_Ω from the first equation of (2-10), $T_\Omega = -A_{\Omega\Omega}^{-1} A_{\Omega\Gamma} T_\Gamma$, and substituting into the other, we obtain $(A_{\Gamma\Gamma} - A_{\Gamma\Omega} A_{\Omega\Omega}^{-1} A_{\Omega\Gamma}) T_\Gamma = B_\Gamma Q_\Gamma$. This expression is a relationship well known in the boundary element method,

$$AT_\Gamma = B_\Gamma Q_\Gamma. \tag{2-11}$$

3. Analytical solution of the inverse problem of heat conduction

The application of the new type of base functions will be illustrated using an analytical solution of an inverse problem for a circular ring (see Figure 5).

The ring has an outer radius $r_o = 1$ and an inner radius $r_i < r_o$. The inverse heat conduction problem may be formulated in dimensionless coordinates by giving the distributions of temperature and heat flow

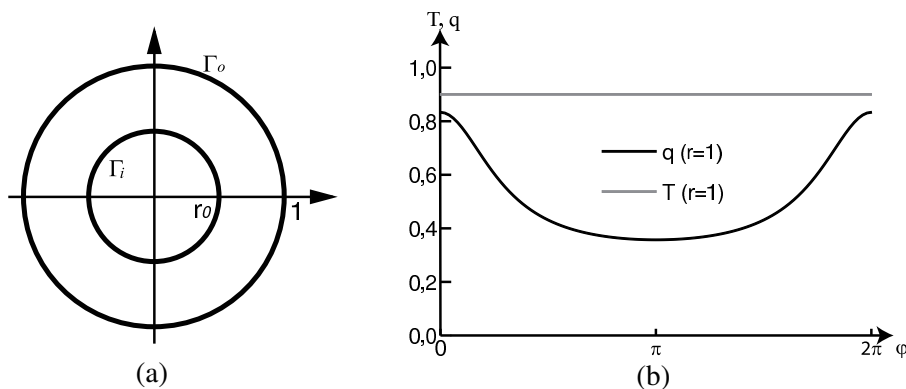


Figure 5. Temperature and heat flow density distributions at the outer boundary of the ring $C = 0.5, a = 0.4, T_c = 0.9, r_i = 0.5$.

density at the outer boundary of the ring [Wróblewska et al. 2008].

$$\Gamma_o : T_{wo} = T_c, \quad q_o = C \cdot \frac{1 - a \cos \varphi}{(1 + a^2 - 2a \cos \varphi)}, \quad a \leq r_i.$$

Moreover, the temperatures in the neighborhoods of the outer and inner boundaries, $T_o = 1$ and $T_i = 0$, are known. The objective is to determine the heat flow and temperature distributions at the inner surface of the ring.

Solution of such a problem is achieved by power series expansion of the q_o function determined at the outer ring boundary,

$$\begin{aligned} q_o &= C \cdot \frac{1 - a \cos \varphi}{(1 + a^2 - 2a \cos \varphi)} = C \cdot \operatorname{Re} \left(\frac{1}{1 - a e^{i\varphi}} \right) \\ &= C \cdot \operatorname{Re} \left(\sum_{m=0}^{\infty} (a \cdot e^{i\varphi})^m \right) = C \cdot \sum_{m=0}^{\infty} a^m \cos(m\varphi), \end{aligned}$$

and hence

$$T(r, \varphi) = T_c + C \cdot \ln(r) + C \cdot \sum_{m=1}^{\infty} \frac{1}{2m} \left[(ar)^m - \left(\frac{a}{r} \right)^m \right] \cos(m\varphi). \tag{3-1}$$

Based on the solution of the inverse problem (3-1) the temperature and heat flow density patterns at the outer boundary (see Figure 5) are determined, for which the inverse problem is to be solved. For the given temperatures outside T_o and inside T_i the ring distributions of normalized heat transfer coefficients with regard to the angle,

$$\Gamma_o : \alpha_o = \frac{q_o}{(T_o - T_{wo})}, \quad \Gamma_i : \alpha_i = \frac{q_i}{(T_i - T_{wi})},$$

are shown in Figure 6.

The vectors of temperatures and heat flow at the ring domain boundary, T_Γ and Q_Γ , that appear in the formula (2-11) are decomposed into the values related to the outer and inner ring boundaries, respectively,

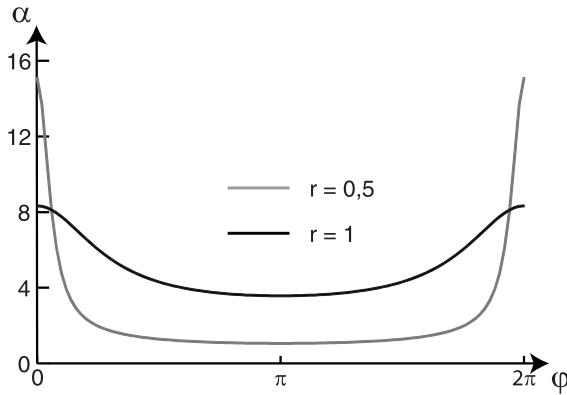


Figure 6. Distributions of heat transfer coefficients α at the inside and outside ring boundaries $C = 0.5, a = 0.4, T_c = 0.9, r_i = 0.5$.

as

$$T_\Gamma = \begin{bmatrix} T_{wo} \\ T_{wi} \end{bmatrix}, \quad Q_\Gamma = \begin{bmatrix} q_o \\ q_i \end{bmatrix}.$$

The relationship (2-11) is then transformed to obtain a solution of the inverse problem [Frąckowiak et al. 2006],

$$\begin{bmatrix} T_{wi} \\ q_i \end{bmatrix} = [-B_i \ A_i]^T [B_o \ -A_o] \begin{bmatrix} T_{wo} \\ q_o \end{bmatrix}. \tag{3-2}$$

This relationship may also be so transformed as to consider the third kind of boundary condition of the direct problem [Frąckowiak et al. 2006]

$$\begin{bmatrix} T_{wo} \\ T_{wi} \end{bmatrix} = [B_o + \alpha_o A_o \ B_i + \alpha_i A_i]^{-1} [\alpha_o A_o \ \alpha_i A_i] \begin{bmatrix} T_o \\ T_i \end{bmatrix}.$$

4. Results of the numerical calculation

The ring, shown in Figure 5, is divided into 450 triangular domains, see Figure 7, thus generating 200 points located at the ring boundary (100 at the inner one and 100 at the outer) and 700 inner points. The direct and inverse problems of ring cooling have been solved according to the method proposed in the present paper.

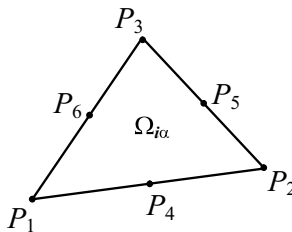


Figure 7. A mesh element.

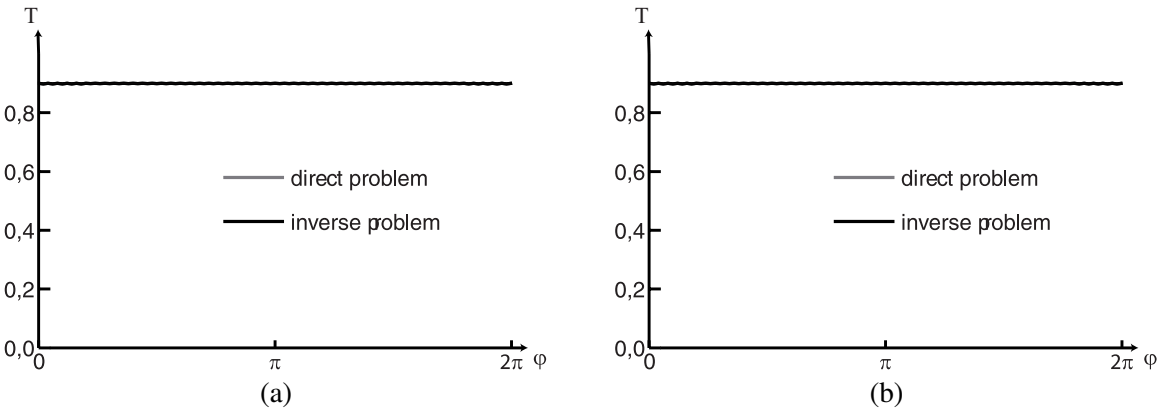


Figure 8. Temperature distribution at the outer (a) and inner (b) boundaries for the direct and inverse problems.

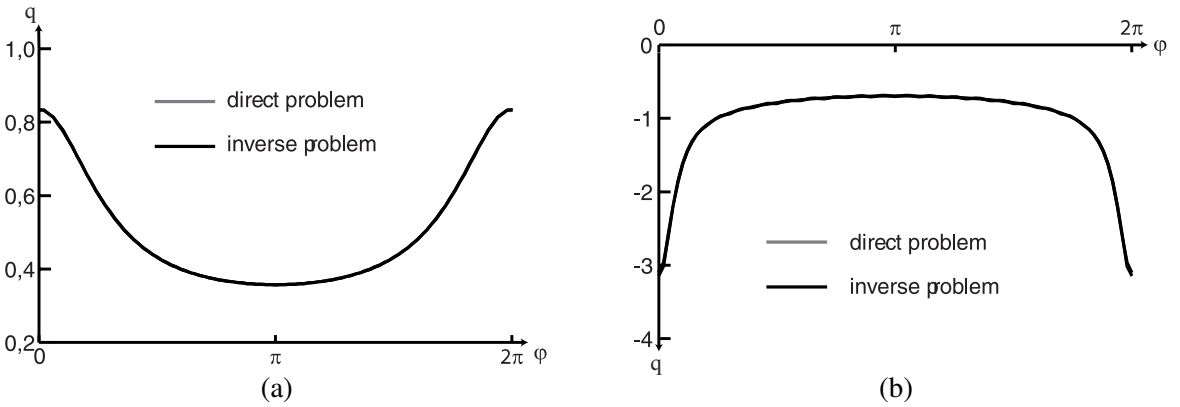


Figure 9. Heat flow density distribution at the outer (a) and inner (b) boundaries for the direct and inverse problems.

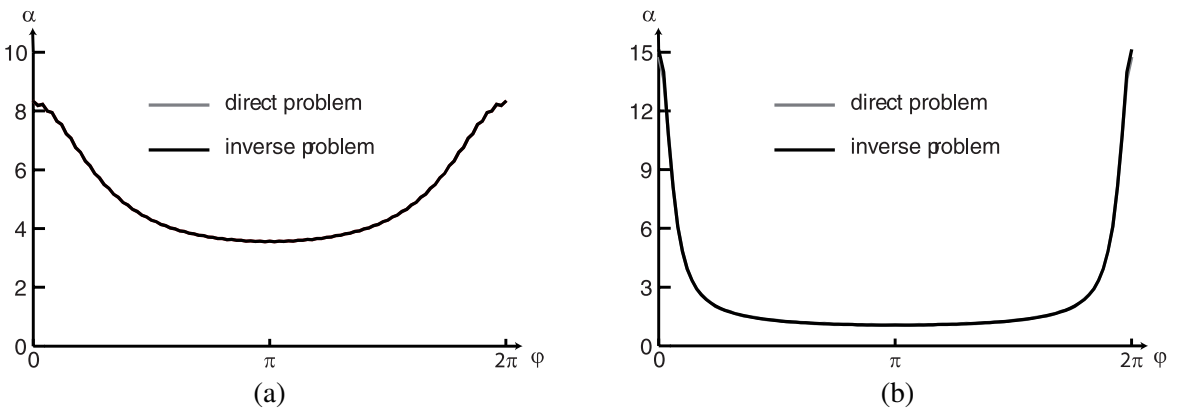


Figure 10. Normalized heat transfer coefficient α distributions at the outer (a) and inner (b) boundaries for the direct and inverse problems.

Type		Temperature error δL_{2T} [%]						
	m	f	$\epsilon_{max}=0$	$\epsilon_{max}=0.1$	$\epsilon_{max}=0.5$	$\epsilon_{max}=1$	$\epsilon_{max}=5$	$\epsilon_{max}=10$
The direct problem			0.03	0.03	0.03	0.04	0.15	0.35
The inverse problem, without smoothing	3		1.71	1.72	1.97	2.81	5.50	23.44
	5		0.16	8.29	49.73	53.14		
	8		0.05					
The inverse problem with smoothed boundary conditions	90	3	1.74	1.74	1.76	1.83	3.12	5.57
		5	0.32	4.32	29.54	51.00		
		8	0.35					
	50	3	1.74	1.74	1.75	1.81	2.47	4.55
		5	0.33	1.74	25.54	30.82		
		8	0.35					
	20	3	1.74	1.74	1.74	1.75	2.37	3.62
		5	0.33	1.81	5.33	14.41		
		8	0.38	1.95	6.19	12.98		
	4	3	2.77	2.77	2.76	2.77	2.88	3.50
		5	2.77	2.77	2.76	2.77	2.83	3.00
		8	2.77	2.77	2.77	2.77	2.85	2.79

Table 1. Relative error of temperature distribution at the ring boundary for various disturbances of the boundary conditions with the error ϵ_{max} [%], various f parameters of the SVD algorithm, and various numbers of base functions m for smoothing of boundary conditions.

The inverse matrix $[-B_i \ A_i]^T$ of the inverse problem has been computed with the SVD (singular value decomposition) algorithm with various values of the f parameter [Frackowiak et al. 2006]. Results of calculation of the direct and inverse problems, for example, the distributions of temperature, heat flow density, and surface film conductance at the inner and outer ring boundaries for undisturbed boundary conditions, and the parameter $f = 5$ (with the f parameter affecting only the inverse task), are shown in Figures 8–10.

Moreover, Tables 1 and 2 present relative errors of temperature and heat flow density at the ring boundaries with regard to the analytical solution given by the formula

$$\delta L_{2T} = \frac{\int_{\Gamma} (T - T_{analyt})^2 ds}{\int_{\Gamma} T_{analyt}^2 ds} \cdot 100\%, \quad \delta L_{2q} = \frac{\int_{\Gamma} (q - q_{analyt})^2 ds}{\int_{\Gamma} q_{analyt}^2 ds} \cdot 100\%. \tag{4-1}$$

The boundary conditions (temperature and heat flow density) in both cases have been disturbed with a relative error given by the formula

$$\epsilon = \epsilon_{max} \cdot (2 \cdot \text{random} - 1), \tag{4-2}$$

Type		Heat flow error δL_{2q} [%]						
	m	f	$\epsilon_{max}=0$	$\epsilon_{max}=0.1$	$\epsilon_{max}=0.5$	$\epsilon_{max}=1$	$\epsilon_{max}=5$	$\epsilon_{max}=10$
The direct problem			0.35	0.35	0.39	0.55	2.42	5.04
The inverse problem, without smoothing		3	18.01	18.04	18.79	21.60	27.68	
		5	3.80					
		8	0.66					
The inverse problem with smoothed boundary conditions	90	3	18.02	18.02	18.08	18.27	22.55	33.28
		5	3.86					
		8	13.47					
	50	3	18.02	18.02	18.05	18.22	20.35	28.91
		5	3.87	34.25				
		8	13.47					
	20	3	18.02	18.02	18.04	18.09	19.47	25.13
		5	3.87	38.05				
		8	13.83	40.52				
	4	3	22.60	22.60	22.61	22.61	23.00	24.88
		5	22.60	22.60	22.60	22.61	22.80	23.55
		8	26.22	26.22	26.22	26.22	26.35	26.26

Table 2. Relative error of heat flow density distribution at the ring boundary for various disturbances of the boundary conditions with the error ϵ_{max} [%], various f parameters of the SVD algorithm, and various numbers of base functions m for smoothing of boundary conditions.

where random is a pseudorandom number in the range (0, 1).

For the inverse problem and disturbed boundary conditions the task has been computed prior to solving it according to the formula (3-2), smoothing temperature and heat flow density at the outer boundary with a trigonometric polynomial [Wróblewska et al. 2008]. The error values (4-1) for various numbers of the trigonometric polynomials used for boundary condition smoothing are shown in Tables 1, 2 and Figures 11, 12.

5. Summary

The FEM method introduced in this paper consists of using base functions φ_i that take zero values at the boundary of the mesh node neighborhood, Figure 2, belonging to the domain Ω . Consequently, the function that approximates the solution of the differential equation in the element is not subject to differentiation.

The method presented in this paper, with disturbed boundary conditions, gave very good values of temperature and flow distributions at the ring boundaries, in the sense of the norm (4-1). In the case of temperature it was below 1%, while for the flow density it was below 14%, with the maximal level of boundary condition disturbance amounting to $\epsilon_{max} = 5\%$.

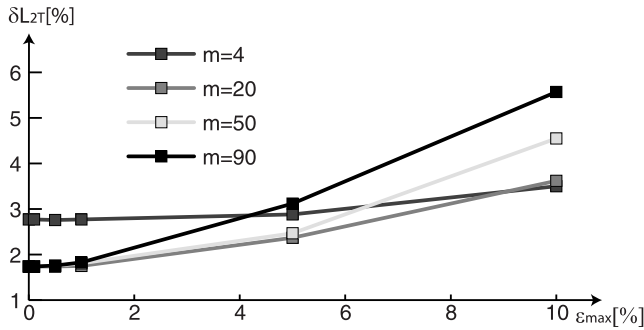


Figure 11. Dependence of relative error of temperature on maximal level of boundary condition disturbance for various numbers of the base functions smoothing the boundary conditions and the parameter $f = 3$.

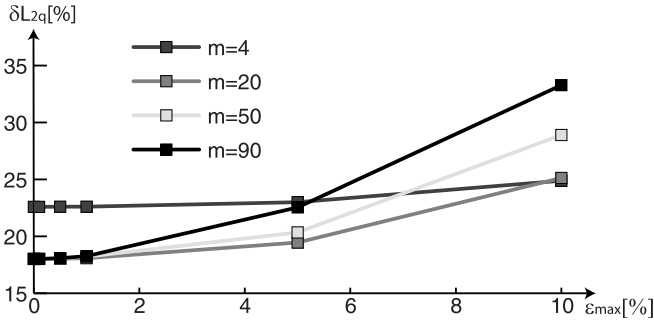


Figure 12. Dependence of relative error of heat flow density on maximal level of boundary condition disturbance for various numbers of the base functions smoothing the boundary conditions and the parameter $f = 3$.

In case of the inverse problem the best results, in the sense of the norm (4-1), have been obtained with the f parameter of the SVD algorithm equal to 3. For temperature it was below 2%, while for the heat flow density below 20%, with a maximal level of temperature and heat flow disturbance at the outer ring boundary amounting to $\epsilon_{max} = 0.5\%$. Smoothing of boundary conditions with the use of linear combination of trigonometric polynomials reduced the error of the norm (4-1). For the flow it dropped below 20% with $\epsilon_{max} = 5\%$ for $f = 3$ and 20 trigonometric functions. In case of higher values of the parameter $f \in (4, 8)$ good results have been achieved only with undisturbed boundary conditions. In case of 4 smoothing functions the error, in the sense of the norm (4-1), remained independent on the parameter f , amounting to less than 3% for the temperature and less than 23% for the flow.

References

[Frąckowiak ≥ 2008] A. Frąckowiak, *Base functions of the Finite Element Method and their properties*, To appear in *Zesz. Nauk. Politech. Poznań*.

[Frąckowiak et al. 2006] A. Frąckowiak, M. Ciałkowski, and J. von Wolfersdorf, "Numerical solution of a two-dimensional inverse heat transfer problem in gas turbine blade cooling", *Arch. Thermodyn.* **27**:4 (2006), 1–8.

[Gresho and Sani 2000] P. M. Gresho and R. L. Sani, *Incompressible flow and the finite element method*, Wiley, New York, 2000.

[Wróblewska et al. 2008] A. Wróblewska, M. Ciałkowski, and F. A., “Numerical solution of a direct and inverse stationary problem of heat transfer with a modified method of elementary balances”, *Arch. Thermodyn.* **29**:1 (2008), 3–18.

Received 7 Feb 2008. Revised 26 Mar 2008. Accepted 2 Apr 2008.

ANDRZEJ FRĄCKOWIAK: andrzej.frackowiak@put.poznan.pl
Poznań University of Technology, Piotrowo 3, 60-965 Poznań, Poland

JENS VON WOLFERSDORF: jens.vonwolfersdorf@itlr.uni-stuttgart.de
Universität Stuttgart, Institut für Thermodynamik der Luft- und Raumfahrt, Pfaffenwaldring 31, 70569 Stuttgart, Germany

MICHAŁ CIAŁKOWSKI: michal.cialkowski@put.poznan.pl
Poznań University of Technology, Piotrowo 3, 60-965 Poznań, Poland

DYNAMICS OF A ROPE AS A RIGID MULTIBODY SYSTEM

PAWEŁ FRITZKOWSKI AND HENRYK KAMINSKI

A preliminary discrete model of a rope is considered both as a scleronomic and a rheonomic system. Numerical experiments are performed and advantages of the applied algorithm are discussed on the basis of energy conservation. The problem of discretization of the rope is presented in terms of efficient computational simulations. A wave-like effect is discussed with regard to energy transfer and velocity of the model tip. The next directions of the model development are outlined.

1. Introduction

The dynamics of a rope may serve as an introduction to the problem of a cracking whip, which has been drawing the attention of scientists for over a hundred years. In the early twentieth century the hypothesis was advanced that the tip of the whip reaches supersonic speed at the crack time. Theoretical explanations of the phenomenon were supported later by numerous experiments, which in fact provided some surprising observations, for example the acceleration of the tip is up to 50000 g and its velocity is about twice the speed of sound in the air [Pierański and Tomaszewski 2005].

Theoretical and experimental works focus not only on the motion of the whip. The dynamics of similar bodies, such as chains and ropes, is analyzed too. However, the results of the experiments cannot be confirmed by any accurate analytical calculations because of the complexity of the problem, which may be approximately described with the use of a complicated system of differential equations. Nevertheless, in such difficult cases computational methods may be very useful.

The papers by Pierański and Tomaszewski [2004; 2005] were the key papers for us on the initial stage of our work. The authors analyze the fall of a chain using a discrete model of the body. Goriely and McMillen [2002] consider the propagation and acceleration of waves in the motion of whips. Their paper is also a kind of introduction to the problem with its history outline.

We concentrate on a simple model, which actually is a rigid, chain-like model and more similar to the rope than the whip. Therefore, it plays a role of a preliminary model only, whose properties will be modified in the future. Applying the Lagrange formulation, we present the equations of motion for such a system both for the scleronomic and the rheonomic one. With the use of numerical methods we obtain an approximate solution to the problem. In several experiments we simulate the behaviour of the given body and analyze it mostly with respect to time dependencies of velocity and acceleration of the system's tip. Also some algorithmic matters of the simulations are considered.

2. Mechanical system and equations of motion

Below we define a discrete model of the rope, also used by Pierański and Tomaszewski [2005]. However, for us this model is introductory as mentioned before. The discussion is made more general by including the rheonomic case.

Keywords: multibody dynamics, discrete model, differential-algebraic equations, energy conservation.

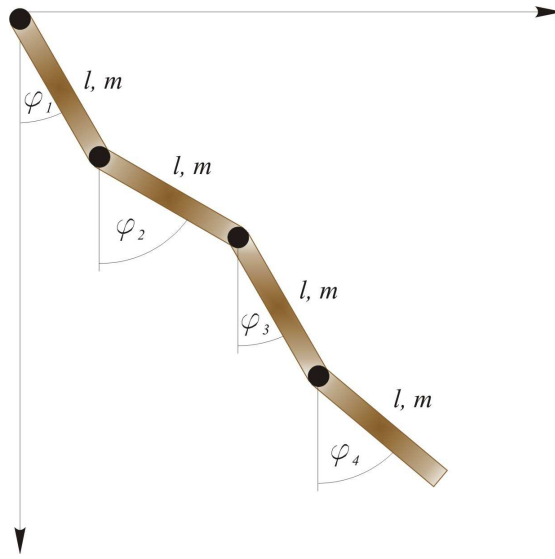


Figure 1. The simplest discrete model of the rope.

2A. A system with scleronomic constraints. Let us denote length of the rope by L and its mass by M . We divide the given body into n segments of length l and mass m each so that $L = nl$ and $M = nm$. They are connected by ideal joints (without friction). Assuming that every element is a rigid cylindrical rod as well, we obtain the simplest discrete model of the rope which actually is a multiple physical pendulum (Figure 1).

We focus on a special case of a mechanical system moving in a gravitational field with no external forces acting on it. One end of the rope is attached to a stationary point whereas the other end moves freely. Furthermore, let us assume that the motion is restricted to take place in a vertical plane only.

To specify the state of the system we introduce angular generalized coordinates. The position of the i th element is described by a variable φ_i which defines the angle from the Y downward axis. The position of each segment (its mass centre) in the Cartesian coordinate system may be written as follows

$$x_i = \sum_{j=1}^{i-1} l \sin \varphi_j + \frac{1}{2}l \sin \varphi_i, \quad y_i = \sum_{j=1}^{i-1} l \cos \varphi_j + \frac{1}{2}l \cos \varphi_i, \tag{2-1}$$

and the velocities of the i th segment in the X and Y directions are expressed by the formulas

$$v_{xi} = \sum_{j=1}^{i-1} \dot{\varphi}_j l \cos \varphi_j + \frac{1}{2} \dot{\varphi}_i l \cos \varphi_i, \quad v_{yi} = - \sum_{j=1}^{i-1} \dot{\varphi}_j l \sin \varphi_j - \frac{1}{2} \dot{\varphi}_i l \sin \varphi_i.$$

Now we can write the kinetic energy of the whole mechanical system according to König's theorem

$$T = \frac{1}{2}m \sum_{i=1}^n v_i^2 + \frac{1}{2}I \sum_{i=1}^n \dot{\varphi}_i^2,$$

where I is the moment of inertia of each element ($I = ml^2/12$). After some simplifications we obtain the kinetic energy in the following form

$$T = ml^2 \sum_{i=1}^n \frac{3(n-i)+1}{6} \dot{\varphi}_i^2 + ml^2 \sum_{i=1}^n \sum_{j=i+1}^n \frac{2(n-j)+1}{2} \dot{\varphi}_i \dot{\varphi}_j \cos(\varphi_i - \varphi_j).$$

The potential energy of the model is given by

$$V = -mgl \sum_{i=1}^n y_i = -mgl \sum_{i=1}^n \frac{2(n-i)+1}{2} \cos \varphi_i.$$

Using the terms above for the Lagrangian $L = T - V$ we can apply the Euler-Lagrange equations to describe behaviour of the system

$$\frac{d}{dt} \left(\frac{\partial L}{\partial \dot{\varphi}_i} \right) - \frac{\partial L}{\partial \varphi_i} = 0, \quad i = 1, 2, \dots, n. \tag{2-2}$$

After substitutions and simplifications we obtain the equations in the final form

$$\sum_{j=1}^n a_{ij} \ddot{\varphi}_j \cos(\varphi_i - \varphi_j) + \sum_{j=1}^n a_{ij} \dot{\varphi}_j^2 \sin(\varphi_i - \varphi_j) + \frac{g}{l} b_i \sin \varphi_i = 0, \quad i = 1, 2, \dots, n, \tag{2-3}$$

where

$$a_{ij} = \begin{cases} \frac{2(n-i)+1}{2}, & \text{for } j < i \\ \frac{3(n-i)+1}{3}, & \text{for } j = i \\ \frac{2(n-j)+1}{2}, & \text{for } j > i \end{cases} \quad \text{and} \quad b_i = \frac{2(n-i)+1}{2}. \tag{2-4}$$

To make it clearer, we present the equations of motion for $n = 3$:

$$\begin{aligned} a_{11} \ddot{\varphi}_1 \cos(\varphi_1 - \varphi_1) + a_{12} \ddot{\varphi}_2 \cos(\varphi_1 - \varphi_2) + a_{13} \ddot{\varphi}_3 \cos(\varphi_1 - \varphi_3) + a_{11} \dot{\varphi}_1^2 \sin(\varphi_1 - \varphi_1) \\ + a_{12} \dot{\varphi}_2^2 \sin(\varphi_1 - \varphi_2) + a_{13} \dot{\varphi}_3^2 \sin(\varphi_1 - \varphi_3) + (g/l) b_1 \sin \varphi_1 = 0, \\ a_{21} \ddot{\varphi}_1 \cos(\varphi_2 - \varphi_1) + a_{22} \ddot{\varphi}_2 \cos(\varphi_2 - \varphi_2) + a_{23} \ddot{\varphi}_3 \cos(\varphi_2 - \varphi_3) + a_{21} \dot{\varphi}_1^2 \sin(\varphi_2 - \varphi_1) \\ + a_{22} \dot{\varphi}_2^2 \sin(\varphi_2 - \varphi_2) + a_{23} \dot{\varphi}_3^2 \sin(\varphi_2 - \varphi_3) + (g/l) b_2 \sin \varphi_2 = 0, \\ a_{31} \ddot{\varphi}_1 \cos(\varphi_3 - \varphi_1) + a_{32} \ddot{\varphi}_2 \cos(\varphi_3 - \varphi_2) + a_{33} \ddot{\varphi}_3 \cos(\varphi_3 - \varphi_3) + a_{31} \dot{\varphi}_1^2 \sin(\varphi_3 - \varphi_1) \\ + a_{32} \dot{\varphi}_2^2 \sin(\varphi_3 - \varphi_2) + a_{33} \dot{\varphi}_3^2 \sin(\varphi_3 - \varphi_3) + (g/l) b_3 \sin \varphi_3 = 0. \end{aligned}$$

Having calculated all the coefficients according to (2-4) we obtain

$$\begin{aligned} \frac{7}{3} \ddot{\varphi}_1 + \frac{3}{2} \ddot{\varphi}_2 \cos(\varphi_1 - \varphi_2) + \frac{1}{2} \ddot{\varphi}_3 \cos(\varphi_1 - \varphi_3) + \frac{3}{2} \dot{\varphi}_2^2 \sin(\varphi_1 - \varphi_2) + \frac{1}{2} \dot{\varphi}_3^2 \sin(\varphi_1 - \varphi_3) + \frac{5}{2} (g/l) \sin \varphi_1 = 0, \\ \frac{3}{2} \ddot{\varphi}_1 \cos(\varphi_2 - \varphi_1) + \frac{4}{3} \ddot{\varphi}_2 + \frac{1}{2} \ddot{\varphi}_3 \cos(\varphi_2 - \varphi_3) + \frac{3}{2} \dot{\varphi}_1^2 \sin(\varphi_2 - \varphi_1) + \frac{1}{2} \dot{\varphi}_3^2 \sin(\varphi_2 - \varphi_3) + \frac{3}{2} (g/l) \sin \varphi_2 = 0, \\ \frac{1}{2} \ddot{\varphi}_1 \cos(\varphi_3 - \varphi_1) + \frac{1}{2} \ddot{\varphi}_2 \cos(\varphi_3 - \varphi_2) + \frac{1}{3} \ddot{\varphi}_3 + \frac{1}{2} \dot{\varphi}_1^2 \sin(\varphi_3 - \varphi_1) + \frac{1}{2} \dot{\varphi}_2^2 \sin(\varphi_3 - \varphi_2) + \frac{1}{2} (g/l) \sin \varphi_3 = 0. \end{aligned}$$

2B. A system with rheonomic constraints. Now let us assume that one end of the rope is attached to a moving support, whose position expressed in the Cartesian coordinates depends explicitly on time

$$x_0 = x_0(t) \quad \text{and} \quad y_0 = y_0(t).$$

The dependencies cause some modifications of the terms (2-1)

$$x_i = x_0 + \sum_{j=1}^{i-1} l \sin \varphi_j + \frac{1}{2}l \sin \varphi_i \quad \text{and} \quad y_i = y_0 + \sum_{j=1}^{i-1} l \cos \varphi_j + \frac{1}{2}l \cos \varphi_i. \quad (2-5)$$

Hence, the terms for the kinetic and the potential energy of the system have a more complex form:

$$T = ml^2 \sum_{i=1}^n \frac{3(n-i)+1}{6} \dot{\varphi}_i^2 + ml^2 \sum_{i=1}^n \sum_{j=i+1}^n \frac{2(n-j)+1}{2} \dot{\varphi}_i \dot{\varphi}_j \cos(\varphi_i - \varphi_j) \\ + \frac{1}{2}mn(\dot{x}_0 + \dot{y}_0)^2 + ml \sum_{i=1}^n \frac{2(n-i)+1}{2} \dot{\varphi}_i (\dot{x}_0 \cos \varphi_i - \dot{y}_0 \sin \varphi_i), \\ V = -mg \sum_{i=1}^n \left(\frac{2(n-i)+1}{2} l \cos \varphi_i + y_0 \right).$$

Still using the general form of the dynamic equations (2-2), one may obtain their final form as follows:

$$\sum_{j=1}^n a_{ij} \ddot{\varphi}_j \cos(\varphi_i - \varphi_j) + \sum_{j=1}^n a_{ij} \dot{\varphi}_j^2 \sin(\varphi_i - \varphi_j) + b_i \frac{1}{l} (g \sin \varphi_i + \ddot{x}_0 \cos \varphi_i - \ddot{y}_0 \sin \varphi_i) = 0, \quad (2-6)$$

where $i = 1, 2, \dots, n$ and the coefficients a and b are defined in (2-4).

It is important to remark that the described mechanical system is not a conservative one as its Lagrangian contains explicit time dependence because the transformation equations (2-5) involve the time explicitly.

3. Numerical experiments

The complexity of the presented dynamic equations and tending towards maximum possible number n of the model elements requires applying numerical methods to obtain an approximate solution to the problem.

In our analysis we have applied the MEBDFV code developed by Abdulla and Cash of Imperial College, London (Department of Mathematics). They implemented the modified extended backward differentiation formulas (MEBDF) of Cash. The algorithm is designed to solve stiff initial value problems for systems of linearly implicit differential algebraic equations (DAEs) of the form

$$\mathbf{M}(\mathbf{q})\dot{\mathbf{q}} = \mathbf{f}(t, \mathbf{q}), \quad (3-1)$$

where the matrix \mathbf{M} depends on \mathbf{q} , which is a vector of dependent variables, and t is the independent variable.

As is typical for computational methods, the system of dynamic equations should be reformulated as a system of first-order differential equations. Such a set of $2n$ equations is presented below in matrix form with initial conditions

$$\begin{bmatrix} 1 & 0 & \dots & 0 & 0 & 0 & \dots & 0 \\ 0 & 1 & \dots & 0 & 0 & 0 & \dots & 0 \\ \vdots & \vdots & \ddots & \vdots & \vdots & \vdots & \ddots & \vdots \\ 0 & 0 & \dots & 1 & 0 & 0 & \dots & 0 \\ 0 & 0 & \dots & 0 & m_{11} & m_{12} & \dots & m_{1n} \\ 0 & 0 & \dots & 0 & m_{21} & m_{22} & \dots & m_{2n} \\ \vdots & \vdots & \ddots & \vdots & \vdots & \vdots & \ddots & 0 \\ 0 & 0 & 0 & 0 & m_{n1} & m_{n2} & \dots & m_{nn} \end{bmatrix} \begin{bmatrix} \dot{\varphi}_1 \\ \dot{\varphi}_2 \\ \vdots \\ \dot{\varphi}_n \\ \dot{\omega}_1 \\ \dot{\omega}_2 \\ \vdots \\ \dot{\omega}_n \end{bmatrix} = \begin{bmatrix} \omega_1 \\ \omega_2 \\ \vdots \\ \omega_n \\ f_1 \\ f_2 \\ \vdots \\ f_n \end{bmatrix}, \tag{3-2}$$

$$\varphi_i(t_0) = \varphi_{i0}, \quad \omega_i(t_0) = \omega_{i0}, \quad i = 1, 2, \dots, n.$$

The elements m_{ij} of the matrix \mathbf{M} depend on the generalized coordinates $m_{ij} = a_{ij} \cos(\varphi_i - \varphi_j)$ with $i, j = 1, 2, \dots, n$, and the components f_i of the right-hand side vector are functions of the generalized coordinates as well as the generalized velocities

$$f_i = - \sum_{j=1}^n a_{ij} \omega_j^2 \sin(\varphi_i - \varphi_j) - b_i \frac{g}{l} \sin \varphi_i, \quad i = 1, 2, \dots, n.$$

For the rheonomic system, the terms for f_i contain the time as an explicit variable:

$$f_i = - \sum_{j=1}^n a_{ij} \omega_j^2 \sin(\varphi_i - \varphi_j) - b_i \frac{1}{l} (g \sin \varphi_i + \ddot{x}_0 \cos \varphi_i - \ddot{y}_0 \sin \varphi_i), \quad i = 1, 2, \dots, n.$$

In general, the applied solver carries out integration in three stages. Firstly, a solution at the current point is predicted and the Newton iterations are performed to improve the values. The next stage uses them to approximate a solution at the next point where the Newton scheme is applied again. The prediction process in the two phases involves the backward finite differences. The last stage plays a role of a corrector and is based on the Newton method again. The same Jacobian matrix is used in the iterations for all the three stages. Moreover, the code includes some strategy to reduce a number of the Jacobian evaluations. For more details on the usage of the modified backward differentiation formulas the reader is referred to Cash and Considine [1992].

First, we deal with the scleronomic system and discuss the simulations mostly from the algorithmic point of view. More physical aspects are taken into account when it comes to the rheonomic constraints. However, we focus only on the function $x_0(t)$ referring to the horizontal direction. All the simulations are performed for the model of total length $nl = 1$ m and total mass $nm = 0.5$ kg. Additionally, zero generalized velocities are assumed at a start point $\dot{\varphi}_i(0) = 0$ for $i = 1, 2, \dots, n$.

Experiment 1. We decided to confront results obtained in our numerical simulations with the results described in Pierański and Tomaszewski [2005] and based on the RADAU5 code developed by Hairer and Wanner. After performing the simulations for the scleronomic system with the same parameters (n, L, M) and initial conditions, we analyzed configurations of the chain. As expected, there was no difference between the compared shapes of the multibody model in certain moments of time, and the time dependencies of the linear velocity of the tip were compatible too.

However, it was impossible to make a comparison between the results of motion in any longer time interval. Pierański and Tomaszewski focused on very short initial phases of the chain fall (from $t = 0.0$ to $t = 0.6$ s) which included the most interesting process namely the evolution of a sharp peak in the

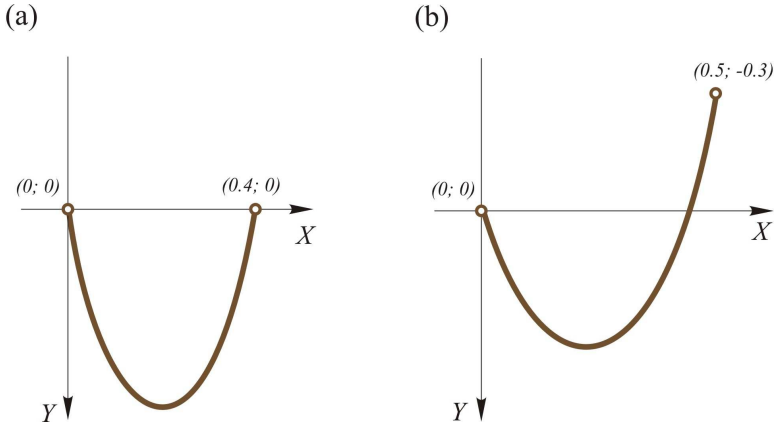


Figure 2. Initial configurations of the mechanical system. Left: Experiment 1; right: Experiment 2.

velocity time dependence of the tip. But even if they dealt with the farther stages, the agreement between the results could be not so good.

Actually, we applied the RADAU5 on the initial stage of our work. Aiming at simulations of the complex model motion in general (not only in a short time), we began to use the MEBDFV code. This was due to the character of the RADAU5, which is a solver for systems of DAEs with a constant matrix \mathbf{M} . A consequence of this is a problem with energy conservation of the model after a short period of good performance. Although one may update the matrix \mathbf{M} frequently, the results do not meet the energy conservation law. All in all, using the RADAU5 code without any significant modifications seems to be inefficient when researching long-lasting motion of such a complex mechanical system.

To show the difference, we performed a numerical experiment using both codes, with the same initial conditions for a catenary curve (Figure 2a) and the same parameters $n = 20$, $M = 0.5 \text{ kg}$, and $L = 1 \text{ m}$.

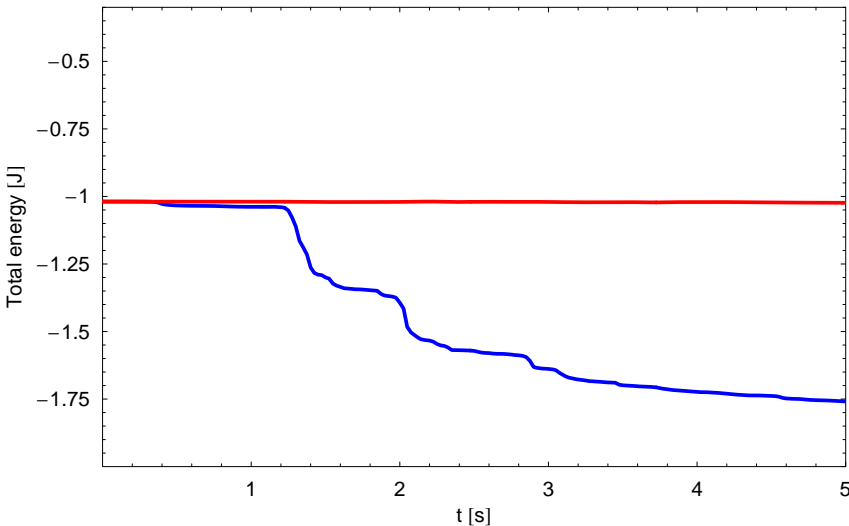


Figure 3. The total energy based on results from RADAU5 (blue) and MEBDFV (red).

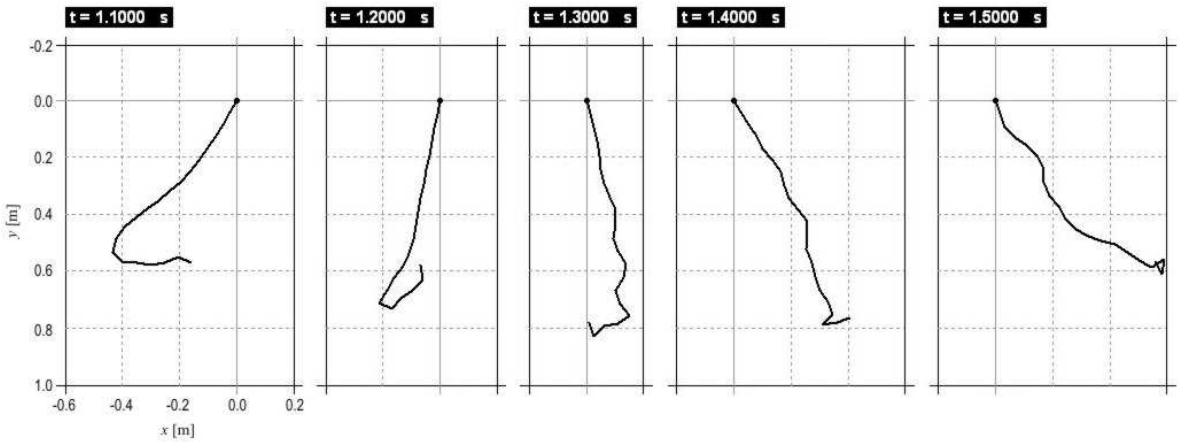


Figure 4. Configurations of the chain found in the numerical experiment with the use of the RADAU5.

Let us concentrate on the time dependence of the total energy of the model and its shape during the motion. According to Figure 3, the results obtained with the use of the RADAU5 show a rapid decrease in the energy around $t = 1.3 \text{ s}$. On the other hand, the red line illustrates the quantity given by the computation based on the other code—dependency with some small fluctuations (constant in the numerical sense). It may serve as the reference level for the former function. The difference between them increases with time and we can clearly see that the results provided by the solver RADAU5 do not meet the energy conservation law.

It is necessary to remark that no procedure designed for testing fulfillment of the conservation principle is embedded in the solvers. Both codes perform the integration process using some internal, numerical convergence tests, which do not refer to mechanics. The user supplies the physical meaning of the solution and involves it in the computation of such quantities as the total energy.

How do the energy losses affect the configurations of the chain? Are there any significant differences between the results again? To answer these questions we compare the configurations related to the RADAU5 code (Figure 4) and the MEBDFV code (Figure 5).

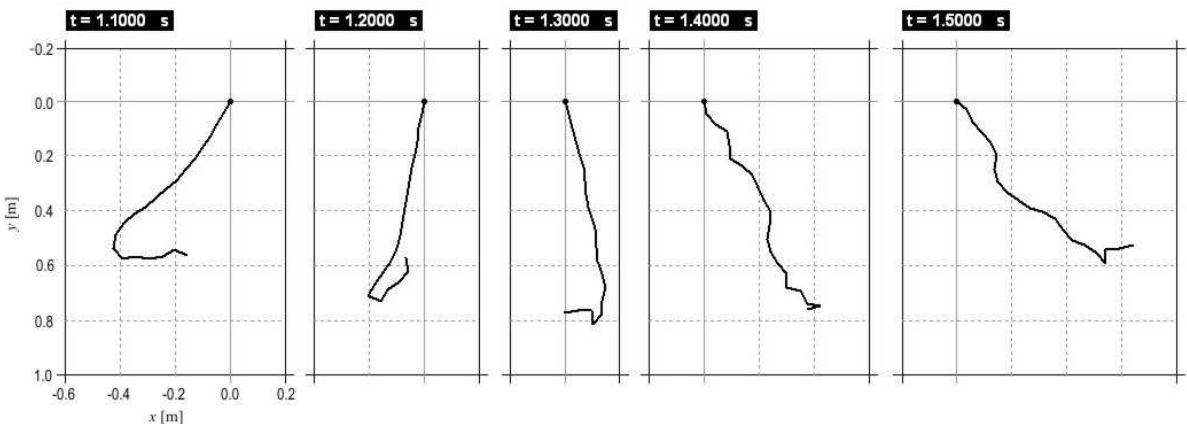


Figure 5. Configurations of the chain found in the numerical experiment with the use of the MEBDFV.

Although not all of the preceding configurations are presented, the shapes of the chain up to $t = 1.2$ s are compatible. Some differences appear at point $t = 1.3$ s and they intensify in time similarly to the ones between the energy dependencies. In general, the shapes of the first chain seems to be smoother, especially in the end phase of the experiment. In the second case, the constant total energy keeps the system going to a chaotic motion, which seems to be obvious when considering such a stiff multibody system. Therefore, the configurations of the latter chain become less and less ordered.

In the present work we do not deal with the theory of chaos and its application to dynamics of the chain, but we feel that this is an area which is worth further attention.

Experiment 2. Let us turn now to the problem of discretization of the rope. The question is how to match the number of the elements of the system to make our simulations efficient?

First, the model should reflect the real body with its physical features. Here we apply the discrete model (convenient in an algorithmic approach), which is to approximate the rope treated as continuum. Theoretically, reaching the idea of continuum is realized when n tends to infinity (and l tends to zero). In practice, it is possible and sufficient to choose some reasonably large number n .

However, it must be remembered that n defines a number of degrees of freedom, and thus the number of Lagrange-Euler equations of motion. In addition, from the numerical point of view the number is doubled when reformulating the system of equations as in (3-2). Thus, the number of the model elements affects the computation time considerably.

In the following experiment we do not specify any optimum. All we do is comparing configurations of the rope in simulations starting from the same initial conditions but from various n . Let us consider three cases: $n = 30$, $n = 45$, and $n = 70$, with the same parameters $M = 0.5$ kg, $L = 1$ m, and the simulation time $t = 2.5$ s. Initial configuration has the shape of a catenary curve (Figure 2b).

It is important to note that we omit the configuration of the rope at $t = 0.5$ s, because the first phase of the motion for different number of segments n looks quite similar. We may say that the numerical integration of the dynamic equations related strictly to a fall of the chain proceeds without any serious problems. Some troubles appear in the next phase of motion, especially when the mechanical system tends to the chaotic-like behaviour. Usually the solver manages to go through the difficulties (it depends on the initial conditions) but it makes the computation time much longer.

First, we compare the shapes of the chain for $n = 30$ and $n = 45$ (Figure 6 and Figure 7). The two initial configurations seem roughly identical. However, there is a small difference. The free end of the model is located slightly lower in the second case (Figure 9). The reason of this is due to the

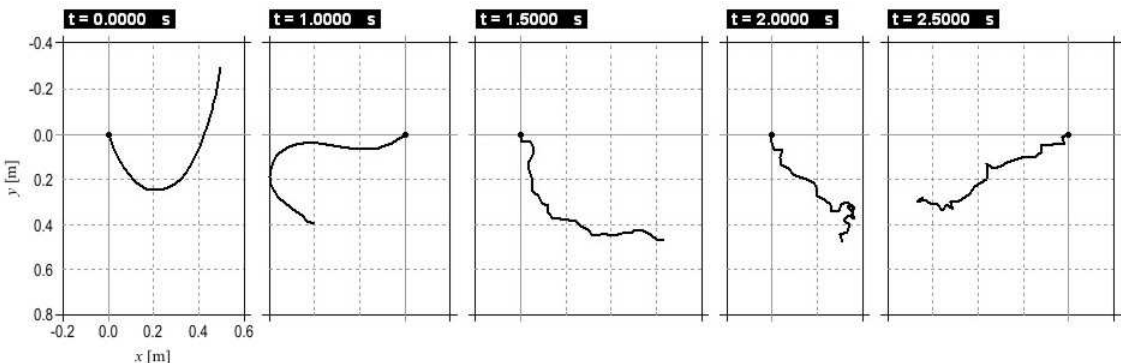


Figure 6. Configurations of the system consisting of $n = 30$ segments.

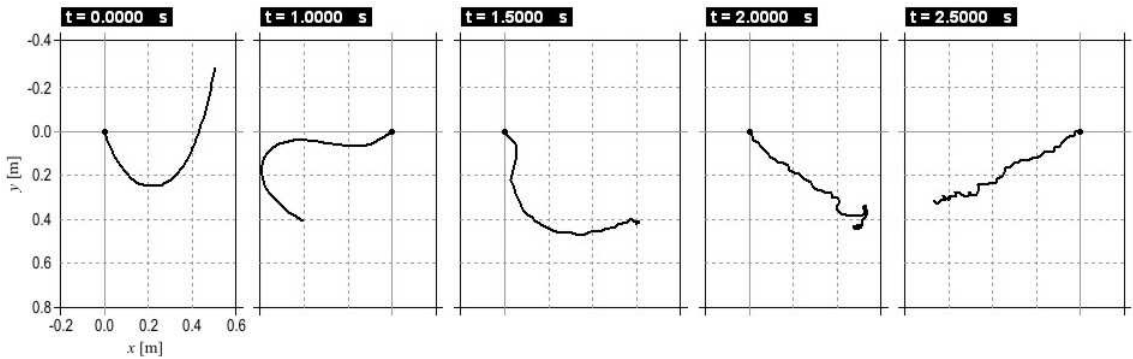


Figure 7. Configurations of the system consisting of $n = 45$ segments.

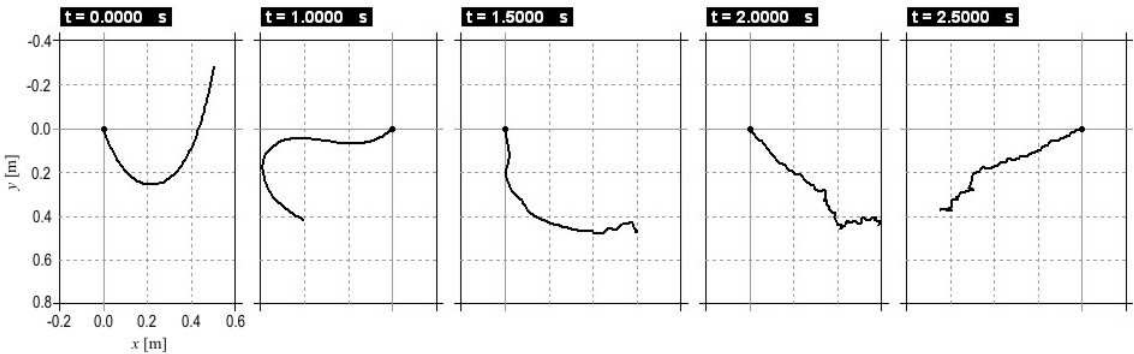


Figure 8. Configurations of the system consisting of $n = 70$ segments.

discretization of the catenary which is hard to do without some small deviations. Nevertheless, it causes no noticeable differences at least for 1 s of the motion (the fall of the folded chain). We can see such differences from the third presented instant ($t = 1.5$ s). As mentioned before, the end phase of the motion is chaotic-like. Therefore, the existing incompatibilities may be the effects of the discretization of the material continuum and/or slightly different initial conditions. The latter ones, in the chaotic dynamics, can produce even a completely new solution at later times.

Comparing the configurations for $n = 45$ and $n = 70$ (Figure 7 and Figure 8), we notice some differences at $t = 1.5$ s again. However, they do not seem so evident. More significant ones are present in the next instant that is shown, and the last configurations differ from each other slightly.

To make our considerations more exact, we present the time dependence of the y -position of the models' tip (Figure 9). It should be emphasized that the dependence cannot be treated as a full measure of the quality of the solutions and their compatibility, since it refers just to one of the body's member (its free end). In addition, we have taken into account the Y direction only.

Obviously, the solutions to the problem for models with identical parameters but various numbers of segments n are more compatible for larger n . However, the number n does not have to tend to very large values. For example, if we presented results for $n = 50$ and compared them with the ones for $n = 70$, no significant difference would be noticed. All in all, attempts to specify some reasonable limits of the discretization merit careful consideration.

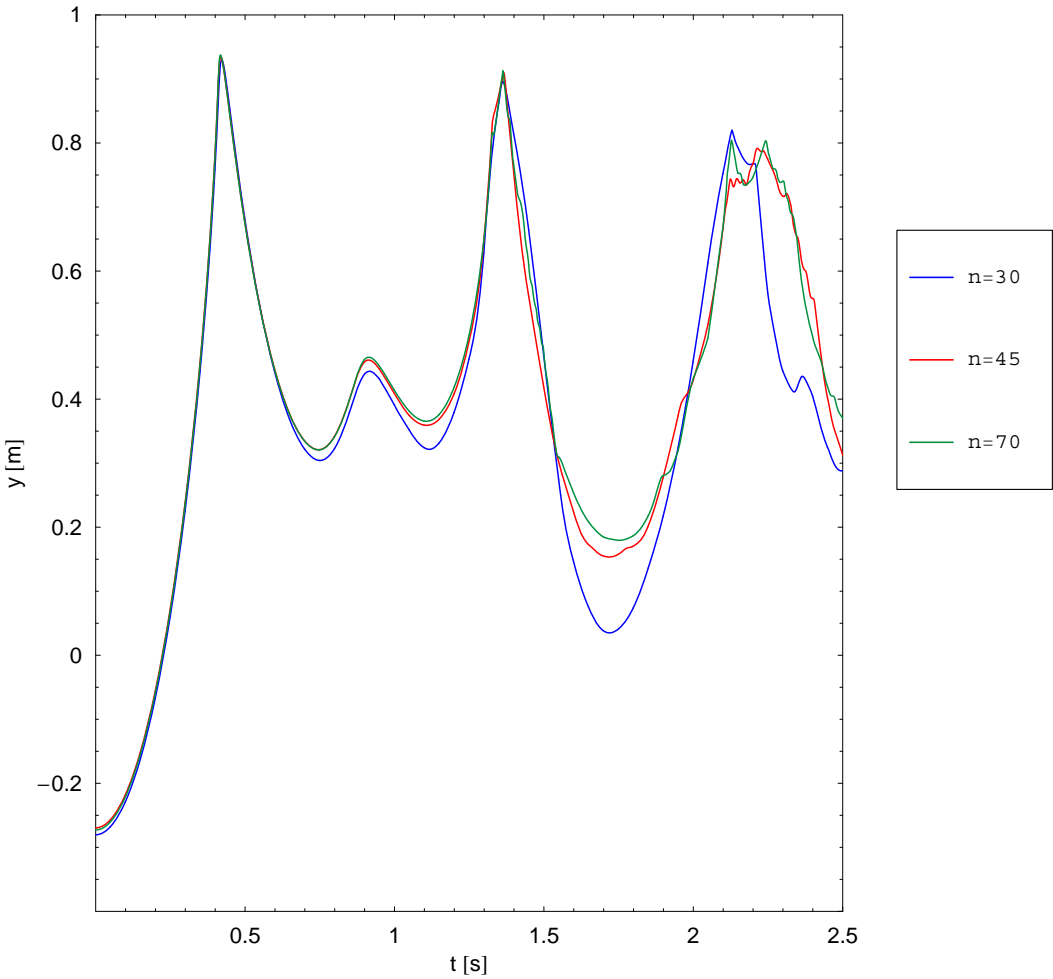


Figure 9. The y -positions of the chain tip for different number of segments.

Experiment 3. Now we turn to the rheonomic case and consider a free-hanging chain where the system resting at full extension so that $\varphi_i(0) = 0$ for $i = 1, 2, \dots, n$. The body will be brought into motion with the use of the following constraint function

$$x_0(t) = A \sin^2(\pi B t), \tag{3-3}$$

where A and B are some constants. Here we take $A = 0.1$ [m] and $B = 5$ [1/s]. Actually, the attachment point is subjected to an oscillatory motion (Figure 10) with an amplitude A . We carry out simulations for two cases, $n = 30$ and $n = 50$, which differ in the number of degrees of freedom.

Let us start the analysis with the time dependencies of the velocity and acceleration at the free end of the system consisting of $n = 30$ segments. As presented in Figure 11, the significant amount of oscillations of the support produces numerous peaks in the tip velocity. However, the velocity increases slowly at the beginning and the first sharp peak occurs when the support velocity reaches its maximal value. The next peaks do not seem to be compatible with the v_{x0} function, since the wave-like effects of the rheonomic constraints overlap in time and influence the tip motion with some delays.

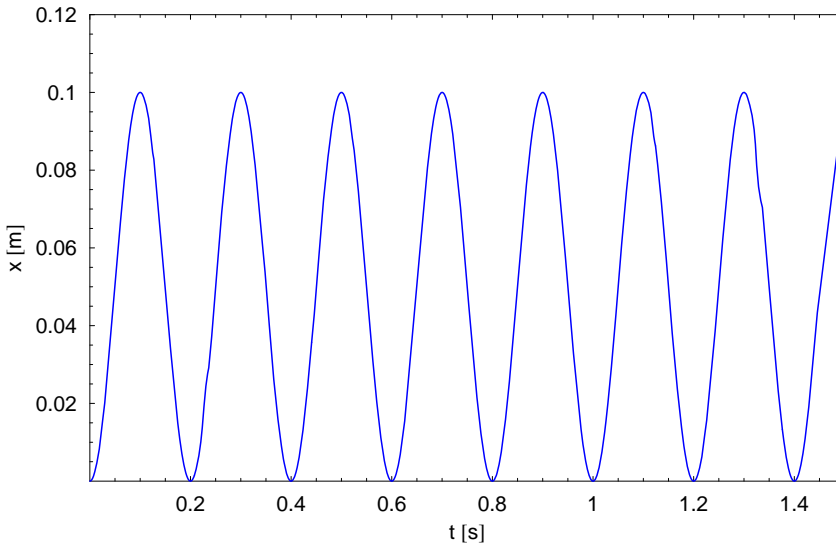


Figure 10. Constraint function $x_0(t)$.

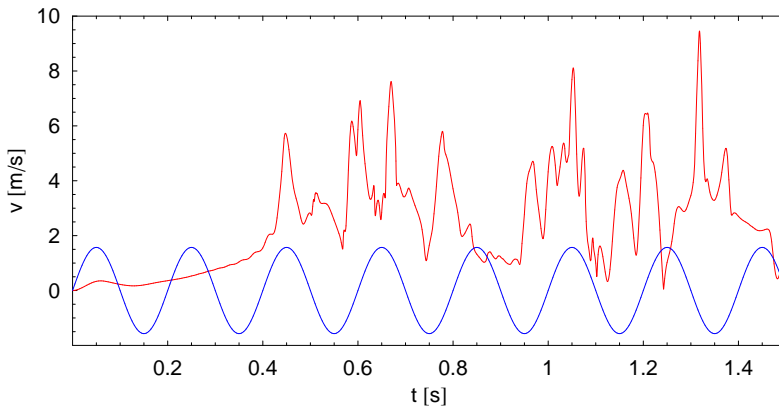


Figure 11. Velocity of the tip (red) and the function v_{x0} (blue) for $n = 30$.

Sharper peaks are visible in the acceleration dependency (Figure 12). They relate mostly to the maxima of velocity. An important conclusion arises from the graphs. Applying a very simple constraint function results in obtaining large values of the acceleration of the tip. For example, at time $t = 0.68$ s the acceleration exceeds $500 g$.

To make the behaviour of the system more imaginable, we show particular phases of motion in Figure 13. It is easy to note that initially the free end of the chain moves upwards only. After four changes of direction of the support motion, in the time range $t = 0.4$ – 0.5 s the tip is pulled horizontally and its acceleration goes up suddenly. Obviously, there is a simultaneous increase in the velocity. The next phases are distinguished by growing disorder. In addition, just the tip seems to be a sort of origin of these effects. However, the details are considered later.

When it comes to the case with $n = 50$ elements, the evolution of the rope motion looks quite similar. Nevertheless, the velocity and acceleration dependencies (Figure 14 and Figure 15) show more peaks

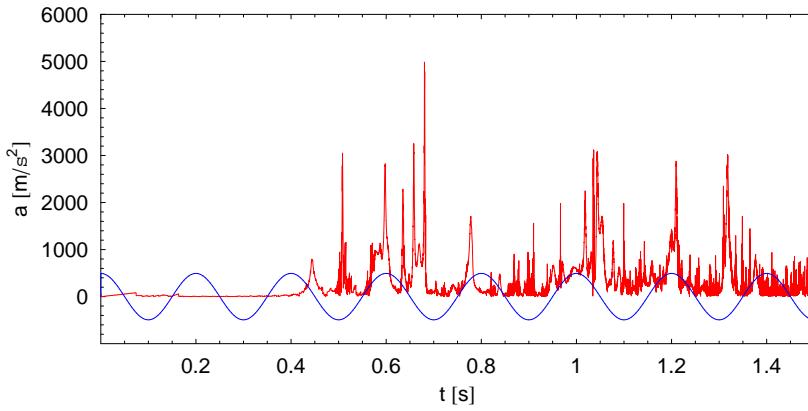


Figure 12. Acceleration of the tip (red) and the function a_{x0} times 10 (blue) for $n = 30$.

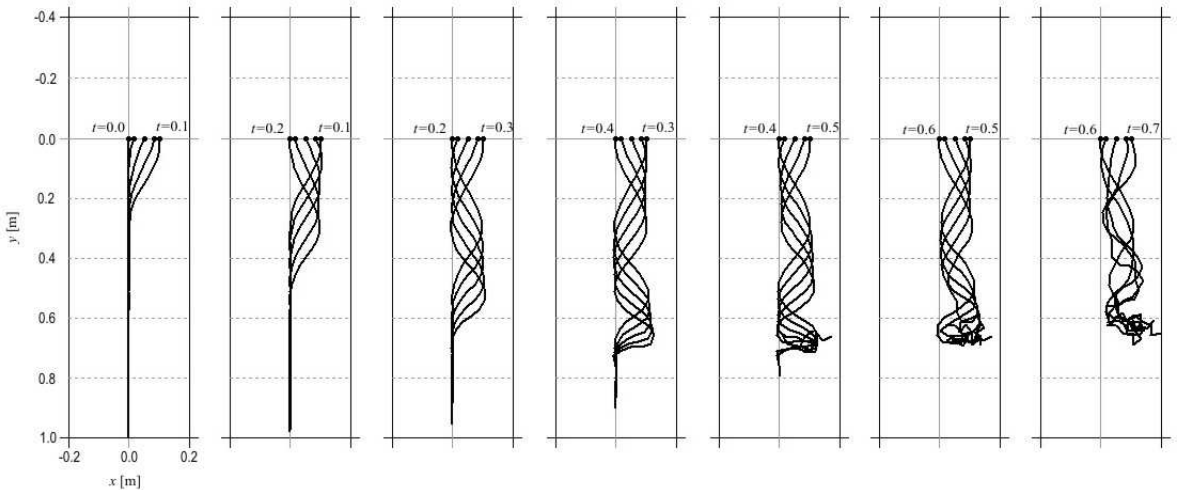


Figure 13. Configurations of the chain in consecutive phases of motion for $n = 30$. The time is given in seconds.

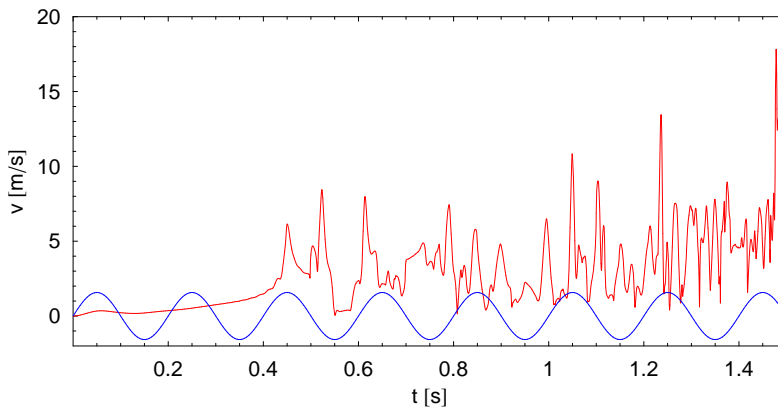


Figure 14. Velocity of the tip (red) and the function v_{x0} (blue) for $n = 50$.

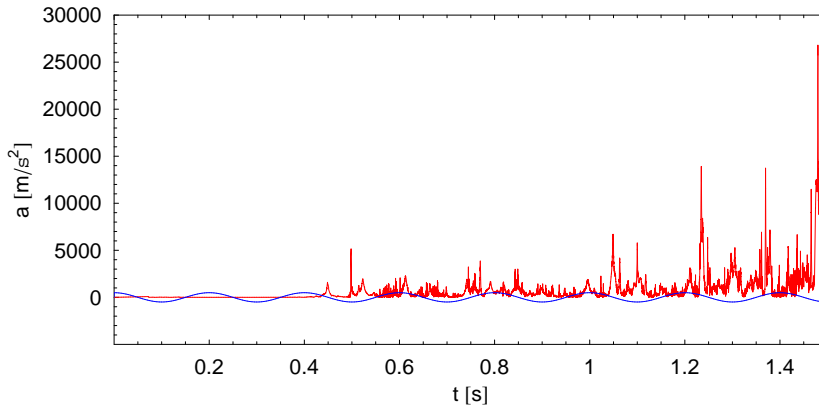


Figure 15. Acceleration of the tip (red) and the function a_{x0} multiplied by 10 (blue) for $n = 50$.

than before. The sharpest one occurs at the end of the simulation time in the chaotic-like phase. It should be remarked that the acceleration of the tip exceeds $2500 g$ at this time.

Compared with the previous case, the configurations (Figure 16) are compatible during the ordered motion. Afterwards some differences appear (see $t = 0.5\text{--}0.7$ s) and the degree of compatibility depends mainly on the difference between the number of segments in the two cases. This matter corresponds to the problem of discretization which we outlined in Experiment 2.

As mentioned, we expect the mechanical system to be nonconservative. Due to periodicity of the constraint function (3-3), energy is provided to the system all the time, except the moments when the support velocity v_{x0} equals zero. A graph of the total energy obtained from the approximate solution is presented in Figure 17. The irregular fluctuations on the advanced stage of motion have a numerical source, which may be also a result of the mechanical disorder.

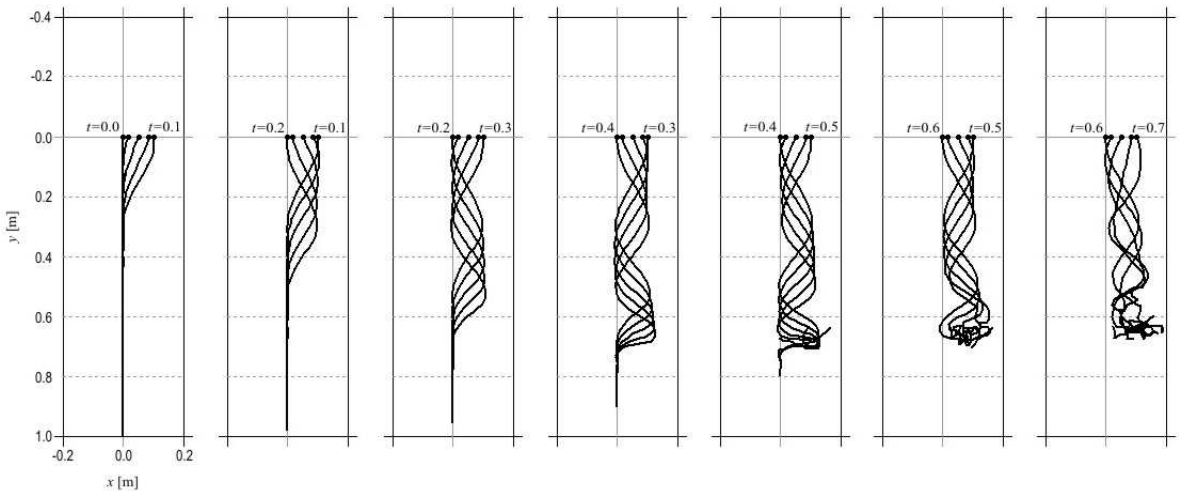


Figure 16. Configurations of the chain in consecutive phases of motion for $n = 50$. The time is given in seconds.

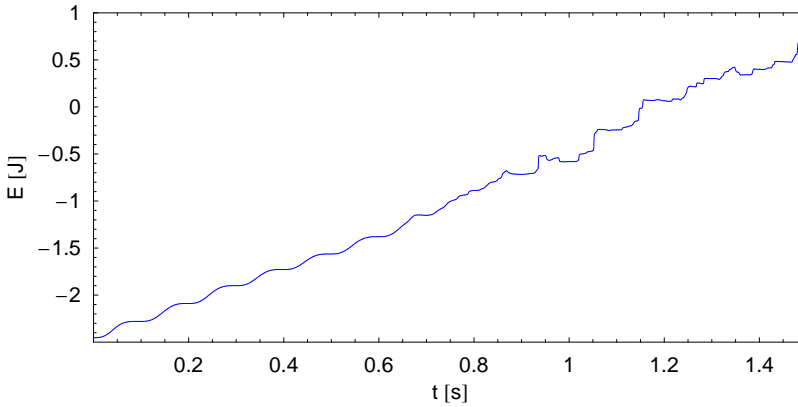


Figure 17. Total energy of the system with $n = 50$ segments.

Experiment 4. This experiment is very similar to the previous one. However, here we wish to show some effects clearer. To do so, let us apply slightly different constraint function

$$x_0(t) = \begin{cases} A \sin^2(\pi B t) & \text{for } t \leq 1/B, \\ 0 & \text{for } t > 1/B, \end{cases}$$

where A and B remain the same, that is, $A = 0.1$ [m] and $B = 5$ [1/s]. In fact, there will be only one period in the support motion, after which its position will be stationary. The function is presented in Figure 21. The initial configuration of the mechanical system is the same too $\varphi_i(0) = 0$ for $i = 1, 2, \dots, n$. The number of degrees of freedom n is equal to 30.

In this case we begin our considerations with the chain’s shape during the evolution. The two initial phases of motion (Figure 18) are identical with the ones from the Experiment 3. A considerable difference arises at the end of the support motion. A fold created from the upper part of the system is traveling along the rope and raising the tip gradually. After the downward propagation the last segments of the body rotate (the simple construction of the model allows them to do so) and a new fold is formed which

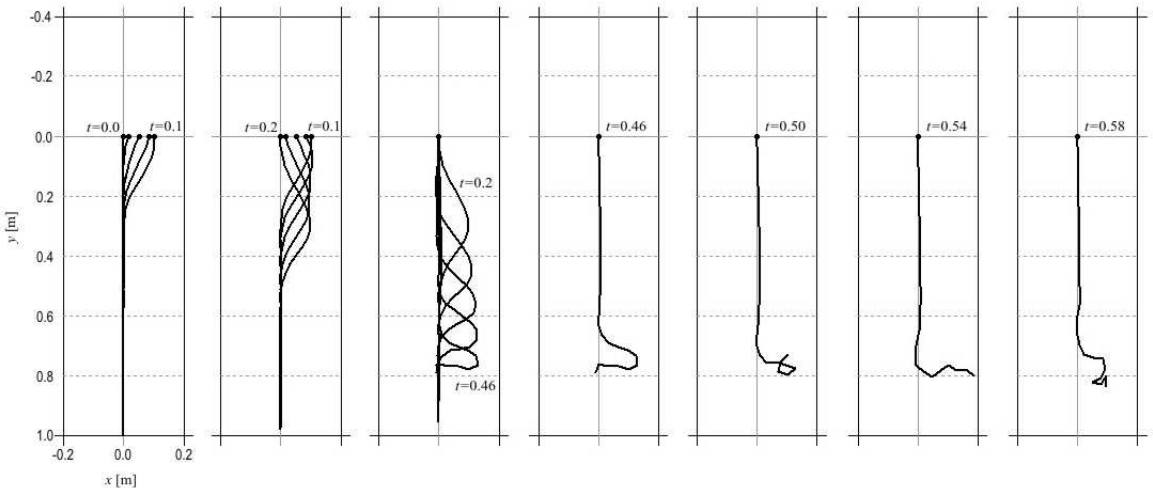


Figure 18. Downward travel of the fold (Experiment 4). Time given in seconds.

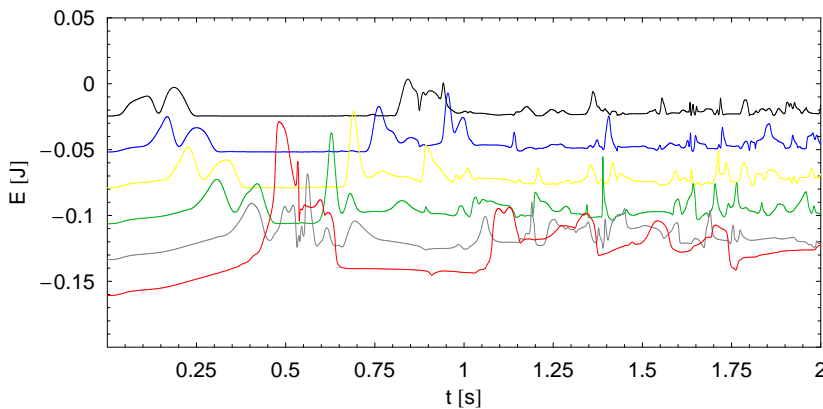


Figure 19. Total energy of the segments: 5 (black), 10 (blue), 15 (yellow), 20 (green), 25 (grey), 30 (red).

tends to go up ($t = 0.6$ s). The upward travel is not so evident but the fold disappears completely just after the next direction change ($t = 1.1$ s).

Actually, a similar situation was present in the previous simulations, but the periodic character of the $x_0(t)$ function caused repetition and overlapping of such effects, which was confusing.

The fold travel seems to be a wave-like phenomenon. It should be remembered that in light of the existing explanations, a shock wave runs down the whip and carries energy which is cumulated on an increasingly smaller section of the whip. Finally, “as the length of this section decreases to zero, the end part of the tip moves with unbounded velocity and cracks as soon as it reaches the velocity of the sound in the air” [Goriely and McMillen 2002].

Although we do not expect such significant results, let us have a look at the energy dependencies. Figure 19 illustrates the flow of the energy along the rope. We choose only several segments but it is clear that as the wave goes down, it involves consecutive elements providing additional energy to them. The greatest increase of the total energy occurs at the last element. Moreover, the inversions of flow direction are visible too. After the second one the dependencies become less meaningful.

As it may be expected, there is a noticeable maximum in velocity of the tip which corresponds to the transfer of energy (Figure 20). The return of the traveling fold to the tip also results in a peak, however, it seems to start a specific series of similar peaks in the end phase of the simulation when the fold disappears.

Finally, we turn our attention to the total energy of the whole mechanical system (Figure 21). Initially, the magnitude increases in the manner presented in the previous experiment as long as the constraints depend on time. Afterwards the energy of the system remains constant at the level forced by the applied constraints. Thus, all the spectacular things connected to the wave-like effect happen in the state in which the total energy is conserved by the system.

4. Conclusions

In the present work we have focused on the simple discrete model of the rope with two types of constraints, scleronomic and rheonomic. The multibody approach produces an expanded system of second order differential equations, which actually need to be solved numerically. Particularly in the case of the scleronomic constraints, the choice of the solver is justified by the energy principle. There is an

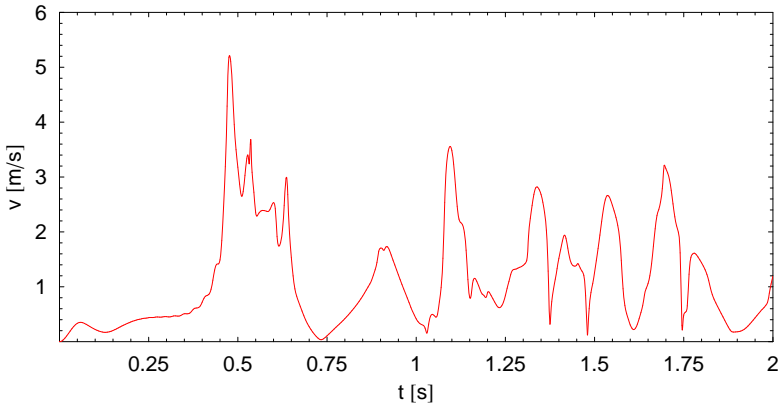


Figure 20. Velocity of the tip (Experiment 2).

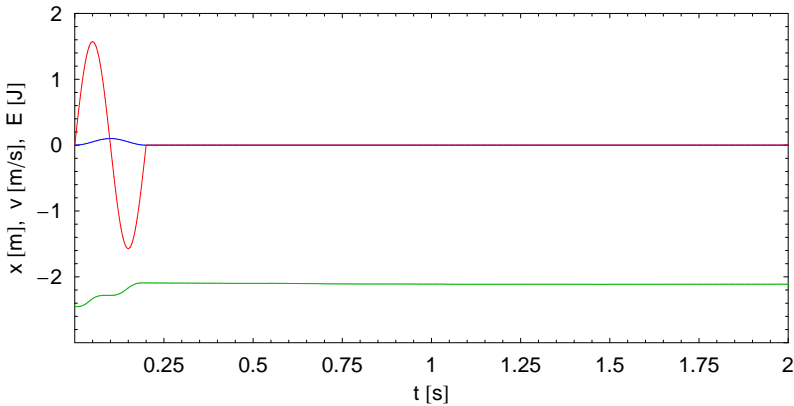


Figure 21. Total energy of the system (green) next to the constraint function x_0 (blue) and its derivative v_{x_0} (red).

agreement between our results of computation and the results of the numerical and laboratory experiments presented in Pierański and Tomaszewski [2005]. However, in order to perform computational simulations without significant energy losses (numerical dissipation) as well as rigorous restrictions related to time, we excluded the assumption that the left-hand side matrix in (3-1) is constant. Hence, the solutions to the problem obtained with the use of the MEBDFV code fulfill the energy conservation law in longer lasting motion.

We have also discussed the problem of discretization of the rope. The performed experiments point at possible improvements of the simulations' efficiency, in terms of shorter computation time and sufficient approximation of continuum by the model. Some reasonable limits of discretization, as an optimum of the number of elements, may not be very demanding when it comes to the computation capabilities.

As shown, the use of appropriate constraint functions results in emerging wave-like effects that are typical for the dynamics of the whip. The occurrence of sharp peaks in the time dependencies of velocity and acceleration of the tip turned out to be a result of the energy transfer between the consecutive elements of the discrete model.

In fact, the considered problem is a very good test for the applied solver. It seems that the code of Abdulla and Cash will succeed in solving dynamic equations for more complex mechanical systems including elasticity and damping. Also the function $y_0(t)$ should be considered to perform various maneuvers moving the entire body and inverting its velocity. The air resistance and the chaotic dynamics are worth studying too.

All in all, the problem provides many possibilities of dynamics analysis, since the challenging multi-body approach in conjunction with computational methods give insight into numerous aspects of mechanics. Thus, we feel that the outlined directions of development are worth the efforts and will be realized successively.

References

- [Cash and Considine 1992] J. R. Cash and S. Considine, "An MEBDF code for stiff initial value problems", *ACM Transactions on Mathematical Software* **18**:2 (1992), 142–155.
- [Goriely and McMillen 2002] A. Goriely and T. McMillen, "Shape of a cracking whip", *Phys. Rev. Let.* **88** (2002), #244301.
- [Pierański and Tomaszewski 2004] P. Pierański and W. Tomaszewski, "Fizyka strzelającego bicza", *Foton* **85** (2004).
- [Pierański and Tomaszewski 2005] P. Pierański and W. Tomaszewski, "Dynamics of ropes and chains, I: The fall of the folded chain", *New Journal of Physics* **7** (2005), #45.

Received 7 Feb 2008. Revised 26 Apr 2008. Accepted 26 Apr 2008.

PAWEŁ FRITZKOWSKI: pawel.fritzkowski@gmail.com

Computational Mechanics of Structures, Poznan University of Technology, Piotrowo 3, 60-965 Poznan, Poland
<http://www.fritzkowski.pl>

HENRYK KAMINSKI: henryk.kaminski@put.poznan.pl

Institute of Applied Mechanics, Poznan University of Technology, Piotrowo 3, 60-965 Poznan, Poland

THE OPTIMAL SHAPE PARAMETER OF MULTIQUADRIC COLLOCATION METHOD FOR SOLUTION OF NONLINEAR STEADY-STATE HEAT CONDUCTION IN MULTILAYERED PLATE

JAN ADAM KOŁODZIEJ AND MAGDALENA MIERZWICZAK

This paper deals with the numerical solution of the nonlinear heat transfer problem in a multilayered plate. Kansa's meshless method is used for the solution of this problem. In this approach, the unknown temperatures in layers are approximated by the linear combination of radial basis functions, while the governing equation and the boundary conditions are imposed directly at the collocation points. The multiquadrics [MQ] are used as the radial basis functions. In the presented method the radial basis functions contains a free parameter C , called the shape parameter. Usually, in the application of radial basis functions, this parameter is chosen arbitrarily depending on the author's experience. In the presented paper, special attention is paid to the optimal choice of the shape parameter for the radial basis functions. This optimal value of the shape parameter is obtained using a formula given by other authors for solution of the linear case.

1. Introduction

In the last two decades, meshless methods were introduced to computational mechanics. The essential feature of these methods is that they only require a set of unconnected nodes to construct the approximation functions. Among all the meshless methods, Kansa's method [1990a; 1990b] has become quite popular due to its simplicity. In this approach, the solution is approximated by a linear combination of the radial basis functions, while the governing equation and the boundary conditions are imposed directly at the collocation points. The most popular radial basis functions are multiquadrics [Hardy 1971]. In the presented method, the radial basis functions contain a free parameter C , called the shape parameter. Usually in the application to radial basis functions this parameter is chosen arbitrarily, depending on the author's experience. However, the shape parameter affects both the accuracy of the approximation and the conditioning of the system of equation, and there are papers in which this parameter is chosen optimally in proposed algorithms of solution, for example, [Golberg et al. 1996; Rippa 1999; Wertz et al. 2006; Huang et al. 2007].

The purpose of this paper is to determine the optimal choice of the shape parameter for the radial basis functions when a nonlinear heat conduction problem in multilayered solid structures is considered. Walls of heat treatment furnaces usually consist of several layers of different materials, with a different temperature inside and outside of the furnace. There are some electronic devices in which heat flow exists in the multi-layered device materials. Accurate thermal analysis of the high-temperature

Keywords: meshless method, heat transfer, Kansa's method, temperature-dependent thermal conductivity, optimal shape parameter, residual error.

The authors made this work in frame of a Grant 21-247/07 BW from the Polish Committee of Scientific Research.

devices must take into account the dependence of the thermal conductivity on the temperature. Usually, for problems with temperature-dependent thermal conductivity, the Kirchhoff transformation is used to convert a nonlinear heat equation into a linear one with nonlinear boundary conditions. However, in the multilayered walls, the nonlinear boundary conditions appear between layers, which makes this transformation generally problematic. In the paper [Bonani and Ghione 1995], the heat flow in only two layers has been considered. Moreover, the authors assumed that the thermal conductivity in layers is linearly dependent, which permits them to use the Kirchhoff transformations. Similarly, in the paper [Pesare et al. 2001], the authors linearized the boundary conditions between layers and used the Fourier transformation.

In this paper we apply Kansa’s method for the numerical solution of nonlinear heat transfer in multi-layered solid structures. Special attention is paid to the optimal choice of the shape parameter for radial basis functions. This optimal value of the shape parameter is obtained using the formula given in the paper [Huang et al. 2007], which was used in the two-dimensional linear case. Here, this formula is examined for the nonlinear one-dimensional case.

2. Formulation of the problem

Let’s consider three cases of multi-layer walls as shown in Figure 1:

- (1) constant thermal conductivity of layers $\lambda_{(i)} = AW(i)$,

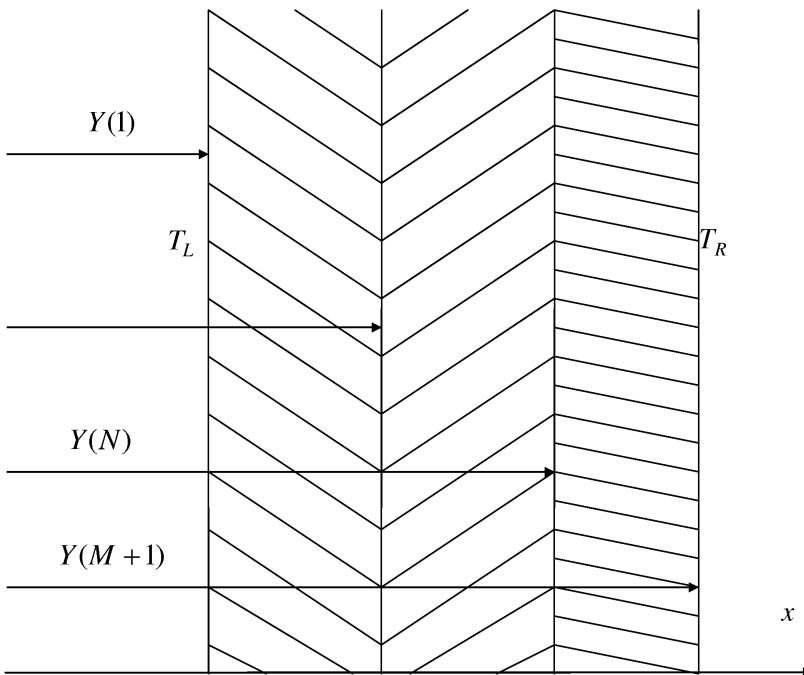


Figure 1. Plane multi-layer wall.

- (2) linear temperature-dependent thermal conductivity $\lambda^{(i)} = AW(i) + BW(i)T^{(i)}$,
 (3) temperature-dependent thermal conductivity of layers

$$\lambda^{(i)} = AW(i) + BW(i)T^{(i)} + CW(i)(T^{(i)})^2, \quad i = 1, 2, \dots, M, \quad (2-1)$$

where $T^{(i)}(x)$ is the temperature field in i th layer, and $AW(i)$, $BW(i)$, and $CW(i)$ are known constants for each layer. On the left and the right hand of the walls the temperatures are T_L and T_R respectively.

The one-dimensional governing equation for steady state heat transfer in multi-layered walls with thermal conductivity dependent on temperature is given as

$$\frac{d}{dx} \left[\lambda(T^{(i)}) \frac{dT^{(i)}}{dx} \right] = 0, \quad \text{for } x \in [Y(i), Y(i+1)], \quad i = 1, \dots, M. \quad (2-2)$$

Equation (2-2) can be expressed as

$$\frac{d^2T}{dx^2} = -\frac{1}{\lambda(T^{(i)})} \frac{d\lambda}{dT^{(i)}} \left(\frac{dT^{(i)}}{dx} \right). \quad (2-3)$$

Substituting Equation (2-1) into Equation (2-3) we have

$$\frac{d^2T}{dx^2} = -\frac{BW(i) + 2CW(i)T^{(i)}}{AW(i) + BW(i)T^{(i)} + CW(i)(T^{(i)})^2} \left(\frac{dT^{(i)}}{dx} \right)^2. \quad (2-4)$$

Equation (2-4) should be solved with the following boundary conditions:

- (1) on the left boundary:

$$T^{(1)} = T_L \quad \text{for } x = Y(1), \quad (2-5)$$

- (2) on the right boundary:

$$T^{(M)} = T_R \quad \text{for } x = Y(M+1), \quad (2-6)$$

- (3) continuity of temperature and heat flux between layers:

$$\begin{aligned} T^{(i)} &= T^{(i+1)}, \\ \lambda(T^{(i)}) \frac{dT^{(i)}}{dx} &= \lambda(T^{(i+1)}) \frac{dT^{(i+1)}}{dx}, \\ \text{for } x &= Y(i+1), \quad i = 1, 2, \dots, M. \end{aligned} \quad (2-7)$$

We introduce the nondimensional variables in the form $\check{T}^{(i)} = T^{(i)}/T_L$, $\check{x}^{(i)} = x^{(i)}/D$, where $D = Y(M+1) - Y(1)$ is the width of a wall. Now, the nondimensional thermal conductivity has the form

$$\check{\lambda}^{(i)} = 1 + \frac{BW(i)}{AW(i)} T_L \check{T}^{(i)} + \frac{CW(i)}{AW(i)} (T_L \check{T}^{(i)})^2 \quad (2-8)$$

$$= 1 + \check{B}W(i) \check{T}^{(i)} + \check{C}W(i) (\check{T}^{(i)})^2, \quad (2-9)$$

where $\check{B}W(i) = \frac{BW(i)}{AW(i)} T_L$, $\check{C}W(i) = \frac{CW(i)}{AW(i)} (T_L)^2$.

The governing Equation (2-4), in the nondimensional thermal conductivity, is now the following:

$$\frac{d^2\check{T}^{(i)}}{d\check{x}^2} = -\frac{\check{B}W(i) + 2\check{C}W(i)\check{T}^{(i)}}{1 + \check{B}W(i)T^{(i)} + \check{C}W(i)(T^{(i)})^2} \left(\frac{d\check{T}^{(i)}}{d\check{x}}\right)^2, \tag{2-10}$$

and is solved with the following boundary conditions in dimensionless form:

(1) on the left boundary:

$$\check{T}^{(1)} = 1, \quad \text{for } \check{x} = \frac{Y(1)}{D}, \tag{2-11}$$

(2) on the right boundary:

$$\check{T}^{(M)} = \frac{T_R}{T_L}, \quad \text{for } \check{x} = \frac{Y(M+1)}{D}, \tag{2-12}$$

(3) continuity between layers:

$$\begin{aligned} \check{T}^{(i)} &= \check{T}^{(i+1)}, \\ \check{\lambda}(\check{T}^{(i)}) \frac{d\check{T}^{(i)}}{d\check{x}} &= \beta^{(i+1)} \cdot \check{\lambda}(\check{T}^{(i+1)}) \frac{d\check{T}^{(i+1)}}{d\check{x}}, \\ \check{x} &= \frac{Y(i+1)}{D}, \quad i = 1, 2, \dots, M, \end{aligned} \tag{2-13}$$

where $\beta^{(i+1)} = \frac{AW(I+1)}{AW(I)}$.

3. Method of solution

According to Kansa’s method the approximate solution is assumed in the form

$$\check{T}^{(i)} = \sum_{j=1}^N D(i, j)\phi_j(\check{x}, \check{x}w(i, j), C), \quad i = 1, 2, \dots, M, \tag{3-1}$$

where $\phi_j(\check{x}, \check{x}w(i, j), C) = \sqrt{(\check{x} - \check{x}w(i, j))^2 + C^2}$ are multiquadrics as radial basis functions, $D(i, j)$ are coefficients to be determined, i is related to i th layer, j is related to interpolation nodes, N is the number of interpolation points in each layer, $\check{x}w(i, j)$ are interpolation points which are determined by the formula

$$\check{x}w(i, j) = \frac{\left(\frac{Y(i+1)}{D} - \frac{Y(i)}{D}\right) \cdot (j - i)}{N - 1} + \frac{Y(i)}{D},$$

and C is the shape factor for which the optimal value will be determined by using error estimation.

Then we can write the solution, Equation (3-1), as

$$\check{T}^{(i)} = \sum_{j=1}^N D(i, j)\sqrt{(\check{x} - \check{x}w(i, j))^2 + C^2}, \quad i = 1, 2, \dots, M, \tag{3-2}$$

The problem can be solved if the coefficients $D(i, j)$, $i = 1, 2, \dots, M$, $j = 1, 2, \dots, N$, are known. These $NG = M \cdot N$ unknown coefficients will be determined with the following equations:

(1) from determination of boundary condition (2-11) at the left side of wall:

$$\check{T}^{(1)}(\check{x}w(1, 1)) = 1, \tag{3-3}$$

(2) determination of boundary condition (2-12) at the right side of wall:

$$\check{T}^{(M)}(\check{x}w(M, N)) = \frac{T_R}{T_L}, \tag{3-4}$$

(3) from the continuity conditions (2-13) between layers, which lead to $2(M - 1)$ equations in the form

$$\check{T}^{(i)}(\check{x}w(i, N)) = \check{T}^{(i+1)}(\check{x}w(i + 1, 1)), \tag{3-5}$$

$$\check{\lambda}(\check{T}^{(i)}) \frac{d\check{T}}{d\check{x}} \Big|_{\check{x}w(i, M)} = \beta^{(i+1)} \check{\lambda}(\check{T}^{(i+1)}) \frac{d\check{T}^{(i+1)}}{d\check{x}} \Big|_{\check{x}w(i+1, j)}. \tag{3-6}$$

(4) from pointwise satisfaction of Equation (2-10) in the inner nodes on each layer, which leads to $M(N - 2)$ equations of the form

$$\frac{d^2\check{T}^{(i)}}{d\check{x}^2} \Big|_{\check{x}w(i, j)} = \left\{ - \frac{\check{B}W(i) + 2\check{C}W(i)\check{T}^{(i)}}{1 + \check{B}W(i)T^{(i)} + \check{C}W(i)(T^{(i)})^2} \left(\frac{d\check{T}^{(i)}}{d\check{x}} \right)^2 \right\} \Big|_{\check{x}w(i, j)}, \tag{3-7}$$

where $i = 1, 2, \dots, M$ and $j = 2, \dots, N - 1$.

Together we have $1 + 1 + 2(M - 1) + M(N - 2) = MN$ nonlinear equations, the same as the number of unknowns $D(i, j)$.

In the presented method, the radial basis functions contain a free parameter C called the shape parameter. Usually in the application of radial basis functions this parameter is chosen arbitrarily, depending on author's experience. However, the shape parameter affects both the accuracy of the approximation and the conditioning of the system of equations, and there are papers in which this parameter is chosen optimally in a proposed algorithm of solution, for example, [Rippa 1999]. For MQ collocation, the shape factor in the basis functions should be increased to its limit. When we push $C \rightarrow \infty$, the theoretical accuracy can be achieved but condition number of solutions matrix becomes huge which leads to the loss of accuracy. We establish an error estimate of

$$\epsilon \approx O(\exp(aC^{3/2} + (\ln \lambda)C^{1/2}h^{-1})), \quad \text{with } 0 < \lambda < 1 \text{ and } a > 0,$$

given in [Huang et al. 2007]. A finite C value for which the error is minimized exists. This optimal value is found to be $C_{\text{opt}} = C_{\text{max}} = -\ln \lambda / (3ah)$. To determine C_{opt} , knowledge of the constants λ and a in the error estimate is needed. In a real world problem, the error is not known because the true solution is not given. Without data, λ and a cannot be determined. This difficulty is overcome by utilizing the residual error, which is a good measure of the error trend, but not the error magnitude. Using residual errors corresponding to a number of C and h values, these two constants λ and a can be estimated by least square data fitting.

For numerical experiments we solve three cases: constant, linear, and nonlinear temperature-dependent thermal conductivity of layers. In order to verify the exactness of the proposed method, as a first example,

one layer with known temperature at the left and right walls and linearly temperature-dependent thermal conductivity $\lambda(T) = AW + BW \cdot T$ was considered. The analytical solution is

$$T(x) = \frac{-AW + \sqrt{AW^2 - 2BW(\kappa_1 \cdot x + \kappa_2)}}{BW},$$

where

$$\kappa_1 = \frac{AW(T_R - T_L) + \frac{1}{2}BW(T_K^2 - T_L^2)}{G} \quad \text{and} \quad \kappa_2 = AW T_L + \frac{1}{2}BWT_L^2,$$

and we can make a comparison of the result from the MQ collocation method with the optimal shape factor and check the accuracy of the method using the maximum error

$$\epsilon_{\max} = \max_{q=1, \dots, N-1} \frac{|T(xr_q) - \check{T}(xr_q)|}{T_{\max}},$$

and square error

$$\epsilon_{\text{sqr}} = \frac{\sqrt{\frac{1}{N-1} \sum_{q=1}^{N-1} [T(xr_q) - \check{T}(xr_q)]^2}}{T_{\max}}.$$

4. Residual error

In a real life problem, we have no knowledge about the exact solution; hence we do not have error data to use at all. We need to find an alternative to the above procedure and estimate the residual error. If we check the residual error at a node xr_q not belonging to the collocation set,

$$\epsilon_R(xr_q) = \frac{d}{dx} \left(\lambda \check{T}(xr_q) \frac{d\check{T}(xr_q)}{dx} \right),$$

the error is generally not zero. The residual error can be used as a good indication of error trend, but it does not give the error magnitude. We can write the estimate of residual error as follows: $\epsilon_r = A\epsilon$, where A is a constant of an unknown order of magnitude. For a given grid h , we can perform two computations using two different C values, C_k and C_{k+1} , to obtain the residual errors $\epsilon_r(C_k)$ and $\epsilon_r(C_{k+1})$. With two such data points, their ratio gives the following linear equation in the two unknowns a and $\ln \lambda$:

$$\ln \frac{\epsilon_R(C_k)}{\epsilon_R(C_{k+1})} = (C_k^{3/2} - C_{k+1}^{3/2})a - \frac{C_k^{1/2} - C_{k+1}^{1/2}}{h} \ln \lambda,$$

The three computations with different C 's can form two equations for the determination of a and $\ln \lambda$. In practice, it is better to obtain a larger number of data points to perform the least squares fitting. Then the obtained constants can be used to determine the C_{opt} value for a finer grid.

5. Numerical results

Linear temperature-dependent thermal conductivity of one layer. In these cases, the exact solutions are unknown so we can estimate the method error magnitude (maximum and square error). In these numerical calculations, 11 and 21 collocation points in one layer were chosen and 10^{-4} for maximal

C	$\ln \epsilon_R$
1.6	0.00121982413
1.8	0.000886213166
2.0	0.000691965229
2.2	0.000571502605
2.4	0.00048876342
2.6	0.000562506018
2.8	1.6346723
3.0	2.36810104
C_{opt}	$\ln \epsilon_R$
2.45619734	0.00046022506

Table 1. Residual error as a function of the shape parameter C for linear temperature-dependent thermal conductivity.

C	$\ln \epsilon_R$
0.005	0.792708032
0.155	0.629296421
0.305	0.0521441337
0.455	0.00555486248
0.605	0.000754166689
0.755	0.000130104558
C_{opt}	$\ln \epsilon_R$
0.786010956	0.000104694988

Table 2. Residual error as a function of the shape parameter C for linear temperature-dependent thermal conductivity.

error in Newton's method was accepted. The first approximation was the solution to the temperature distribution for a constant thermal conductivity coefficient (independent of the temperature).

For 11 collocation points the optimal shape factor is $C_{\text{opt}} = 2.45619734$ for which the residual error $\epsilon_R = 0.00046$ and maximum and square error between approximated and analytic solution is, $\epsilon_{\text{max}} = 3.81 \times 10^{-005}$, $\epsilon_{\text{sqr}} = 2.27 \times 10^{-005}$ respectively (Table 1).

For 21 collocation points $C_{\text{opt}} = 0.786010956$, $\epsilon_R(C_{\text{opt}}) = 0.0001047$, $\epsilon_{\text{max}} = 3.46 \times 10^{-005}$, $\epsilon_{\text{sqr}} = 2.84 \times 10^{-005}$ (Table 2). The values of maximum and square errors show that the accuracy of the method is high and the approximate solution agrees with the theoretical solution. The above figures show that the numerical and theoretical solutions are similar and the MQ collocation method with optimized shape procedure is an effective tool to solve heat transfer problems.

Constant thermal conductivity of multilayer plane. We considered three cases:

C	$\ln \epsilon_R$	C	$\ln \epsilon_R$
0.05	3.0710643	0.1	2.64531052
0.2	0.447483879	0.2	0.53068379
0.35	0.150444561	0.3	0.174990457
0.5	0.086741511	0.4	0.09438661
0.65	0.065856967	0.5	0.068759911
0.8	0.057433939	0.6	0.058639665
0.95	0.053670263	0.7	0.054148311
1.1	0.051987961	0.8	0.052033416
1.25	0.095730805	0.9	0.05100849
1.4	0.074601817	1.0	0.050664394
1.55	0.064468031	1.1	0.08348719
C_{opt}	$\ln \epsilon_R$	C_{opt}	$\ln \epsilon_R$
0.594536825	0.000310218	0.386502402	0.015555844

Table 3. Residual error as a function of the shape parameter C for constant thermal conductivity. Left: one-layer wall with 21 collocation points. Right: two-layer wall with 11 collocation points.

The first case experiment is performed at one layer with 21 collocation points. The calculated shape factor is $C_{opt} = 0.594536825$ for which the residual error is $\epsilon_R(C_{opt}) = 0.00031$ (Table 3, left).

In the second case, a two layer wall is taken with 11 collocation points. The calculated shape factor is $C_{opt} = 0.386502402$ for which the residual error is $\epsilon_R(C_{opt}) = 0.01556$ (Table 3, right).

In the third case, a three layer wall is considered with 11 collocation points. The optimal shape factor is $C_{opt} = 0.687803178$ and the residual error is $\epsilon_R(C_{opt}) = 0.0328$ (Table 4).

C	$\ln \epsilon_R$	C	$\ln \epsilon_R$	C	$\ln \epsilon_R$
0.1	1.97888189	0.35	0.042408028	0.6	0.033871399
0.15	0.532822138	0.4	0.037617988	0.65	0.056527116
0.2	0.177169659	0.45	0.035414293	0.7	0.074507336
0.25	0.083325356	0.5	0.034366375	0.75	0.19534613
0.3	0.053618929	0.55	0.033893021	0.8	0.886799178
		C_{opt}	$\ln \epsilon_R$		
		0.687803178	0.032803874		

Table 4. Residual error as a function of the shape parameter C for constant thermal conductivity, for a three-layer wall with 11 collocation points.

C	$\ln \epsilon_R$	C	$\ln \epsilon_R$
0.01	1.53630798	0.005	2.11501089
0.11	1.41237822	0.13	1.66547618
0.21	0.246053512	0.255	0.168228737
0.31	0.048526885	0.38	0.023131902
0.41	0.010647406	0.505	0.004399075
0.51	0.00258324	0.63	0.001125429
0.61	0.000698235	0.755	0.000375851
0.71	0.000209848	0.88	0.000161322
0.81	0.00048872	1.005	0.066491517
C_{opt}	$\ln \epsilon_R$	C_{opt}	$\ln \epsilon_R$
0.791210985	8.34×10^{-05}	0.812596263	0.000245721

Table 5. Residual error as a function of the shape parameter C . Left: one-layer wall with 21 collocation points. Right: two-layer wall with 11 collocation points.

Temperature-dependent thermal conductivity of layers. Next we considered the nonlinear temperature-dependent thermal conductivity, so we solved the nonlinear system using Newton's method.

In the first case, the experiment is performed at one layer with 21 collocation points. The calculated shape factor is $C_{\text{opt}} = 0.791210985$ for which the residual error is $\epsilon_R(C_{\text{opt}}) = 8.34 \times 10^{-05}$ (Table 5, left).

In the second case, a two layer wall is taken into account with 11 collocation points. The calculated shape factor is $C_{\text{opt}} = 0.812596263$ for which the residual error is $\epsilon_R(C_{\text{opt}}) = 2.46 \times 10^{-04}$ (Table 5, right).

In the third case, a three layer wall is taken into account with 11 collocation points. The optimal shape factor is $C_{\text{opt}} = 0.618039263$ and the residual error is $\epsilon_R(C_{\text{opt}}) = 1.11 \times 10^{-04}$ (Table 6).

C	$\ln \epsilon_R$
0.005	4.89989774
0.13	0.910910183
0.255	0.0331283856
0.38	0.00237394996
0.505	0.000305350558
0.63	0.00172510558
C_{opt}	$\ln \epsilon_R$
0.618039263	0.000111371465

Table 6. Residual error as a function of the shape parameter C , for a three-layer wall with 11 collocation points.

6. Conclusion

In this paper, the meshless method has been successfully used to solve the nonlinear heat transfer problem in multilayer wall insulation with a temperature-dependent thermal conductivity. Special attention was paid to the optimal choice of the shape parameter for the radial basis functions. For a calculated optimal value $C_{\text{opt}} = -(\ln \lambda)/(3ah)$, we can minimize the solution error. We find a constant $\ln \lambda$ using the residual error and least square method. The proposed method can be very easily implemented. The proposed algorithm of calculation is based on the Kansas's method, which numerically leads to a relatively simple nonlinear system of algebraic equations. The use of the calculated optimal shape factor guarantees a quick convergence with Newton's method for nonlinear system equations.

References

- [Bonani and Ghione 1995] F. Bonani and G. Ghione, "On the application of the Kirchhoff transformation to the steady-state thermal analysis of semiconductor devices with temperature-dependent and piecewise inhomogeneous thermal conductivity", *Solid-State Electronics* **38** (1995), 1409–1511.
- [Golberg et al. 1996] M. A. Golberg, C. S. Chen, and S. Karur, "Improved multiquadric approximation for partial differential equations", *Engineering Analysis with Boundary Elements* **18** (1996), 9–17.
- [Hardy 1971] R. L. Hardy, "Multiquadric equations of topography and other irregular surfaces", *Journal of geophysics research* **76** (1971), 1905–1915.
- [Huang et al. 2007] C.-S. Huang, C.-F. Lee, and A. H.-D. Cheng, "Error estimate, optimal shape factor, and high precision computation of multiquadric collocation method", *Engineering Analysis with Boundary Elements* **31** (2007), 614–623.
- [Kansa 1990a] E. J. Kansa, "Multiquadrics—a scattered data approximation scheme with applications to computational fluid-dynamics. I. Surface approximations and partial derivative estimates", *Comput. Math. Appl.* **19**:8-9 (1990), 127–145.
- [Kansa 1990b] E. J. Kansa, "Multiquadrics—a scattered data approximation scheme with applications to computational fluid-dynamics. II. Solutions to parabolic, hyperbolic and elliptic partial differential equations", *Comput. Math. Appl.* **19**:8-9 (1990), 147–161.
- [Pesare et al. 2001] M. Pesare, A. Giorgio, and A. G. Perri, "An analytical method for thermal layout optimization of multi-layer structures solid-state devices", *Solid-State Electronics* **45** (2001), 511–517.
- [Rippa 1999] S. Rippa, "An algorithm for selecting a good value for the parameter c in radial basis function interpolation", *Adv. Comput. Math.* **11**:2-3 (1999), 193–210. Radial basis functions and their applications.
- [Wertz et al. 2006] J. Wertz, E. J. Kansa, and L. Ling, "The role of the multiquadric shape parameters in solving elliptic partial differential equations", *Comput. Math. Appl.* **51**:8 (2006), 1335–1348.

Received 7 Feb 2008. Revised 26 Apr 2008. Accepted 26 Apr 2008.

JAN ADAM KOŁODZIEJ: jan.kolodziej@put.poznan.pl

Institute of Applied Mechanics, Poznan University of Technology, ul. Piotrowo 3, 60-965 Poznan, Poland

MAGDALENA MIERZWICZAK: magdalena.mierzwickzak@wp.pl

Institute of Applied Mechanics, Poznan University of Technology, ul. Piotrowo 3, 60-965 Poznan, Poland

THE APPLICATION OF THE METHOD OF FUNDAMENTAL SOLUTIONS TO A SIMULATION OF THE TWO-DIMENSIONAL SLOSHING PHENOMENON

JAN ADAM KOŁODZIEJ AND MAGDALENA MIERZWICZAK

This paper describes the application of the method of fundamental solutions (MFS) and the collocation method to the simulation of the sloshing phenomenon on an ideal fluid in a two-dimensional rectangular vessel. The phenomenon is governed by the Laplace equation with respect to the velocity potential. The equation is solved with nonlinear boundary conditions. The velocity potential is approximated by a linear superposition of fundamental solutions with the appropriate coefficients at each time step.

1. Introduction

Free surface fluctuation, also called liquid sloshing, is the most prominent phenomenon of liquid motion in either stationary or moving tanks subjected to forced external perturbations. The problem of liquid sloshing inside of moving or stationary containers remains of great concern to the aerospace, civil, and nuclear engineers, physicists, and designers of road or ship tankers. This phenomenon can be observed on the oil vessel of a tanker sailing on the ocean; as the tanker oscillates, the oil may spill. Another example is the cooling of a water vessel in an atomic power reactor that is oscillated by an earthquake. It is important to study the motion of a liquid fuel inside a tank during a rocket launch. Excessive liquid sloshing may cause structural failure and manipulation loss, which can lead to loss of economic, human, and environmental resources.

Usually the sloshing problem is formulated as a two-dimensional initial boundary-value problem in terms of the velocity potential, assuming that the fluid is inviscid, incompressible, and that the flow is irrotational (such that the viscosity, which causes the rotational motion, may be negligible). In such a case, the governing equation is the Laplace equation, which is solved with the appropriate boundary conditions. The surface profile and the boundary conditions on the free surface are updated from the potential value and its derivatives. Due to the nonlinear boundary conditions on the free surface and because the free surface is not known a priori, this problem is difficult and is usually solved numerically. This phenomenon has been simulated by using boundary and finite element methods [Abe and Sakuraba 1999; Hamano et al. 2003; Cho and Lee 2004; Sriram et al. 2006]. These methods, however, have some difficulties. The finite element method needs remeshing at each time step, and the computational time is very extensive. When we use the boundary element method with the boundary discretization alone, and therefore the mesh regeneration cost is cheaper, another difficulty arises due to the singularity of the fundamental solutions, and the calculation of the potential derivatives is somewhat troublesome.

Keywords: method of fundamental solutions (MFS), collocation points, source points, substantive (material) derivative, sloshing phenomenon.

This work was supported by Grant 21-247/07 BW from the Polish Committee of Scientific Research.

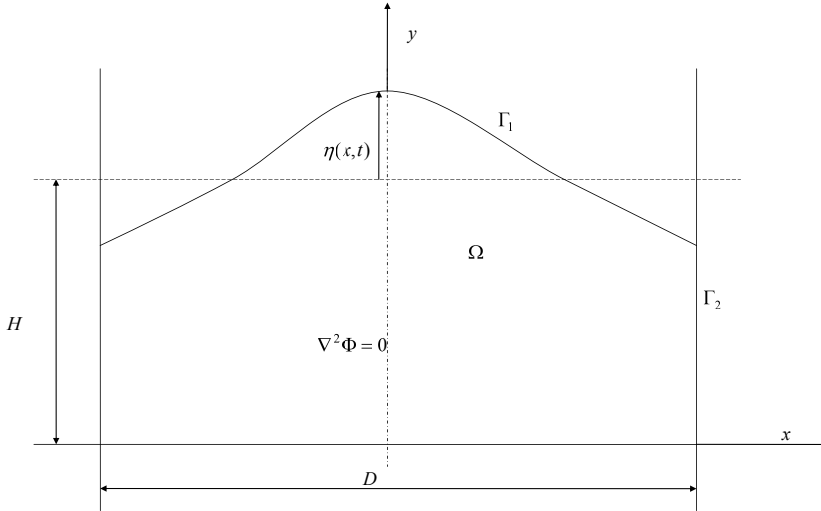


Figure 1. Rectangular vessel.

To overcome these difficulties, we propose using the meshless method of fundamental solutions (MFS). The velocity potential is approximated by the superposition of the fundamental solutions with unknown parameters that will be determined from the boundary condition. The calculation of the first and second derivatives is relatively easy. Therefore, we can treat the nonlinear boundary condition with Euler’s extended algorithm [Kita et al. 2004].

2. The governing equation’s boundary and initial conditions

Let’s consider an ideal fluid contained in a rectangular tank in two dimensions (Figure 1). For free vibrations of the fluid, the initial displacement of the free surface is assumed to be known. The object domain occupied by the fluid, the free surface of the fluid, and the wall of the vessel are indicated by Ω , Γ_1 , Γ_2 , respectively. The x and y axes of the Cartesian coordinates are taken in the horizontal and vertical directions, respectively. The origin of coordinates is located in the center, at the bottom of the tank. The width of the tank is D , the height of the undisturbed fluid is H , $\eta(x, t)$ is the vertical displacement of the fluid surface (displacement from the undisturbed fluid level), and $\xi(x, t)$ is the horizontal displacement of a fluid element on the free surface. By simplifying the flow problem (the fluid is incompressible, the flow irrotational, and forces due to viscosity are neglected), fluid flow can be defined by the Laplace equation involving a velocity potential $\Phi(x, y)$,

$$\frac{\partial^2 \Phi}{\partial x^2} + \frac{\partial^2 \Phi}{\partial y^2} = 0. \tag{2-1}$$

The boundary conditions are as follows:

- (1) The bottom and lateral walls are rigid and flat, so that

$$\frac{\partial \Phi}{\partial y} = 0 \quad \text{for } y = -H, \quad \frac{\partial \Phi}{\partial x} = 0 \quad \text{for } x = \pm \frac{D}{2}.$$

- (2) The kinematic condition on the free surface states that a particle of fluid which is at some time on the free surface will always remain on the free surface. Since the equation of the surface is $y - \eta = 0$, it follows that

$$\frac{D}{Dt}(y - \eta) = 0.$$

This equation may be expanded to give

$$\frac{\partial \eta}{\partial t} + \frac{\partial \Phi}{\partial x} \frac{\partial \eta}{\partial x} - \frac{\partial \Phi}{\partial y} = 0. \quad (2-2)$$

- (3) The dynamic condition on the free surface is implemented through the Bernoulli equation for unsteady irrotational motion:

$$\frac{\partial \Phi}{\partial t} + \frac{P}{\rho} + \frac{1}{2} \nabla \Phi \circ \nabla \Phi + g\eta = 0.$$

When the atmospheric pressure is taken as zero, the P will be zero, and

$$\frac{\partial \Phi}{\partial t} + \frac{1}{2} \left(\left(\frac{\partial \Phi}{\partial x} \right)^2 + \left(\frac{\partial \Phi}{\partial y} \right)^2 \right) + g\eta = 0. \quad (2-3)$$

The initial conditions are the following (the initial displacement of the free surface is assumed to be known):

$$\xi(x, 0) = \xi_0(x), \quad \eta(x, 0) = \eta_0(x). \quad (2-4)$$

3. Solving the sloshing phenomenon

The solution for the two-dimensional Laplace Equation (2-1) is given as follows:

$$\Phi(x, y, t) = \sum_{i=1}^N A_i(t) \ln \sqrt{(x - xs_i)^2 + (y - ys_i)^2}, \quad (3-1)$$

where (xs_i, ys_i) are the source points placed outside of the considered domain, N is the total number of source points, $\{A_1(t), A_2(t), \dots, A_n(t)\}$ denotes the vector of unknown functions of time, which is determined by the satisfaction of the appropriate boundary condition by means of the collocation method and initial conditions. It is easy to calculate the potential first and second-derivatives:

$$\begin{aligned} \frac{\partial \Phi}{\partial x} &= \sum_{i=1}^N A_i(t) \frac{(x - xs_i)}{(x - xs_i)^2 + (y - ys_i)^2}, & \frac{\partial \Phi}{\partial y} &= \sum_{i=1}^N A_i(t) \frac{(y - ys_i)}{(x - xs_i)^2 + (y - ys_i)^2}, \\ \frac{\partial^2 \Phi}{\partial x^2} &= \sum_{i=1}^N A_i(t) \frac{(y - ys_i)^2 - (x - xs_i)^2}{((x - xs_i)^2 + (y - ys_i)^2)^2}, & \frac{\partial^2 \Phi}{\partial y^2} &= \sum_{i=1}^N A_i(t) \frac{(x - xs_i)^2 - (y - ys_i)^2}{((x - xs_i)^2 + (y - ys_i)^2)^2}, \\ \frac{\partial^2 \Phi}{\partial x \partial y} &= \sum_{i=1}^N A_i(t) \frac{-2(x - xs_i)(y - ys_i)}{((x - xs_i)^2 + (y - ys_i)^2)^2}, \end{aligned}$$

Let's consider a collocation point in the free surface which moves from (ξ^k, η^k) at time t to a new position (ξ^{k+1}, η^{k+1}) at time $t + \Delta t$. If the time interval is small, the new position and the associated velocity potential can be obtained by Taylor series expansion:

$$\begin{aligned} \Phi^{k+1} &= \Phi^k + \Delta t \frac{D\Phi}{Dt} + \frac{1}{2} (\Delta t)^2 \frac{D^2\Phi}{Dt^2}, \\ \xi^{k+1} &= \xi^k + \Delta t \frac{D\xi}{Dt} + \frac{1}{2} (\Delta t)^2 \frac{D^2\xi}{Dt^2}, \\ \eta^{k+1} &= \eta^k + \Delta t \frac{D\eta}{Dt} + \frac{1}{2} (\Delta t)^2 \frac{D^2\eta}{Dt^2}. \end{aligned} \tag{3-2}$$

The substantive derivatives are estimated as follows:

$$\frac{D\Phi}{Dt} = \frac{1}{2} \nabla\Phi \circ \nabla\Phi - g\eta, \quad \frac{D\eta}{Dt} = \frac{\partial\Phi}{\partial y} = v_y, \quad \frac{D\xi}{Dt} = \frac{\partial\Phi}{\partial x} = v_x, \tag{3-3}$$

$$\begin{aligned} \frac{D^2\eta}{Dt^2} &= \frac{D}{Dt} \left(\frac{D\eta}{Dt} \right) = \frac{\partial}{\partial y} \left(\frac{\partial\Phi}{\partial t} \right) + \frac{\partial\Phi}{\partial x} \frac{\partial^2\Phi}{\partial x\partial y} + \frac{\partial\Phi}{\partial y} \frac{\partial^2\Phi}{\partial y^2}, \\ \frac{D^2\xi}{Dt^2} &= \frac{D}{Dt} \left(\frac{D\xi}{Dt} \right) = \frac{\partial}{\partial x} \left(\frac{\partial\Phi}{\partial t} \right) + \frac{\partial\Phi}{\partial x} \frac{\partial^2\Phi}{\partial x^2} + \frac{\partial\Phi}{\partial y} \frac{\partial^2\Phi}{\partial x\partial y}, \\ \frac{D^2\Phi}{Dt^2} &= \frac{D}{Dt} \left(\frac{1}{2} \nabla\Phi \circ \nabla\Phi - g\eta \right) = v_x \frac{D^2\xi}{Dt^2} + v_y \frac{D^2\eta}{Dt^2} - gv_y, \end{aligned} \tag{3-4}$$

The time derivative $\partial\Phi/\partial t = \Phi_t$ is calculated by solving the following boundary value problem using MFS, where the time derivative velocity potential is approximated by a linear combination of appropriate functions:

$$\begin{cases} \nabla^2\Phi_t = 0 & (\text{in } \Omega), \\ \Phi_t = -\frac{1}{2} (v_x^2 + v_y^2) - gy & (\text{on } \Gamma_1), \\ \partial\Phi_t/\partial n = 0 & (\text{on } \Gamma_2), \end{cases} \tag{3-5}$$

Computational accuracy is checked using the conservation of the fluid volume V in the container and of the total energy E , using the equations

$$V = \int_{\Omega} dV, \quad E = \int_{\Omega} \left(\frac{1}{2} \nabla\Phi \cdot \nabla\Phi + gy \right) dV. \tag{3-6}$$

4. The algorithm

(1) Specify the initial profile of the free surface and the initial velocity potential on the free surface:

$$\Phi_0 = -g\eta_0.$$

(2) Initialize the time step: $k \leftarrow 0$.

(3) Substitute $\Phi_k \leftarrow \Phi_0, \quad \eta_k \leftarrow \eta_0, \quad \xi_k \leftarrow \xi_0$.

(4) Solve the boundary-value problem for Φ give by

$$\begin{cases} \nabla^2 \Phi = 0 & (\text{in } \Omega), \\ \Phi = \Phi_0 & (\text{on } \Gamma_1), \\ \partial \Phi / \partial n = 0 & (\text{on } \Gamma_2). \end{cases} \quad (4-1)$$

(5) Estimate the derivatives

$$\frac{\partial \Phi}{\partial x}, \quad \frac{\partial \Phi}{\partial y}, \quad \frac{\partial^2 \Phi}{\partial x^2}, \quad \frac{\partial^2 \Phi}{\partial y^2}, \quad \frac{\partial^2 \Phi}{\partial x \partial y}.$$

(6) Solve the boundary-value problem for Φ_t given by

$$\begin{cases} \nabla^2 \Phi_t = 0 & (\text{in } \Omega), \\ \Phi_t = -\frac{1}{2} (v_x^2 + v_y^2) - gy & (\text{on } \Gamma_1), \\ \partial \Phi_t / \partial n = 0 & (\text{on } \Gamma_2). \end{cases} \quad (4-2)$$

(7) Estimate the derivatives given in Equation (3-4):

$$\frac{D^2 \eta}{Dt^2}, \quad \frac{D^2 \xi}{Dt^2}, \quad \frac{D^2 \Phi}{Dt^2}.$$

(8) Use Equation (3-2) to calculate Φ^{k+1} , ξ^{k+1} , η^{k+1} .

(9) Smooth the free surface profile using cubic spline interpolation.

(10) Correct the vertical positions of free surface fluid particles with respect to the constant volume of the fluid.

(11) Update the free surface profile and the boundary condition on it:

$$\Phi \leftarrow \Phi_{k+1}, \quad \eta \leftarrow \eta_{k+1}, \quad \xi \leftarrow \xi_0.$$

(12) Increment the time step $k \leftarrow k + 1$.

(13) Go to step (4).

5. Numerical examples

We consider a two-dimensional rectangular vessel with an ideal fluid. The width of the tank is $D = 1$ m, and the height of the undisturbed fluid is $H = 1$ m. The initial form of the free surface is sinusoidal (Figure 1), and the initial amplitude is $A = 0.1$ m. The collocation and source points are placed uniformly on the whole boundary. The distance from the source points to the boundary walls or free surface is $s = 0.1$ m. Simulations are performed using different time-steps Δt , and different numbers of source and collocation points on the free surface and on the boundary tanks.

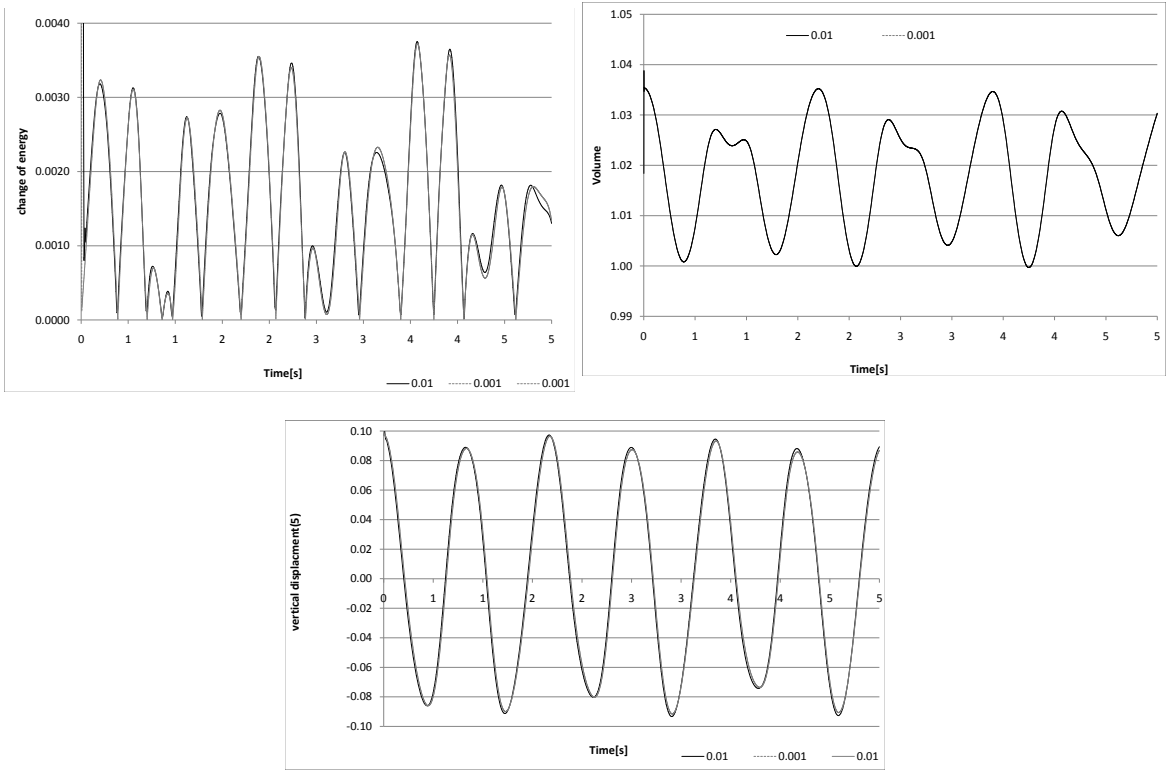


Figure 2. Top: Fluctuation of energy (left) and fluid volume (right) as a function of time. Bottom: Vertical displacement of point number 5 in the free surface. A total of 44 collocation and source points were used (see text).

6. Results

For a set of simulations with 11 collocation and source points on each of the tank's three walls plus the free surface (for a total of 44 collocation points), we compare simulation results for time step $\Delta t = 0.01$ and $\Delta t = 0.001$. Figure 2 shows the history of volume, the change in energy, and the vertical displacement for a free surface point, for different time steps. We see that the results are similar, and for equal time steps we obtained good results.

For the next case, when $\Delta t = 0.005$ and 11 (source, collocation) points are placed on the free surface and 7 (source, collocation) points are placed on the bottom, right, and left walls of the tank (for a total of 31 collocation and source points), the results are presented in Figure 3. Whether or not we observe fluctuations in the total fluid volume or energy, the algorithm is stable for many time steps.

When we take a time step of $\Delta t = 0.01$ and 15 (source, collocation) points in free surface, 11 (source, collocation) points on the bottom, right and left wall of the tank (for a total of 48 collocation and source points), the algorithm loses its stability after a number of time steps (see Figure 4).

Taking the last time step equal to $\Delta t = 0.001$ with the same numbers of collocation and source points, the algorithm is still unstable after some time steps, at which point the total energy rapidly increases (Figure 5).

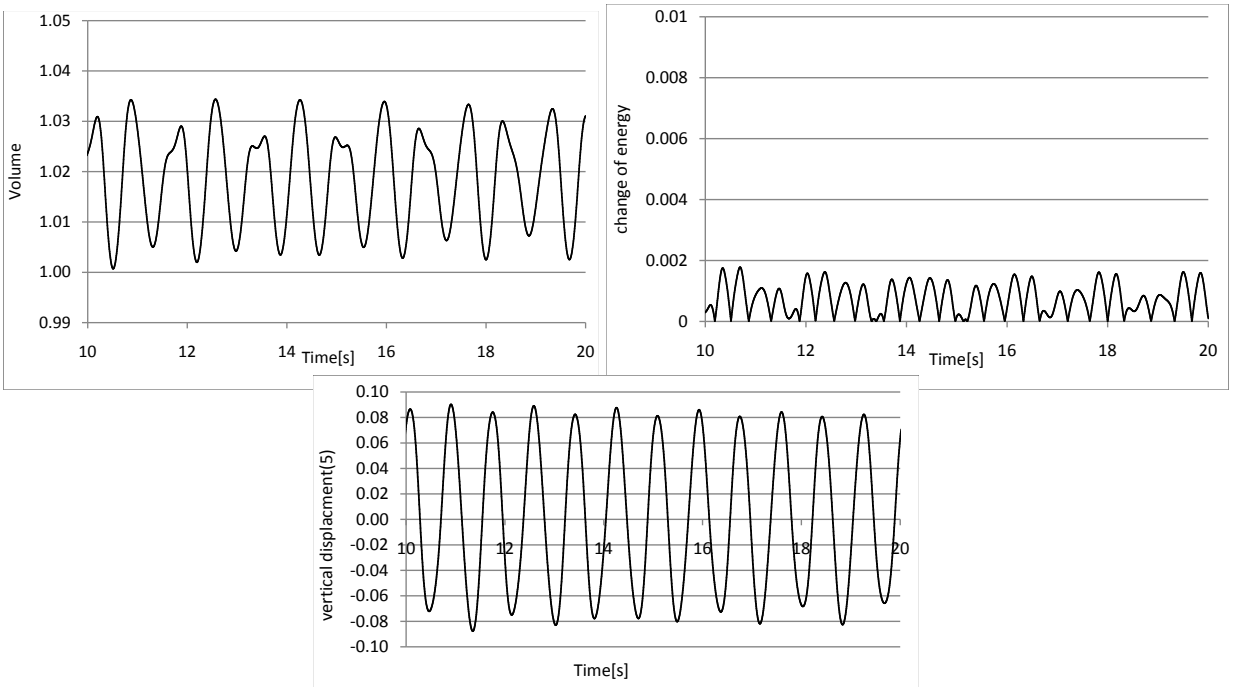


Figure 3. Same as Figure 2, but with 31 collocation points.

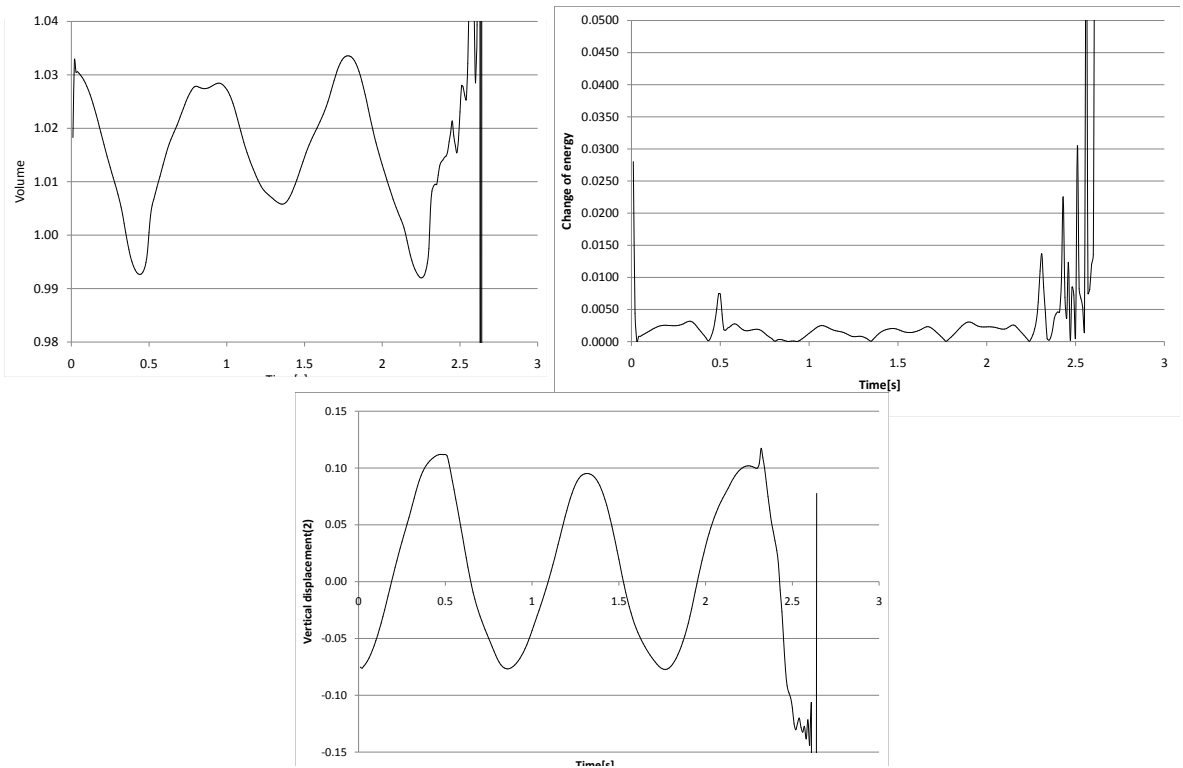


Figure 4. Same as Figure 2, but with 48 collocation points.

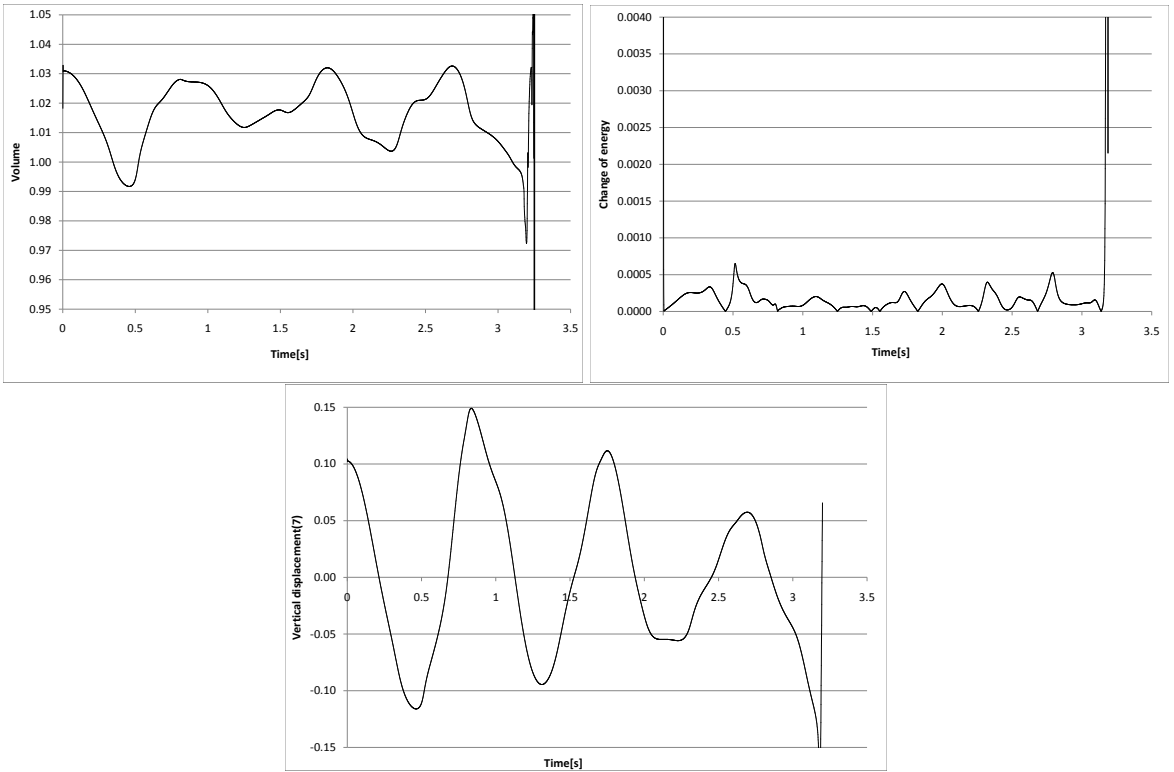


Figure 5. Same as Figure 4, but with $\Delta t = 0.001$.

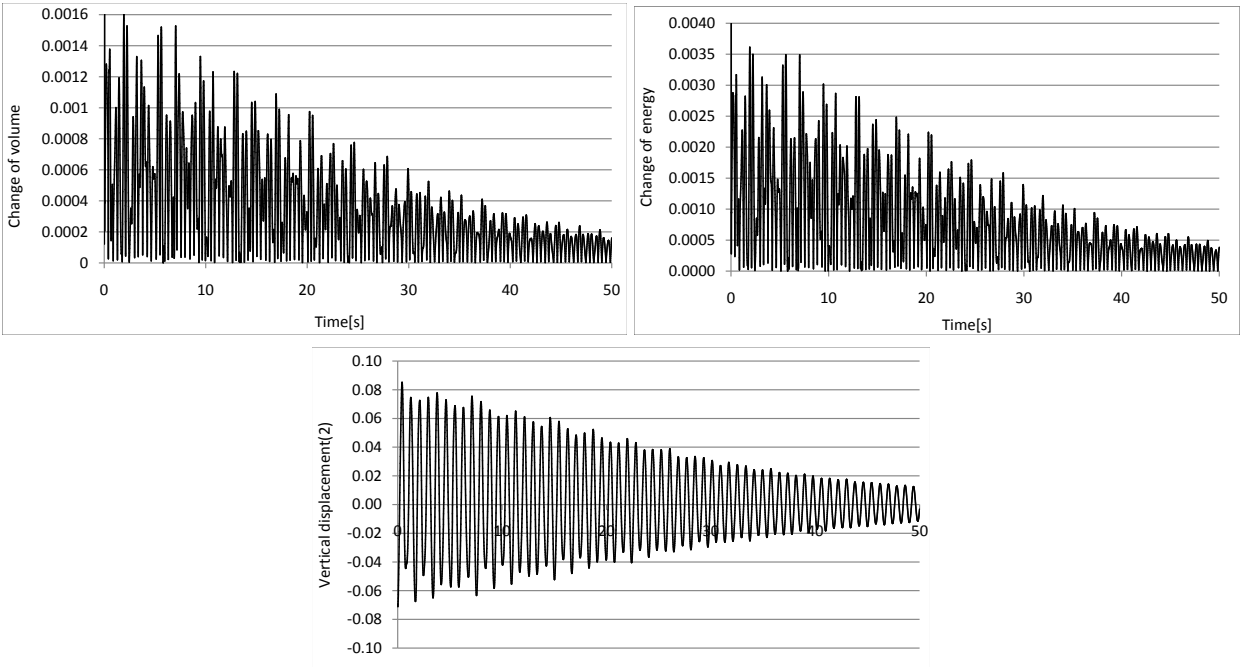


Figure 5. Same as Figure 4, but with 60 collocation points.

The algorithm becomes stable when we increase the number of collocation and source points (15) on the bottom, right and left wall of the tank at $\Delta t = 0.01$ (see Figure 5).

7. Conclusions

We applied a meshless numerical method to simulate the sloshing phenomenon. The method is "meshless" or "element-free", thus simplifying the geometric representation of the solution domain and eliminating the need for constructing and booking element connectivity. This comes in handy particularly when a moving boundary is involved, which may require frequent remeshing. Using the fundamental solution of the Laplace equation and locating the source points outside the computational domain, the problem is solved by collocation of a few boundary points. We used a mixed Eulerian and Lagrangian method (ALE). The numerical simulation was validated by checking the accuracy, including the errors in total volume and energy, and the convergence of the simulation was studied by changing the number of collocation and source points while varying the time interval. The results presented show that for some input parameters the algorithm is stable (Figures 2 and 3), but for others, after some number of time steps (300), the algorithm becomes unstable (Figures 4 and 5). In the last example, we observed damping of the change of energy and damping of the free surface motion for many time steps (Figure 5). We suppose that the reason for this simulation behavior is the lack of an energy correction. In future algorithms, conservation of energy will also be investigated.

References

- [Abe and Sakuraba 1999] K. K. Abe and S. Sakuraba, "An hr-adaptive boundary element for water free-surface problems", *Engineering Analysis with Boundary Elements* **23** (1999), 223–232.
- [Cho and Lee 2004] K. J. R. Cho and H. W. Lee, "Numerical study on liquid sloshing in baffled tank by nonlinear finite element method", *Comput. Methods Appl. Mech. Engrg* **193** (2004), 2581–2598.
- [Hamano et al. 2003] K. Hamano, S. Murashige, and K. Hayami, "Boundary element simulation of large amplitude standing waves in vessels.", *Engineering Analysis with Boundary Elements* **27** (2003), 565–574.
- [Kita et al. 2004] K. E. Kita, J. Katsuragawa, and N. Kamiya, "Application of Trefftz-type boundary element method to simulation of two-dimensional sloshing phenomenon", *Engineering Analysis with Boundary Elements* **28** (2004), 677–683.
- [Sriram et al. 2006] K. V. Sriram, S. A. Sannasiraj, and V. Sundar, "Simulation of two-dimensional nonlinear waves using finite element method with cubic spline approximation", *Journal of Fluids and Structures* **22** (2006), 663–681.

Received 7 Feb 2008. Accepted 28 Apr 2008.

JAN ADAM KOŁODZIEJ: jan.kolodziej@put.poznan.pl

Institute of Applied Mechanics, Poznan University of Technology, ul. Piotrowo 3, 60-965 Poznan, Poland

MAGDALENA MIERZWICZAK: magdalena.mierzwiczak@wp.pl

Institute of Applied Mechanics, Poznan University of Technology, ul. Piotrowo 3, 60-965 Poznan, Poland

PROPAGATION OF A SURFACE WAVE IN A VORTEX ARRAY ALONG A SUPERCONDUCTING HETEROSTRUCTURE

BOGDAN T. MARUSZEWSKI, ANDRZEJ DRZEWIECKI AND ROMAN STAROSTA

We analyze the propagation conditions and dispersion relations for SH surface waves (Love-like waves) running along a vortex array in a superconducting heterostructure consisting of a layer and a half-space. Investigations allowed us to estimate a new interval for the wave phase velocity values different from the classical estimate and to show that the structure has filtering properties.

1. Introduction

Superconductors generally fall into two classes. A type-I superconductor expels magnetic flux from the material and hence is in the Meissner state. That is possible only at an applied magnetic field strength less than the determined critical value. In contrast a type-II superconductor behaves in another way. For an applied field less than the lower critical field a type-II superconductor will exhibit the usual Meissner effect. Applied fields greater than the upper critical field strength destroy the superconductivity altogether. In between the lower H_{c1} and upper H_{c2} magnetic field strengths the superconductor is in the mixed or vortex state. The second variable that determines the existence of that state is the temperature $T < T_c$, where T_c denotes the critical phase transition temperature [Tilley and Tilley 1974; Tinkham 1975; Orlando and Delin 1991; Cyrot and Pavuna 1992; Blatter et al. 1994; Brandt 1995; Lüthi 2005; Fossheim and Sudbø 2004]. Magnetic flux can penetrate a type-II superconductor in the form of Abrikosov vortices (also called flux lines, flux tubes, or fluxons) each carrying a quantum of magnetic flux. These tiny vortices of supercurrent tend to arrange themselves in a triangular or quadratic flux-line lattice [Cyrot and Pavuna 1992; Fossheim and Sudbø 2004] which is more or less perturbed by material inhomogeneities that pin the flux lines. Pinning is caused by imperfections of the crystal lattice, such as dislocations, point defects grain boundaries, etc. Hence a honeycomb-like pattern of the vortex array presents some thermomechanical properties.

In the natural state of any superconductor the thermomechanical field comes from atomic and/or molecular interactions both within crystalline (solid) and amorphous (fluid) states of the material in the presence of temperature changes. Such a situation transfers itself to the vortex state as well.

Since the vortices are formed by the applied magnetic field and the supercurrent flows around each vortex, there are also Lorentz force interactions among the vortices. Those interactions form an origin of an additional thermomechanical (stress) field occurring in the type-II superconductor. Near the lower critical magnetic intensity limit H_{c1} , this field has an elastic character. However, if the density of the supercurrent is above its critical value and/or the temperature is sufficiently high, a flow of vortex lines occurs in the superconducting body. Within such a situation vortices behave rather as a fluid than as an

Keywords: magnetic vortex array mechanics, superconductivity, surface waves in unconventional media.
The paper has been partially supported by MEiN 1101/T02/2006/30 grant.

elastic lattice. The fluidity of the vortex array is also observed when the applied magnetic field tends to its upper critical limit H_{c2} (same references as on page 1097). In this way we meet a very interesting situation in a type-II superconductor. We can say that there are two coexisting thermomechanical fields in the medium. One field is of a pure thermoelastic character coming from the mechanical properties of the crystal lattice of the superconductor. The second field comes from the vortex array, which keeps its thermoelastic character near the lower magnetic field strength limit H_{c1} and transfers smoothly into a "fluid" near the upper magnetic field strength limit H_{c2} . The above phenomenon (transfer and coexistence) occurs in the $\{(H(T), T) : H_{c1} < H < H_{c2}, T < T_c\}$ space. However, the vortex field also has a viscous character. The motion of vortices is damped by a force proportional to the vortex velocity. There are two reasons for that damping. The first reason comes from simultaneous interactions among magnetic, mechanical, and thermal fields. The second reason occurs because the resistivity in area of vortex creep is the same as the resistivity of a current which would flow inside the vortex core. Hence the viscosity coefficient reads, from [Cyrot and Pavuna 1992],

$$\eta = \frac{\Phi_0 \mu_0 H_{c2}}{\rho_n}, \quad (1)$$

where Φ_0 is the magnetic flux, μ_0 denotes the permeability of vacuum, and ρ_n is the resistivity in the normal state.

Since the vortices may be described within a macroscopic phenomenology, except for the description presented in [Blatter et al. 1994; Ketterson and Song 1999], an unconventional model of magneto-thermomechanical processes running in the vortex array in a continuous manner has been proposed [Maruszewski and Restuccia 1999; Maruszewski 1998; 2007; Maruszewski et al. 2007]. Following that model, field equations have been obtained and their form shows that not only diffusion, creep, or flow of the vortices are possible in the superconducting material but also wave propagation (transmission of signals) [Restuccia and Maruszewski 1998; 1999; Maruszewski and Restuccia 2001; Drzewiecki et al. 2002a; 2002b].

This paper deals with Love's wave propagation along the superconducting heterostructure consisting of two II-type superconductors (the layer on the half-space) placed in an external magnetic field perpendicular to characteristic planes of the structure. The analysis has been based on [Achenbach 1976; Maruszewski et al. 2007; Maruszewski and van de Ven 1995; Drzewiecki et al. 2004]. We focus only on magnetoelastic interactions within the vortex lattice (the applied magnetic field intensity is close to the lower magnetic field limit H_{c1} , satisfying the inequality $H^0 > H_{c1}$).

2. Magnetoelastic Love's waves

Let us consider a superconducting heterostructure consisting of a layer of thickness h and a half-space. That heterostructure is placed in an external constant magnetic field $\mathbf{H} = [H^0, 0, 0]$. Along the interface between the structure components Love's wave propagates with a velocity v . The propagation direction is x_2 . The complete geometry of the problem is presented in Figure 1.

The general linearized equations describing the propagation of harmonic waves in the above heterostructure (solely in the vortex field) read as follows (see [Maruszewski and Restuccia 1999; Maruszewski 2007; Maruszewski et al. 2007; Maruszewski and van de Ven 1995; Restuccia and Maruszewski 1999;

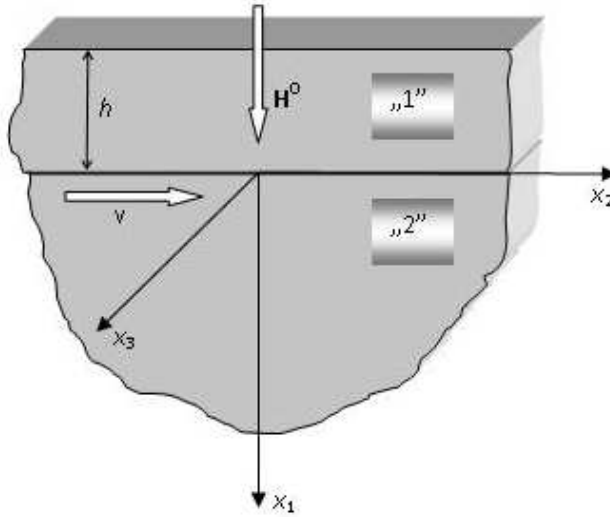


Figure 1. Geometry of the problem.

Drzewiecki et al. 2002a]):

$$\begin{aligned} \mu u_{i,jj} + \eta \dot{u}_{i,jj} + (\lambda + \mu) u_{j,ij} + \frac{1}{3} \eta \dot{u}_{j,ij} + \mu_0 (h_{r,i} - h_{i,r}) H_r^0 - \rho \ddot{u}_i &= 0, \\ \lambda_0^2 h_{i,kk} - h_i + u_{i,k} H_k^0 - u_{k,k} H_i^0 &= 0. \end{aligned} \tag{2}$$

Since the viscosity coefficient (1) is very small we neglect the damping features in the vortex field in the sequel. The linearization has been done assuming the total magnetic field in the structure of the form

$$\mathbf{H} = \mathbf{H}^0 + \mathbf{h}, \quad |\mathbf{h}| \ll |\mathbf{H}^0|, \quad \mathbf{H}^0 = [H_1^0, 0, 0], \quad H_1^0 = \text{const}, \tag{3}$$

where \mathbf{h} is the small contribution to the total magnetic field \mathbf{H} coupled with the displacement vector \mathbf{u} . Lamé's constants, λ and μ , have been calculated from H^0 and H_{c1} [Blatter et al. 1994; Ketterson and Song 1999], μ_0 is the permeability of vacuum, and λ_0 is the London penetration depth. Note that Equations (2) are valid simultaneously for both arrays 1 and 2 in Figure 1.

Now assuming that the solutions of (2) in the geometry shown in Figure 1 are in the following form

$$f(x_1, x_2, t) = \bar{f}(x_1) \exp[i(\omega t - kx_2)], \tag{4}$$

where $f(x_1, x_2, t)$ stands for all fields in (2), that is,

$$f(x_1, x_2, t) = \{ {}^0u_3, {}^0h_3 \}(x_1, x_2, t), \tag{5}$$

where Love's mode concerns only the u_3 component, Equations (2) may be rewritten in the form (see [Achenbach 1976; Maruszewski and van de Ven 1995])

$$\mu_K u_{3,jj}^K - \mu_0 h_{3,1}^K H_1^0 - \rho_K \ddot{u}_3^K = 0 \quad \text{and} \quad \lambda_0 h_{3,jj}^0 - k_3^K + u_{3,1}^K H_1^0 = 0 \quad \text{both with } j = 1, 2, \tag{6}$$

where $K = 1, 2$ distinguishes the layer (1) from the half-space (2).

To facilitate the investigation of (6) and the analysis of its solutions, we convert the above formula to a dimensionless form with the help of the relations

$$\begin{aligned}
 x_1 = hx, \quad x_2 = hy, \quad x_3 = hz, \quad t = T\tau, \quad T = h\sqrt{\frac{\rho_1}{\mu_1}} = \frac{h}{v_{T1}}, \\
 H_1^0 = H_{c1}H_0, \quad h_3^K = H_{c1}h_z^K, \quad u_3^K = hu_z^K, \quad \Omega = \omega T, \quad V = \frac{v}{v_{T1}}, \\
 k = \frac{\omega}{v} = \frac{\Omega}{vT} = \frac{\Omega}{Vh}, \quad \tilde{\rho}_K = \frac{\rho_K h^2}{T^2 \mu_1}, \quad \tilde{\lambda}_K = \frac{\lambda_K}{\mu_1}, \quad \tilde{\mu}_K = \frac{\mu_K}{\mu_1}, \quad \tilde{\mu}_0 = \frac{\mu_0 H_{c1}^2}{\mu_1}, \quad \tilde{\lambda}_{0K}^2 = \frac{\lambda_{0K}^2}{h^2},
 \end{aligned} \tag{7}$$

where v_{TK} denotes the transverse elastic mode phase velocity in the layer and the substrate.

Recasting the set (6) dimensionless form using Equations (4), (5), and (7), we obtain

$$\begin{aligned}
 \tilde{\mu}_K \frac{d^2 u_z^K}{dx^2} + \frac{\Omega^2}{V^2} (V^2 \tilde{\rho}_K - \tilde{\mu}_K) u_z^K + \tilde{\mu}_0 H_0 \frac{dh_z^K}{dx} = 0, \\
 \tilde{\lambda}_{0K} \frac{d^2 h_z^K}{dx^2} - \left(\tilde{\lambda}_{0K}^2 \frac{\Omega^2}{V^2} + 1 \right) h_z^K + H_0 \frac{du_z^K}{dx} = 0.
 \end{aligned} \tag{8}$$

The boundary and jump conditions for the variables in (7) across the characteristic planes of the heterostructure are

$$\text{at } x = -1 : \quad \begin{cases} h_z^1 = 0 & \text{(continuity of the tangent component of the magnetic field),} \\ u_{z,x}^1 = 0 & \text{(the plane is stress free),} \end{cases}$$

and

$$\text{at } x = 0 : \quad \begin{cases} [[h_z]] = h_z^1 - h_z^2 = 0, \\ [[u_z]] = u_z^1 - u_z^2 = 0 & \text{(continuity of displacements),} \\ [[u_{z,x}]] = u_{z,x}^1 - u_{z,x}^2 = 0 & \text{(continuity of stress).} \end{cases}$$

The characteristic equation of (8) for both layer and substrate reads

$$\lambda_{0K}^2 \mu_K p^4 + [\lambda_{0K}^2 B_K(\Omega, V) - F_K(\Omega, V) \mu_K - \mu_0 H_0^2] p^2 - F_K(\Omega, V) B_K(\Omega, V) = 0, \tag{9}$$

where the solutions of (8) were assumed to be in the form

$$\{u_z^K, h_z^K\} = \{^0u_z^K, ^0h_z^K\} e^{px} \tag{10}$$

and

$$B_K(\Omega, V) = \frac{\Omega^2}{V^2} (V^2 \tilde{\rho}_K - \tilde{\mu}_K), \quad F_K(\Omega, V) = \tilde{\lambda}_{0K}^2 \frac{\Omega^2}{V^2} + 1 > 0.$$

The waves under consideration propagate if the solutions of (10), u_z^1 and h_z^1 , are convergent, that is, the squares of the roots p_1 and p_2 of the characteristic equation (9) in the layer are both real and p_3 and p_4 in the substrate are of opposite signs. To avoid divergence of solutions (10) in the substrate, we assume additionally that u_z^2 and h_z^2 vanish if $x \rightarrow \infty$. The requirements above for p_1 – p_4 are satisfied, if for

$$\begin{aligned}
 p_1, p_2 : B_1(\Omega, V) < 0 \rightarrow V^2 < \tilde{\mu}_1 / \tilde{\rho}_1, \\
 p_3, p_4 : B_2(\Omega, V) > 0 \rightarrow V^2 > \tilde{\mu}_2 / \tilde{\rho}_2.
 \end{aligned}$$

Hence we obtain a very important condition for Love’s phase velocity wave if its propagation is possible

$$\tilde{\mu}_2/\tilde{\rho}_2 < V^2 < \tilde{\mu}_1/\tilde{\rho}_1 \quad (\text{dimensionless form})$$

or

$$v_{T2} < v < v_{T1} \quad (\text{dimensional form}). \tag{11}$$

That is a new result and it differs from the classical result for the elastic Love’s wave propagation condition which run along interface between two elastic materials (layer and substrate); see [Achenbach 1976]. For the latter case the inequality (11) is reciprocal.

As a result, the solutions (10) for the layer are, in detailed form,

$$u_z^1 = S_1 e^{p_1 x} + S_2 e^{-p_1 x} + S_3 e^{p_2 x} + S_4 e^{-p_2 x} \tag{12}$$

and

$$h_z^1 = -M(p_1, \Omega, V) S_1 e^{p_1 x} + M(p_1, \Omega, V) S_2 e^{-p_1 x} - M(p_2, \Omega, V) S_3 e^{p_2 x} - M(p_2, \Omega, V) S_4 e^{-p_2 x}, \tag{13}$$

where

$$M(p_i, \Omega, V) = \frac{p_i}{\tilde{\mu}_0 H_0} + \frac{\Omega^2 (V^2 - 1)}{V^2 H_0 p_i}, \quad i = 1, 2. \tag{14}$$

For the substrate the solutions are

$$u_z^2 = S_5 e^{-p_3 x}, \quad h_z^1 = N(p_3, \Omega, V) S_5 e^{-p_3 x}, \quad \text{where } N(p_3, \Omega, V) = \frac{\tilde{\mu}_2 p_3}{\tilde{\mu}_0 H_0} + \frac{\Omega^2 (V^2 \tilde{\rho}_2 - \tilde{\mu}_2)}{V^2 \tilde{\mu}_0 H_0 p_3}.$$

Now using solutions (12)–(15) for the boundary and jump conditions, we arrive at the homogeneous algebraic equations

$$W_{mn}(\Omega, V) S_n = 0, \quad m, n = 1, \dots, 5. \tag{15}$$

Equation (15) has nontrivial solutions only if its determinant satisfies the relation below

$$\det W_{mn}(\Omega, V) = 0. \tag{16}$$

We have thus proved that Love’s waves can propagate in a superconducting heterostructure and that their dispersion relation is given by (16).

3. Numerical results

The numerical analysis of the problem considered in the paper has been done for the superconducting heterostructure consisting of two ceramics, YBa₂Cu₃O_{6+x} (YBCO) as the layer and La_{1-x}Sr_xCuO₄ as the half-space. All the necessary data are collected in Table 1. The results of using these data in the dispersion relation (16) are presented in Figures 2–3.

The first very important result from Equation (16) is that the waves considered are able to propagate only if the thickness of the layer satisfies

$$10^{-7} < h < 10^{-5}. \tag{17}$$

Then from Figures 2–3 it is seen that there are two frequency regions where waves are nondispersive. This means that they can be stably modulated in order to transmit signals carrying information. Between

Quantity	YBa ₂ Cu ₃ O _{6+x}	La _{1-x} Sr _x CuO ₄	Unit
λ_0	$4 \cdot 10^{-7}$	$2.5 \cdot 10^{-7}$	m
ρ	10^{-6}	$5 \cdot 10^{-6}$	kg/m ³
H_{c1}	$0.01/\mu_0$	$0.01/\mu_0$	A/m
H_{c2}	$120/\mu_0$	$120/\mu_0$	A/m
ξ	10^{-9}	$1.5 \cdot 10^{-9}$	m
H_c	$H_{c2}\xi/(\lambda_0\sqrt{2})$	$H_{c2}\xi/(\lambda_0\sqrt{2})$	A/m
c_{11}	$\mu_0 H_1^{02}/4\pi$	$\mu_0 H_1^{02}/4\pi$	N/m ²
c_{66}	$(H_c^2/16\pi)(1-0.29b)(1-b)^2b$	$(H_c^2/16\pi)(1-0.29b)(1-b)^2b$	N/m ²
b	$\mu_0 H_1^0/H_{c2}$	$\mu_0 H_1^0/H_{c2}$	Vs/Am
μ	c_{66}	c_{66}	N/m ²
λ	$c_{11}-2c_{66}$	$c_{11}-2c_{66}$	N/m ²
μ_0	$4\pi \cdot 10^{-7}$	$4\pi \cdot 10^{-7}$	Vs/Am

Table 1. Data for the superconducting heterostructure.

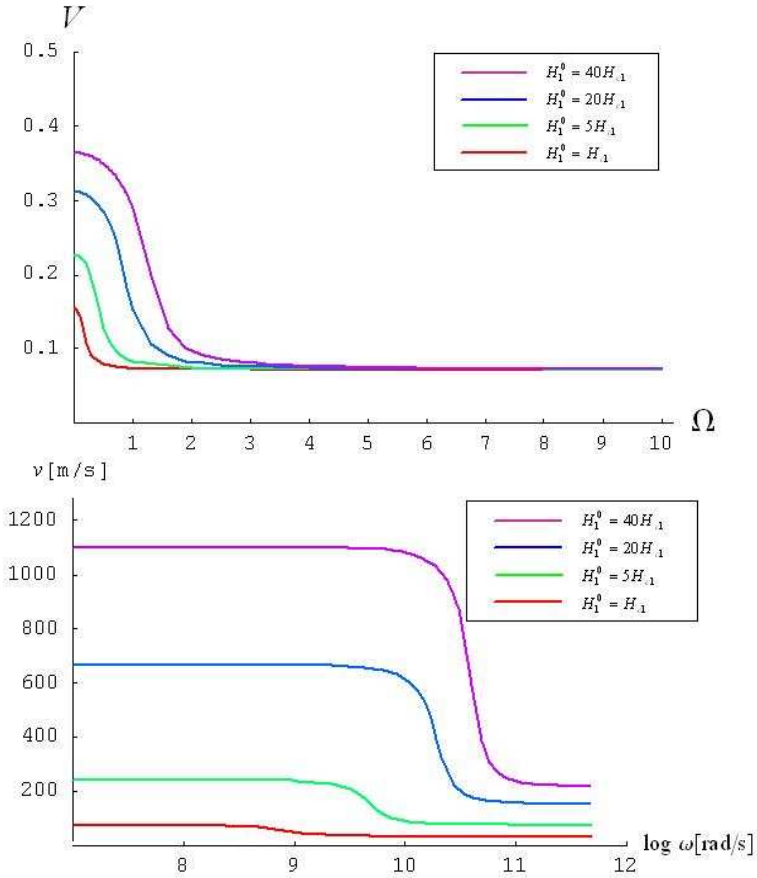


Figure 2. Dispersion for various intensities of applied magnetic field and fixed layer thickness $h = 10^{-7}$ m for the dimensionless (top) and dimensional (bottom) version.

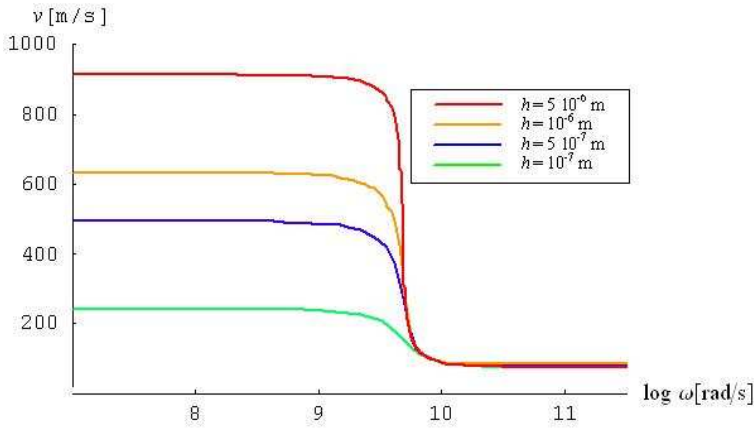


Figure 3. Dispersion for various layer thicknesses and fixed magnetic field intensities $H_1^0 = 20H_{c1}$.

those regions there is a forbidden interval (for frequencies)

$$10^8 < \omega < 10^{12}, \quad (18)$$

where strong dispersion of Love's wave is observed.

These properties are not typical if we compare them to those related to classical ones, concerning waves in a elastic material heterostructure.

4. Conclusions

- (i) The paper proves that Love's waves can propagate within a vortex array existing in a superconducting heterostructure.
- (ii) The anomalous range of the phase velocity of (11) indicates that in this case the layer should have a higher vortex density and the substrate should have a lower vortex density contrary to the classical elastic material case.
- (iii) The thickness of the layer allowing wave propagation is limited; see Equation (17).
- (iv) There are two dispersionless regions concerning Love's modes in the structure. The similar property has been observed in the case of bulk waves in the vortex array existing in the superconducting space [Drzewiecki et al. 2002a; 2004].
- (v) There is a forbidden region where the dispersion is very high.
- (vi) The waves under consideration propagate with an acoustic phase velocity and an optical wave frequency. This is another anomalous feature about them.

References

- [Achenbach 1976] J. Achenbach, *Wave propagation in elastic solids*, North-Holland, Amsterdam, 1976.
- [Blatter et al. 1994] G. Blatter, M. V. Feigelman, V. B. Geshkenbein, A. I. Larkin, and V. M. Vinokur, "Vortices in high-temperature superconductors", *Rev. Mod. Phys.* **66** (1994), 1125–1388.

- [Brandt 1995] E. H. Brandt, “The flux-line lattice in superconductors”, *Rep. Prog. Phys.* **58** (1995), 1465–1594.
- [Cyrot and Pavuna 1992] M. Cyrot and D. Pavuna, *Introduction to superconductivity and high- T materials*, World Scientific, Singapore, 1992.
- [Drzewiecki et al. 2002a] A. Drzewiecki, J. A. Koł odziej, and B. T. Maruszewski, “Viscomagnetoelastic interactions in a vortex array in type-II superconductor”, *Tech. Mech.* **22**:3 (2002), 167–174.
- [Drzewiecki et al. 2002b] A. Drzewiecki, B. T. Maruszewski, and L. Restuccia, “Waves in a type-II superconducting halfspace. Vortex lattice case”, pp. 41–49 in *Structured media TRECOP’ 01*, edited by B. T. Maruszewski, Publ. House of Poznan University of Technology, Poznan, 2002.
- [Drzewiecki et al. 2004] A. Drzewiecki, B. T. Maruszewski, J. A. Kołodziej, and L. Restuccia, “Rayleigh and Love’s waves in a vortex field of the II-type superconductor”, pp. 111–127 in *Trends in continuum physics TRECOP’04*, edited by B. T. Maruszewski et al., Publ. House of Poznan University of Technology, Poznan, 2004.
- [Fossheim and Sudbø 2004] K. Fossheim and A. Sudbø, *Superconductivity, physics and applications*, Wiley, Chichester, 2004.
- [Ketterson and Song 1999] J. B. Ketterson and S. N. Song, *Superconductivity*, Cambridge University Press, Cambridge, 1999.
- [Lüthi 2005] B. Lüthi, *Physical acoustics of the solid state*, Springer, Berlin, 2005.
- [Maruszewski 1998] B. T. Maruszewski, “Superconducting fullerenes in a nonconventional thermodynamical model”, *Arch. Mech.* **50** (1998), 497–508.
- [Maruszewski 2007] B. T. Maruszewski, “On a nonclassical thermoviscoelastic stress in the vortex field in type-II superconductor”, *Phys. Status Solidi (b)* **244** (2007), 919–927.
- [Maruszewski and Restuccia 1999] B. T. Maruszewski and L. Restuccia, “Mechanics of vortex lattice in superconductors. Phenomenological approach”, pp. 220–230 in *Trends in continuum physics, TRECOP’98*, edited by B. T. Maruszewski et al., World Scientific, Singapore, 1999.
- [Maruszewski and Restuccia 2001] B. T. Maruszewski and L. Restuccia, “Magnetoelastic waves in a vortex fluid in a type-II high T_c superconductors”, pp. 47–50 in *Fourth international congress on thermal stresses THERMAL STRESSES’ 01*, edited by N. Noda and R. B. Hetnarski, Osaka, 2001.
- [Maruszewski and van de Ven 1995] B. Maruszewski and A. A. F. van de Ven, “Plasmomagnetoelastic waves in a semiconducting heterostructure. II. SH-magnetoelastic modes,” in *Nonlinear waves in solids*, edited by J. L. Wegner and F. R. Norwood, AMR **137**, ASME, New York, NY, 1995.
- [Maruszewski et al. 2007] B. T. Maruszewski, A. Drzewiecki, and R. Starosta, “Anomalous features of thermomagnetoelastic field in a vortex array in superconductor, propagation of Love’s waves”, *J. Therm. Stresses* **30** (2007), 1049–1065.
- [Orlando and Delin 1991] T. P. Orlando and K. A. Delin, *Foundations of applied superconductivity*, Addison-Wesley Publ. Co., Reading, 1991.
- [Restuccia and Maruszewski 1998] L. Restuccia and B. T. Maruszewski, “Magnetoelastic surface waves in superconductors”, pp. 413–418 in *Suplemento ai Rendiconti del Circolo Matematico di Palermo, Serie II Numero 57*, 1998.
- [Restuccia and Maruszewski 1999] L. Restuccia and B. T. Maruszewski, “Vortex lattice waves in a high- T_c superconductor”, pp. 89–92 in *Third international congress on thermal stresses THERMAL STRESSES’99*, edited by J. J. Skrzypek and R. B. Hetnarski, Cracow, 1999.
- [Tilley and Tilley 1974] D. R. Tilley and J. Tilley, *Superfluidity and superconductivity*, Van Nostrand Reinhold Co., New York, 1974.
- [Tinkham 1975] M. Tinkham, *Introduction to superconductivity*, McGraw-Hill Book Co., 1975.

Received 7 Feb 2008. Accepted 25 Mar 2008.

BOGDAN T. MARUSZEWSKI: bogdan.maruszewski@put.poznan.pl
Poznan University of Technology, Institute of Applied Mechanics, ul. Piotrowo 3, 60-965 Poznan, Poland

ANDRZEJ DRZEWIECKI: andrzej.drzewiecki@put.poznan.pl
Poznan University of Technology, Institute of Applied Mechanics, ul. Piotrowo 3, 60-965 Poznan, Poland

ROMAN STAROSTA: roman.starosta@put.poznan.pl
Poznan University of Technology, Institute of Applied Mechanics, ul. Piotrowo 3, 60-965 Poznan, Poland

ON NONLINEAR KINETIC EFFECTS IN THE VORTEX ARRAY IN SUPERCONDUCTORS

BOGDAN T. MARUSZEWSKI

The motion of vortices in a type II superconductor is accompanied by a heat flux coming from the vortices themselves. It leads to such thermogalvanomagnetic effects like the Nernst, Ettingshausen and Righi-Leduc effects. Moreover, besides the linear thermoelectric Seebeck and Peltier effects, the Hall effect also occurs. That situation seems to be very interesting because it does not take place during common electric conductivity processes but during diffusion and/or creep of magnetic vortices in superconductors. It is known that each vortex line carries a quantum of magnetic field and around it a supercurrent flows. But inside the vortex core a normal current exists. Therefore, the above kinetic linear and nonlinear effects are possible in the vortex array. The paper aims at the formulation of an unconventional thermodynamical model of the above kinetic phenomena including their relaxation properties. As a result we have obtained forms of the constitutive laws related to those processes.

1. Introduction

Magnetic flux can penetrate a type II superconductor in the form of Abrikosov vortices (also called flux lines, flux tubes or fluxons) each carrying a quantum of magnetic flux [Tilley 1974; Tinkham 1975; Orlando and Delin 1991; Cyrot and Pavuna 1992; Blatter et al. 1994; Brant 1995]. These tiny vortices tend to arrange themselves in a triangular or quadratic flux-line lattice, which is more or less perturbed by material inhomogeneities that can pin those flux lines. Pinning is caused by imperfections of a crystal lattice of a superconducting material, such as dislocations, point effects, grain boundaries, etc. Hence a honeycomb or quadratic pattern of the vortex array presents some mechanical properties. They come mainly from force interactions observed in the field of vortices. Indeed, the vortices are created by the applied magnetic field which penetrates the superconductor. Now, around each vortex the supercurrent flows, so there are Lorentz-like force interactions among those lines. Such a situation is a cause of the previously mentioned mechanical (stress) field occurring in the medium, besides the common one coming from the type II superconducting material itself. That field near the lower critical magnetic intensity limit H_{C1} is also of an elastic character. However, if the intensity of the supercurrent is above its critical value, the temperature is sufficiently high, and/or the value of the applied magnetic field tends to its upper critical limit H_{C2} , a flow (creep or diffusion) of the vortices occurs. The vortex array then loses its configuration and behaves as a fluid.

It has been observed that the vortex motion is accompanied by an energy dissipation. That motion is damped by a force proportional to the velocity of the vortex field point. Hence, except for the elastic properties, the vortex field is also of a viscous character. The resistivity in area of the vortex motion is the same as the resistivity of a current which would flow inside the vortex core where the material is

Keywords: nonlinear kinetics in magnetic vortices, thermodynamical modelling of vortex field, superconductivity.

in the normal state and where Ohm's law holds true. The result of the above superconducting material properties is a temperature gradient along the vortices and a heat flux that occurs in the vortex field.

In superconductors the vortex lattice mostly consists of a parallel straight vortex line set whose cross section forms the previously mentioned symmetries [Orlando and Delin 1991; Cyrot and Pavuna 1992]. However, recent research shows that the vortex lines can be curved or even tangled along the material [Blatter et al. 1994; Brant 1995]. Moreover, since the vortices form, among others, sets called twisted triplets, twisted quadruplets, single loops or pairs [Schönenberger et al. 1997], the vortex field can be considered even in three dimensions. Because of the fact that each vortex line has a sign (has the definite vorticity), lines of the opposite signs annihilate.

In the paper we focus solely on the kinetic part of interactions occurring in the vortex field of the type II superconductor. The subject of our considerations are the reciprocal links between normal current, supercurrent, heat flux and vortex diffusion flux in the vortex array. Those links are the source of kinetic laws, both linear (Fourier's, Fick's, Ohm's, London's, Soret's, Dufour's, Seebeck's, Peltier's, etc.) and nonlinear (Righi-Leduc's, Ettingshausen-Nernst's, Hall's, etc.), all of which describe thermogalvanoelectromagnetic effects extended on interactions with the supercurrent [Maruszewski 1984; 1988; Sirotnin and Šaskolskaya 1979; Freimuth 2002]. All these laws have a purely kinetic character but from the thermodynamical model presented in the paper laws of relaxation-kinetic nature like the generalized Maxwell-Cattaneo equation, the generalized Fick-Nonnemacher equation, and the generalized first London's equation result as well [Kluitenberg 1981; Restuccia and Kluitenberg 1987].

2. The unconventional thermodynamical model

Let us consider the elastic vortex array that exists in the type II superconductor placed in an external magnetic field. For the sake of simplicity we deal solely with soft (depinned) vortices to avoid direct material connections between the superconducting medium and the vortex medium (to ensure our description is related only to the vortex array).

Following the above properties the unconventional (extended-like) thermodynamical model for the viscoelastic field of vortices in the type II superconductor is presented below. We have assumed that the mass density ρ of the vortex field concerns the density of the material in the normal state as the counterpart in the mixed type II superconductor [Kopnin 2002] (that is, the mass of the normal part of the body related to the total volume of the material), and the energy dissipation occurs only because of the Ohmic-like resistivity (normal-state resistivity) inside the vortex core [Blatter et al. 1994]. Hence the general form of the state vector (the set of independent variables) reads [Maruszewski and Restuccia 1999; Schönenberger et al. 1997]

$$C = \{\varepsilon_{ij}, \varphi, A_i, T, T_{,i}, c, c_{,i}, \psi, \psi^*, \psi_{,i}, \psi_{,i}^*, q_i, j_i^c, j_i^S\}, \quad (1)$$

where ε_{ij} denotes the strain tensor, φ and A_i are the scalar and vector potentials, respectively, T is the absolute temperature, ψ is the order parameter (the wave function of a Cooper pair) and ψ^* is its complex conjugate, j_i^S is the supercurrent density, j_i^c is the diffusion flux of vortices and q_i is the heat flux in the vortex field. c denotes the concentration of vortices defined as $c = \frac{\rho}{\rho_{tot}}$, where ρ_{tot} is the density of the superconducting material.

The fundamental laws, which govern the set (1), are the *balances*

$$\rho \dot{c} + j_{k,k}^c = 0, \quad \rho \dot{v}_k - \sigma_{jk,j} - \epsilon_{kij} j_i B_j - f_k = 0, \quad \epsilon_{ijk} \sigma_{jk} = 0, \quad \rho \dot{U} - \sigma_{ji} v_{i,j} + q_{k,k} - j_i \mathcal{E}_i - \rho r = 0, \quad (2)$$

the *evolution equations*

$$\dot{q}_k^* - Q_k(C) = 0, \quad \dot{j}_k^c - j_k^c(C) = 0, \quad \dot{j}_k^S - j_k^S(C) = 0, \quad \dot{\psi} - \Psi(C) = 0, \quad \dot{\psi}^* - \Psi^*(C) = 0, \quad (3)$$

where the superimposed asterisk denotes the Zaremba–Jaumann time derivative, *Maxwell's equations*

$$\epsilon_{ijk} E_{k,j} + \frac{\partial B_i}{\partial t} = 0, \quad \epsilon_{ijk} H_{k,j} - j_i = 0, \quad D_{k,k} = 0, \quad B_{k,k} = 0, \quad (4)$$

where $j_i = j_i^N + j_i^S$, and the *balance of superelectrons* [van de Ven 1991]

$$\frac{\partial n^S}{\partial t} + j_{k,k}^S = N^S(C), \quad j_{k,k}^S - N^S(C) = (\psi^* \psi_{,k} + \psi \psi_{,k}^*) - [\psi^* \Psi(C) + \psi \Psi^*(C)]. \quad (5)$$

Here v_k denotes the velocity of the vortex field point, σ_{ik} is the viscoelastic stress tensor, j_i^N is the normal current, B_j is the magnetic induction and H_j is the magnetic field strength, f_k is the body force, U is the internal energy density, \mathcal{E}_i is the electromotive intensity in a moving frame and E_i is the electromotive intensity in a resting frame, r is the heat source distribution, and n^S is the number density of superelectrons (Cooper pairs). The sets (2), (3), (4), and (5) consist of the equation whose form ensures conservation of the vortex mass in the sense indicated above, the momentum balance in the vortex field where elastic interactions are due to the Lorentz force, the equation determining the symmetry of the stress tensor, the internal energy balance of the vortex field where the dissipation term comes only from the Joule-like heat produced by the total current, the first law of thermodynamics, the evolution equation for heat flux, the evolution equation for diffusion flux, the evolution equation for supercurrent, the evolution equations for Cooper pairs wave function as the order parameter (internal variable) evolution equations, the electromagnetic field evolution equations, and the balance equations for superelectrons. Such equations form the structure of an unconventional thermodynamical model based on extended thermodynamics with internal variables [Maruszewski 1990]. The extended-like thermodynamical description has been chosen here since all the interactions run within low temperatures. Moreover, for the electromagnetic field quantities the following relations hold

$$D_k = \epsilon E_k, \quad B_k = \mu_0 H_k, \quad E_k = -\varphi_{,k} - \frac{\partial A_k}{\partial t}, \quad B_k = \epsilon_{ijk} A_{j,i}, \quad \mathcal{E}_i = E_i + \epsilon_{ijk} v_j B_k.$$

In the sequel we follow the assumption that φ vanishes because of gauging [Orlando and Delin 1991; Yeh and Chen 1993].

The use of the second law of thermodynamics in the form of entropy inequality is to ensure solutions of the set (2)–(5) to be related to description of real physical processes.

The *entropy inequality* is taken in its classical form

$$\rho \dot{S} + \Phi_{k,k} - \frac{\rho r}{T} \geq 0, \quad (6)$$

where S is the entropy density and Φ_k denotes the entropy flux.

Now, the inequality (6) gives us a possibility of determining all the constitutive functions which in our case form the set of dependent variables

$$Z = \{\sigma_{ij}, \mu^c, U, Q_k, \Psi, \Psi^*, J_k^c, J_k^S, N^S, S, \Phi_k\}, \quad Z = Z(C). \tag{7}$$

We omit from now on investigations and analysis of the above thermodynamical structure for laws concerning states of the vortex field [Maruszewski 2007; Maruszewski et al. 2007]. Our attention is focused only on laws dealing with processes running in the vortex array, that is, kinetic relations.

A detailed analysis of the entropy inequality and the introduction of the free energy density

$$F = U - TS, \quad F = F^N(\varepsilon_{ij}, T, c, q_i, j_i^c, j_i^S) + F^S(\varepsilon_{ij}, T, c, A_i, \psi, \psi^*, \psi_{,k}, \psi_{,k}^*)$$

[van de Ven 1991; Maruszewski 1998; Maugin 1992] lead us to the residual inequality

$$-\frac{1}{T}q_k T_{,k} - h_c j_k^c c_{,k} + j_i^N \mathcal{E}_i - \rho \frac{\partial F}{\partial q_i} \dot{q}_i - \rho \frac{\partial F}{\partial j_i^c} \dot{j}_i^c - \rho \frac{\partial F}{\partial j_i^S} \dot{j}_i^S - \left[\rho \frac{\partial F}{\partial \psi} - \left(\rho \frac{\partial F}{\partial \psi_{,k}} \right)_{,k} \right] \frac{\partial \psi}{\partial t} - \left[\rho \frac{\partial F}{\partial \psi^*} - \left(\rho \frac{\partial F}{\partial \psi_{,k}^*} \right)_{,k} \right] \frac{\partial \psi^*}{\partial t} \geq 0, \tag{8}$$

which stands for the kinetic part of the modelled and described interaction among the elastic, thermal, diffusion, and electromagnetic fields in the vortex array. Here $h_c = \partial \mu^c / \partial c$ [Maruszewski 1997], where μ^c is the vortex chemical potential,

As we see, the residual inequality has a bilinear form and can be presented as follows:

$$J_\alpha X_\alpha \geq 0, \tag{9}$$

where J_α are the generalized fluxes and X_α denote generalized forces. Based on the irreversible thermodynamical model, the relation between generalized fluxes and forces is linear

$$J_\alpha = \ell^{\alpha\beta} X_\beta, \tag{10}$$

where the phenomenological coefficients $\ell^{\alpha\beta}$ satisfy Onsager–Casimir’s reciprocity relations

$$\ell^{\alpha\beta} = \ell^{\beta\alpha}. \tag{11}$$

The use of (9), (10), and (11) in (8) allows us to determine matrices of generalized fluxes, forces and phenomenological coefficients, as follows:

$$J_\alpha = \begin{pmatrix} q_k \\ j_k^c \\ j_k^N \\ \dot{q}_k \\ j_k^c \\ j_k^S \\ \dot{\psi} \\ \dot{\psi}^* \end{pmatrix}, \quad X_\beta = \begin{pmatrix} -(1/T)T_{,k} \\ -h_c c_{,k} \\ \mathcal{E}_i \\ -\rho \partial F / \partial q_i \\ -\rho \partial F / \partial j_i^c \\ -\rho \partial F / \partial j_i^S \\ -[\rho \partial F / \partial \psi - (\rho \partial F / \partial \psi_{,k})_{,k}] \\ -[\rho \partial F / \partial \psi^* - (\rho \partial F / \partial \psi_{,k}^*)_{,k}] \end{pmatrix}, \tag{12}$$

$$\ell^{\alpha\beta} = \begin{pmatrix} \ell^{11} & \ell^{12} & \ell^{13} & 0 & 0 & 0 & 0 & 0 \\ \ell^{21} & \ell^{22} & \ell^{23} & 0 & 0 & 0 & 0 & 0 \\ \ell^{31} & \ell^{32} & \ell^{33} & 0 & 0 & 0 & 0 & 0 \\ 0 & 0 & 0 & \ell^{44} & \ell^{45} & \ell^{46} & 0 & 0 \\ 0 & 0 & 0 & \ell^{54} & \ell^{55} & \ell^{56} & 0 & 0 \\ 0 & 0 & 0 & \ell^{64} & \ell^{65} & \ell^{66} & 0 & 0 \\ 0 & 0 & 0 & 0 & 0 & 0 & \ell^{77} & \ell^{78} \\ 0 & 0 & 0 & 0 & 0 & 0 & \ell^{87} & \ell^{88} \end{pmatrix}. \tag{13}$$

The basic thermogalvanomagnetic effects and effects which include relaxation features of the considered processes can be described, in the first approximation, if the phenomenological coefficients are assumed in the following form [Maruszewski 1984; Sirotin and Šaskolskaya 1979] $\ell_{ij}^{\alpha\beta}(H_k) = \ell_{ij}^{\alpha\beta(0)} + \ell_{ijk}^{\alpha\beta(1)} H_k$. After laborious but routine calculations, the final forms of the expected kinetic relations both without and with relaxation properties (for the sake of simplicity and easy interpretation we present them in the isotropic form assuming that $\ell_{kj}^{\alpha\beta(0)} = \ell^{\alpha\beta(0)} \delta_{kj}$, $\ell_{kjl}^{\alpha\beta(1)} = \ell^{\alpha\beta(1)} \epsilon_{kjl}$, [Orlando and Delin 1991; Cyrot and Pavuna 1992; Maruszewski 1984; 1988; 1990; 1997; Sirotin and Šaskolskaya 1979; Freimuth 2002; Kluitenberg 1981; Restuccia and Kluitenberg 1987]) become the *generalized Fourier law*

$$\mathbf{q} = -\kappa \nabla T + \frac{1}{T} \ell \nabla T \times \mathbf{H} - h_c \kappa^c \nabla c + h_c K^c \nabla c \times \mathbf{H} + \kappa^e \mathcal{E} + N \mathcal{E} \times \mathbf{H}, \tag{14}$$

the *generalized Fick law*

$$\mathbf{j}^c = -\frac{1}{T} \kappa^c \nabla T + \frac{1}{T} K^c \nabla T \times \mathbf{H} - \rho D \nabla c + M h_c \nabla c \times \mathbf{H} + \Sigma^c \mathcal{E} + \Gamma^c \mathcal{E} \times \mathbf{H}, \tag{15}$$

the *generalized Ohm law*

$$\mathbf{j}^N = -\frac{1}{T} \kappa^e \nabla T + \frac{1}{T} N \nabla T \times \mathbf{H} - h_c \Sigma^c \nabla c + \rho D \nabla c + h_c \Gamma^c \nabla c \times \mathbf{H} + \sigma \mathcal{E} + R \mathcal{E} \times \mathbf{H}, \tag{16}$$

the *generalized Maxwell–Cattaneo law*

$$\tau^q \dot{\mathbf{q}} = \kappa \nabla T - \frac{1}{T} \ell \nabla T \times \mathbf{H} + h_c \kappa^c \nabla c - h_c K^c \nabla c \times \mathbf{H} + \kappa^e \mathcal{E} - N \mathcal{E} \times \mathbf{H} - \mathbf{q} - D^c \mathbf{j}^c - D^S \mathbf{j}^S, \tag{17}$$

the *generalized Fick–Nonnenmacher law*

$$\tau^c \dot{\mathbf{j}}^c = \frac{1}{T} \kappa^c \nabla T - \frac{1}{T} K^c \nabla T \times \mathbf{H} + \rho D \nabla c - M h_c \nabla c \times \mathbf{H} + \Sigma^c \mathcal{E} - \Gamma^c \mathcal{E} \times \mathbf{H} - D^q \mathbf{q} - \mathbf{j}^c - D^{Sq} \mathbf{j}^S, \tag{18}$$

and the *generalized first London equation*

$$\tau^S \dot{\mathbf{j}}^S = P^T T \nabla T - \frac{1}{T} R^T \nabla T \times \mathbf{H} + P^c \nabla c - h_c R^c \nabla c \times \mathbf{H} + \frac{1}{\mu_0 \lambda_0^2} \mathcal{E} - R^e \mathcal{E} \times \mathbf{H} - D^q \mathbf{q} - \mathbf{j}^S - D^{cS} \mathbf{j}^c. \tag{19}$$

In Eqs. (14), (15), (16), (17), (18), and (19) we recognize the following phenomena and effects described by definite coefficients:

κ	heat conductivity	D^c	thermodiffusive constant
ℓ	Righi–Leduc effect coefficient	D^S	thermosupercurrent constant

h^c	diffusion constant [Sirotn and Šaskolskaya 1979]	τ^c	diffusive relaxation time
κ^c	Dufour–Soret effect coefficient	D^q	diffusive-thermal constant
K^c	magnetothermodiffusive kinetic coefficient	D^{Sq}	diffusive-supercurrent constant
κ^e	Peltier effect coefficient	τ^S	supercurrent relaxation time
N	Ettingshausen–Nernst effect coefficient	P^T	superthermal constant
D	diffusion coefficient	R^T	supermagnetothermal constant
M	magnetodiffusive kinetic coefficient	P^c	superdiffusive constant
Σ^c	electrodiffusive kinetic coefficient	R^c	supermagnetodiffusive constant
Γ^c	electromagnetodiffusive kinetic coefficient	R^e	superelectromagnetic constant
σ	electric conductivity	D^{qS}	superthermal kinetic constant
R	Hall constant	D^{cS}	superdiffusive kinetic constant
τ^q	thermal relaxation time		

In addition, (3), (12), and (13) still yield the generalized Ginzburg–Landau kinetic equation as well [Orlando and Delin 1991; Maruszewski 1998]. Since we have, however, decided that the gauge can be chosen such that the scalar electric potential vanishes [Yeh and Chen 1993], then we use the experimental observations that the supercurrent exists reasonably long in time and we assume that the local density of Cooper pairs to be constant (this approach is true in many practical situations where the local fluctuations of the density of superelectrons in steady state are of such length and time scales that they are too small to be of engineering interest [Orlando and Delin 1991]). That fact leads to the conclusion that $X_7 = X_8 = 0$ in (12). Hence, we assume that the generalized Ginzburg–Landau equation in such a situation (within the model of interactions presented in the paper) can be neglected.

3. Conclusions

The paper has proved, in the opinion of the author, that the dynamics of the vortex field in a type II superconductor is very rich in interesting phenomena. The kinetic part of interactions and processes running in that array show that reciprocal links among heat transfer, diffusion of vortices and normal electron conduction (the Ohmic-like current) with relaxation of heat flux, diffusion flux, and supercurrent result in known and unknown linear and nonlinear kinetic effects. Those effects, particularly nonlinear ones, demand detailed physical analysis and interpretation. Finally, experimentation should verify and answer the fundamental question: do all the effects presented in (14)–(19) really exist?

References

- [Blatter et al. 1994] G. Blatter, M. V. Feigelman, V. B. Geshkenbein, A. I. Larkin, and V. M. Vinokur, “Vortices in high-temperature superconductors”, *Rev. Mod. Phys.* **66** (1994), 1125–1388.
- [Brant 1995] E. H. Brant, “The flux-line lattice in superconductors”, *Rep. Prog. Phys.* **58** (1995), 1465–1594.
- [Cyrot and Pavuna 1992] M. Cyrot and D. Pavuna, *Introduction to superconductivity and high- T_c materials*, World Scientific, Singapore, 1992.
- [Freimuth 2002] A. Freimuth, “Vortex dynamics in a temperature gradient”, pp. 321–340 in *Vortices in unconventional superconductors and superfluids*, edited by R. P. Huebner et al., Springer, Berlin, 2002.
- [Kluitenberg 1981] G. A. Kluitenberg, “On vectorial internal variables and dielectric and magnetic relaxation phenomena”, *Physica A* **109** (1981), 91–122.

- [Kopnin 2002] N. B. Kopnin, "Vortex dynamics and the problem of the transverse force in clean superconductors and Fermi superfluids", pp. 99–118 in *Vortices in unconventional superconductors and superfluids*, edited by R. P. Huebner et al., Springer, Berlin, 2002.
- [Maruszewski 1984] B. Maruszewski, "Efekty termogalwanomagnetyczne w sprężystych półprzewodnikach", *Biuletyn Wojskowej Akademii Technicznej* **33**:1 (377) (1984), 87–95.
- [Maruszewski 1988] B. Maruszewski, "Evolution equations of thermodiffusion in paramagnets", *Int. J. Engn. Sci.* **26** (1988), 1217–1230.
- [Maruszewski 1990] B. Maruszewski, "Non-classical thermodynamical description of interactions of physical fields in solids", *Atti Accad. Peloritana dei Pericolanti, Cl. I Sci. Fis. Mat. Nat.* **68** (1990), 101–115.
- [Maruszewski 1997] B. Maruszewski, "Thermomechanical interactions in superconducting fullerenes", pp. 691–694 in *Proc. Second Int. Symposium on Thermal Stresses and Related Topics* (Rochester, NY), 1997.
- [Maruszewski 1998] B. Maruszewski, "Superconducting fullerenes in a nonconventional thermodynamical model", *Arch. Mech.* **50** (1998), 497–508.
- [Maruszewski 2007] B. T. Maruszewski, "On a nonclassical thermoviscoelastic stress in the vortex field in the type-II superconductor", *Phys. Stat. Solidi B* **244**:3 (2007), 919–927.
- [Maruszewski and Restuccia 1999] B. T. Maruszewski and L. Restuccia, "Mechanics of a vortex lattice in superconductors: phenomenological approach", pp. 220–230 in *Trends in continuum physics*, edited by B. T. Maruszewski et al., World Scientific, Singapore, 1999.
- [Maruszewski et al. 2007] B. T. Maruszewski, A. Drzewiecki, and R. Starosta, "Anomalous features of the thermomagnetoelastic field in a vortex array in superconductor: Propagation of Love's waves", *J. Thermal Stresses* **30** (2007), 1049–1065.
- [Maugin 1992] G. A. Maugin, "Irreversible thermodynamics of deformable superconductors", *C. R. Acad. Sci. Paris. Ser. II* **314** (1992), 889–994.
- [Orlando and Delin 1991] T. P. Orlando and K. A. Delin, *Foundations of applied superconductivity*, Addison-Wesley, Reading, MA, 1991.
- [Restuccia and Kluitenberg 1987] L. Restuccia and G. A. Kluitenberg, "On possible interactions among dielectric relaxation, magnetic relaxation, heat conduction, electric conduction, diffusion phenomena, viscous flow and chemical reactions in fluid mixtures", *Atti Accad. Peloritana dei Pericolanti, Cl. I Sci. Fis. Mat. Nat.* **65** (1987), 310–336.
- [Schönenberger et al. 1997] A. Schönenberger, A. Larkin, E. Heeb, V. Geshkenbein, and G. Blatter, "Strong pinning and plastic deformations of a vortex lattice", private communication, 1997.
- [Sirotnin and Šaskolskaya 1979] Y. I. Sirotnin and M. P. Šaskolskaya, *Основы кристаллофизики*, Nauka, Moscow, 1979.
- [Tilley 1974] D. R. Tilley, *Superfluidity and superconductivity*, Van Nostrand, New York, 1974.
- [Tinkham 1975] M. Tinkham, *Introduction to superconductivity*, McGraw-Hill, New York, 1975.
- [van de Ven 1991] A. A. F. van de Ven, "A note on 'A nonequilibrium theory of thermoelastic superconductors' by S.-A. Zhou, K. Miya", *Int. J. Appl. Electromagn. Mat.* **2** (1991), 169–175.
- [Yeh and Chen 1993] C. S. Yeh and K. C. Chen, "A phenomenological theory for elastic superconductors", *Continuum Mech. Thermodyn.* **5** (1993), 127–144.

Received 7 Feb 2008. Accepted 25 Mar 2008.

BOGDAN T. MARUSZEWSKI: bogdan.maruszewski@put.poznan.pl

Poznań University of Technology, Institute of Applied Mechanics, ul. Piotrowo 3, 60-965 Poznań, Poland

www.put.poznan.pl

THERMODYNAMICS OF INHOMOGENEOUS FERROELECTRICS

GERARD A. MAUGIN AND LILIANA RESTUCCIA

In a previous paper within the framework of the theory of inhomogeneities, the balance law of the so-called *pseudomomentum* for ferroelectrics was worked out exploiting the presence of *material forces*. Electric polarization density per unit mass and its gradient were introduced as state variables in the state vector. In this paper, starting from the pseudomomentum balance equation, we construct, in a systematic way, the material energy balance law for ferroelectrics which plays a crucial role in applications related to the study of fracture.

1. Introduction

Ferroelectrics are dielectric materials which possess the essential property of exhibiting a local spontaneous electrical polarization. Ferroelectricity generally disappears above a certain temperature, called the transition temperature or Curie point θ_c , at which a ferroelectric crystal passes from a polarized state of low temperature to a nonpolarized state of high temperature. Thermic agitation tends to destroy ferroelectric order. Ferroelectric crystals which don't have a Curie point exist, because they melt before reaching a ferroelectric phase. Rochelle salt has two Curie points, one higher and one lower, between which this crystal is ferroelectric. Ferroelectrics have applications in computer science, in the technology of integrated circuits, and in the fields of electronic microscopy, electronic sensors, optoelectronics, and other technological sectors. Ferroelectric media are characterized by the fact that two ordered structures coexist in them: a crystalline structure which has as order parameter the deformation of the elementary cell (tensorial parameter), and the ferroelectric order parameter consisting of the specific polarization vector. We use in our description a phenomenological approach to deformable ferroelectric crystals, derived in [Maugin 1977a; 1977b; Maugin and Pouget 1980]. Dissipative processes in ferroelectrics were investigated in [Francaviglia et al. 2004]. Electric polarization density per unit mass, possessing its own dynamics and inertia, and its gradient, responsible for nonlocal interactions and the typical ferroelectric ordering, are introduced as state variables in the state vector. In this paper, within the framework of the theory of inhomogeneities [Maugin 1993], from the pseudomomentum balance equation, worked out in [Restuccia and Maugin 2004], the material energy balance law is constructed for inhomogeneous ferroelectrics in the presence of configurational forces. This law plays a crucial role in applications related to the fracture study and the computation of the so-called energy-release rate (energy dissipated at the phase-transition fronts). Inhomogeneities can be caused by abrupt changes of material properties such as density, module of elasticity, and existence of different elements and parts, and by the presence of transition fronts, dislocations, and defects such as cavities, cracks, and inclusions, which can self-propagate during the processes of fabrication because of changed conditions or surrounding conditions

Keywords: Eshelbian mechanics, material inhomogeneities, fracture mechanics.

that are favorable [Cherepanov 1979]. Such defect propagation can provoke a premature fracture [Maugin 1992]. A crack is one of the most common defects, and it can self-propagate when a critical threshold of a certain strength is reached. To prevent this fracture criteria for propagation of a crack can be introduced in the study of the mechanics of solids [Maugin 1992]. The critical threshold of propagation of a crack can be evaluated by introducing, for instance, the rate of energy restitution and the contour integral (more precisely, Rice’s integral). This critical threshold is a precise breaking condition because of the fracture instability of a fractured medium. Fracture criteria were introduced long ago for elastic materials (Lhemon, 1888, on the mesomorphic phase of the matter; Volterra, 1907, on distortions in matter). The technological evolution of the science of materials has introduced new materials into industry that exhibit an interaction between mechanical stress elastic fields and polarization field. One of the first works on inhomogeneities is by Eshelby [1951] (see also [Eshelby 1969; Maugin 1995]), who studied a particular case of inhomogeneity: the presence of a defect in an elastic material. He introduced a fictitious force (the material force) in order to give a more detailed description of energy variation related to a position of imperfection. This force is not to be confused with surface and bulk forces. Eshelby showed that this force can be obtained starting with a contour integral on any surface surrounding the defect. In the absence of a defect, this integral becomes zero and reduces itself to a strict conservation law. Following Maugin, the material force of inhomogeneity is put into evidence by projecting the balance equations of a continuum body onto a material frame [Maugin 1992]. Also Kalpakides and Agiasofitou [2002], Vukobrat [1994] and Huang and Batra [1996] investigated ferroelectrics where the gradient of electric polarization or electric fields is considered.

2. Governing equations for ferroelectrics

We use the standard Cartesian tensor notation in rectangular coordinate systems. The general nonlinear deformation of a body, between a configurational reference \mathcal{K}_R and a current configuration \mathcal{K}_t at the time t , is represented by the diffeomorphism

$$\mathbf{x} = \chi(\mathbf{X}, t), \quad \mathbf{X} = \chi^{-1}(\mathbf{x}, t),$$

where \mathbf{x} represents Eulerian coordinates and \mathbf{X} the material coordinates of the same material particle P .

We have the following relations: $F^i_K = \partial x^i / \partial X^K = x^i_{,K}$ (denoting the components of the deformation gradient \mathbf{F}), $(F^{-1})^K_j = \partial X^K / \partial x_j = X^K_{,j}$, $J_F = \det(F^i_K) > 0$ (the Jacobian of \mathbf{F}), $x^i_{,K} X^K_{,j} = \delta^i_j$, $F^i_K (F^{-1})^K_j = \delta^i_j$, $X^K_{,i} x^i_{,L} = \delta^K_L$, $(F^{-1})^K_i F^i_L = \delta^K_L$. From the kinematic description one defines the physical and material velocities by $v^i = (\partial x^i / \partial t)|_{\mathbf{x}}$, $V^K = (\partial X^K / \partial t)|_{\mathbf{X}}$, where we have explicitly indicated the time derivatives at fixed \mathbf{X} (the so-called “material derivative”) and at fixed \mathbf{x} . Now consider in a current configuration \mathcal{K}_t the general equations that govern the quasielectrostatics of thermoelastic ferroelectric insulators [Maugin and Pouget 1980; Restuccia and Maugin 2004]. Suppose that *the material may present continuously distributed material inhomogeneities*, that the range of the considered temperatures is much below the Curie ferroelectric phase-transition temperature θ_c , and that the body occupies the simply connected material volume V_t with regular boundary ∂V_t having unit outward normal \mathbf{n} in \mathcal{K}_t , while it occupies the volume V_R with regular boundary ∂V_R having unit outward normal \mathbf{N} in \mathcal{K}_R .

We now discuss the governing equations.

Maxwell equations in the quasielectrostatic approximation. Let \mathbf{E} , \mathbf{B} , \mathbf{D} , \mathbf{H} , \mathbf{P} and \mathbf{M} denote the electric field, the magnetic induction, the electric displacement, the magnetic field, the electric polarization and the magnetization per unit volume, all evaluated in a fixed Galilean frame at time t . In the quasielectrostatic case Maxwell's equations read [Maugin 1988]

$$\nabla \times \mathbf{E} = \mathbf{0}, \quad \nabla \times \mathbf{H} = \mathbf{0}, \quad \nabla \cdot \mathbf{D} = 0, \quad \nabla \cdot \mathbf{B} = 0,$$

where Lorentz–Heaviside units are used and neither currents nor electric charge are present. Further

$$\mathbf{D} = \mathbf{E} + \mathbf{P}, \quad \mathbf{H} = \mathbf{B}, \quad \mathbf{M} = \mathbf{0},$$

and the associated jump conditions on ∂V_t are:

$$\mathbf{n} \times \llbracket \mathbf{E} \rrbracket = \mathbf{0}, \quad \mathbf{n} \cdot \llbracket \mathbf{B} \rrbracket = 0, \quad \mathbf{n} \times \llbracket \mathbf{H} \rrbracket = \mathbf{0}, \quad \mathbf{n} \cdot \llbracket \mathbf{D} \rrbracket = 0,$$

where $\llbracket \mathbf{A} \rrbracket = \mathbf{A}^+ - \mathbf{A}^-$, \mathbf{A}^+ and \mathbf{A}^- being the field limits as the boundary is approached from outside and from inside. In the Galilean approximation, calling \mathcal{E} , \mathcal{B} , \mathcal{H} , \mathcal{P} and \mathcal{M} the same fields as \mathbf{E} , \mathbf{B} , \mathbf{H} , \mathbf{P} and \mathbf{M} , but referring to an element of matter at time t in a frame $\mathcal{K}_c(\mathbf{x}, t)$, we have

$$\mathcal{E} = \mathbf{E} + c^{-1} \mathbf{u} \times \mathbf{B}, \quad \mathcal{B} = \mathbf{B} - c^{-1} \mathbf{u} \times \mathbf{E}, \quad \mathcal{H} = \mathbf{B} - \mathcal{M} = \mathcal{B}, \quad \mathcal{D} = \mathbf{D}, \quad \mathcal{M} = \mathbf{0}, \quad \mathcal{P} = \mathbf{P}, \quad (1)$$

where \mathbf{u} is the velocity of the reference \mathcal{K}_c with respect to the current reference \mathcal{K}_t . In the quasielectrostatic approximation, terms in \mathbf{u} are irrelevant. Further, let $\boldsymbol{\pi}$ denote the *polarization vector* per unit mass in \mathcal{K}_t :

$$\boldsymbol{\pi} = \boldsymbol{\pi}(\mathbf{X}, t) = \mathbf{P}/\rho,$$

where $\rho(\mathbf{x}, t)$ is the mass density.

Conservation of mass. This equation reads

$$\dot{\rho} + \rho \nabla \cdot \mathbf{v} = 0 \quad \text{in } V_t, \quad (2)$$

where $\dot{\rho}(\mathbf{X}, t) = \left. \frac{\partial \rho(\mathbf{X}, t)}{\partial t} \right|_{\mathbf{X}}$ is the material time derivative of ρ and $\mathbf{v} = \left. \frac{\partial \boldsymbol{\chi}(\mathbf{X}, t)}{\partial t} \right|_{\mathbf{X}}$. Moreover,

$$\left. \frac{\partial \rho_0}{\partial t} \right|_{\mathbf{X}} = 0, \quad \text{i.e.,} \quad \rho_0(\mathbf{X}) = J_F \rho, \quad \text{in } V_R. \quad (3)$$

Relation (3)₂ indicates that ρ_0 depends at most on \mathbf{X} . It depends on \mathbf{X} when the considered body presents *inertial material inhomogeneities*.

Motion equation. In the absence of body force (of purely mechanical origin) this equation reads

$$\text{div } \mathbf{t} + \mathbf{f}^{\text{em}} = \rho \dot{\mathbf{v}} \quad \text{in } V_t, \quad (4)$$

with the boundary condition

$$t_{ij} n_j = T_i^{\text{em}} \quad \text{on } \partial V_t,$$

where \mathbf{f}^{em} and \mathbf{T}^{em} are, in the quasielectrostatic approximation, the volume ponderomotive force in a nonrelativistically moving nonmagnetizable dielectric medium and the corresponding surface traction of purely mechanical origin, given by

$$f_i^{\text{em}} = P_j \mathcal{E}_{i,j}, \quad \mathbf{f}^{\text{em}} = (\mathbf{P} \cdot \nabla) \mathcal{E} = -(\nabla \cdot \mathbf{P}) \mathcal{E} + \nabla \cdot (\mathcal{E} \otimes \mathbf{P}), \quad \mathbf{T}^{\text{em}} = \llbracket \mathcal{E} \otimes \mathbf{P} + \mathbf{E} \otimes \mathbf{E} - \frac{1}{2} (E^2) \mathbf{1} \rrbracket \cdot \mathbf{n},$$

and t^{ij} is the nonsymmetric Cauchy stress tensor defined by

$$t^{ij} = \sigma^{ij} + (t^{\text{int}})^{[ij]}. \tag{5}$$

In (5) σ^{ij} is the *intrinsic stress tensor* (the symmetric Cauchy tensor)

$$\sigma^{ij} = \sigma^{ji}$$

and $(t^{\text{int}})^{ij}$ is the *interaction stress tensor* defined by

$$(t^{\text{int}})^{ij} = \rho^L E^i \pi^j - {}^L \mathbb{E}^{ip} \pi_{,p}^j, \quad \text{with } t^{[ij]} = (t^{\text{int}})^{[ij]}. \tag{6}$$

This equation is the local statement of the balance of moment of momentum.

In Equation (6)₁ ${}^L \mathbf{E} \equiv ({}^L E^i)$ is called the *local electric field vector* and represents the electric anisotropy field, accounting for the interaction between the polarization of different molecular species with the crystal lattice, while ${}^L \mathbb{E} \equiv ({}^L \mathbb{E}^{ip})$ accounts for polarization gradients and has the name of *shell-shell interaction tensor*, by identification or analogy with results from the lattice theory of alkali halides. ${}^L \mathbb{E}$ is responsible for the typical ferroelectric ordering. In fact, in this phenomenological model, derived in [Maugin 1977a; 1977b; Maugin and Pouget 1980], it is assumed that the medium is formed by n coexisting molecular species $\alpha = 1, 2, \dots, n$, each one of them giving rise to a field of electric dipoles, which when suitably averaged is represented by a volume density \mathbf{P}_α of electrical polarization. Then, the polarization vector per unit volume is the sum of the polarization vectors per unit volume of each molecular species: $\mathbf{P} = \Sigma_\alpha \mathbf{P}_\alpha$. Letting ρ_α be the density of α molecules, $c_\alpha \equiv \rho_\alpha / \rho$ being the corresponding concentration, we define $\boldsymbol{\pi}_\alpha \equiv \mathbf{P}_\alpha / \rho_\alpha$, where \mathbf{P}_α and $\boldsymbol{\pi}_\alpha$ are the polarization vectors per unit volume and mass in \mathcal{K}_t for the molecular species α .

Balance equation for the polarization vector. A theorem in [Maugin and Pouget 1980] states that the balance equation for the polarization vector in a deformable nonmagnetizable ferroelectric medium reads (see also [Maugin 1977a; 1977b; Maugin and Pouget 1980])

$$\mathcal{E}^i + {}^L E^i + \rho^{-1} {}^L \mathbb{E}_{,j}^{ij} = I \ddot{\pi}^i \quad \text{in } V_t, \tag{7}$$

where I is the so-called polarization inertia and \mathcal{E} is the *electromotive intensity* due to external sources; see (1)₁. This equation resembles Newton's law of motion.

After the introduction of the symmetric stress tensor ${}^E t^{ij}$ (*elastic stress tensor*) defined by

$${}^E t^{ij} = \sigma^{ij} - \rho^L E^{(i} \pi^{j)} + {}^L \mathbb{E}^{(ik} \pi_{,k}^{j)} = {}^E t^{ji},$$

Equation (5) reads

$$t^{ij} = {}^E t^{ij} + \rho^L E^i \pi^j - {}^L \mathbb{E}^{ik} \pi_{,k}^j = {}^E t^{ij} + (t^{\text{int}})^{ij}. \tag{8}$$

Conservation of energy. The first law of thermodynamics, in the absence of a heat source by radiation, reads

$$\rho \dot{e} = t^{ji} v_{i,j} - \rho^L E^i \dot{\pi}_i + {}^L \mathbb{E}^{ij} (\dot{\pi}_i)_{,j} - q_{,k}^k. \tag{9}$$

Entropy inequality and Clausius–Duhem inequality. In this paper we use the following form of the entropy inequality:

$$\rho \dot{\eta} + \nabla \cdot \mathbf{j}_s \geq 0,$$

where η is the entropy per unit mass and \mathbf{j}_s is the entropy flux, defined by $\mathbf{j}_s = \mathbf{q}/\theta$.

Introducing Helmholtz's free energy per unit mass $\psi = e - \eta\theta$ by a *Legendre transformation* and using the energy balance equation, the following Clausius–Duhem inequality is obtained:

$$-\rho(\dot{\psi} + \eta\dot{\theta}) + t^{ji} v_{i,j} - \rho {}^L E^i \dot{\pi}_i + {}^L \mathbb{E}^{ij} (\dot{\pi}_i)_{,j} - \theta^{-1} q^k \theta_{,k} \geq 0,$$

where $0 < \theta \ll \theta_c$.

3. A thermodynamical model for ferroelectrics

In [Restuccia and Maugin 2004], following the general philosophy exposed in the theory of the inhomogeneities [Maugin 1993], in order to put in evidence the material force of inhomogeneity, balance equations of continuum were projected onto \mathcal{K}_R material frame, effecting the following *Piola transformations* (see also [Maugin and Pouget 1980; Lax and Nelson 1976]):

$$\begin{aligned} \mathbf{T} &= J_F \mathbf{F}^{-1} \cdot \mathbf{t}, & T^{Ki} &= J_F (F^{-1})_j^K t^{ji}, \\ {}^E \mathbf{T} &= J_F \mathbf{F}^{-1} \cdot {}^E \mathbf{t}, & {}^E T^{Ki} &= J_F (F^{-1})_j^K {}^E t^{ji}, \\ {}^L \mathbb{E} &= J_F \mathbf{F}^{-1} \cdot {}^L \mathbb{E}, & {}^L \mathbb{E}^{Ki} &= J_F (F^{-1})_j^K {}^L \mathbb{E}^{ji}, \\ \mathbf{Q} &= J_F \mathbf{F}^{-1} \cdot \mathbf{q}, & Q^K &= J_F (F^{-1})_j^K q^j, \\ \mathbf{J}_s &= J_F \mathbf{F}^{-1} \cdot \mathbf{j}_s, & J_s^K &= J_F (F^{-1})_j^K j_s^j, \\ {}^L \mathbf{E} &= \mathbf{F}^T \cdot {}^L \mathbf{E}, & {}^L E_K &= {}^L E_i F_K^i, \\ {}^L E^s &= \delta^{si} {}^L E_i = \delta^{si} (F^{-1})_i^K {}^L E_K, \\ \mathbb{E} &= \mathbf{F}^T \mathcal{E}, & \mathbb{E}_K &= \mathcal{E}_i F_K^i, \\ \mathbf{\Pi} &= J_F \mathbf{F}^{-1} \cdot \mathbf{P}, & \Pi^K &= J_F (F^{-1})_j^K P^j. \end{aligned}$$

Multiplying (8) by $J_F (F^{-1})_i^K$, the following Piola transformation was derived:

$$T^{Ki} = {}^E T^{Ki} + \rho_0 (F^{-1})_l^K {}^L E^l \pi^i - {}^L \mathbb{E}^{Kl} \pi_{,l}^i, \quad (10)$$

where \mathbf{T} is the first *Piola–Kirchhoff* stress.

Further, multiplying the balance of energy by J_F , we obtain

$$\dot{E} = (T^{Ki} \delta_{ij}) \dot{F}_k^j - \rho_0 \delta^{is} (F^{-1})_s^K {}^L E_K \dot{\pi}_i + {}^L \mathbb{E}^{iK} (\dot{\pi}_i)_{,K} - Q_{,K}^K, \quad (11)$$

where $E = \rho_0 e$; doing the same to the entropy inequality and the Clausius–Duhem inequality we get

$$\begin{aligned} \theta \dot{S} &\geq -Q_{,K}^K + \theta^{-1} Q^K \theta_{,K}, \\ -(\dot{W} + S\dot{\theta}) + (T^{Ki} \delta_{ij}) \dot{F}_K^j - \rho_0 \delta^{is} (F^{-1})_s^K {}^L E_K \dot{\pi}_i + {}^L \mathbb{E}^{iK} (\dot{\pi}_i)_{,K} - \theta^{-1} Q^K \theta_{,K} &\geq 0, \end{aligned}$$

where $S = \rho_0 \eta$ and $W = \rho_0 \psi = E - S\theta$.

In [Restuccia and Maugin 2004] a thermodynamical model for materially inhomogeneous thermoelastic ferroelectric insulators was proposed, choosing the following state vector

$$C = C(\mathbf{F}, \boldsymbol{\pi}, \nabla_R \boldsymbol{\pi}, \theta, \nabla_R \theta; \mathbf{X}), \tag{12}$$

where the physical fields $\boldsymbol{\pi}$ and $\nabla_R \boldsymbol{\pi}$ are responsible for the internal structure of the medium, the relaxation properties of the thermal field are taken into account, and the explicit dependence on \mathbf{X} reflects the material inhomogeneity. In (12) the symbol ∇_R denotes the gradient operator in material space. The constitutive dependent variables of the set

$$\mathbf{Z} = \mathbf{Z}(W, S, \mathbf{T}, {}^L\mathbf{E}, {}^L\boldsymbol{\Xi}, \mathbf{Q}),$$

were determined as functions of the set C , that is, $\mathbf{Z} = \mathbf{Z}(C)$, and using the expression

$$W = W(\mathbf{F}, \boldsymbol{\pi}, \nabla_R \boldsymbol{\pi}, \theta, \nabla_R \theta; \mathbf{X})$$

and the Clausius–Duhem inequality, the *nonlinear constitutive equations*, the *dissipation inequality*, and other results were worked out:

$$T^{Ki} = \frac{\partial W}{\partial F_K^j} \delta^{ji}, \quad {}^L E_K = -\rho_0^{-1} \frac{\partial W}{\partial \pi_i} (\mathbf{F})_K^i, \quad {}^L \Xi^{iK} = \frac{\partial W}{\partial \pi_{i,K}}, \tag{13}$$

$$S = -\frac{\partial W}{\partial \theta}, \quad \frac{\partial W}{\partial \theta_{,K}} = 0, \quad -\theta^{-1} Q^K \theta_{,K} \geq 0. \tag{14}$$

Then

$$W = W(\mathbf{F}, \boldsymbol{\pi}, \nabla_R \boldsymbol{\pi}, \theta; \mathbf{X}),$$

but

$$Q^K = Q^K(\mathbf{F}, \boldsymbol{\pi}, \nabla_R \boldsymbol{\pi}, \theta, \nabla_R \theta; \mathbf{X}),$$

with $\lim_{\nabla_R \theta \rightarrow 0} Q^K(\mathbf{F}, \boldsymbol{\pi}, \nabla_R \boldsymbol{\pi}, \theta, \nabla_R \theta; \mathbf{X}) = 0$ (continuity condition).

From (11), using the constitutive relations and the Legendre transformation $W = E - S\theta$, the energy equation can be rewritten as

$$\theta \frac{\partial S}{\partial t} \Big|_{\mathbf{X}} + \nabla_R \cdot \mathbf{Q} = 0, \quad \text{or} \quad \frac{\partial S}{\partial t} \Big|_{\mathbf{X}} + \nabla_R \cdot \mathbf{J}_s = -\theta^{-2} Q^K \theta_{,K}. \tag{15}$$

4. Material energy balance

In [Restuccia and Maugin 2004], following the philosophy of the theory of the inhomogeneities exposed in [Maugin 1993], in order to place the presence of *material forces* and to obtain the balance of material momentum (called balance of pseudomomentum), the motion equation (4) was projected onto the material manifold \mathcal{M}^3 by applying the operator $J_F \mathbf{F}^T$ at the left of equation (4). This operation is called *convection* or *pull-back*. First, by multiplying Equation (4) by J_F , the following Piola–Kirchhoff form was obtained:

$$T_{i,K}^K + J_F f_i^{\text{em}} = J_F \rho \dot{v}_i = \rho_0 \dot{v}_i, \quad \text{div}_R \mathbf{T} + J_F \mathbf{f}^{\text{em}} = \frac{\partial \mathbf{p}_R}{\partial t} \Big|_{\mathbf{X}}, \tag{16}$$

where $\mathbf{p}_R = \rho_0 \mathbf{v}$ is defined as the *physical linear momentum per unit volume* in \mathcal{K}_R .

Next, applying the pull-back operator (\mathbf{F}^T) on the left-hand side of (16)₁,

$$F_L^i T_{i,K}^K + J_F F_L^i f_i^{\text{em}} = F_L^i \frac{\partial}{\partial t} (\rho_o v_i) \Big|_{\mathbf{X}},$$

the following balance of pseudomomentum projected on \mathcal{M}^3 was obtained:

$$\frac{\partial \mathcal{P}}{\partial t} \Big|_{\mathbf{X}} - \text{div}_R \hat{\mathbf{b}} = \mathbf{f}^{\text{inh}} + \mathbf{f}^{\text{th}} + \mathbf{f}^{\text{fer}}, \quad (17)$$

where

$$\begin{aligned} \mathcal{P} &= -\rho_0 \mathbf{F}^T \cdot \mathbf{v} - (\nabla_R \boldsymbol{\pi}) \cdot (\rho_0 I \dot{\boldsymbol{\pi}}), \\ \hat{\mathbf{b}} &= -(\hat{\mathcal{L}} \mathbf{1}_R + \mathbf{T} \cdot \mathbf{F} + (\nabla_R \boldsymbol{\pi}) \cdot {}^L \boldsymbol{\Xi}), \\ \hat{\mathcal{L}} &= \rho_0(\mathbf{X}) \left(\frac{1}{2} \mathbf{v}^2 + \frac{1}{2} I \dot{\boldsymbol{\pi}}^2 + \boldsymbol{\mathcal{E}} \cdot \boldsymbol{\pi} \right) - W(\mathbf{F}, \boldsymbol{\pi}, \nabla_R \boldsymbol{\pi}, \theta; \mathbf{X}), \\ \mathbf{f}^{\text{inh}} &= \nabla_R \rho_0(\mathbf{X}) \left(\frac{1}{2} \mathbf{v}^2 + \frac{1}{2} I \dot{\boldsymbol{\pi}}^2 + \boldsymbol{\mathcal{E}} \cdot \boldsymbol{\pi} \right) - \nabla_R \mathbf{W}|_{\text{expl}}, \\ \mathbf{f}^{\text{th}} &= S \nabla_R \theta, \\ \mathbf{f}^{\text{fer}} &= \rho_0 \boldsymbol{\pi} \cdot \nabla_R \boldsymbol{\mathcal{E}} - \mathbf{F}^T \cdot (\boldsymbol{\Pi} \cdot \nabla_R) \boldsymbol{\mathcal{E}}. \end{aligned} \quad (18)$$

In these expressions \mathcal{P} is the *pseudomomentum*, a material *covector* on \mathcal{M}^3 , $\hat{\mathbf{b}}$ is referred to as the *Eshelby* (material) stress tensor accounting for ferroelectric exchange effects, \mathbf{f}^{inh} is the *material inhomogeneity* force, \mathbf{f}^{th} is called the *thermal material force*, and \mathbf{f}^{fer} is a new material force which reflects the presence of ferroelectric effects (see also [Maugin and Pouget 1980]). The inhomogeneity force \mathbf{f}^{inh} here has its canonical definition

$$\mathbf{f}^{\text{inh}} = \frac{\partial \hat{\mathcal{L}}}{\partial \mathbf{X}} \Big|_{\text{expl}},$$

where the potential $\hat{\mathcal{L}}$ would be the Lagrangian density if irreversible processes were not present. Now, although (11) already provides an expression of the local energy equation, we construct the expression of the material energy balance that plays a crucial role in applications related to the study of fracture in a medium. Using the already obtained results, upon scalar multiplication of (17) by the material velocity, we obtain

$$\frac{\partial \mathcal{P}}{\partial t} \Big|_{\mathbf{X}} \cdot \mathbf{V} - (\text{div}_R \hat{\mathbf{b}}) \cdot \mathbf{V} = \mathbf{f}^{\text{inh}} \cdot \mathbf{V} + \mathbf{f}^{\text{th}} \cdot \mathbf{V} + \mathbf{f}^{\text{fer}} \cdot \mathbf{V}. \quad (19)$$

We evaluate each contribution separately, systematically using the following relations (see [Fomethé and Maugin 1996]):

$$\begin{aligned} \mathbf{V} &= \frac{\partial \boldsymbol{\chi}^{-1}(\mathbf{x}, t)}{\partial t} \Big|_{\mathbf{x}}, \quad v^i = -F_K^i V^K, \quad V^K = -(F^{-1})_i^K v^i, \\ \dot{\mathbf{A}}(\mathbf{X}, t) &= \frac{\partial \mathbf{A}(\mathbf{X}, t)}{\partial t} \Big|_{\mathbf{X}}, \quad \dot{\mathbf{A}} = \frac{\partial \mathbf{A}}{\partial t} \Big|_{\mathbf{x}} + \mathbf{v} \cdot \nabla \mathbf{A}, \quad \frac{\partial \mathbf{A}}{\partial t} \Big|_{\mathbf{x}} = \dot{\mathbf{A}} + \mathbf{V} \cdot \nabla_R \mathbf{A}, \\ A_{,K}^i &= A_{,j}^i F_K^j, \quad A_{,j}^i = A_{,K}^i (F^{-1})_j^K, \quad \mathbf{v} \cdot \nabla \mathbf{A} = \frac{\partial \mathbf{A}}{\partial t} \Big|_{\mathbf{x}} - \frac{\partial \mathbf{A}}{\partial t} \Big|_{\mathbf{X}}, \quad \mathbf{V} \cdot \nabla_R \mathbf{A} = \frac{\partial \mathbf{A}}{\partial t} \Big|_{\mathbf{x}} - \frac{\partial \mathbf{A}}{\partial t} \Big|_{\mathbf{X}}, \\ \dot{F}_K^i &= v_{,K}^i = v_{,j}^i F_K^j, \quad v_{,j}^i v^j = \frac{\partial v^i}{\partial t} \Big|_{\mathbf{x}} - \frac{\partial v^i}{\partial t} \Big|_{\mathbf{X}}, \quad \frac{\partial \rho_0}{\partial t} \Big|_{\mathbf{x}} = 0, \end{aligned}$$

where the objective vector field \mathbf{A} is a geometrical time-dependent object which is form invariant under rigid-body changes of coordinate frames in K_t and its components transform tensorially. Then, from equations (18) and (19) we have

$$\frac{\partial}{\partial t}(-\rho_0 \mathbf{F}^T \cdot \mathbf{v}) \Big|_{\mathbf{x}} \cdot \mathbf{V} = \frac{\partial}{\partial t}(\rho_0 v^2) \Big|_{\mathbf{x}} - \rho_0 \frac{\partial}{\partial t} \left(\frac{1}{2} v^2 \right) \Big|_{\mathbf{x}} \quad (20)$$

and

$$\begin{aligned} -\frac{\partial}{\partial t} [\nabla_R \boldsymbol{\pi} \cdot (\rho_0 I \dot{\boldsymbol{\pi}})] \Big|_{\mathbf{x}} \cdot \mathbf{V} &= -(\rho_0 I \ddot{\pi}_{i,L} + \rho_0 I \dot{\pi}^i \dot{\pi}_{i,L}) V^L \\ &= -\rho_0 I \ddot{\pi}^i \frac{\partial \pi_i}{\partial t} \Big|_{\mathbf{x}} + \rho_0 I \dot{\pi}^i \frac{\partial \pi_i}{\partial t} \Big|_{\mathbf{x}} - \rho_0 I \dot{\pi}^i \frac{\partial \dot{\pi}_i}{\partial t} \Big|_{\mathbf{x}} + \rho_0 I \dot{\pi}^i \frac{\partial \dot{\pi}_i}{\partial t} \Big|_{\mathbf{x}}. \end{aligned} \quad (21)$$

The second term on the left-hand side of (19) gives

$$(\operatorname{div}_R \hat{\mathbf{b}}) \cdot \mathbf{V} = -\hat{\mathcal{L}}_{,L} V^L - (T_i^K F_L^i + {}^L \boldsymbol{\Xi}^{iK} \pi_{i,L})_{,K} V^L. \quad (22)$$

Evaluating the contributions in the right side of (22) we have

$$-\hat{\mathcal{L}}_{,L} V^L = -\frac{\partial \hat{\mathcal{L}}}{\partial t} \Big|_{\mathbf{x}} + \frac{\partial \hat{\mathcal{L}}}{\partial t} \Big|_{\mathbf{x}},$$

where

$$\begin{aligned} -\frac{\partial \hat{\mathcal{L}}}{\partial t} \Big|_{\mathbf{x}} &= \frac{\partial W}{\partial F_K^j} \frac{\partial F_K^j}{\partial t} \Big|_{\mathbf{x}} + \frac{\partial W}{\partial \pi_i} \frac{\partial \pi_i}{\partial t} \Big|_{\mathbf{x}} + \frac{\partial W}{\partial \pi_{i,K}} \frac{\partial \pi_{i,K}}{\partial t} \Big|_{\mathbf{x}} + \frac{\partial W}{\partial \theta} \frac{\partial \theta}{\partial t} \Big|_{\mathbf{x}} + \frac{\partial W}{\partial X^L} \Big|_{\text{expl}} \frac{\partial X^L}{\partial t} \Big|_{\mathbf{x}} \\ &\quad - \left(\frac{1}{2} v^2 + \frac{1}{2} I \dot{\pi}^2 + \boldsymbol{\mathcal{E}} \cdot \boldsymbol{\pi} \right) \frac{\partial \rho_0}{\partial t} \Big|_{\mathbf{x}} - \rho_0 \frac{\partial}{\partial t} \left(\frac{1}{2} v^2 + \frac{1}{2} I \dot{\pi}^2 + \boldsymbol{\mathcal{E}} \cdot \boldsymbol{\pi} \right) \Big|_{\mathbf{x}} \end{aligned} \quad (23)$$

and

$$\frac{\partial \hat{\mathcal{L}}}{\partial t} \Big|_{\mathbf{x}} = \frac{\partial}{\partial t} \left[\rho_0(\mathbf{X}) \left(\frac{1}{2} v^2 + \frac{1}{2} I \dot{\pi}^2 + \boldsymbol{\mathcal{E}} \cdot \boldsymbol{\pi} \right) \right] \Big|_{\mathbf{x}} - \frac{\partial W}{\partial t} \Big|_{\mathbf{x}}. \quad (24)$$

In the following, we use the constitutive equations (13) and (14)₁ at fixed \mathbf{x} in the term $(\partial \hat{\mathcal{L}} / \partial t) \Big|_{\mathbf{x}}$. We further have

$$-(T_i^K F_L^i)_{,K} V^L = T_{i,K}^K v^i - T_i^K \frac{\partial F_K^i}{\partial t} \Big|_{\mathbf{x}} + T_i^K v_{i,K} = \nabla_R \cdot (\mathbf{T} \cdot \mathbf{v}) - T_i^K \frac{\partial F_K^i}{\partial t} \Big|_{\mathbf{x}}, \quad (25)$$

$$-({}^L \boldsymbol{\Xi}^{iK} \pi_{i,L})_{,K} V^L = -{}^L \boldsymbol{\Xi}_{,K}^{iK} \frac{\partial \pi_i}{\partial t} \Big|_{\mathbf{x}} + {}^L \boldsymbol{\Xi}_{,K}^{iK} \frac{\partial \pi_i}{\partial t} \Big|_{\mathbf{x}} - {}^L \boldsymbol{\Xi}^{iK} \frac{\partial \pi_{i,K}}{\partial t} \Big|_{\mathbf{x}} + {}^L \boldsymbol{\Xi}^{iK} \frac{\partial \pi_{i,K}}{\partial t} \Big|_{\mathbf{x}}, \quad (26)$$

$${}^L \boldsymbol{\Xi}_{,K}^{iK} \frac{\partial \pi_i}{\partial t} \Big|_{\mathbf{x}} + {}^L \boldsymbol{\Xi}^{iK} \frac{\partial \pi_{i,K}}{\partial t} \Big|_{\mathbf{x}} = \nabla_R \cdot ({}^L \boldsymbol{\Xi} \cdot \dot{\boldsymbol{\pi}}), \quad (27)$$

$$\mathbf{f}^{\text{inh}} \cdot \mathbf{V} = \left(\frac{1}{2} v^2 + \frac{1}{2} I \dot{\pi}^2 + \boldsymbol{\mathcal{E}} \cdot \boldsymbol{\pi} \right) \frac{\partial \rho_0}{\partial t} \Big|_{\mathbf{x}} - \frac{\partial W}{\partial t} \Big|_{\text{expl}}, \quad (28)$$

and

$$\mathbf{f}^{\text{th}} \cdot \mathbf{V} = S \theta_{,L} V^L = S \frac{\partial \theta}{\partial t} \Big|_{\mathbf{x}} - S \dot{\theta} = S \frac{\partial \theta}{\partial t} \Big|_{\mathbf{x}} + \dot{W} - \dot{E} - \nabla_R \cdot \mathbf{Q}, \quad (29)$$

where we have used the relation $-S \dot{\theta} = \dot{W} - \dot{E} - \nabla_R \cdot \mathbf{Q}$, obtained by the Legendre transformation $W = E - S \theta$ and the entropy balance equation (15)₁.

Finally, using the relations

$$\rho_0 \pi^i \mathcal{E}_{i,L} V^L = \rho_0 (\pi^i \mathcal{E}_i)_{,L} V^L - \rho_0 \mathcal{E}_i \pi^i_{,L} V^L, \quad \mathbf{f}^{\text{fer}} \cdot \mathbf{V} = \rho_0 \pi^i \mathcal{E}_{i,L} V^L - F_L^i \Pi^K \mathcal{E}_{i,K} V^L,$$

$$\rho_0 I \ddot{\pi}^i \frac{\partial \pi_i}{\partial t} \Big|_{\mathbf{x}} = \rho_0 I \dot{\pi}^i \frac{\partial \dot{\pi}_i}{\partial t} \Big|_{\mathbf{x}} = \rho_0 \frac{\partial}{\partial t} \left(\frac{1}{2} I \dot{\pi}^2 \right) \Big|_{\mathbf{x}},$$

the balance equation for the polarization vector (7) multiplied by $\rho_0 \frac{\partial \pi_i}{\partial t} \Big|_{\mathbf{x}}$,

$$\rho_0 \mathcal{E}^i \frac{\partial \pi_i}{\partial t} \Big|_{\mathbf{x}} + \rho_0 {}^L E^i \frac{\partial \pi_i}{\partial t} \Big|_{\mathbf{x}} + {}^L \mathbb{E}^{i,K} \frac{\partial \pi_i}{\partial t} \Big|_{\mathbf{x}} = \rho_0 I \ddot{\pi}^i \frac{\partial \pi_i}{\partial t} \Big|_{\mathbf{x}},$$

operating some transformations and substituting all the contributions (20)–(29) in (19), we obtain the energy balance equation in the form

$$\frac{\partial}{\partial t} \left[E + \rho_0(\mathbf{X}) \left(\frac{1}{2} v^2 + \frac{1}{2} I \dot{\pi}^2 - \mathcal{E} \cdot \boldsymbol{\pi} \right) \right] \Big|_{\mathbf{x}} - \nabla_R \cdot (\mathbf{T} \cdot \mathbf{v} + {}^L \mathbb{E} \cdot \dot{\boldsymbol{\pi}} - \mathbf{Q}) = H, \quad (30)$$

where

$$H = -\rho_0 \boldsymbol{\pi} \cdot \dot{\boldsymbol{\mathcal{E}}} - \mathbf{F}^T \cdot (\boldsymbol{\Pi} \cdot \nabla_R) \boldsymbol{\mathcal{E}} \cdot \mathbf{V}. \quad (31)$$

In the left-hand side of (30) there appear the partial time derivatives at fixed \mathbf{X} of the internal energy E , the kinetic energy of the material lattice, the kinetic energy of the polarization vector that has own inertia, the interaction energy between the electric and the polarization fields and the material energy fluxes related to the Piola–Kirchhoff stress \mathbf{T} , the shell-shell interaction tensor ${}^L \mathbb{E}$ and the negative of the heat flux. In the right-hand side there are energy sources due to material forces which reflect the presence of ferroelectric effects.

Next we have

$$\begin{aligned} \mathbf{f}^{\text{fer}} \cdot \mathbf{V} &= \rho_0 \pi^i \mathcal{E}_{i,L} V^L - F_L^i \Pi^K \mathcal{E}_{i,K} V^L = -\rho_0 \pi^i (F^{-1})^L{}_q v^q \mathcal{E}_{i,L} - \rho_0 F_L^i (F^{-1})^K{}_j \pi^j \mathcal{E}_{i,K} V^L \\ &= -\rho_0 \pi^i \mathcal{E}_{i,q} v^q + \rho_0 \pi^j \mathcal{E}_{i,j} v^i = -\rho_0 \pi^i v^j (\mathcal{E}_{i,j} - \mathcal{E}_{j,i}) = 0, \end{aligned}$$

where we have taken into consideration that $\nabla \times \boldsymbol{\mathcal{E}} = 0$ (we are in quasielectrostatic approximation) and

$$\Pi^K = J_F (F^{-1})^K{}_j P^j = \rho J_F (F^{-1})^K{}_j \pi^j = \rho_0 (F^{-1})^K{}_j \pi^j.$$

Then $\mathbf{f}^{\text{fer}} \cdot \mathbf{V} \equiv 0$. That means \mathbf{f}^{fer} has no dissipative content. Now we transform H :

$$\begin{aligned} H &= -\rho_0 \boldsymbol{\pi} \cdot \dot{\boldsymbol{\mathcal{E}}} - \mathbf{F}^T \cdot (\boldsymbol{\Pi} \cdot \nabla_R) \boldsymbol{\mathcal{E}} \cdot \mathbf{V} = -\rho_0 \pi^i \dot{\mathcal{E}}_i - F_L^j \Pi^K \mathcal{E}_{j,K} V^L \\ &= -\rho_0 \pi^i \dot{\mathcal{E}}_i - \rho_0 F_L^j (F^{-1})^K{}_q \pi^q \mathcal{E}_{j,K} V^L = -\rho_0 \pi^i \dot{\mathcal{E}}_i + \rho_0 \pi^i \mathcal{E}_{i,j} v^j = -\rho_0 \pi^i \left(\frac{\partial \mathcal{E}_i}{\partial t} \right) \Big|_{\mathbf{x}}. \end{aligned}$$

Using the relations $\boldsymbol{\mathcal{E}} = -\nabla \varphi(x, t)$ and $\rho_0 \boldsymbol{\pi} \cdot \nabla \equiv \boldsymbol{\Pi} \cdot \nabla_R$, we then obtain

$$H = \rho_0 \boldsymbol{\pi} \cdot \nabla \left(\frac{\partial \varphi}{\partial t} \right) \Big|_{\mathbf{x}} = (\boldsymbol{\Pi} \cdot \nabla_R) \left(\frac{\partial \varphi}{\partial t} \right) \Big|_{\mathbf{x}} = \nabla_R \cdot \left(\boldsymbol{\Pi} \frac{\partial \varphi}{\partial t} \Big|_{\mathbf{x}} \right) - (\nabla_R \cdot \boldsymbol{\Pi}) \frac{\partial \varphi}{\partial t} \Big|_{\mathbf{x}}. \quad (32)$$

Finally, using (32) the energy balance equation (30) reads

$$\frac{\partial}{\partial t} \left[E + \rho_0(\mathbf{X}) \left(\frac{1}{2} v^2 + \frac{1}{2} I \dot{\pi}^2 - \mathcal{E} \cdot \boldsymbol{\pi} \right) \right] \Big|_{\mathbf{x}} + \nabla_R \cdot \left(\mathbf{T} \cdot \mathbf{v} + \boldsymbol{\Pi} \frac{\partial \varphi}{\partial t} \Big|_{\mathbf{x}} + {}^L \mathbb{E} \cdot \dot{\boldsymbol{\pi}} - \mathbf{Q} \right) = H, \quad (33)$$

with

$$H = -(\nabla_R \cdot \mathbf{\Pi}) \frac{\partial \varphi}{\partial t} \Big|_{\mathbf{x}}, \quad E = \bar{E}(\mathbf{F}, \boldsymbol{\pi}, \nabla_R \boldsymbol{\pi}, \theta; \mathbf{X}). \quad (34)$$

Although it is not given as a strict conservation law, this expression of the energy conservation is of interest because (i) it can be used directly for the evaluation of the *energy-release rate* in the fracture study (compare to the case of classical dielectric-piezoelectrics in [Maugin and Dascalu 1993]), and (ii) it makes the comparison with classical electroelasticity easy in the appropriate reduction.

Indeed, in this simplified case we have

$$I = 0, \quad {}^L \mathbf{E} = 0$$

and, for quasielectrostatics, equations (33) and (34) yield

$$\frac{\partial}{\partial t} [E - \rho_0(\mathbf{X}) \boldsymbol{\mathcal{E}} \cdot \boldsymbol{\pi}] - \nabla_R \cdot \left(\mathbf{T} \cdot \mathbf{v} + \mathbf{\Pi} \frac{\partial \varphi}{\partial t} \Big|_{\mathbf{x}} - \mathbf{Q} \right) = -(\nabla_R \cdot \mathbf{\Pi}) \frac{\partial \varphi}{\partial t} \Big|_{\mathbf{x}}. \quad (35)$$

Simultaneously, equations (7) and (13)₂ yield $\mathcal{E}^i + {}^L E^i = 0$,

$$\mathcal{E}_i = -{}^L E_i = -(F^{-1})_i^K {}^L E_K = \rho_0^{-1} \frac{\partial W}{\partial \pi_j} (F^{-1})_i^K F_K^j, \quad \mathcal{E}_i = \rho_0^{-1} \frac{\partial W}{\partial \pi_i}.$$

Thus, $E - \rho_0 \boldsymbol{\pi} \cdot \boldsymbol{\mathcal{E}} = W + S\theta - \rho_0 \boldsymbol{\pi} \cdot \boldsymbol{\mathcal{E}}$. Setting

$$\bar{W} = W(\mathbf{F}, \boldsymbol{\pi}, \theta) - \rho_0 \boldsymbol{\pi} \cdot \boldsymbol{\mathcal{E}} = \bar{W}(\mathbf{F}, \boldsymbol{\mathcal{E}}, \theta; \mathbf{X}), \quad \pi_j = \rho_0^{-1} \frac{\partial \bar{W}}{\partial \mathcal{E}_j},$$

we finally obtain from equation (35)

$$\frac{\partial}{\partial t} \bar{W}(\mathbf{F}, \boldsymbol{\mathcal{E}}, \theta; \mathbf{X}) \Big|_{\mathbf{x}} - \nabla_R \cdot \left(\mathbf{T} \cdot \mathbf{v} + \mathbf{\Pi} \frac{\partial \varphi}{\partial t} \Big|_{\mathbf{x}} - \mathbf{Q} \right) = -(\nabla_R \cdot \mathbf{\Pi}) \frac{\partial \varphi}{\partial t} \Big|_{\mathbf{x}},$$

which is equation (21) in [Maugin and Dascalu 1993] if we discard the temperature effect.

Acknowledgements

This work has been partially supported by GNFM of INDAM. Restuccia is grateful to W. Muschik for useful remarks and stimulating discussions.

References

- [Cherepanov 1979] G. P. Cherepanov, *Mechanics of brittle fracture*, McGraw-Hill, New York, 1979.
- [Eshelby 1951] J. D. Eshelby, "The force on an elastic singularity", *Phil. Tran. Roy. Soc. A* **244** (1951), 87–112.
- [Eshelby 1969] J. D. Eshelby, "Energy relations and energy momentum tensor in continuous mechanics", pp. 77–115 in *Inelastic behavior of solids*, edited by M. F. Kanninen et al., McGraw-Hill, New York, 1969.
- [Fomethé and Maugin 1996] A. Fomethé and G. A. Maugin, "Material forces in elastic ferromagnets", *Cont. Mech. and Thermodynam.* **8** (1996), 275–292.
- [Francaviglia et al. 2004] M. Francaviglia, L. Restuccia, and P. Rogolino, "Entropy production in polarizable bodies with internal variables", *Journal of Non-Equilibrium Thermodynamics* **29** (2004), 221–235.
- [Huang and Batra 1996] Y. N. Huang and R. C. Batra, "Energy-momentum tensors in nonsimple elastic dielectrics", *J. Elasticity* **42** (1996), 275–281.

- [Kalpakides and Agiasofitou 2002] V. K. Kalpakides and E. K. Agiasofitou, “On material equations in second gradient electroelasticity”, *J. Elasticity* **67** (2002), 205–227.
- [Lax and Nelson 1976] M. Lax and D. F. Nelson, “Maxwell equations in material form”, *Phys. Rev. B* **13** (1976), 1785–1796.
- [Maugin 1977a] G. A. Maugin, “Deformable dielectrics, II: Voigt’s intramolecular force balance in elastic dielectrics”, *Arch. Mech. (Poland)* **29** (1977), 143–159.
- [Maugin 1977b] G. A. Maugin, “Deformable dielectrics, III: A model of interactions,”, *Arch. Mech. (Poland)* **29** (1977), 251–258.
- [Maugin 1988] G. A. Maugin, *Continuum mechanics and electromagnetic solids*, North-Holland, Amsterdam, 1988.
- [Maugin 1992] G. A. Maugin, *Thermomechanics of plasticity and fracture*, Cambridge University Press, Cambridge, 1992.
- [Maugin 1993] G. A. Maugin, *Material inhomogeneities in elasticity*, Chapman and Hall, London, 1993.
- [Maugin 1995] G. A. Maugin, “Material forces: concepts and applications”, *Appl. Mech. Rev. (ASME)* **48** (1995), 213–245.
- [Maugin and Dascalu 1993] G. A. Maugin and C. Dascalu, “Energy-release rates and path-independent integrals in electroelasticity: an assessment”, pp. 41–50 in *Mechanics of electromagnetic materials and structures*, edited by J. S. Lee et al., ASME Proceedings **AMD-161/MD-42**, ASME, New York, 1993.
- [Maugin and Pouget 1980] G. A. Maugin and J. Pouget, “Electroacoustic equations for one-domain ferroelectric bodies”, *J. Acoust. Soc. Am.* **68**:2 (1980), 575–587.
- [Restuccia and Maugin 2004] L. Restuccia and G. A. Maugin, “Pseudomomentum and material forces in ferroelectrics”, pp. 310–325 in *Proc. of The International Symposium on Trends in Continuum Physics (TRECOP’04)* (Poznan, 2004), edited by B. T. Maruszewski et al., Publishing House of the Poznan University of Technology, 2004.
- [Vukobrat 1994] M. Vukobrat, “*J*-integral and energy-release rate in elastic dielectrics”, *Int. J. Engng. Sci.* **32** (1994), 1151–1155.

Received 13 Mar 2008. Accepted 26 Apr 2008.

GERARD A. MAUGIN: gerard.maugin@upmc.fr

Université Pierre et Marie Curie, Institut Jean Le Rond d’Alembert, Case 162, 4 place Jussieu, 75252 Paris Cedex 05, France

LILIANA RESTUCCIA: lrest@dipmat.unime.it

Università di Messina, Dipartimento di Matematica, Contrada Papardo, Salita Sperone 31, 98166, Sant’ Agata Messina, Italy

EXPLOITATION OF THE DISSIPATION INEQUALITY, IF SOME BALANCES ARE MISSING

WOLFGANG MUSCHIK, VITA TRIANI AND CHRISTINA PAPENFUSS

The balance equations of continuum thermodynamics need constitutive equations in order to solve them under the constraint that the entropy production appearing in the entropy balance equation must be not negative. This dissipation inequality represents the second law of thermodynamics. There are two procedures which exploit the dissipation inequality to obtain constitutive equations which are in agreement with the second law: the Coleman–Noll and the Liu techniques. Here we use the Liu technique in the special case in which not all balance equations are taken into account when exploiting the dissipation inequality. This case is of interest because often not all balances are known, or only the energy balance is considered. It is also proved that in this abridged exploitation of the dissipation inequality, thermodynamic restrictions for the constitutive equations are obtained, so that these satisfy the second law. These restrictions represent a smaller class of materials than that obtained when all balances are taken into account.

1. Introduction

The balance equations of continuum thermodynamics have the shape

$$\dot{\mathbf{X}} + \nabla \cdot \mathbf{Y} = \mathbf{R}. \quad (1)$$

The fields $\mathbf{X}(\mathbf{x}, t)$, $\mathbf{Y}(\mathbf{x}, t)$, and $\mathbf{R}(\mathbf{x}, t)$ can be divided into three classes [Muschik et al. 2001]: They may be wanted (or basic) fields, they may be constitutive equations which are defined on the chosen state space \mathbf{Z} spanned by the fields of the state space variables $\mathbf{z}(\mathbf{x}, t)$,

$$\mathbf{z}(\mathbf{x}, t) \in \mathbf{Z}, \quad \mathbf{X}(\mathbf{z}(\mathbf{x}, t)), \quad \mathbf{Y}(\mathbf{z}(\mathbf{x}, t)), \quad \mathbf{R}(\mathbf{z}(\mathbf{x}, t)), \quad (2)$$

and they may be external given fields $\mathbf{X}(\mathbf{x}, t)$, $\mathbf{Y}(\mathbf{x}, t)$, $\mathbf{R}(\mathbf{x}, t)$.

A special balance is that of the local entropy density $s(\mathbf{x}, t)$

$$\sigma_s = \dot{s} + \nabla \cdot \mathbf{J}_s - r_s \geq 0. \quad (3)$$

This inequality represents the second law of continuum thermodynamics, and is called the dissipation inequality. The fields of the entropy production density $\sigma_s(\mathbf{Z})$, of the entropy flux density $\mathbf{J}_s(\mathbf{Z})$, and of the entropy supply density $r_s(\mathbf{Z})$ are constitutive equations. Consequently, according to Equation (2), these fields depend on the state space variables $\mathbf{z}(\mathbf{x}, t)$, and consequently depend indirectly on space-time.

Keywords: dissipation inequality, reduced set of balances, abridged exploitation of the dissipation inequality, second law exploitation, Coleman–Noll procedure, Liu procedure.

The paper was prepared during Triani's stay at the Institut für Theoretische Physik, TU Berlin, and was partly delivered by Muschik at TRECOP'07, Trends in Continuum Physics, Sept. 16–20, 2007, Lviv/Briukhovichi, Ukraina.

Performing the derivatives in Equation (1), we obtain terms which are linear in the so-called higher derivatives

$$\mathbf{y} := (\dot{\mathbf{z}}, \nabla \mathbf{z}), \tag{4}$$

which are outside the state space, and we obtain other terms from \mathbf{R} in (1) which are independent of the higher derivatives. Consequently, after having performed the derivatives in (1) and (3), we obtain the so-called balances on the state space [Muschik 1990] and the dissipation inequality, which both have the shape of an algebraic system which is linear in the higher derivatives, (4), and are given as

$$\mathbf{A} \cdot \mathbf{y} = \mathbf{C}, \quad \mathbf{B} \cdot \mathbf{y} \geq D. \tag{5}$$

Here \mathbf{A} and \mathbf{B} are constitutive equations $\mathbf{A}(\mathbf{z}(\mathbf{x}, t))$, $\mathbf{B}(\mathbf{z}(\mathbf{x}, t))$, and \mathbf{C} and D also consist of constitutive equations, or are given external fields $\mathbf{C}(\mathbf{x}, t)$, $D(\mathbf{x}, t)$.

We now have to exploit the dissipation inequality, (5)₂. For this reason, we use the second law in the Coleman–Mizel formulation [1964] (see also [Muschik et al. 2001]):

$$\{\wedge \mathbf{y} \mid \mathbf{A} \cdot \mathbf{y} = \mathbf{C}\} \longrightarrow \mathbf{B} \cdot \mathbf{y} \geq D, \tag{6}$$

This can be proved by an amendment of the second law, “Except in equilibrium subspace, no reversible process directions exist” [Muschik and Ehretraut 1996], and it shows the material selectivity of the second law; \mathbf{A} , \mathbf{B} , \mathbf{C} , and D are not arbitrary, but have to satisfy the second law, (6).

Two celebrated procedures for the exploitation of the second law (in Coleman–Mizel formulation) are the Coleman–Noll procedure [Truesdell and Noll 1965] and the Liu technique [Liu 1972; Muschik and Ehretraut 1996]. These procedures are different from a mathematical point of view, but are equivalent if all balance equations are taken into account in both procedures [Triani et al. 2008]. Using the Liu procedure, by which the higher derivatives \mathbf{y} are removed from the balances (5)₁ and from the dissipation inequality (5)₂, we obtain

$$\Lambda \cdot \mathbf{A} = \mathbf{B}, \quad \Lambda \cdot \mathbf{C} \geq D. \tag{7}$$

The so-called Lagrange parameters Λ are functions on the chosen state space (2).

If the matrix \mathbf{A} has maximal rank, there exists a right-hand reciprocal of \mathbf{A} ,

$$\mathbf{A} \cdot \bar{\mathbf{A}} = \mathbf{1}, \tag{8}$$

and we obtain from (7) the Lagrange parameters

$$\Lambda = \mathbf{B} \cdot \bar{\mathbf{A}}. \tag{9}$$

Inserting this into (7)₂, we obtain the constraints on the constitutive equations in form of an inequality,

$$\mathbf{B} \cdot \bar{\mathbf{A}} \cdot \mathbf{C} \geq D. \tag{10}$$

We now ask the question of what happens when we make an abridged exploitation of the dissipation inequality by not taking all balance equations into account, a procedure which is often performed [Erickson 1991] (this occurs because people forget some balance equations or do not know all balances). In this paper we prove that an abridged exploitation of the second law restricts the class of materials [Muschik 1990], but this restricted class does satisfy the second law. This means that neglecting balance equations

in the exploitation procedure does not result in mistakes with respect to the second law, but the found class of materials is too small with respect to that class derived by taking all balances into account.

2. The general case

We start out with the balances on the state space $(5)_1$ and with the corresponding dissipation inequality $(5)_2$, both in matrix formulation. Because there are more higher derivatives \mathbf{y} than balance equations the matrix \mathbf{A} is singular, which means there exists a set of \mathbf{y}^0 spanning the nonvanishing kernel of \mathbf{A} ,

$$\mathbf{y}^0 \in \ker \mathbf{A} \leftrightarrow \mathbf{A} \cdot \mathbf{y}^0 = \mathbf{0}, \quad \dim(\ker \mathbf{A}) < n. \quad (11)$$

We now introduce a projector \mathbf{P} as

$$\ker \mathbf{P} \neq \emptyset, \quad \mathbf{P} \cdot \hat{\mathbf{C}} = \mathbf{0}, \quad \hat{\mathbf{C}} \neq \mathbf{0}, \quad (12)$$

which reduces the number of balances which are taken into account, $\mathbf{P} \cdot \mathbf{A} \cdot \mathbf{y} = \mathbf{P} \cdot \mathbf{C}$. The projected balances have other solutions \mathbf{Y} than $(5)_1$,

$$\mathbf{P} \cdot \mathbf{A} \cdot \mathbf{Y} = \mathbf{P} \cdot \mathbf{C}. \quad (13)$$

The dissipation inequality $(5)_2$ transforms into another inequality,

$$\mathbf{B}_P \cdot \mathbf{Y} \geq D_P, \quad (14)$$

which belongs to the projected balances (13). First of all, the connection between (\mathbf{B}, D) and (\mathbf{B}_P, D_P) remains open. The reduced system of balances on the state space (13) and of the dissipation inequality (14) now replaces the original ones, $(5)_1$ and $(5)_2$. The consequences of this replacement are investigated in this paper.

Next we ask the question, if $\hat{\mathbf{C}}$ in (12) is a solution of $(5)_1$, then

$$\mathbf{A} \cdot \hat{\mathbf{y}} = \hat{\mathbf{C}}. \quad (15)$$

According to (11), all solutions of this set of balance equations can be written down in the form

$$\hat{\mathbf{y}} = \bar{\mathbf{A}} \cdot \hat{\mathbf{C}} + \mathbf{y}^0, \quad (16)$$

where $\bar{\mathbf{A}}$ is the existing right-hand reciprocal (8) of \mathbf{A} (because \mathbf{A} has less rows than columns and is presupposed to have maximal rank). Introducing (16) into (15) results, by using (11), in

$$\mathbf{A} \cdot \bar{\mathbf{A}} \cdot \hat{\mathbf{C}} = \hat{\mathbf{C}}.$$

According to (8), this shows that (16) is a solution of (15). Because of $(12)_3$, we state that for all solutions of (15)

$$\hat{\mathbf{y}} \notin \ker \mathbf{A}, \quad (17)$$

is valid.

Applying the projector to (15) and using $(12)_2$, we obtain $\mathbf{P} \cdot \mathbf{A} \cdot \hat{\mathbf{y}} = \mathbf{P} \cdot \hat{\mathbf{C}} = \mathbf{0}$, which means that

$$\hat{\mathbf{y}} \in \ker(\mathbf{P} \cdot \mathbf{A}). \quad (18)$$

Because of

$$\mathbf{A} \cdot \mathbf{y}^0 = \mathbf{0} \quad \rightarrow \quad \mathbf{P} \cdot \mathbf{A} \cdot \mathbf{y}^0 = \mathbf{0}, \quad (19)$$

we obtain

$$\mathbf{y}^0 \in \ker \mathbf{A} \quad \rightarrow \quad \mathbf{y}^0 \in \ker(\mathbf{P} \cdot \mathbf{A}).$$

From (18) and (17), it follows that there are $\hat{\mathbf{y}}$ with the property

$$\hat{\mathbf{y}} \notin \ker \mathbf{A} \quad \leftarrow \quad \hat{\mathbf{y}} \in \ker(\mathbf{P} \cdot \mathbf{A}).$$

Consequently, we obtain for the dimension of the kernels

$$\dim(\ker(\mathbf{P} \cdot \mathbf{A})) > \dim(\ker \mathbf{A}). \quad (20)$$

This means that if the balance equations are neglected the dimension of the kernel belonging to the set of the new balance equations becomes greater. This fact also has consequences for the dissipation inequality (5)₂.

The balance equations on state space are related to the dissipation inequality by the Coleman–Mizel formulation of the second law [Coleman and Mizel 1964]: “Each solution of the balance equations satisfies the dissipation inequality.” This is also true for the projected balances (13) on state space. Consequently, we have the inductions

$$\begin{aligned} \mathbf{A} \cdot (\mathbf{y}^* + \mathbf{y}^0) = \mathbf{C} &\quad \rightarrow \quad \mathbf{B} \cdot (\mathbf{y}^* + \mathbf{y}^0) \geq D, \\ \mathbf{P} \cdot \mathbf{A} \cdot (\bar{\mathbf{Y}} + \hat{\mathbf{Y}}) = \mathbf{P} \cdot \mathbf{C} &\quad \rightarrow \quad \mathbf{B}_P \cdot (\bar{\mathbf{Y}} + \hat{\mathbf{Y}}) \geq D_P. \end{aligned}$$

Because \mathbf{y}^0 and $\hat{\mathbf{Y}}$ are arbitrary elements of the kernels of \mathbf{A} and $\mathbf{P} \cdot \mathbf{A}$, we obtain, in order to maintain the dissipation inequalities,

$$\begin{aligned} \mathbf{B} \cdot \mathbf{y}^0 = 0 &\quad \rightarrow \quad \mathbf{B} \perp \ker \mathbf{A}, \\ \mathbf{B}_P \cdot \hat{\mathbf{Y}} = 0 &\quad \rightarrow \quad \mathbf{B}_P \perp \ker(\mathbf{P} \cdot \mathbf{A}). \end{aligned}$$

This results in

$$\begin{aligned} \dim(\text{span } \mathbf{B}) + \dim(\ker \mathbf{A}) &= n, \\ \dim(\text{span } \mathbf{B}_P) + \dim(\ker(\mathbf{P} \cdot \mathbf{A})) &= n. \end{aligned}$$

Subtracting both the equations from each other,

$$\dim(\text{span } \mathbf{B}) - \dim(\text{span } \mathbf{B}_P) + \dim(\ker \mathbf{A}) - \dim(\ker(\mathbf{P} \cdot \mathbf{A})) = 0,$$

and according to (20) this results in

$$\dim(\text{span } \mathbf{B}) > \dim(\text{span } \mathbf{B}_P). \quad (21)$$

The inequality (21) can be interpreted as follows: If balance equations are not taken into account when exploiting the dissipation inequality, the found class of materials [Muschik et al. 2001] becomes smaller and the dissipation inequality remains valid. Neglecting balance equations in the process of exploiting the dissipation inequality does not result in violations of the second law, but the acquired class of materials is too small. Correct exploitation, considering all balance equations, results in a greater class of materials than when we neglect some of the balances.

3. An example

3.1. Unabridged system of balances. We consider a state space [Muschik et al. 2001; Muschik 2004] spanned by the internal energy density ε and by two additional vector fields, \mathbf{z} and \mathbf{w} ,

$$\mathbf{Z} = \{\varepsilon, \mathbf{z}, \mathbf{w}\}. \quad (22)$$

The local balances (3), of internal energy ε and entropy s , read

$$\dot{\varepsilon} + \nabla \cdot \mathbf{q} - r = 0, \quad \dot{s} + \nabla \cdot \mathbf{J}_s - r_s \geq 0, \quad (23)$$

where \mathbf{q} is the heat flux density and r the heat supply density. The second law of thermodynamics forces the entropy production (3) to be nonnegative.

The set of governing equations for \mathbf{z} and \mathbf{w} is assumed to have balance form, and represent constraints for the state space variables

$$\dot{\mathbf{z}} + \nabla \cdot \Psi = \pi, \quad \dot{\mathbf{w}} + \nabla \cdot \Delta = \delta. \quad (24)$$

Here Ψ is the flux of \mathbf{z} , Δ is the flux of \mathbf{w} , and π and δ are their productions and supplies, respectively. The relaxation equations of \mathbf{z} and/or \mathbf{w} are included by setting $\Psi \equiv \mathbf{0}$ and/or $\Delta \equiv \mathbf{0}$.

Let us now introduce two additional constitutive functions M and \mathbf{W} , which are not in the state space, and for which we also have balances

$$\dot{M}(\varepsilon, \mathbf{z}, \mathbf{w}) + \nabla \cdot \Upsilon(\varepsilon, \mathbf{z}, \mathbf{w}) = \Sigma(\varepsilon, \mathbf{z}, \mathbf{w}), \quad (25)$$

$$\dot{\mathbf{W}}(\varepsilon, \mathbf{z}, \mathbf{w}) + \nabla \cdot \Xi(\varepsilon, \mathbf{z}, \mathbf{w}) = \Omega(\varepsilon, \mathbf{z}, \mathbf{w}). \quad (26)$$

The balance laws (23)–(26) and the entropy inequality (3) can be written in matrix formulation [Muschik et al. 2001], with the shape of (5)₁ and (5)₂, as

$$\mathbf{A} \cdot \mathbf{y} = \mathbf{C}, \quad \mathbf{B} \cdot \mathbf{y} \geq D, \quad (27)$$

where \mathbf{y} represents the higher derivatives of the chosen state space (22), $\mathbf{y} = \{\dot{\varepsilon}, \dot{\mathbf{z}}, \dot{\mathbf{w}}, \nabla \varepsilon, \nabla \mathbf{z}, \nabla \mathbf{w}\}$. The matrices \mathbf{A} and \mathbf{C} follow from the five balance equations (23)–(26),

$$\mathbf{A} = \begin{bmatrix} 1 & 0 & 0 & \frac{\partial \mathbf{q}}{\partial \varepsilon} & \frac{\partial \mathbf{q}}{\partial \mathbf{z}} & \frac{\partial \mathbf{q}}{\partial \mathbf{w}} \\ 0 & 1 & 0 & \frac{\partial \Psi}{\partial \varepsilon} & \frac{\partial \Psi}{\partial \mathbf{z}} & \frac{\partial \Psi}{\partial \mathbf{w}} \\ 0 & 0 & 1 & \frac{\partial \Delta}{\partial \varepsilon} & \frac{\partial \Delta}{\partial \mathbf{z}} & \frac{\partial \Delta}{\partial \mathbf{w}} \\ \frac{\partial M}{\partial \varepsilon} & \frac{\partial M}{\partial \mathbf{z}} & \frac{\partial M}{\partial \mathbf{w}} & \frac{\partial \Upsilon}{\partial \varepsilon} & \frac{\partial \Upsilon}{\partial \mathbf{z}} & \frac{\partial \Upsilon}{\partial \mathbf{w}} \\ \frac{\partial \mathbf{W}}{\partial \varepsilon} & \frac{\partial \mathbf{W}}{\partial \mathbf{z}} & \frac{\partial \mathbf{W}}{\partial \mathbf{w}} & \frac{\partial \Xi}{\partial \varepsilon} & \frac{\partial \Xi}{\partial \mathbf{z}} & \frac{\partial \Xi}{\partial \mathbf{w}} \end{bmatrix}, \quad \mathbf{C} = \begin{bmatrix} r \\ \pi \\ \delta \\ \Sigma \\ \Omega \end{bmatrix}. \quad (28)$$

From the entropy balance (23)₂, it follows that

$$\mathbf{B} = \left[\frac{\partial s}{\partial \varepsilon} \quad \frac{\partial s}{\partial \mathbf{z}} \quad \frac{\partial s}{\partial \mathbf{w}} \quad \frac{\partial \mathbf{J}_s}{\partial \varepsilon} \quad \frac{\partial \mathbf{J}_s}{\partial \mathbf{z}} \quad \frac{\partial \mathbf{J}_s}{\partial \mathbf{w}} \right], \quad D = r_s. \quad (29)$$

The balances and the dissipation inequality (27) are now exploited by the Liu procedure [Liu 1972; Muschik and Ehrentraut 1996], by which the higher derivatives are removed. We introduce the so-called Lagrange parameters,

$$\Lambda := \{ \lambda^\varepsilon \quad \lambda^{\mathbf{z}} \quad \lambda^{\mathbf{w}} \quad \lambda^M \quad \lambda^{\mathbf{W}} \}, \quad (30)$$

and, taking (28)–(29) into account, the Liu equations, (7)₁, become

$$\begin{aligned}
 \lambda^\varepsilon + \lambda^M \frac{\partial M}{\partial \varepsilon} + \lambda^{\mathbf{W}} \cdot \frac{\partial \mathbf{W}}{\partial \varepsilon} &= \frac{\partial s}{\partial \varepsilon}, \\
 \lambda^z + \lambda^M \frac{\partial M}{\partial \mathbf{z}} + \lambda^{\mathbf{W}} \cdot \frac{\partial \mathbf{W}}{\partial \mathbf{z}} &= \frac{\partial s}{\partial \mathbf{z}}, \\
 \lambda^{\mathbf{w}} + \lambda^M \frac{\partial M}{\partial \mathbf{w}} + \lambda^{\mathbf{W}} \cdot \frac{\partial \mathbf{W}}{\partial \mathbf{w}} &= \frac{\partial s}{\partial \mathbf{w}}, \\
 \lambda^\varepsilon \frac{\partial \mathbf{q}}{\partial \varepsilon} + \lambda^z \cdot \frac{\partial \Psi}{\partial \varepsilon} + \lambda^{\mathbf{w}} \cdot \frac{\partial \Delta}{\partial \varepsilon} + \lambda^M \frac{\partial \Upsilon}{\partial \varepsilon} + \lambda^{\mathbf{W}} \cdot \frac{\partial \Xi}{\partial \varepsilon} &= \frac{\partial \mathbf{J}_s}{\partial \varepsilon}, \\
 \lambda^\varepsilon \frac{\partial \mathbf{q}}{\partial \mathbf{z}} + \lambda^z \cdot \frac{\partial \Psi}{\partial \mathbf{z}} + \lambda^{\mathbf{w}} \cdot \frac{\partial \Delta}{\partial \mathbf{z}} + \lambda^M \frac{\partial \Upsilon}{\partial \mathbf{z}} + \lambda^{\mathbf{W}} \cdot \frac{\partial \Xi}{\partial \mathbf{z}} &= \frac{\partial \mathbf{J}_s}{\partial \mathbf{z}}, \\
 \lambda^\varepsilon \frac{\partial \mathbf{q}}{\partial \mathbf{w}} + \lambda^z \cdot \frac{\partial \Psi}{\partial \mathbf{w}} + \lambda^{\mathbf{w}} \cdot \frac{\partial \Delta}{\partial \mathbf{w}} + \lambda^M \frac{\partial \Upsilon}{\partial \mathbf{w}} + \lambda^{\mathbf{W}} \cdot \frac{\partial \Xi}{\partial \mathbf{w}} &= \frac{\partial \mathbf{J}_s}{\partial \mathbf{w}},
 \end{aligned} \tag{31}$$

and the residual inequality, (7)₂, becomes

$$\lambda^\varepsilon r + \lambda^z \cdot \pi + \lambda^{\mathbf{w}} \cdot \delta + \lambda^M \Sigma + \lambda^{\mathbf{W}} \cdot \Omega \geq r_s. \tag{32}$$

The Liu equations (31) and the residual dissipation inequality (32) represent the constraints on the constitutive equations M , \mathbf{W} , \mathbf{q} , Ψ , Δ , Υ , and Ξ caused by the second law.

According to (8) and (7)₁ the Lagrange parameters are given by (9), and the constraints on the constitutive equations have the form of an inequality, as in (10).

3.2. Reduced system of balances. Now we introduce the matrix projector \mathbf{P} , cutting the balance (26) as

$$\mathbf{P} = \begin{bmatrix} 1 & 0 & 0 & 0 & 0 \\ 0 & 1 & 0 & 0 & 0 \\ 0 & 0 & 1 & 0 & 0 \\ 0 & 0 & 0 & 1 & 0 \\ 0 & 0 & 0 & 0 & 0 \end{bmatrix}. \tag{33}$$

The original system of balances, (27), is now replaced by the system (13)

$$\mathbf{P} \cdot \mathbf{A} \cdot \mathbf{Y} = \mathbf{P} \cdot \mathbf{C}, \quad \mathbf{Y} \neq \mathbf{y}, \quad \dim(\text{span } \mathbf{Y}) > \dim(\text{span } \mathbf{y}), \quad \dim(\text{span } (\mathbf{P} \cdot \mathbf{C})) < \dim(\text{span } \mathbf{C}).$$

With this replacement we are not taking into account the balance of the constitutive function \mathbf{W} according to (33). The Liu equations and the residual dissipation inequality, obtained by using the Liu technique [Muschik et al. 2001], have the same algebraic form as (7) in the case of complete exploitation, considering all balances,

$$\Lambda_P \cdot \mathbf{P} \cdot \mathbf{A} = \mathbf{B}_P, \quad \Lambda_P \cdot \mathbf{P} \cdot \mathbf{C} \geq D_P. \tag{34}$$

According to (30) we have

$$\Lambda_P = \{ \lambda_P^\varepsilon \ \lambda_P^z \ \lambda_P^{\mathbf{w}} \ \lambda_P^M \ \lambda_P^{\mathbf{W}} \}, \quad \Lambda_P \cdot \mathbf{P} = \{ \lambda_P^\varepsilon \ \lambda_P^z \ \lambda_P^{\mathbf{w}} \ \lambda_P^M \ 0 \} =: \Lambda_P^0. \tag{35}$$

The projected balances of (34),

$$\Lambda_P^0 \cdot \mathbf{A} = \mathbf{B}_P, \quad \Lambda_P^0 \cdot \mathbf{C} \geq D_P, \tag{36}$$

differ from (7) by setting $\lambda^{\mathbf{W}}$ formally to zero. Consequently, (36) becomes, if (31) and (32) are taken into account,

$$\begin{aligned} \lambda_P^\varepsilon + \lambda_P^M \frac{\partial M}{\partial \varepsilon} &= \left. \frac{\partial S}{\partial \varepsilon} \right|_P, \\ \lambda_P^z + \lambda_P^M \frac{\partial M}{\partial \mathbf{z}} &= \left. \frac{\partial S}{\partial \mathbf{z}} \right|_P, \\ \lambda_P^w + \lambda_P^M \frac{\partial M}{\partial \mathbf{w}} &= \left. \frac{\partial S}{\partial \mathbf{w}} \right|_P, \\ \lambda_P^\varepsilon \frac{\partial \mathbf{q}}{\partial \varepsilon} + \lambda_P^z \cdot \frac{\partial \Psi}{\partial \varepsilon} + \lambda_P^w \cdot \frac{\partial \Delta}{\partial \varepsilon} + \lambda_P^M \frac{\partial \Upsilon}{\partial \varepsilon} &= \left. \frac{\partial \mathbf{J}_s}{\partial \varepsilon} \right|_P, \\ \lambda_P^\varepsilon \frac{\partial \mathbf{q}}{\partial \mathbf{z}} + \lambda_P^z \cdot \frac{\partial \Psi}{\partial \mathbf{z}} + \lambda_P^w \cdot \frac{\partial \Delta}{\partial \mathbf{z}} + \lambda_P^M \frac{\partial \Upsilon}{\partial \mathbf{z}} &= \left. \frac{\partial \mathbf{J}_s}{\partial \mathbf{z}} \right|_P, \\ \lambda_P^\varepsilon \frac{\partial \mathbf{q}}{\partial \mathbf{w}} + \lambda_P^z \cdot \frac{\partial \Psi}{\partial \mathbf{w}} + \lambda_P^w \cdot \frac{\partial \Delta}{\partial \mathbf{w}} + \lambda_P^M \frac{\partial \Upsilon}{\partial \mathbf{w}} &= \left. \frac{\partial \mathbf{J}_s}{\partial \mathbf{w}} \right|_P, \end{aligned} \tag{37}$$

and

$$\lambda_P^\varepsilon r + \lambda_P^z \cdot \pi + \lambda_P^w \cdot \delta + \lambda_P^M \Sigma \geq r_s^P. \tag{38}$$

The equations (37) and the dissipation inequality (38) are the thermodynamic constraints due to the second law, if the balance (26) of the constitutive function \mathbf{W} is not taken into account. These relations are analogous to (31) and to (32). We will compare them in the next section.

3.3. Comparison. A comparison of the original Liu equations, (31), with the projected ones, (37), shows how different spaces are generated by the Lagrange parameters. Because, according to (30) and (35)₂, $5 = \dim(\text{span } \Lambda) > \dim(\text{span } \Lambda_P^0) = 4$ is valid, we obtain, according to the maximal rank of \mathbf{A} and to (7)₁ and (36)₁, $\dim(\text{span } \mathbf{B}) > \dim(\text{span } \mathbf{B}_P)$, the inequality (21), which was expected according to the considerations of the general case.

The class of materials becomes smaller by the reduction of the balances. This yields a comparison of the projected balances, (37), with the original ones, (31). All solutions of the projected balance equations are also solutions of the original balance equations in the case of $\lambda^{\mathbf{W}} = 0$.

3.3.1. The supplies. Comparing the dissipation inequalities (32) and (38), we see that the energy supply r is insensitive to canceling (26). The same is presupposed for the entropy supply

$$r_s^P \doteq r_s. \tag{39}$$

Because energy supply and entropy supply are connected by the temperature Θ ,

$$r_s = \frac{r}{\Theta}, \tag{40}$$

and we obtain from (32) and (38) with (39) and (40)

$$\left[\lambda^\varepsilon - \frac{1}{\Theta} \right] r + \lambda^z \cdot \pi + \lambda^w \cdot \delta + \lambda^M \Sigma + \lambda^{\mathbf{W}} \cdot \Omega \geq 0, \quad \left[\lambda_P^\varepsilon - \frac{1}{\Theta} \right] r + \lambda_P^z \cdot \pi + \lambda_P^w \cdot \delta + \lambda_P^M \Sigma \geq 0.$$

Because the energy supply is independent of all the other quantities which appear in these dissipation inequalities and because the sign of the energy supply can be positive or negative, we obtain

$$\lambda^\varepsilon = \frac{1}{\Theta} = \lambda_P^\varepsilon.$$

In the next section it is proved that the entropy production is sensitive to the reduction of the balance equations.

3.3.2. The entropy production. We now calculate relations between (\mathbf{B}, D) and (\mathbf{B}_P, D_P) . From (7) and (34) we obtain

$$\mathbf{B} = \Lambda \cdot \mathbf{A}, \quad \mathbf{B}_P = \Lambda_P \cdot \mathbf{P} \cdot \mathbf{A}, \quad \Lambda \cdot \mathbf{C} \geq D, \quad \Lambda_P \cdot \mathbf{P} \cdot \mathbf{C} \geq D_P,$$

which results, by use of (35)₂, in

$$\mathbf{B} - \mathbf{B}_P = (\Lambda - \Lambda_P^0) \cdot \mathbf{A}. \tag{41}$$

Because \mathbf{A} is of maximal rank, and $\Lambda \neq \Lambda_P^0$ follows from (30) and (35)₂, we obtain from (41) that $\mathbf{B} \neq \mathbf{B}_P$.

Starting out with (30)₂ and (36)₂, and taking (29)₂ and (39) into account,

$$\Lambda \cdot \mathbf{C} \geq D = r_s, \quad \Lambda_P^0 \cdot \mathbf{C} \geq D_P = r_s^P = r_s,$$

and we obtain for the entropy production

$$\sigma = \Lambda \cdot \mathbf{C} - r_s, \quad \sigma_P = \Lambda_P^0 \cdot \mathbf{C} - r_s \quad \longrightarrow \quad \sigma \neq \sigma_P. \tag{42}$$

Taking (9) and the corresponding relation, $\Lambda_P^0 = \mathbf{B}_P \cdot \bar{\mathbf{A}}$, into account, (42) results in $\sigma = \mathbf{B} \cdot \bar{\mathbf{A}} \cdot \mathbf{C} - r_s \geq 0$ and $\sigma_P = \mathbf{B}_P \cdot \bar{\mathbf{A}} \cdot \mathbf{C} - r_s \geq 0$. We have proved that the entropy production changes when the balance equations are reduced. But it is not clear that the entropy production becomes smaller in the reduced case compared with the original one. Comparing (32) with (38), we do not know that $\lambda^W \cdot \Omega$ is positive. Beyond that, we do not know the values of the remaining terms in which Λ is replaced by Λ_P^0 .

4. Conclusion

It is well known that the second law represents a constraint on the constitutive equations of a system under consideration [Muschik et al. 2001], which means the second law, represented by the dissipation inequality, is material-selective. When exploiting the dissipation inequality by the Liu technique, usually one has to take into account all balance equations of the system [Triani et al. 2008]. There are several reasons why not all balances would be included in the exploitation of the dissipation inequality: not all balance equations are known, only the energy balance is taken into account [Ericksen 1991], or some balances are forgotten. In these cases, an interesting question arises: What happens if not all balances are taken into account when exploiting the dissipation inequality? The answer is that we obtain a smaller class of materials than in the nonreduced case! This smaller class of materials does obey the second law. Therefore, no mistakes appear with respect to the second law, if we forget some balances in its exploitation: we are punished with a smaller class of materials, which has a different nonnegative entropy production than in the nonreduced case. This result is important with respect to the fact that there are

former papers in which an abridged exploitation of the dissipation inequality was performed without any comment or notice.

The results mentioned above are obtained by choosing an abstract large state space (no after-effects) [Muschik et al. 2001] on which the constitutive equations are defined, starting out with the Coleman–Mizel formulation of the second law [Coleman and Mizel 1964; Muschik and Ehretraut 1996], using the Liu procedure for exploiting the dissipation inequality [Liu 1972; Muschik and Ehretraut 1996], and by presupposing that the entropy supply is insensitive to reducing the number of balances.

References

- [Coleman and Mizel 1964] B. D. Coleman and V. J. Mizel, “Existence of caloric equations of state in thermodynamics”, *J. Chem. Phys.* **40** (1964), 1116–1125. MR 28 #4780
- [Ericksen 1991] J. L. Ericksen, *Introduction to the thermodynamics of solids*, vol. 1, Applied Mathematics and Mathematical Computation, Chapman & Hall, London, 1991. MR 93d:73010
- [Liu 1972] I. S. Liu, “Method of Lagrange multipliers for exploitation of the entropy principle”, *Arch. Rational Mech. Anal.* **46** (1972), 131–148. MR 49 #1936
- [Muschik 1990] W. Muschik, *Aspects of nonequilibrium thermodynamics*, vol. 9, Series in Theoretical and Applied Mechanics, World Scientific Publishing Co. Inc., Teaneck, NJ, 1990. Six lectures on fundamentals and methods. MR 92h:80007
- [Muschik 2004] W. Muschik, “Remarks on thermodynamical terminology”, *Non-Equilib. Thermodyn.* **29** (2004), 199.
- [Muschik and Ehretraut 1996] W. Muschik and H. Ehretraut, “An amendment to the second law”, pp. 163–171 in *Proceedings of the Third Meeting on Current Ideas in Mechanics and Related Fields (Segovia, 1995)*, vol. 11, 1996. MR 97j:80002
- [Muschik et al. 2001] W. Muschik, C. Papenfuss, and H. Ehretraut, “A sketch of continuum thermodynamics”, *J. Non-Newtonian Fluid Mech.* **96** (2001), 255–290.
- [Triani et al. 2008] V. Triani, C. Papenfuss, V. Cimmelli, and W. Muschik, “Exploitation of the second law: Coleman–Noll and Liu procedure in comparison”, *Non-Equilib. Thermodyn.* **33** (2008), 47–60.
- [Truesdell and Noll 1965] C. Truesdell and W. Noll, “The non-linear field theories of mechanics”, pp. 1–602 in *Handbuch der Physik, Band III/3*, Springer-Verlag, Berlin, 1965. MR 33 #2030

Received 7 Feb 2008. Revised 26 Mar 2008. Accepted 2 Apr 2008.

WOLFGANG MUSCHIK: muschik@physik.tu-berlin.de

Institut für Theoretische Physik, EW 7-1, Technische Universität Berlin, Hardenbergstraße 36, 10623 Berlin, Germany

VITA TRIANI: vitriani@virgilio.it

Dipartimento di Matematica ed Informatica, Università degli Studi della Basilicata, Campus Macchia Romana, Potenza, 85100, Italy

CHRISTINA PAPENFUSS: c.papenfuss@gmx.de

Institut für Mechanik, Technische Universität Berlin, Strasse des 17. Juni, 10623 Berlin, Germany

VARIATIONAL PRINCIPLES FOR HEAT CONDUCTION IN DISSIPATIVE CONTINUA

STANISŁAW SIENIUTYCZ

Applying some results of nonequilibrium statistical mechanics obtained in the framework of Grad's theory we evaluate nonequilibrium corrections Δs to the entropy s of resting incompressible continua in terms of the nonequilibrium density distribution function, f . To find corrections Δe to the energy e or kinetic potential L we apply a relationship that links energy and entropy representations of thermodynamics. We also evaluate the coefficients of the wave model of heat conduction, such as relaxation time, propagation speed, and thermal inertia. With corrections to L we then formulate a quadratic Lagrangian and a variational principle of Hamilton's (least action) type for a fluid with heat flux, or other random-type effect, in the field or Eulerian representation of the fluid motion. Results that are significant in the hydrodynamics of real incompressible fluids at rest and their practical applications are discussed. In particular, we discuss canonical and generalized conservation laws and show the satisfaction of the second law of thermodynamics under the constraint of canonical conservation laws. We also show the significance of thermal inertia and so-called thermal momentum in the variational formulation.

Glossary of symbols

ϕ, Ψ	Lagrange multipliers	p_i	probabilities
Γ	momentum density	P	pressure
ρ_e	energy density	Q	energy flux
τ	relaxation time	q	heat flux
θ	thermal inertia	R	gas constant
ε	equilibrium energy density	R_j	resistance of j th process
\mathcal{A}	action	r_j	rate of j th process
C	peculiar velocity	S	total entropy
c_0	propagation speed	$S_v = \rho_s$	entropy density
e	specific energy	s	specific entropy
f	distribution function	T	temperature
G^{jk}	matter tensor	$T^{\alpha\beta}$	stress tensor
g	inertial factor	u	macroscopic velocity
H	Hamiltonian	v	diffusion velocity
j	flux density	V	potential function
k_B	Boltzmann constant	W	total work

Keywords: wave equations, variational principles, thermal inertia, conservation laws.

The author acknowledges a support from the Warsaw TU grant: *Simulation and optimization of thermal and mechanical separation processes in 2007/2008.*

L	kinetic potential	w	specific work
m	mass of microobject	\mathbf{x}	radius vector
n	particle number	z	Pontryagin's adjoint

1. Introduction

In this research we embed variational principles of heat transfer into the framework of extended thermodynamics and discuss what can be obtained from statistical theories when describing local disequilibria and evaluating kinetic or flux-dependent terms in energies and macroscopic Lagrangians. Assuming an incompressible continuum in the case of fluids we consider them locally at rest, which let us eliminate the effects of hydrodynamic velocity and focus on the heat transfer and the only phenomenon of interest. Sections 2–4 treat statistical aspects of thermodynamic and transport properties of nonequilibrium fluids with heat flow by applying an analysis that uses Grad's results [1958] to determine nonequilibrium corrections Δs or Δe to the energy e or entropy s in terms of the nonequilibrium density distribution function f . To find corrections to the energy e or kinetic potential L we use corrections Δs and a relationship that links energy and entropy representations of thermodynamics. We also evaluate coefficients of the wave model of heat conduction, such as relaxation time, propagation speed and thermal inertial factors, g and θ . With these data we discuss in Sections 5–7 a variational principle of Hamilton's (least action) type for incompressible continua with heat flux in the field or Eulerian representation. We display an approach that adjoins a given set of constraints to a kinetic potential L and transfers the original variational formulation to the space of associated Lagrange multipliers. Also, we evaluate canonical (physical) and formal (Noether's) components of the energy-momentum tensor along with associated conservation laws. We show that despite of the generally noncanonical form of the conservation laws produced by Noether's theorem the approach that adjoints constraints to given kinetic potential works efficiently. In fact, the approach leads to exact embedding of constraints in the potential space of Lagrange multipliers, implying that the appropriateness of the constraining set should be verified by physical rather than mathematical criteria. In fact, the approach is particularly useful in the field (Eulerian) description of transport phenomena, where equations of the thermal field follow from variational principles containing state adjoints rather than original physical variables. An example of the process is hyperbolic heat transfer, but the approach can also be applied to coupled parabolic transfer of heat, mass, and electric charge. With various gradient or nongradient representations of physical fields in terms of state adjoints (quantities similar to those used by Clebsch in his velocity representation [Sieniutycz 1994]), useful action-type criteria emerge. Symmetry principles are effective, and components of the formal energy-momentum tensor can be evaluated. While we focus on heat flow in incompressible continua our work represents, in fact, a quite general approach that shows the methodological advantage of approaches borrowed from the optimal control theory in variational descriptions of irreversible transport phenomena.

2. Information obtained from statistical theories

For irreversible thermodynamic systems statistical theories may be useful [Grad 1958] to evaluate nonequilibrium corrections to energy and other thermodynamic potentials in situations when a continuum is inhomogeneous and this inhomogeneity is associated with presence of irreversible fluxes. To illustrate

benefits resulting from suitable findings in the field of nonequilibrium statistical thermodynamics, heat transfer processes in locally nonequilibrium fluids can be analyzed [Sieniutycz and Berry 1989].

Quite essential in these analyses is the connection between various representations of thermodynamics of nonequilibrium fluids and a relationship that links energy and entropy representations (resembling the Gouy–Stodola law). Thanks to this relationship nonequilibrium corrections to the energy function can be found from those known for the entropy function of Grad’s theory. These energy corrections will next be used to construct suitable kinetic potentials L and formulate variational principles.

In this paper we work in the energy and Lagrangian representations of thermodynamics and focus on the formulation of a linear variational description for heat transfer in incompressible continua. While the linearity of the theory is certainly an approximation, it is simple and lucid enough to illustrate the effectiveness of a (relatively unknown) variational approach based on adjoining known process equations as constrains to a kinetic potential which is the integrand of the action functional.

The present approach differs from more conventional variational ones in that the action functional is systematically constructed rather than assumed from the beginning. Once a variational theory is developed for an assumed kinetic potential L it can easily be modified for improved kinetic potentials which take more subtle effects into consideration. Equations of constraints (reversible or irreversible) follow in the form of their representations in the space of Lagrange multipliers as extremum conditions of a composite (constraint involving) Lagrangian Λ or its gauge counterparts. We show that as long as representations describing physical variables of state are known in their explicit form, which expresses these variables in terms of Lagrange multipliers, the whole variational formalism can be transferred to the adjoint space of these multipliers, that is, a variational principle can be formulated in this (adjoint) space. We also show how to use the Lagrangian of the problem to obtain the energy-momentum tensor for the continuum with heat flow and formulate associated conservation laws. Finally we discuss the coincidence conditions for formal and canonical conservation laws.

3. Thermodynamics of heat flow in energy and entropy representations

Here we recall some basic knowledge on the thermodynamics of heat flow without local equilibrium. A process description will be developed that will next be used to construct suitable Lagrangians, variational principles, and conservation laws. We work in the framework of extended thermodynamics of fluids [Jou et al. 2001]. We restrict ourselves to an incompressible, one-component continuum with heat flow. In absence of an external magnetic field the rotation of the system does not change the form of nonequilibrium function $e(s, \rho, \mathbf{j}_s)$ which depends then only on the length of the vector \mathbf{j}_s .

Restricting to second order terms, the following is the McLaurin expansion of e with respect to $\mathbf{j}_s = 0$:

$$e(s, \rho, \mathbf{j}_s) \cong e(s, \rho, 0) + \frac{1}{2}(\partial^2 e / \partial \mathbf{j}_s^2)_{\rho, s} \mathbf{j}_s^2, \quad (1)$$

where $e(s, \rho, 0) = e(s, \rho)$ is the familiar equilibrium function of specific energy. Since $(\partial e / \partial \mathbf{j}_s)_{\rho, s}$ vanishes at equilibrium, the first-order term is absent in expansion (1), thus the first nonvanishing term is that quadratic with respect to \mathbf{j}_s . This notion pertains, of course, to any variable vanishing at equilibrium. Clearly, as the second derivative $(\partial^2 e / \partial \mathbf{j}_s^2)$ in (1) is determined at constant s and ρ , it depends on these quantities as parameters.

With Equation (1) and for \mathbf{j}_s as an independent variable describing nonequilibrium deviations, and not too far from the equilibrium, the following equation for the perfect differential of the specific internal energy e is deduced:

$$de(s, \rho, \mathbf{j}_s) = [T(s, \rho) + \Delta T(s, \rho, \mathbf{j}_s)] ds + [\rho^{-2} P(s, \rho) + \Delta \rho^{-2} P(s, \rho, \mathbf{j}_s)] d\rho + \mathbf{a}_s(s, \rho, \mathbf{j}_s) \cdot d\mathbf{j}_s, \quad (2)$$

where $\mathbf{a}_s = (\partial^2 e / \partial \mathbf{j}_s^2)_{\rho, s} \mathbf{j}_s$, from Equation (1). As, roughly, entropy flux \mathbf{j}_s is proportional to its momentum density (*thermal momentum* [Sieniutycz and Berry 1989]), the vector quantity \mathbf{a}_s is a measure of the associated velocity of entropy diffusion, $\mathbf{v} = \mathbf{u}_s - \mathbf{u}$, where \mathbf{u}_s is the absolute velocity of the entropy transfer and \mathbf{u} is the hydrodynamic (barycentric) velocity. The latter is, of course zero in the case of the resting fluid we consider. Equation (2) contains corrections ΔT and $\Delta \rho$ which should be added to equilibrium intensities $T(\rho, s)$ and $\rho^{-2} P(\rho, s)$ to obtain proper nonequilibrium values $T(\rho, s, \mathbf{j}_s)$ and $\rho^{-2} P(\rho, s, \mathbf{j}_s)$. From Equation (2) one obtains the quantities called *nonequilibrium temperatures and pressures*. They are limited in the sense that they are only measures of partial derivatives of the energy with particular nonequilibrium variables chosen to be held constant in a particular frame of variables

$$T(s, \rho, \mathbf{j}_s) = \partial e(s, \rho, \mathbf{j}_s)_{\rho, \mathbf{j}_s} / \partial s \quad \text{and} \quad P(s, \rho, \mathbf{j}_s) = \rho^2 \partial e(s, \rho, \mathbf{j}_s)_{\rho, \mathbf{j}_s} / \partial \rho.$$

The last quantity we define is the vector variable $\mathbf{a}_s(s, \rho, \mathbf{j}_s)$ adjoint with respect to the entropy flux \mathbf{j}_s such that

$$\mathbf{a}_s(s, \rho, \mathbf{j}_s) = \partial \Delta e(s, \rho, \mathbf{j}_s)_{\rho, s} / \partial \mathbf{j}_s,$$

where $\Delta e = e(s, \rho, \mathbf{j}_s) - e(s, \rho, 0)$. We will also use the entropy flux adjoint based on the correction to the energy of unit volume $\Delta \rho_e$

$$\mathbf{i}_s(s, \rho, \mathbf{j}_s) = \partial \Delta \rho_e(s, \rho, \mathbf{j}_s)_{\rho, \mathbf{j}_s} / \partial \mathbf{j}_s, \quad (3)$$

which has units of momentum per unit entropy and is more important than \mathbf{a}_s . A discussion on the role of \mathbf{a}_s and \mathbf{i}_s in the definition of invariant nonequilibrium temperatures is given in Sieniutycz and Berry [1989]. Restricted to the quadratic approximation of Δe in Equation (1) in the case of small flux \mathbf{j}_s , on the basis of Equations (2), (3), (4) and (5), the nonequilibrium corrections ΔT and ΔP caused by the presence of flux \mathbf{j}_s are

$$\Delta T(s, \rho, \mathbf{j}_s) = \frac{1}{2} (\partial^3 \Delta e(s, \rho, \mathbf{j}_s) / \partial \mathbf{j}_s^2 \partial s)_{\text{eq}} \mathbf{j}_s^2, \quad (4)$$

with an analogous formula for ΔP . These are quadratic functions of \mathbf{j}_s . From Equations (1) and (3) the entropy flux adjoint \mathbf{i}_s is

$$\mathbf{i}_s(s, \rho, \mathbf{j}_s) = (\partial^2 \rho_e(s, \rho, \mathbf{j}_s) / \partial \mathbf{j}_s^2)_{\text{eq}} \mathbf{j}_s. \quad (5)$$

The equilibrium subscript in Equations (4)–(6) means that the corresponding derivatives are evaluated at the limit of $\mathbf{j}_s = 0$.

When the curvature of the Gibbs' surface can be neglected, corresponding to the near-equilibrium situation, the energy and entropy excesses are linked by an equality resembling the Gouy–Stodola law

$$(e - e_{\text{eq}})_{s, \rho} = -T(s - s_{\text{eq}})_{e, \rho}. \quad (6)$$

Equation (6) is derived in [Callen 1998, Appendix]. As Figure 1 shows if q is close to zero, an approximation of the same temperature in points A , B , and C can be made. While heat flux densities can be

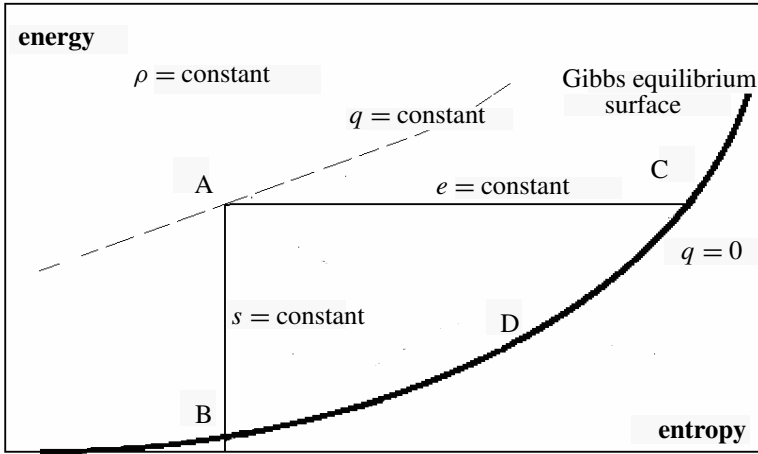


Figure 1. For a given nonequilibrium state, point *A*, two equilibrium reference states at points *B* and *C* correspond, respectively, to the energy and entropy representation. A researcher knowing energy *e* formulates his description of state *A* in terms of equilibrium parameters at *C* for a set of nonequilibrium variables (here heat flux *q*). However, a researcher who knows entropy *s* (for example from distribution function *f* corresponding to *A*) can base his modeling on the equilibrium properties at *B*. When point *A* moves the background, equilibrium states (*B* and *C*) vary. The conventional picture of motion in terms of Hamilton’s principle corresponds to following the behavior of *B* and the kinetic energy of entropy flux, whereas the kinetic theory view corresponds to tracking of *C* and the deviation of entropy from equilibrium. The transition from one view to the other is possible [Sieniutycz and Berry 1989].

finite, they must be small and they are always small otherwise the definition of temperature will lose it meaning. Therefore the small-flux approximation makes sense. Equation (6) is thus interpreted in Figure 1 in the case when the curvature of the line *BDC* can be neglected and a common temperature *T* can be attributed to all reference points (*B*, *C*, or *D*) which is allowed for not-too-large distances of point *A* from equilibrium. The equation states that the energy released during the isoentropic relaxation equals the product of the absolute temperature and the entropy deficiency in the system caused by the presence of an ordered quantity such as the heat flux *q* or the entropy flux, *j_s*.

4. Corrections to energy or entropy in terms of nonequilibrium distribution function *f*

It is the entropy representation that is assumed in the formalism of the kinetic theory of Grad. The function ϕ_1 obtained in Grad’s method when the system’s disequilibrium is maintained by a heat flux *q* is

$$\phi_1 = \frac{2}{5}(m/Pk_B^2T^2)(\frac{1}{2}mC^2 - \frac{5}{2}k_B T)C \cdot q, \tag{7}$$

where *m* is the mass of a molecule. Hence one obtains for the entropy deviation

$$\Delta s = -\frac{1}{5}(m/\rho Pk_B T^2)q^2. \tag{8}$$

See [Grad 1958; Sieniutycz and Berry 1989; Jou et al. 2001] for more information about Equations (7) and (8). Now Equation (6) is applied to evaluate the related energy deviation in terms of the entropy flux $\mathbf{j}_s = \mathbf{q}T^{-1}$

$$\Delta e = \frac{1}{5}(m^2/k_B\rho^2)\mathbf{j}_s^2 = \frac{1}{2}\rho^{-2}g\mathbf{j}_s^2. \quad (9)$$

Equations (8) and (9) hold to the accuracy of the thirteenth moment of the velocity [Grad 1958]. When passing from Equation (8) to (9) the state equation $P = \rho k_B T m^{-1}$ is used and the constant g of the Taylor expansion of (9) defined as $g(\rho, s) \equiv \rho_{\text{eq}}^2(\partial^2 e / \partial \mathbf{j}_s^2)_{\text{eq}}$ is obtained in the form

$$g \equiv \frac{2mT\rho}{5Pk_B} = \frac{2m^2}{5k_B^2}. \quad (10)$$

Here we have abandoned the entropy representation and use the energy representation.

The knowledge of inertial coefficients, such as g , from statistical mechanics considerations helps calculate two basic quantities in the model of heat transfer in continua with finite wave speed. They are thermal relaxation time τ and the propagation speed, c_0 . Of the several formulae available that link quantities τ and g , probably the following expression

$$\tau = kg(\rho T)^{-1} \quad (11)$$

is the most useful [Sieniutycz 1994, p. 199]. Its virtue is that it holds not only for fluids but for arbitrary continua. It links thermal relaxation time τ with thermal conductivity k , inertia g , and thermodynamic state parameters of the system.

As, by definition, the propagation speed of the thermal wave $c_0 = (a/\tau)^{1/2}$, where $a = k/(\rho c_p)$ is the thermal diffusivity, the quantity c_0 satisfies the formula

$$c_0 = \left(\frac{a}{\tau}\right)^{1/2} = \left(\frac{T}{c_p g}\right)^{1/2}.$$

Substituting to this expression the ideal gas data, that is, g of Equation (10) and $c_p = 5k_B/(2m)$, yields the propagation speed in the ideal gas

$$c_0 = \left(\frac{T}{c_p g}\right)^{1/2} = \left(\frac{k_B T}{m}\right)^{1/2}. \quad (12)$$

Thus the results of nonequilibrium statistical mechanics help to estimate numerical values of damped-wave model of heat transfer. The data of τ and c_0 are used below in a variational principle for wave heat transfer. One more coefficient that is quite useful in the wave theory of heat is the coefficient describing a thermal mass per unit of entropy $\theta = T c_0^{-2}$. For the ideal gas, Equation (12) yields the coefficient $\theta = m k_B^{-1}$. We can now establish a variational principle for linear wave heat flow (Cattaneo model).

5. Adjoining a given set of constraints to a kinetic potential

For a heat conduction process described in the entropy representation by the Cattaneo equation of heat and the conservation law for internal energy, the set of constraints is

$$\frac{\partial \mathbf{q}}{c_0^2 \partial t} + \frac{\mathbf{q}}{c_0^2 \tau} + \nabla \rho_e = 0 \quad \text{and} \quad \frac{\partial \rho_e}{\partial t} + \nabla \cdot \mathbf{q} = 0, \quad (13)$$

where the density of equilibrium thermal energy ρ_e satisfies $d\rho_e = \rho c_v dT$, c_0 is propagation speed for the thermal wave, τ is thermal relaxation time, and $D = c_0^2 \tau$ is the thermal diffusivity.

The energy-representation of the Cattaneo equation

$$\frac{\partial \mathbf{j}_s}{c_s^2 \partial t} + \frac{\mathbf{j}_s}{c_s^2 \tau} + \nabla T = 0 \quad (14)$$

uses diffusive entropy flux \mathbf{j}_s instead of heat flux \mathbf{q} . The coefficient c_s is defined as $c_s \equiv (\rho c_v \theta^{-1})^{1/2}$, where $\theta = T c_0^{-2}$, and thermal diffusivity $k \equiv \rho c_v c_0^2 \tau$. Equation (14) is Kaliski's equation [Sieniutycz 1994]. For an incompressible medium one may apply this equation in the form

$$\frac{\partial \mathbf{j}_s}{c_0^2 \partial t} + \frac{\mathbf{j}_s}{c_0^2 \tau} + \nabla \rho_s = 0, \quad (15)$$

which uses the entropy density ρ_s and the propagation speed c_0 instead of c_s .

An action is assumed that absorbs constraints (13) by the Lagrange multipliers, the vector $\boldsymbol{\psi}$ and the scalar ϕ . Its kinetic potential L , Equation (17) below, has a Hamilton's form

$$A = \int_{t_1, V}^{t_2} \varepsilon^{-1} \left\{ \frac{1}{2} \frac{\mathbf{q}^2}{c_0^2} - \frac{1}{2} \rho_e^2 - \frac{1}{2} \varepsilon^2 + \boldsymbol{\psi} \cdot \left(\frac{\partial \mathbf{q}}{c_0^2 \partial t} + \frac{\mathbf{q}}{c_0^2 \tau} + \nabla \rho_e \right) + \phi \left(\frac{\partial \rho_e}{\partial t} + \nabla \cdot \mathbf{q} \right) \right\} dV dt. \quad (16)$$

Since the continuum is at rest, no kinetic energy appears in the above equation. As the kinetic potentials can be diverse (with accuracy to a four-divergence), the conservation laws for energy and momentum substantiate the form (16). In (16) ε is the energy density at an equilibrium reference state, the constant which ensures the action dimension for A but otherwise is unimportant. We assume that the actual energy density ρ_e is close to ε so that the variable ρ_e can be identified with the constant ε in suitable approximations.

We call the multiplier-free term of the integrand of Equation (16) the kinetic potential of Hamilton type for heat transfer

$$L \equiv \frac{1}{2} \varepsilon^{-1} \left\{ \mathbf{q}^2 / c_0^2 - \rho_e^2 - \varepsilon^2 \right\}. \quad (17)$$

It is based on the quadratic form of an indefinite sign, and it has the usual units of the energy density. Remember that we deal with a nonrelativistic theory and in nonrelativistic theories kinetic potentials are always assumed and then tested on their outcomes, never derived. This is what one should remember before he decides to do a variational work. Yet, there may be a hint from Hamilton's principle to define the structure of L in the Hamiltonian form as the difference between the kinetic and static (internal) energy. Functional (17) satisfies this property in the framework of a linear theory that we develop first, because it leads to an explicit analytical solution. It may be shown that Equation (17) is a quadratic approximation of the more exact Hamilton's functional (32) below. This approximation is obtained after the Taylor expansion of the internal energy density around and the subsequent rejection of terms linear in ρ_e which do not influence the extremum conditions of the action integral (16).

Vanishing variations of action A with respect to multipliers $\boldsymbol{\psi}$ and ϕ recover constraints, whereas those with respect to state variables \mathbf{q} and ρ_e yield representations of state variables in terms of $\boldsymbol{\psi}$ and ϕ . For the accepted Hamilton-like structure of L , Equation (17), the Euler-Lagrange equations yield

$$\mathbf{q} = \frac{\partial \boldsymbol{\psi}}{\partial t} - \frac{\boldsymbol{\psi}}{\tau} + c_0^2 \nabla \phi$$

and

$$\rho_e = -\nabla \psi - \frac{\partial \phi}{\partial t}. \tag{18}$$

6. Variational formulation in the space of Lagrange multipliers

In terms of the adjoints ψ and ϕ , the action A , Equation (16), assumes the form

$$A = \int_{t_1, V}^{t_2} \varepsilon^{-1} \left\{ \frac{1}{2c_0^2} \left(\frac{\partial \psi}{\partial t} - \frac{\psi}{\tau} + c_0^2 \nabla \phi \right)^2 - \frac{1}{2} \left(\nabla \cdot \psi + \frac{\partial \phi}{\partial t} \right)^2 - \frac{1}{2} \varepsilon^2 \right\} dV dt. \tag{19}$$

Its Euler–Lagrange equations with respect to ψ and ϕ are respectively

$$\frac{\partial}{\partial t} \left\{ \frac{1}{c_0^2} \left(\frac{\partial \psi}{\partial t} - \frac{\psi}{\tau} + c_0^2 \nabla \phi \right) \right\} + \frac{1}{\tau c_0^2} \left(\frac{\partial \psi}{\partial t} - \frac{\psi}{\tau} + c_0^2 \nabla \phi \right) - \nabla \cdot \left(\nabla \cdot \psi + \frac{\partial \phi}{\partial t} \right) = 0 \tag{20}$$

and

$$-\frac{\partial}{\partial t} \left(\nabla \cdot \psi + \frac{\partial \phi}{\partial t} \right) + \nabla \cdot \left(\frac{\partial \psi}{\partial t} - \frac{\psi}{\tau} + c_0^2 \nabla \phi \right) = 0. \tag{21}$$

It is easy to see that (20) and (21) are the original equations of the thermal field, Equations (13), in terms of the potentials ψ and ϕ . Their equivalent form below shows the damped wave nature of the transfer process. In fact, Lagrange multipliers ψ and ϕ of this (sourceless) problem satisfy certain inhomogeneous wave equations. In terms of the modified quantities Ψ and Φ satisfying $\Psi = \psi \tau c_0^2$ and $\Phi = -\phi \tau c_0^2$; these equations are

$$\nabla^2 \Psi - \frac{\partial^2 \Psi}{c_0^2 \partial t^2} + \frac{\partial \Psi}{\tau c_0^2 \partial t} = \mathbf{q} \quad \text{and} \quad \nabla^2 \Phi - \frac{\partial^2 \Phi}{c_0^2 \partial t^2} + \frac{\partial \Phi}{\tau c_0^2 \partial t} = \rho_e.$$

As both original state variables (\mathbf{q}, ρ_e) and adjoints (ψ, ϕ) appear in these equations, they represent, in fact, mixed formulations of the theory. Still they are interesting as they show that for given densities \mathbf{q} and ρ_e thermal energy transfer can be broken down to potentials. The situation is similar to that in electromagnetic theory or in gravitation theory, where the specification of sources defines the behavior of the field potentials.

Numerical simulation of thermal fields described by (20) and (21) involves the above equations for known potential functions $\psi(\mathbf{x}, t)$ and $\phi(\mathbf{x}, \tau)$ and given coefficients of wave model, c_0 and τ . The way to calculate the fields $\psi(\mathbf{x}, t)$ and $\phi(\mathbf{x}, \tau)$ is provided by the variational principle (19). The principle ensures, in fact, optimal values of thermal fields $\psi(\mathbf{x}, t)$ and $\phi(\mathbf{x}, \tau)$ that are simultaneously solutions of Cattaneo and energy balance equations. In particular, the simulation can involve behavior of imperfect fluids, the application case being polymeric fluids where the quantitative role of relaxation terms is pronounced. Of course, in case of these fluids one should no longer use the ideal gas data but general thermodynamic formulae for coefficients of the wave model, that is, Equation (11), should be applied.

7. Source term in internal energy equation

However, while simple and useful, the method of construction of a suitable action A in the space of potentials by the direct substitution of the representation equations to the kinetic potential L is limited

to cases with linear constraints that do not contain sources. This may be exemplified when the internal energy balance contains a source term $a'q^2$, where a' is a positive constant. The augmented action integral, generalizing Equation (16), should now contain the negative term $-a'q^2$ in its ϕ term

$$-\nabla \cdot \mathbf{q} = \frac{\partial \rho_e}{\partial t} - a'q^2. \tag{22}$$

The energy representation is unchanged, but the heat flux representation follows in a generalized form

$$\mathbf{q} = (1 - 2a'\phi c_0^2)^{-1} \left(\frac{\partial \boldsymbol{\psi}}{\partial t} - \frac{\boldsymbol{\psi}}{\tau} + c_0^2 \nabla \phi \right). \tag{23}$$

Substituting Equations (18) and (23) into action A of Equation (16) (L of (17)) shows that in terms of the potentials the action acquires the form

$$A = \int_{t_1, V}^{t_2} \varepsilon^{-1} \left\{ \frac{1}{2c_0^2} (1 - 2a'\phi c_0^2)^{-2} \left(\frac{\partial \boldsymbol{\psi}}{\partial t} - \frac{\boldsymbol{\psi}}{\tau} + c_0^2 \nabla \phi \right)^2 - \frac{1}{2} \left(\nabla \cdot \boldsymbol{\psi} + \frac{\partial \phi}{\partial t} \right)^2 - \frac{1}{2} \varepsilon^2 \right\} dV dt. \tag{24}$$

However, the Euler–Lagrange equations for this action are not the process constraints in terms of potentials, that is, the method fails to provide a correct variational formulation for constraints with sources. The way to improve the situation is to substitute the obtained representations to a transformed augmented action in which the only terms rejected are total time or space derivatives. The latter can be selected via partial differentiation within the integrand of the original action A . (As we know from the theory of functional extrema the addition of negative terms with total derivatives and divergences do not change extremum properties of a functional.) When this procedure is applied to the considered problem and total derivatives are rejected, a correct action follows in the form

$$A = \int_{t_1, V}^{t_2} \varepsilon^{-1} \left\{ \frac{1}{2c_0^2} (1 - 2a'\phi c_0^2)^{-1} \left(\frac{\partial \boldsymbol{\psi}}{\partial t} - \frac{\boldsymbol{\psi}}{\tau} + c_0^2 \nabla \phi \right)^2 - \frac{1}{2} \left(\nabla \cdot \boldsymbol{\psi} + \frac{\partial \phi}{\partial t} \right)^2 - \frac{1}{2} \varepsilon^2 \right\} dV dt. \tag{25}$$

This form differs from that of Equation (24) only by the power of the term containing the constant a' , related to the source. With the related representation equations (18) and (23), action (25) yields the proper Cattaneo constraint (13) (left) and the generalized balance of internal energy which extends (13) (right) by the source term $a'q^2$.

Equation (24) proves that four-dimensional potential space $(\boldsymbol{\psi}, \phi)$ is sufficient to accommodate an exact variational formulation for the problem with a source. Yet, due to the presence of this source, the formulation does not exist in the original four-dimensional original space (\mathbf{q}, ρ_e) , and, if somebody insists to exploit this space plus possibly a necessary part of the potential space, the following action is obtained from Equations (18), (23), and (25)

$$A = \int_{t_1, V}^{t_2} \varepsilon^{-1} \left\{ (1 - 2a'\phi c_0^2) \frac{\mathbf{q}^2}{2c_0^2} - \frac{1}{2} \rho_e^2 + \frac{1}{2} \varepsilon^2 \right\} dV dt. \tag{26}$$

This form of A shows that, when original state space is involved, the state space required to accommodate the variational principle must be enlarged by inclusion of the Lagrange multiplier ϕ as an extra variable. In fact, Equation (26) proves that original state space (physical space) is lacking sufficient symmetry (Vainberg’s theorem [Sieniutycz 1994]). Yet, as Equation (26) shows, the adjoint space of

potentials (ψ, ϕ) , while also four-dimensional as space (\mathbf{q}, ρ_e) , can accommodate the variational formulation. Why is this so? Because the representation equations do adjust themselves to the extremum requirement of A at given constraints, whereas the given constraints without controls cannot exhibit any flexibility.

Somewhat surprisingly, it follows that a source term in the internal energy balance, as in Equation (22), should be the necessary property of the Cattaneo model, else the energy conservation will be violated. Indeed, aimed at the evaluation of energy conservation we multiply the nontruncated Cattaneo formula

$$\frac{\partial \mathbf{q}}{c_0^2 \partial t} + \frac{\mathbf{q}}{c_0^2 \tau} + \nabla \rho_e = 0$$

by the heat flux \mathbf{q} . The result is an equation

$$\frac{\partial \mathbf{q}^2}{2\epsilon c_0^2 \partial t} - \frac{\rho_e}{\epsilon} \nabla \cdot \mathbf{q} + \nabla \cdot (\epsilon^{-1} \mathbf{q} \rho_e) = -\frac{\mathbf{q}^2}{\epsilon c_0^2 \tau}, \quad (27)$$

which describes an energy balance. We observe that the combination of this balance with the sourceless balance of internal energy,

$$\frac{\partial \rho_e}{\partial t} + \nabla \cdot \mathbf{q} = 0,$$

leads to a differential result

$$\frac{\partial \mathbf{q}^2}{2\epsilon c_0^2 \partial t} + \frac{\rho_e}{\epsilon} \frac{\partial \rho_e}{\partial t} + \nabla \cdot (\epsilon^{-1} \mathbf{q} \rho_e) = -\frac{\mathbf{q}^2}{\epsilon c_0^2 \tau},$$

which — under the linear approximations of the present theory — does not yield a conservation law for the total energy but a balance formula with an energy source

$$\frac{\partial}{\partial t} \left(\frac{\mathbf{q}^2}{2\epsilon c_0^2} + \rho_e \right) + \nabla \cdot (\epsilon^{-1} \mathbf{q} \rho_e) = -\frac{\mathbf{q}^2}{\epsilon c_0^2 \tau}.$$

This shows violation of the total energy conservation for the sourceless internal energy of the model, and leads to the conclusion that the model composed of the Cattaneo equation and sourceless balance of internal energy is physically admissible only in the reversible case of an infinite τ . Certainly, this is not a demanded property of the energy transfer model, thus a further analysis is required. The solution of the dilemma seems to admit a sufficiently large, yet a nonvanishing, source in the internal energy balance.

Admitting a source of the internal energy, as in Equation (22), and using Equation (22) in Equation (27) we find

$$\frac{\partial \mathbf{q}^2}{2\epsilon c_0^2 \partial t} + \frac{\rho_e}{\epsilon} \frac{\partial \rho_e}{\partial t} - \frac{\rho_e}{\epsilon} a' \mathbf{q}^2 + \nabla \cdot (\epsilon^{-1} \mathbf{q} \rho_e) = -\frac{\mathbf{q}^2}{\epsilon c_0^2 \tau}.$$

From this formula we observe that for a' satisfying

$$a' = \frac{1}{\rho c_0^2 \tau} = \frac{1}{\rho c_v D_h T} = \frac{1}{kT}. \quad (28)$$

and — under the approximation of the linear theory — conservation of total energy is satisfied by the sourceless equation

$$\frac{\partial}{\partial t} \left(\frac{\mathbf{q}^2}{2\epsilon c_0^2} + \rho_e \right) + \nabla \cdot (\epsilon^{-1} \mathbf{q} \rho_e) = 0. \tag{29}$$

The positive value of a' in Equation (28) implies generation of the internal energy in the heat transfer process, as described by Equation (22). Still, the internal energy equation with the positive source caused by the quadratic heat flux is a dubious structure. Nonetheless, it is a step forward in comparison with sourceless internal energy balance as we may observe that this generation awkwardly mimics the entropy production with the coefficient $a = T a' = 1/k$. This finally leads us to the conclusion that it is the entropy balance with the source \mathbf{j}^2/k and that it should replace Equation (22).

Replacing Equation (22) with a' of Equation (28) by its conserved counterpart expressed in entropy terms $T \frac{\partial \rho_s}{\partial t} = -\nabla \cdot \mathbf{q}$, where ρ_s is equilibrium entropy density, we expect to obtain better results. After rearranging

$$\frac{\partial \rho_s}{\partial t} = -\nabla \cdot \left(\frac{\mathbf{q}}{T} \right) + \mathbf{q} \cdot \nabla T^{-1}$$

and using in this result a suitable form of the Cattaneo equation (13) (left)

$$-\frac{\tau}{\lambda T^2} \frac{\partial \mathbf{q}}{\partial t} + \nabla T^{-1} - \frac{\mathbf{q}}{\lambda T^2} = 0,$$

we obtain

$$\frac{\partial \rho_s}{\partial t} = -\nabla \cdot \left(\frac{\mathbf{q}}{T} \right) + \mathbf{q} \cdot \left(\frac{\tau}{\lambda T^2} \frac{\partial \mathbf{q}}{\partial t} + \frac{\mathbf{q}}{\lambda T^2} \right),$$

and hence the second law balance for the entropy of extended thermodynamics is

$$\frac{\partial}{\partial t} \left(\rho_s - \frac{\tau}{2\lambda T^2} \mathbf{q}^2 \right) + \nabla \cdot (\mathbf{q} T^{-1}) = \frac{\mathbf{q}^2}{\lambda T^2}.$$

The total energy is conserved in the linearized form (29) or in an exact form

$$\frac{\partial}{\partial t} \left(\frac{T \tau \mathbf{j}_s^2}{2k} + \rho_e \right) + \nabla \cdot (T \mathbf{j}_s) = 0. \tag{30}$$

We shall now see what can be obtained in the energy representation.

8. Action and extremum conditions in variables \mathbf{j}_s and ρ_s

The theory developed so far gives an important hint on how to proceed to a more general formulation which is capable of including the effects of hydrodynamic motion and compressibility of the continuum. Here we shall only outline this problem restricting the variational formulation to the case of resting fluids and relegating all details of the generalized variations to a future paper. In the generalized description we shall proceed to the energy representation, where the constraining set includes Kaliski's counterpart of the Cattaneo equation, Equation (15), and the entropy balance with a source

$$\frac{\partial \rho_s}{\partial t} + \nabla \cdot (\rho_s u + \mathbf{j}_s) = a \mathbf{j}_s^2. \tag{31}$$

The coefficient a is a positive constant, equal to the reciprocal of thermal conductivity k . The form (31) is valid in both classical and extended thermodynamics. The virtue of using the energy representation is that in this frame there is no need to restrict to the special quadratic form of Equation (17). In fact, here is the proper context to include hydrodynamic effects and to design quite diverse nonlinear expressions of Hamilton's type describing the difference between kinetic and internal energies. Assuming as before the absence of external fields, the kinetic potential L of a general process with hydrodynamic effects follows in the form

$$L = \rho \frac{u^2}{2} + \frac{\mathbf{j}_s^2}{2c_s^2} - \rho_e(\rho_s, \rho), \tag{32}$$

where a variable mass density of the fluid is ρ . Equation (32) contains the same kinetic energy of heat which is present in Equation (17), but here this energy is expressed in terms of the entropy flux rather than heat flux. Below we outline the related resting-medium theory.

For a resting medium with a constant density ρ the composite action A assumes the form

$$A = \int_{t_1, V}^{t_2} \left\{ \frac{\mathbf{j}_s^2}{2c_s^2} - \rho_e(\rho_s, \rho) + \eta \left(\frac{\partial \rho_s}{\partial t} - a \mathbf{j}_s^2 + \nabla \cdot \mathbf{j}_s \right) + \boldsymbol{\psi} \cdot \left(\frac{\partial \mathbf{j}_s}{c_0^2 \partial t} + \frac{\mathbf{j}_s}{c_0^2 \tau} + \nabla \rho_s \right) \right\} dV dt. \tag{33}$$

Again, the Lagrange multipliers, scalar η and vector $\boldsymbol{\psi}$, absorb the process constraints. Equation (33) is a truncated form of a more general action that describes the heat and fluid flow in the case when mass density changes and a finite mass flux (represented by the convection velocity \mathbf{u}) is present. This general action is not considered here. The simplified form (33) is sufficient to our present purpose; it selects the heat transfer as the basic process of investigation.

The representations of physical variables in terms of $\boldsymbol{\psi}$, η and ϕ follow from the stationarity conditions of A . These are

$$\delta \mathbf{j}_s : (c_s^{-2} - 2a\eta) \mathbf{j}_s = \frac{\partial \boldsymbol{\psi}}{c_0^2 \partial t} - \frac{\boldsymbol{\psi}}{c_0^2 \tau} + \nabla \eta, \tag{34}$$

$$\delta \rho_s : T(\rho_s, \rho) = -\nabla \cdot \boldsymbol{\psi} - \frac{\partial \eta}{\partial t}. \tag{35}$$

From Equation (34) we obtain a nongradient representation of the diffusive entropy flux in terms of the Lagrange multipliers

$$\mathbf{j}_s = (c_s^{-2} - 2a\eta)^{-1} \left(\frac{\partial \boldsymbol{\psi}}{c_0^2 \partial t} - \frac{\boldsymbol{\psi}}{c_0^2 \tau} + \nabla \eta \right). \tag{36}$$

The Lagrange multipliers are potentials in terms of which a variational formulation is constructed. Yet, there is no theoretical argument to assume that the extremum properties of the action applying the above representations in the kinetic potential (32) should generally be the same as those of the augmented quantity (33). The constraint term (with multipliers), while vanishing, also contributes to the extremum properties. What is possible, however, is the partial integration, which ensures that the Euler–Lagrange equations of the augmented and transformed functional are the same. For the functional (33) the partial integration yields the transformed action

$$A' = \int_{t_1, V}^{t_2} \left\{ \frac{\mathbf{j}_s^2}{2c_s^2} - \rho_e(\rho_s, \rho) - \rho_s \frac{\partial \eta}{\partial t} - \eta a \mathbf{j}_s^2 - \mathbf{j}_s \cdot \nabla \eta - \mathbf{j}_s \cdot \frac{\partial \boldsymbol{\psi}}{c_0^2 \partial t} + \frac{\boldsymbol{\psi} \cdot \mathbf{j}_s}{c_0^2 \tau} - \rho_s \nabla \cdot \boldsymbol{\psi} \right\} dV dt. \tag{37}$$

Since the mass density is not varied, we obtain with the representations (35) and (36) a transformed action that includes the free energy density $f_e = \rho_e - T\rho_s$

$$A' = \int_{t_1, V}^{t_2} \left\{ (2a\eta c_s^2 - 1) \frac{\mathbf{j}_s^2}{2c_s^2} - (\rho_e - T\rho_s) \right\} dV dt. \tag{38}$$

Taking into account that the case of nonvaried mass density corresponds here to the vanishing chemical potential μ , it may be shown that this quantity constitutes a particular type of the pressure action similar to that known in perfect fluid theory. Yet the action obtained includes the Lagrange multiplier η of the entropy balance with the positive source $a\mathbf{j}_s^2$. The situation is similar to that in the process with a source of internal energy, Equation (25). Namely, to obtain an action functional for an irreversible process of heat transfer, associated with a finite entropy source, the state space required to accommodate the variational principle must be enlarged by inclusion of the Lagrange multiplier η as an extra variable. Yet, in the adjoint space only Lagrange multipliers (potentials) and their derivatives are the arguments of the action integrand. The potential representation of action (38) has the form

$$A' = \int_{t_1, V}^{t_2} \left\{ -\frac{c_s^2}{2(1 - 2a\eta c_s^2)} \left(\frac{\partial \psi}{c_0^2 \partial t} - \frac{\psi}{c_0^2 \tau} + \nabla \eta \right)^2 - f_e \left(-\nabla \cdot \psi - \frac{\partial \eta}{\partial t}, \rho \right) \right\} dV dt. \tag{39}$$

Its Euler–Lagrange conditions are Equations (15) and (31) with variables ρ_s and \mathbf{j}_s expressed in terms of η and ψ , Equations (35) and (36). Thus the variational principle is established.

9. Energy conservation and source term in entropy equation

For Equation (31), the entropy source satisfies $\sigma_s = -\partial L'/\partial \eta$. The total entropy production corresponding to action (39) assures the satisfaction of the second law of thermodynamics

$$S_\sigma = -\frac{\partial A'}{\partial \eta} = \int_{t_1, V}^{t_2} \left\{ \frac{ac_s^4}{(1 - 2a\eta c_s^2)^2} \left(\frac{\partial \psi}{c_0^2 \partial t} - \frac{\psi}{c_0^2 \tau} + \nabla \eta \right)^2 \right\} dV dt = \int_{t_1, V}^{t_2} a\mathbf{j}_s^2 dV dt.$$

Let us analyze the differential entropy source in some detail. After transforming the variational stationarity condition of action (37) with respect to ψ

$$\frac{\partial \mathbf{j}_s}{c_0^2 \partial t} + \frac{\mathbf{j}_s}{c_0^2 \tau} + \nabla \rho_s = 0$$

to the form

$$\frac{\partial \mathbf{j}_s}{c_0^2 \partial t} + \frac{\mathbf{j}_s}{c_0^2 \tau} = -\rho c_v \nabla T^{-1},$$

and using the relation between coefficients c_s and c_0 , $c_s^2 = c_0^2(\rho c_v T^{-1})$, we obtain Kaliski’s equation of entropy transfer [1965] with the explicit temperature gradient

$$\frac{\partial \mathbf{j}_s}{c_s^2 \partial t} + \frac{\mathbf{j}_s}{c_s^2 \tau} + \nabla T = 0.$$

After multiplying Kaliski’s equation above by \mathbf{j}_s we find

$$\frac{\partial \mathbf{j}_s^2}{2c_s^2 \partial t} + \nabla \cdot (T \mathbf{j}_s) - T \nabla \cdot \mathbf{j}_s = -\frac{\mathbf{j}_s^2}{c_s^2 \tau}. \tag{40}$$

Under the assumption of the entropy conservation Equation (40) would yield an equation

$$\frac{\partial \mathbf{j}_s^2}{2c_s^2 \partial t} + \nabla \cdot (T \mathbf{j}_s) + T \frac{\partial \rho_s}{\partial t} = -\frac{\mathbf{j}_s^2}{c_s^2 \tau},$$

thus leading to the following energy balance

$$\frac{\partial}{\partial t} \left(\frac{\mathbf{j}_s^2}{2c_s^2} + \rho_e \right) + \nabla \cdot (T \mathbf{j}_s) = -\frac{\mathbf{j}_s^2}{c_s^2 \tau}.$$

This result implies a nonvanishing source of the energy and means that the assumption of the conserved entropy would result in the violation of the energy conservation law.

Yet, for the physical entropy satisfying the nonconserved balance

$$-\nabla \cdot \mathbf{j}_s = \frac{\partial \rho_s}{\partial t} - a \mathbf{j}_s^2, \tag{41}$$

with the coefficient a equal to the reciprocal of thermal conductivity

$$a = \frac{1}{T c_s^2 \tau} = \frac{1}{k}. \tag{42}$$

Total energy balance follows from Equations (40)–(42) in a form that is conservative because the two source terms mutually cancel:

$$\frac{\partial}{\partial t} \left(\frac{\mathbf{j}_s^2}{2c_s^2} + \rho_e \right) + \nabla \cdot (T \mathbf{j}_s) - T a \mathbf{j}_s^2 = -\frac{\mathbf{j}_s^2}{c_s^2 \tau}. \tag{43}$$

The action A' that assures the energy conservation is

$$A' = \int_{t_1, V}^{t_2} \left\{ \left(\frac{2\eta - T\tau}{k} \right) \frac{\mathbf{j}_s^2}{2} - (\rho_e - T\rho_s) \right\} dV dt.$$

Importantly, even when the conservation laws are satisfied in irreversible processes in their canonical form, the related extremum action and potential representations of physical variables do explicitly contain potentials not only their derivatives.

We may thus claim that whenever a irreversible process occurs with the coefficient a satisfying Equation (42), canonical conservation laws can be obtained from Noether’s theorem. In particular the energy conservation law has the form

$$\frac{\partial}{\partial t} \left(\frac{\mathbf{j}_s^2}{2c_s^2} + \rho_e \right) + \nabla \cdot (T \mathbf{j}_s) = 0.$$

As the coefficient $c_s^2 = k(T\tau)^{-1}$, the above equation is equivalent with Equation (30)

$$\frac{\partial}{\partial t} \left(\frac{T\tau \mathbf{j}_s^2}{2k} + \rho_e \right) + \nabla \cdot (T \mathbf{j}_s) = 0.$$

In conclusion, the mathematical scheme obtained preserves the conservation of energy and simultaneous production of the entropy in accordance with laws of thermodynamics.

10. Concluding remarks

Our statistical evaluation of corrections ΔL to the kinetic potential L has led to the variational wave model of heat conduction containing relaxation time, propagation speed, and thermal inertia as the basic coefficients. Applying the corresponding action functional and the variational principle of Hamilton's type we have proved generalized conservation laws for energy and momentum which include terms responsible for the effects associated with the heat inertia and obtained the associated second law of thermodynamics. The most important properties of the generalization are a finite momentum of heat and the nonclassical terms in the stress tensor caused by the heat flux. With all this one still has both the first and the second law satisfied. Here the product of temperature T and the positive entropy source of Equation (41) (quadratic in \mathbf{j}_s) emerges as the kinetic energy of heat in the energy balance (43). While this result is simple, its role is nontrivial for the existence of the variational formulation. Let us recall that in the variational dynamics of real fluids it is always extremely difficult to simultaneously satisfy both laws of thermodynamics (the classical Hamilton's principle holds only for reversible processes, that is, those without entropy production).

In irreversible situations, it may be necessary to absorb more constraints in the action functional. In fact, thermodynamic irreversibility complicates potential representations of physical fields in comparison with the representations describing the reversible evolution.

The problem of thermal energy transfer can be broken down to the problem of related potentials, as in the case of electromagnetic and gravitational fields. We have displayed inhomogeneous equations describing heat transfer in terms of thermal potentials and sources of the field. These equations show that sources of the thermal field are heat flux q and energy density ρ_e . In heat transfer theory, these results yield a situation similar to that in electromagnetic or gravitational field theories, where specification of sources (electric four-current or the matter tensor, respectively) defines the behavior of the potentials.

References

- [Callen 1998] H. Callen, *Thermodynamics and an introduction to thermostatistics*, Wiley, New York, 1998. 2nd edition.
- [Grad 1958] H. Grad, "Principles of the theory of gases", pp. 1 in *Handbook der Physik*, vol. 12, edited by S. Flugge, Springer, Berlin, 1958.
- [Jou et al. 2001] D. Jou, J. Casas-Vazquez, and G. Lebon, *Extended irreversible thermodynamics*, 3rd ed., Springer, Heidelberg, 2001. pp. 121 and 172.
- [Kaliski 1965] S. Kaliski, "Wave equation of heat conduction", *Bull. Acad. Pol. Sci. Ser. Sci. Tech.* **13** (1965), 211–219.
- [Sieniutycz 1994] S. Sieniutycz, *Conservation laws in variational thermo-hydrodynamics*, Kluwer, Dordrecht, 1994.
- [Sieniutycz and Berry 1989] S. Sieniutycz and R. S. Berry, "Conservation laws from Hamilton's principle for nonlocal thermodynamic equilibrium fluids with heat flow", *Phys. Rev. A* **40** (1989), 348–361.

Received 29 Dec 2007. Revised 26 Mar 2008. Accepted 2 Apr 2008.

STANISŁAW SIENIUTYCZ: sieniutycz@ichip.pw.edu.pl

Warsaw University of Technology, Faculty of Chemical and Process Engineering, 1 Waryńskiego Street, 00-645, Warszawa, Poland

www.ichip.pw.edu.pl

NON-NEWTONIAN FLUID FLOW IN A POROUS MEDIUM

ANITA USCIOLOWSKA

This paper presents the properties of non-Newtonian fluid flow in a porous medium. A numerical study on Brinkman flow is considered. It is assumed that the flow is isothermal. The governing equations are included. The steady-state problem is considered. The problem is nonlinear, described by coupled equations and boundary conditions. To solve the problem, a method based on the method of fundamental solutions for solving nonlinear boundary problems is proposed. The numerical experiment is performed and results are discussed.

1. Introduction

Dynamic porous media analysis is a powerful tool used for solving many everyday engineering problems, such as earthquake engineering, soil-structure interaction, biomechanics, et cetera. Moreover, the non-Newtonian fluid flow in porous media is very important due to its practical engineering applications, such as oil recovery, food processing, and materials processing. NonNewtonian fluids in porous media exhibit a nonlinear behaviour that is different from that of Newtonian fluids. An analysis of flow behaviour of non-Newtonian fluids is presented by Skerget and Sames [1999]. The boundary domain integral method for the numerical simulation of unsteady incompressible Newtonian fluid flow is extended to analyse the effects of available non-Newtonian viscosity. The method was applied to the Rayleigh–Benard natural convection problem. The problem mentioned above was solved also in [Huang et al. 1999] using the finite element method. In [Bernal and Kindelan 2007] the problem of injecting a non-Newtonian fluid into a thin cavity was considered. Using the Hele–Shaw approximation the problem reduces to a moving boundary problem in which the pressure is described by a two-dimensional nonlinear, elliptic equation. Mesh-free methods are very well suited for the numerical solution of moving boundary problems since no remeshing is needed at each time step to correctly represent the boundary. Among these methods, Bernal and Kindelan [2007] have chosen the asymmetric RBF collocation method (Kansa’s method), a mesh-free method. The numerical experiment is performed to test different boundary conditions. The other method to simulate the turbulent non-Newtonian flow was proposed in [Rudman and Blackburn 2006]. A spectral element Fourier method for direct numerical simulation of the turbulent flow of non-Newtonian fluids is described and the particular requirements for non-Newtonian rheology are discussed.

For non-Newtonian fluids the phenomena of natural convection in porous media has attracted more attention during recent years. The problem is discussed in the literature by many authors [Hadim 2006; Cheng 2006]. Some numerical methods have been proposed for solving the considered problem. The purpose of [Jecl and Skerget 2003] was to present the use of the boundary element method in the analysis of the natural convection in the porous cavity saturated by the non-Newtonian fluid. The results of

Keywords: non-Newtonian fluid, porous media, fundamental solutions method, Carreau model, Brinkman equation, method of fundamental solutions.

hydrodynamic and heat transfer evaluations were reported for the configuration in which the enclosure is heated from a side wall while the horizontal walls are insulated. The flow in the porous medium was modelled using the modified Brinkman extended Darcy model taking into account the nonDarcy viscous affects. Sarler et al. [2004] described the solution of a steady natural convection problem in porous media by the dual reciprocity boundary element method. The boundary element method for the coupled set of mass, momentum and energy equations in two dimensions was structured by the fundamental solution of the Laplace equation. Numerical examples were presented. The solution was assessed by comparison with reference results of the fine-mesh finite volume method.

The main purpose of this work is to consider an isothermal flow of non-Newtonian fluid in a porous medium. The problem is described by the equation of mass conservation and Brinkman equation. These equations give boundary value problem consisted of a system of nonlinear coupled equations and non-linear coupled boundary conditions. The method of fundamental solutions (MFS) is implemented to solve the nonlinear problem. The algorithm for the nonlinear coupled equations with nonlinear boundary conditions is proposed and applied to the considered problem.

2. Problem description

The steady-state problem in a porous medium is considered. The porous medium is saturated with non-Newtonian fluid. The considered region is presented in Figure 1. The edges of the considered reservoir are insulated, except for two pieces of edge which are open. There is a difference between pressure on two open edges that causes the fluid to flow. The following assumptions are made:

- (i) the only phase flowing is the fluid of constant composition;
- (ii) The fluid is non-Newtonian;
- (iii) flow is isothermal;
- (iv) the permeability of the porous medium is constant and uniform;
- (v) gravitational forces are neglected.

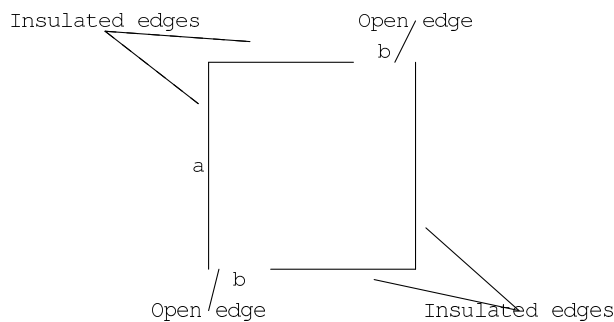


Figure 1. Geometry of the porous medium.

3. The non-Newtonian fluid

To introduce the equations governing the non-Newtonian fluid flow, some general auxiliary parameters are described. The shear-thinning non-Newtonian fluids are ones whose rheology is described by a generalised Newtonian model. Such fluids have an isotropic viscosity that is a function of flow properties. Extra stress tensor S is commonly known as a tensor which is related to the deformation rate by the constitutive equation

$$S_{ij} = \alpha \delta_{ij} + \beta G_{ij} + \gamma G_{ij} G_{ij}, \quad (1)$$

where α , β and γ are functions of three scalar invariants of G_{ij}

$$I_1 = G_{ii}, \quad I_2 = G_{ij} G_{ji}, \quad I_3 = G_{ij} G_{jk} G_{ki}, \quad (2)$$

so

$$\alpha = \alpha(I_1, I_2, I_3), \quad \beta = \beta(I_1, I_2, I_3), \quad \gamma = \gamma(I_1, I_2, I_3), \quad (3)$$

and the deformation rate tensor (the rate of strain tensor) is defined as

$$\mathbf{G} = \nabla \mathbf{v} + (\nabla \mathbf{v})^T, \quad (4)$$

where \mathbf{v} is the velocity field.

Equation (1) is the most general formula for the extra stress of the viscous shear flow. Such fluids are usually called Reiner–Rivlin fluids. For incompressible materials, I_1 equals zero and α , β and γ are considered as functions of I_2 and I_3 . It is recognised that it is far too general to solve a specific flow problem. In order to numerically solve different types of flow problems, there have been many constitutive models in the fluid flow literature proposed by investigators. There is, however, a fairly large category of fluids for which the velocity is not independent of the rate of shear and these fluids are referred to as non-Newtonian. If the viscosity is considered as a function of the invariant I_2 many more practical flow problems can be solved. Then $\mathbf{S} = \eta(I_2)\mathbf{G}$, which represents a generalised Newtonian fluid. The shear rate is defined by $\dot{\gamma} = \sqrt{\frac{1}{2}I_2}$.

Several models are known for non-Newtonian fluids, such as power law fluids or Carreau fluids. In this paper the Carreau fluid is considered. The viscosity for the model is described by the formula

$$\mu = \mu_\infty + (\mu_0 - \mu_\infty) \left(1 + (A\dot{\gamma})^2\right)^{\frac{B-1}{2}},$$

where μ_0 and μ_∞ are asymptotic viscosities (measured in Pa) at large and small strain rates, respectively. A , B are fluid-specific constants (measured in s^{-1}) determined by plotting the observed viscosity as a function of strain rate on a log-log plot, for example. The Carreau model is particularly well-suited for certain dilute, aqueous, polymer solutions and melts.

4. The equations of non-Newtonian fluid flow in porous media

The motion of the fluid in porous media is described by the Brinkman equation for a viscous incompressible isothermal fluid (the momentum equation), the continuity equation and the thermal diffusion equation. The Brinkman equation is in the form

$$\rho_0 \frac{\partial \mathbf{v}}{\partial t} = -\nabla p + \nabla \cdot \mathbf{S} + \frac{\eta}{k} \mathbf{v} + \mathbf{F}, \quad (5)$$

where ρ_0 is the mass density of the fluid, \mathbf{v} is the velocity field, p is the pressure, μ is the viscosity, k is the permeability of the porous structure. In the case of incompressible fluid the equation of the continuity reads

$$\nabla \cdot \mathbf{v} = 0. \tag{6}$$

The considered problem is two-dimensional, so the system of equations (5), (6) has the form

$$\begin{aligned} \eta \nabla^2 v_1 &= -\frac{\partial p}{\partial x_1} + 2\left(\frac{\partial \eta}{\partial x_1} \frac{\partial v_1}{\partial x_1} + \frac{\partial \eta}{\partial x_2} \left(\frac{\partial v_1}{\partial x_2} + \frac{\partial v_2}{\partial x_1}\right)\right) - \frac{\eta}{k} v_1, \\ \eta \nabla^2 v_2 &= -\frac{\partial p}{\partial x_2} + 2\left(\frac{\partial \eta}{\partial x_2} \frac{\partial v_2}{\partial x_2} + \frac{\partial \eta}{\partial x_1} \left(\frac{\partial v_1}{\partial x_2} + \frac{\partial v_2}{\partial x_1}\right)\right) - \frac{\eta}{k} v_2, \\ \nabla^2 p &= 2\left(\frac{\partial^2 \eta}{\partial x_1^2} \frac{\partial v_1}{\partial x_1} + \frac{\partial^2 \eta}{\partial x_2^2} \frac{\partial v_2}{\partial x_2} + \frac{\partial^2 \eta}{\partial x_1 \partial x_2} \left(\frac{\partial v_1}{\partial x_2} + \frac{\partial v_2}{\partial x_1}\right)\right) \\ &\quad + \frac{\partial \eta}{\partial x_1} \left(\nabla^2 v_1 + \frac{\partial^2 v_1}{\partial x_2^2} + \frac{v_1}{k}\right) + \frac{\partial \eta}{\partial x_2} \left(\nabla^2 v_2 + \frac{\partial^2 v_2}{\partial x_1^2} + \frac{v_2}{k}\right). \end{aligned} \tag{7}$$

The boundary conditions are detailed below. For the boundaries of the region the no-slip condition is applied. This means that

$$v_1 = 0, \quad v_2 = 0, \tag{8}$$

for

$$\begin{aligned} \{(x, y) \mid ((b < x < a) \cap (y = 0)) \cup ((x = a) \cap (0 < y < a)) \\ \cup ((0 < x < a - b) \cap (y = a)) \cup ((x = 0) \cap (0 < y < a))\}. \end{aligned}$$

The velocities on the open edges should meet the conditions

$$\frac{\partial v_1}{\partial n} = 0, \quad \frac{\partial v_2}{\partial n} = 0, \tag{9}$$

for $\{(x, y) \mid ((0 < x < b) \cap (y = 0)) \cup ((a - b < x < a) \cap (y = a))\}$. The boundary condition for the pressure field at insulated edges is

$$\nabla p - \nabla \cdot \eta(\nabla \mathbf{v} + (\nabla \mathbf{v})^T) = 0, \tag{10}$$

for

$$\begin{aligned} \{(x, y) \mid ((b < x < a) \cap (y = 0)) \cup ((x = a) \cap (0 < y < a)) \\ \cup ((0 < x < a - b) \cap (y = a)) \cup ((x = 0) \cap (0 < y < a))\}, \end{aligned}$$

where $\mathbf{v} = (v_1, v_2)$. The flow is imposed by pressure difference on both open edges. Therefore, the boundary conditions are

$$p = p_1 \quad \text{for} \quad \{(x, y) \mid ((0 < x < b) \cap (y = 0))\}, \tag{11}$$

$$p = p_2 \quad \text{for} \quad \{(x, y) \mid ((a - b < x < a) \cap (y = a))\}. \tag{12}$$

Moreover, the condition $p_1 > p_2$ has to be introduced. The problem consisting of equations (7) and boundary conditions (8)–(12) was solved in this paper using the method of fundamental solutions supported by Picard iterations.

5. Method of fundamental solutions for nonlinear problems

The nonlinear problem is written in a general form

$$A_n \mathbf{u}(\mathbf{x}) = f_n(\mathbf{x}), \quad (13)$$

for $\mathbf{x} \in \Omega$, where N_e is the number of equations, $n = 1, \dots, N_e$, A_n is a nonlinear partial differential operator, f_n are known functions and Ω is a region in which the equations are determined. The coordinates of the points are given by $\mathbf{x} = (x_1, \dots, x_N)$. The solution requires to calculate $\mathbf{u}(\mathbf{x}) = (u_1(\mathbf{x}), \dots, u_{N_e}(\mathbf{x}))$. For the considered problem the boundary conditions are given by

$$B_l \mathbf{u}(\mathbf{x}) = g_l(\mathbf{x}), \quad (14)$$

for $\mathbf{x} \in \Gamma$ and $l = 1, \dots, N_{bc}$, where Γ is the boundary of the region Ω and N_{bc} is a number of all boundary conditions defined for the considered problem.

In the case that the nonlinear operator can be written as a sum of linear and nonlinear operators, the method of Picard iterations is applied. The nonlinear operator A_n is rewritten as

$$A_n = L_n + N_n, \quad (15)$$

where L_n is the linear partial differential operator of A_n and N_n is a nonlinear partial differential operator. The system of differential equations (13) is written as a system of linear differential equations. The nonlinearity of equation is added to the inhomogeneous part of the equation. Therefore, the considered system of equations has the form

$$L_n \mathbf{u}(\mathbf{x}) = f_n(\mathbf{x}) - N_n \mathbf{u}(\mathbf{x}), \quad (16)$$

for $\mathbf{x} \in \Omega$, where $n = 1, \dots, N_e$. Of course, the boundary conditions (14) are still valid. The proposed transformation of the system of coupled nonlinear equations gives the system of quasilinear equations in implicit form. In order to solve such a system of equations the Picard iterations are implemented. The iterative fashion of the considered system of equations is given as

$$L_n \mathbf{u}^{(k)}(\mathbf{x}) = f_n(\mathbf{x}) - N_n \mathbf{u}^{(k-1)}(\mathbf{x}), \quad (17)$$

for $\mathbf{x} \in \Omega$, where $n = 1, \dots, N_e$ and $k = 1, 2, \dots$. Each of the equations determined in k -th iteration step is solved with the method of fundamental solutions with boundary conditions

$$B_l \mathbf{u}^{(k)}(\mathbf{x}) = g_l(\mathbf{x}), \quad (18)$$

for $\mathbf{x} \in \Gamma$ and $l = 1, \dots, N_{bc}$. The inhomogeneous part of each equation is approximated by radial basis functions and polynomials.

The iterative process begins with initial approximations of the solution, which is obtained by solving the auxiliary boundary value problem

$$L_n \mathbf{u}^{(0)}(\mathbf{x}) = f_n(\mathbf{x}), \quad (19)$$

for $n = 1, \dots, N_e$. The set of equations (19) can be viewed as a system of uncoupled linear equations. Each equation is solved by method of fundamental solutions with proper boundary condition

$$B_l \mathbf{u}^{(0)}(\mathbf{x}) = g_l(\mathbf{x}), \tag{20}$$

for $\mathbf{x} \in \Gamma$ and $l = 1, \dots, N_{bc}$. If the functions $f_n(\mathbf{x})$ do not equal zero, they are approximated by radial basis functions and polynomials. The iterative process has to be stopped if the obtained results reach demanded accuracy. There are some criteria. In this paper the convergence is defined by thresholding the error of obtained solution

$$E_a = \max_{1 \leq i \leq N_C} \max_{1 \leq n \leq N_e} \left| u_n^{(k)}(x_i^C) - u_n^{(k-1)}(x_i^C) \right|, \tag{21}$$

where $\{x_i^C\}_{i=1}^{N_C}$ is a set of trial points with arbitrary chosen number of trial points N_C . Than the condition to stop the iteration problem is

$$E_a < \epsilon, \tag{22}$$

where ϵ denotes a threshold which a small number such as 10^{-5} .

6. Numerical experiment

For considered problem of non-Newtonian fluid flow in porous media the following notation is introduced

$$\mathbf{x} = (x_1, x_2), \quad \mathbf{u}(\mathbf{x}) = (u_1(\mathbf{x}), u_2(\mathbf{x}), u_3(\mathbf{x})) = (v_1(\mathbf{x}), v_2(\mathbf{x}), p(\mathbf{x})). \tag{23}$$

Then, the set (13) is rewritten as

$$A_1 \mathbf{u} = f_1(\mathbf{x}), \quad A_2 \mathbf{u} = f_2(\mathbf{x}), \quad A_3 \mathbf{u} = f_3(\mathbf{x}), \tag{24}$$

with proper boundary conditions. The boundary conditions (14) are the conditions coupling the flow velocities and pressure in porous media. Moreover, one of these conditions consists of a nonlinear operator. Therefore, at every iteration step it is modified using the solution of previous iteration step. In the considered method the set (17) is rewritten in the form of iterative equations

$$\begin{aligned} \nabla^2 u_1^{(k)}(\mathbf{x}) &= f_1(\mathbf{x}) - N_1 \mathbf{u}^{(k-1)}(\mathbf{x}), \\ \nabla^2 u_2^{(k)}(\mathbf{x}) &= f_2(\mathbf{x}) - N_2 \mathbf{u}^{(k-1)}(\mathbf{x}), \\ \nabla^2 u_3^{(k)}(\mathbf{x}) &= f_3(\mathbf{x}) - N_3 \mathbf{u}^{(k-1)}(\mathbf{x}), \end{aligned} \tag{25}$$

for $k = 1, 2, \dots$

Equation (25) are Poisson equations. The inhomogeneous part in each equation is a sum of the functions of independent variables ($f_1(\mathbf{x}), f_2(\mathbf{x}), f_3(\mathbf{x})$) and the part determined by nonlinear operators ($N_1 \mathbf{u}(\mathbf{x}), N_2 \mathbf{u}(\mathbf{x}), N_3 \mathbf{u}(\mathbf{x})$). The system of equations (25) is solved with modified boundary conditions at each iteration step. At the k -th step of procedure the boundary conditions are computed with equations given above. On the boundary the no-slip condition is

$$\begin{aligned} u_1^{(k)} &= 0, & u_2^{(k)} &= 0, \\ \nabla u_3^{(k)} - \nabla \cdot \eta \left(\nabla(u_1^{(k)}, u_2^{(k)}) + (\nabla(u_1^{(k)}, u_2^{(k)}))^T \right) &= 0, \end{aligned} \tag{26}$$

for

$$\{(x, y) \mid ((b < x < a) \cap (y = 0)) \cup ((x = a) \cap (0 < y < a)) \cup ((0 < x < a - b) \cap (y = a)) \cup ((x = 0) \cap (0 < y < a))\}.$$

In the case of an open edge on a boundary the normal flow is defined with

$$\frac{\partial u_1^{(k)}}{\partial y} = 0, \quad \frac{\partial u_2^{(k)}}{\partial y} = 0, \tag{27}$$

for $\{(x, y) \mid ((0 < x < b) \cap (y = 0)) \cup ((a - b < x < a) \cap (y = a))\}$. Pressure is given as

$$u_3^{(k)} = p_1, \tag{28}$$

for $\{(x, y) \mid ((a - b < x < a) \cap (y = a))\}$. At the beginning of the iterative procedure the initial values of unknown variables are set. In the considered case initial values are chosen as

$$u_1^{(0)} = 0, \quad u_2^{(0)} = 0, \quad u_3^{(0)} = 0, \tag{29}$$

$$\frac{\partial u_1^{(0)}}{\partial x} = 0, \quad \frac{\partial u_1^{(0)}}{\partial y} = 0, \quad \frac{\partial u_2^{(0)}}{\partial x} = 0, \quad \frac{\partial u_2^{(0)}}{\partial y} = 0. \tag{30}$$

Then the system of Poisson equations is obtained

$$\nabla^2 u_1^{(1)} = f_1(\mathbf{x}), \quad \nabla^2 u_2^{(1)} = f_2(\mathbf{x}), \quad \nabla^2 u_3^{(1)} = f_3(\mathbf{x}) - N_3 \mathbf{u}^{(1)}(\mathbf{x}), \tag{31}$$

with the boundary conditions (26)–(28) applied with $k = 1$.

The solution is obtained in five iterations. Figures 2, 3 and 4 show, respectively, the vertical component of a velocity field, the horizontal component of the velocity field and the pressure field in a porous medium. It can be observed on the graphs that the boundary conditions for velocity and pressure are met.

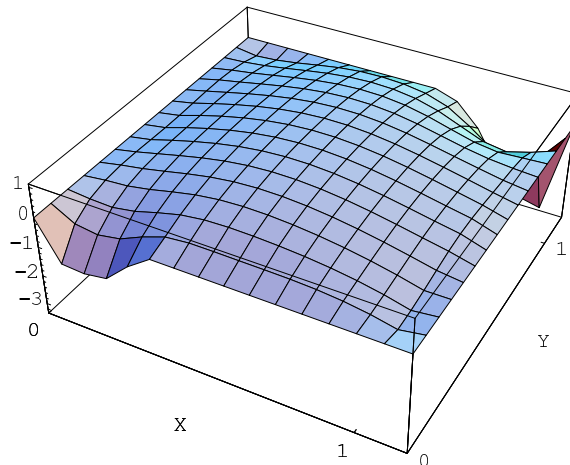


Figure 2. Component v_1 of velocity of non-Newtonian fluid in the porous medium.

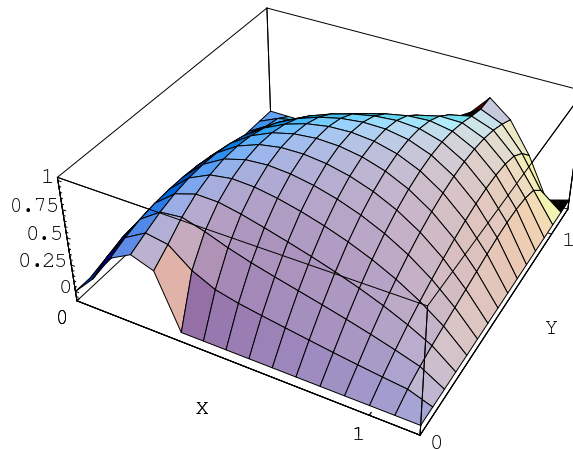


Figure 3. Component v_2 of velocity of non-Newtonian fluid in the porous medium.

The velocity of a non-Newtonian fluid flow in a porous medium, presented in Figure 2 and Figure 3, has the maximum value at the centre point of the considered region. On the boundary with a no-slip condition, velocity equals zero. This fact is observed in Figures 2 and 3. This shows that the implemented method meets the imposed boundary conditions. Near the open edges the component of velocity has positive values, indicating the direction of the flow. Of course, the fluid flows from the edge of higher pressure to the edge of lower pressure. At some distance from the open edges the component changes sign and becomes negative. This results in turbulence. Figure 4, consisting of the pressure field in considered region, confirms fulfilling boundary conditions determined in the problem. On the open edges, the values of pressure have been imposed and kept during implementation of method of fundamental solutions.

The results of numerical experiment show that the numerical method implemented for considered problem is sufficient and correct for nonlinear problems. The method is supported by Picard iterations and

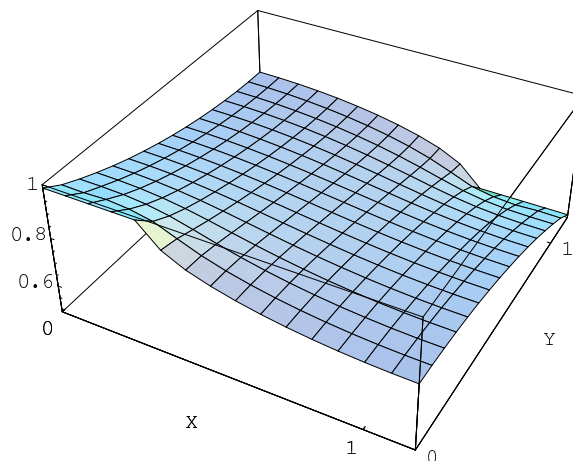


Figure 4. Pressure field in the porous medium.

method of fundamental solutions. For the considered problem the iteration process has been convergent. The satisfactory precision of obtained results has been achieved in five iterations. The presented results are compatible with expected ones.

7. Conclusions

In this paper the flow of non-Newtonian fluid in a porous medium has been considered. The governing equations were written and applied for two dimensional problem. Than the numerical algorithm has been proposed to solve the considered problem. The implementation of the method of fundamental solutions for the system of nonlinear coupled equations with nonlinear coupled boundary conditions has been presented. The numerical experiment, performed for the considered problem gives proper results, compatible with expected ones.

References

- [Bernal and Kindelan 2007] F. Bernal and M. Kindelan, “RBF meshless modelling on non-Newtonian Hele–Shaw flow”, *Eng. Anal. Bound. Elem.* **31** (2007), 863–874.
- [Cheng 2006] C.-Y. Cheng, “Natural convection heat and mass transfer of non-Newtonian power law fluids with yield stress in porous media from a vertical plate with variable wall heat and mass fluxes”, *Int. Commun. Heat Mass.* **33** (2006), 1156–1164.
- [Hadim 2006] H. Hadim, “Non-Darcy natural convection of a non-Newtonian fluid in a porous cavity”, *Int. Commun. Heat Mass.* **33** (2006), 1179–1189.
- [Huang et al. 1999] H. C. Huang, Z. H. Li, and A. Usmani, *Finite element analysis of non-Newtonian flow*, Springer, London, 1999.
- [Jecl and Skerget 2003] R. Jecl and L. Skerget, “Boundary element method for natural convection in non-Newtonian fluid saturated square porous cavity”, *Eng. Anal. Bound. Elem.* **27** (2003), 963–975.
- [Rudman and Blackburn 2006] M. Rudman and H. M. Blackburn, “Direct numerical simulation of turbulent non-Newtonian flow using a spectral element method”, *Appl. Math. Model.* **30** (2006), 1229–1248.
- [Sarler et al. 2004] B. Sarler, J. Perko, D. Gobin, B. Goyeau, and H. Power, “Dual reciprocity boundary element method solution of natural convection in Darcy-Brinkman porous media”, *Eng. Anal. Bound. Elem.* **28** (2004), 23–41.
- [Skerget and Sames 1999] L. Skerget and N. Sames, “BEM for non-Newtonian fluid flow”, *Eng. Anal. Bound. Elem.* **23** (1999), 435–442.

Received 7 Feb 2008. Accepted 25 Mar 2008.

ANITA USCILOWSKA: anita.uscilowska@put.poznan.pl

Institute of Applied Mechanics, Poznan University of Technology, ul. Piotrowo 3, 60-965 Poznan, Poland

INTERNAL ENERGY IN DISSIPATIVE RELATIVISTIC FLUIDS

PÉTER VÁN

Liu procedure is applied to special relativistic fluids. It is shown that a reasonable relativistic theory is an extended one, where the basic state space contains the momentum density. This property follows from the structure of the energy-momentum balance and the Second Law of thermodynamics. Moreover, we derive that the entropy depends on both the energy density and the momentum density in a specific way, indicating that the local rest frame energy density cannot be interpreted as the internal energy, and that the local rest frame momentum density should be considered, too. The corresponding constitutive relations for the stress and the energy flux are derived.

1. Introduction

Nonrelativistic nonequilibrium thermodynamics separates the dissipative and nondissipative parts of the evolving physical quantities. This separation is based on the construction of the internal energy balance [Eckart 1940a; Groot and Mazur 1962; Gyarmati 1970]. According to the classical interpretation, the internal energy is the difference of the total energy and the special energies of known type. The entropy function depends directly on the internal energy. The internal energy is distributed equally among the molecular degrees of freedom. The process by which other energy types are converted to internal energy is called dissipation. This approach is common in all theories of nonequilibrium thermodynamics, including classical irreversible thermodynamics, where the hypothesis of local equilibrium applies. However, there is no internal energy in this sense in relativistic irreversible thermodynamics. In fact, there is practically no relativistic irreversible thermodynamics at all because the local equilibrium theory is plagued by serious inconsistencies. Only extended theories, theories beyond local equilibrium, are considered as viable. The reason for this is that the classical theory of Eckart [1940b] is for relativistic fluids simple and elegant, but produces generic instabilities [Hiscock and Lindblom 1985]. The more developed extended theories incorporate the theory of Eckart, but suppress the instabilities [Hiscock and Lindblom 1987; Geroch 1995; Lindblom 1996].

In this paper we investigate the possibility of local equilibrium in relativistic hydrodynamics by methods of continuum thermodynamics. In Section 2 the balances of energy-momentum and entropy are introduced. In Section 3, we calculate the dissipation inequality for first-order (local equilibrium) relativistic hydrodynamics using the Liu procedure. The need of second-order (extended, or weakly nonlocal) theories is indicated by the emergent structure. A new concept of relativistic internal energy follows. Based on these results, Section 4 shows the constitutive equations of the simplest extended theory by the heuristic arguments of irreversible thermodynamics.

Keywords: relativistic nonequilibrium thermodynamics, Liu procedure, relativistic internal energy.

This work has been supported by the Hungarian National Science Fund OTKA (T49466, T48489), by the EU-I3HP project, and by a Bolyai scholarship of the Hungarian Academy of Sciences.

2. Basic balances of relativistic fluids

For the metric (Lorentz form) we use $g^{\mu\nu} = \text{diag}(-1, 1, 1, 1)$, employing the usual convention that the speed of light $c = 1$. Therefore, for a four-velocity u^α we have $u_\alpha u^\alpha = -1$. $\Delta^\alpha_\beta = g^\alpha_\beta + u^\alpha u_\beta$ denotes the u -orthogonal projection. With these conventions in mind, we proceed to form the basic balances of energy-momentum and entropy.

The energy-momentum density tensor is given with the help of the rest-frame quantities

$$T^{\alpha\beta} = e u^\alpha u^\beta + u^\alpha q^\beta + u^\beta q^\alpha + P^{\alpha\beta}, \quad (1)$$

where $e = u_\alpha u_\beta T^{\alpha\beta}$ is the *density of the energy*, $q^\beta = -u_\alpha \Delta^\beta_\gamma T^{\alpha\gamma}$ is the *energy flux* or *heat flow*, $q^\alpha = -u_\beta \Delta^\alpha_\gamma T^{\gamma\beta}$ is the *momentum density*, and $P^{\alpha\beta} = \Delta^\alpha_\gamma \Delta^\beta_\mu T^{\gamma\mu}$ is the *pressure tensor*. The momentum density, energy flux, and pressure are spacelike in the comoving frame, therefore $u_\alpha q^\alpha = 0$, $u_\beta q^\beta = 0$, and $u_\alpha P^{\alpha\beta} = u_\alpha P^{\beta\alpha} = 0^\beta$. The energy-momentum tensor is symmetric, because we assume that the internal spin of the material is zero. In this case, the energy flux and the momentum density are equal. Let us emphasize that the form (1) of the symmetric energy-momentum tensor is completely general for one-component fluids, but it is expressed by the local rest frame quantities.

Now the conservation of energy-momentum $\partial_\beta T^{\alpha\beta} = 0$ is expanded to

$$\partial_\beta T^{\alpha\beta} = \dot{e} u^\alpha + e u^\alpha \partial_\beta u^\beta + \dot{e} u^\alpha + u^\alpha \partial_\beta q^\beta + q^\beta \partial_\beta u^\alpha + \dot{q}^\alpha + q^\alpha \partial_\beta u^\beta + \partial_\beta P^{\alpha\beta}, \quad (2)$$

where $\dot{e} = \frac{d}{d\tau} e = u^\alpha \partial_\alpha e$ denotes the derivative of e by the proper time τ . Its timelike part in a local rest frame gives the balance of the energy

$$-u_\alpha \partial_\beta T^{\alpha\beta} = \dot{e} + e \partial_\alpha u^\alpha + \partial_\alpha q^\alpha + q^\alpha \dot{u}_\alpha + P^{\alpha\beta} \partial_\beta u_\alpha = 0. \quad (3)$$

The spacelike part in the local rest frame describes the balance of the momentum

$$\Delta^\alpha_\gamma \partial_\beta T^{\gamma\beta} = \dot{e} u^\alpha + q^\alpha \partial_\beta u^\beta + q^\beta \partial_\beta u^\alpha + \Delta^\alpha_\gamma \dot{q}^\gamma + \Delta^\alpha_\gamma \partial_\beta P^{\gamma\beta} = 0^\alpha. \quad (4)$$

The entropy density and flux can also be combined into a four-vector, using local rest frame quantities:

$$S^\alpha = s u^\alpha + J^\alpha, \quad (5)$$

where $s = -u_\alpha S^\alpha$ is the *entropy density* and $J^\alpha = S^\alpha - u^\alpha s = \Delta^\alpha_\beta S^\beta$ is the *entropy flux*. The entropy flux is u -spacelike, therefore $u_\alpha J^\alpha = 0$. In this framework, the Second Law of thermodynamics is expressed by the following inequality

$$\partial_\alpha S^\alpha = \dot{s} + s \partial_\alpha u^\alpha + \partial_\alpha J^\alpha \geq 0. \quad (6)$$

3. Thermodynamics

The thermodynamical background in relativistic theories is usually based on analogies with nonrelativistic thermostatics. However, nonequilibrium thermodynamics has developed beyond the simple, ‘let us substitute everything into the entropy balance and see what happens’ theory since Eckart. It is important to check the dynamic consistency of the Second Law, considering the evolution equations as constraints for the entropy balance. This method of nonequilibrium thermodynamics is constructive, gives important information for new theories, and reveals some deeper interrelations. Here we exploit the Second Law

by Liu's procedure [Liu 1972], introducing a first-order weakly nonlocal state space in all basic variables, and thus restricting ourselves to a local equilibrium theory. One can find a general treatment of nonrelativistic classical and extended irreversible thermodynamics from this point of view in [Ván 2003]. Our aim here is to investigate the relativistic fluids with similar methods, and to get the relativistic equivalent of the classical Fourier–Navier–Stokes system of equations for one component fluids.

Our most important assumption regarding relativistic thermodynamics is that the constitutive equations are local rest frame expressions. As material interactions are local, this is natural from a physical point of view.

The *basic state space* of the theory is spanned by the energy density e and by the velocity field u^α . The *constitutive state space* is spanned by the basic state variables and their first derivatives, is therefore first-order weakly nonlocal. Hence, the constitutive functions depend on the variable set $C = (e, u_\alpha, \partial_\alpha e, \partial_\alpha u_\beta)$. The *constitutive functions* are the energy flux/momentum density q^α , the pressure $P^{\alpha\beta}$, the entropy density s and the entropy flux J^α . The derivatives of the constitutive functions are denoted by the number of the corresponding variable in the constitutive space, for example, $\frac{\partial s}{\partial(\partial_\alpha e)} = \partial_3 s$. With this notation we can distinguish easily between the derivatives by the constitutive and spacetime variables. A nonequilibrium thermodynamic theory is considered to be solved if all other constitutive quantities are expressed by the entropy density and its derivatives.

According to the procedure of Liu, the balance of energy-momentum (2) is a constraint to the entropy balance (6) with the Lagrange–Farkas multiplier Λ_α ,

$$\partial_\alpha S^\alpha - \Lambda_\alpha \partial_\beta T^{\alpha\beta} \geq 0. \quad (7)$$

Let us remember that here, the spacelike components of the four quantities and the entropy density are the constitutive quantities depending on the introduced constitutive variables C . Therefore, in the above inequality we can develop the derivatives of the composite functions. The coefficients of the derivatives that are not in the constitutive space must be zero. As a result, we get the following Liu-equations:

$$\begin{aligned} \partial_{\alpha\beta} e : \quad & (\partial_3 S^\alpha)^\beta - \Lambda_\mu (\partial_3 T^{\mu\alpha})^\beta = 0^{\alpha\beta}, \\ \partial_{\alpha\beta} u_\gamma : \quad & (\partial_4 S^\alpha)^{\beta\gamma} - \Lambda_\mu (\partial_4 T^{\mu\alpha})^{\beta\gamma} = 0^{\alpha\beta\gamma}. \end{aligned} \quad (8)$$

The simple structure of the Liu equations suggests the assumption that the Lagrange multiplier is a local function, and does not depend on the derivatives of the basic state variables

$$\Lambda_\gamma = \Lambda_\gamma(n, e). \quad (9)$$

A general solution of (8) is

$$S^\alpha - \Lambda_\gamma T^{\gamma\alpha} - A^\alpha = 0^\alpha, \quad (10)$$

where $A^\alpha = A^\alpha(n, e)$ is an arbitrary local function.

Let us introduce the splitting of the vector multiplier and the four-vector A^α into spacelike and timelike parts in the local rest frame as

$$\begin{aligned} \Lambda^\alpha &= -\Lambda u^\alpha + l^\alpha, \\ A^\alpha &= A u^\alpha + a^\alpha, \end{aligned}$$

where for the spacelike components $u_\alpha l^\alpha = u_\alpha a^\alpha = 0$. Now, Equation (10) gives

$$u^\alpha (s - \Lambda e - l_\gamma q^\gamma - A) + (J^\alpha - \Lambda q^\alpha - l_\gamma P^{\gamma\alpha} - a^\alpha) = 0^\alpha. \tag{11}$$

Here both the timelike and spacelike parts are zero, resulting in

$$s = \Lambda e + l_\gamma q^\gamma + A, \tag{12}$$

$$J^\alpha = \Lambda q^\alpha + l_\gamma P^{\gamma\alpha} + a^\alpha. \tag{13}$$

After the identification of the Liu equations, we expand the *dissipation inequality* as

$$\begin{aligned} \partial_\alpha e [(\partial_1 s)u^\alpha + \partial_1 J^\alpha - \Lambda u^\alpha - \Lambda \partial_1 q^\alpha - l_\gamma \partial_1 P^{\gamma\alpha} - l_\gamma \partial_1 q^\gamma u^\alpha] \\ + \partial_\alpha u_\beta [(s - \Lambda e - l_\gamma q^\gamma) \Delta^{\alpha\beta} + (\partial_2 s)^\beta u^\alpha + (\partial_2 J^\alpha)^\beta \\ - l^\beta e u^\alpha - l^\beta q^\alpha - \Lambda (\partial_2 q^\beta)^\alpha - \Lambda_\gamma (\partial_2 P^{\gamma\alpha})^\beta - \Lambda_\gamma u^\alpha (\partial_2 q^\gamma)^\beta] \geq 0. \end{aligned} \tag{14}$$

Here we exploited the fact that partial differentiation by e can be exchanged with a multiplication by the four velocity u^α .

In the dissipation inequality one should consider the solution of the Liu equations. Substituting (12) and (13) into (14) we get

$$\begin{aligned} \partial_\alpha e [(\partial_1 s - \Lambda - l_\gamma \partial_1 q^\gamma)u^\alpha + q^\alpha \partial_1 \Lambda + P^{\gamma\alpha} \partial_1 l_\gamma + \partial_1 a^\alpha] \\ + \partial_\alpha u_\beta [A \Delta^{\alpha\beta} + q^\alpha (\partial_2 \Lambda)^\beta + P^{\gamma\alpha} (\partial_2 l_\gamma)^\beta + (\partial_2 a^\alpha)^\beta \\ + u^\alpha ((\partial_2 s)^\beta - l_\gamma (\partial_2 q^\gamma)^\beta - l^\beta e - \Lambda q^\beta) - l^\beta q^\alpha - \Lambda P^{\alpha\beta}] \geq 0, \end{aligned} \tag{15}$$

where the following identities

$$\begin{aligned} u_\gamma \partial_{u_\beta} q^\gamma &= \partial_{u_\beta} (u_\gamma q^\gamma) - q^\gamma \partial_{u_\beta} u_\gamma = -q^\gamma \Delta_\gamma^\beta = -q^\beta, \\ u_\gamma \partial_{u_\beta} P^{\gamma\alpha} &= \partial_{u_\beta} (u_\gamma P^{\gamma\alpha}) - P^{\gamma\alpha} \partial_{u_\beta} u_\gamma = -P^{\gamma\alpha} \Delta_\gamma^\beta = -P^{\beta\alpha}. \end{aligned}$$

were applied to simplify the last term ($\partial_2 = \partial_{u_\beta}$).

Observing the first term in the last form of the dissipation inequality, one can eliminate the direct velocity dependence of the entropy function, recognizing that the entropy may depend on the energy flux in the form

$$s(e, u^\alpha, \partial_\alpha e, \partial_\alpha u^\beta) = \hat{s}(e, q^\gamma(e, u^\alpha, \partial_\alpha e, \partial_\alpha u^\beta)). \tag{16}$$

Therefore, the entropy is local, and is independent of the derivatives of the basic state space variables and the velocity field. Entropy does, however, depend on the energy flux, which can depend on the derivatives because it is, according to our initial assumptions, a constitutive function. Taking this into account, the Lagrange–Farkas multipliers are determined by the entropy derivatives

$$\partial_e \hat{s} = \Lambda, \quad \partial_{q^\alpha} \hat{s} = l_\alpha. \tag{17}$$

We introduce a temperature T as

$$\partial_e \hat{s} = \Lambda = \frac{1}{T}. \tag{18}$$

We recognize that a full thermostatic compatibility requires that in (12), $A := \frac{p}{T}$, where p is the pressure. This consequence is completely analogous to the results of the nonrelativistic nonequilibrium thermodynamic theory, where thermostatics arises from the structure of the balance form evolution equations used as constraints to the Second Law.

Finally, we assume that entropy flux is classical, and the additional term a^α [Müller 1967] is zero

$$a^\alpha = 0^\alpha. \quad (19)$$

The dissipation inequality, then, reduces to the following simple form

$$q^\alpha \partial_\alpha \frac{1}{T} - \frac{1}{T} (P^{\alpha\beta} + T l^\beta q^\alpha - p \Delta^{\alpha\beta}) \partial_\alpha u_\beta - P^{\alpha\gamma} \partial_\alpha l_\gamma - \left(\frac{q^\alpha}{T} + e l^\alpha \right) \dot{u}_\alpha \geq 0. \quad (20)$$

As we do not want an acceleration-dependent entropy production, we require that the last term vanishes. According to (17) and (18)

$$e \partial_{q_\alpha} \hat{s} + q^\alpha \partial_e \hat{s} = 0. \quad (21)$$

The general solution of (21) can be given as

$$\hat{s} = \tilde{s}(e^2 - q^\alpha q_\alpha) + B, \quad (22)$$

where $B = \text{const}$. The entropy must depend on the energy density e and the momentum density q^α in a very particular but simple way. As a consequence of this functional form of the entropy function, the Gibbs relation can be given with the help of the entropy derivatives (17) as

$$de - \frac{q^\alpha}{e} dq_\alpha = T ds. \quad (23)$$

We may require first-order homogeneity of the entropy density (extensivity) in (22) without loss of generality. To do so, we introduce $E = \sqrt{|e^2 - q_\alpha q^\alpha|}$ as a variable of the entropy density. In this way, the entropy is a first-order homogeneous functions both of the energy density e and the momentum density q^α . With this property, it is unique.

The corresponding potential relation can be constructed according to the first-order homogeneity (extensivity) of the physical quantities as

$$e - \frac{q^\alpha q_\alpha}{e} = Ts - p. \quad (24)$$

The previous thermostatic relations require the interpretation of E as internal energy. On the other hand, let us recognize that E is the absolute value of the energy vector

$$E = \|E^\alpha\| = \|-u_\beta T^{\beta\alpha}\| = \|eu^\alpha + q^\alpha\| = \sqrt{|e^2 - q_\alpha q^\alpha|}. \quad (25)$$

One should note that the $1/T$ introduced in (18) is not the derivative of the entropy function according to E .

Finally, the entropy flux from (13) and (19) is

$$J^\alpha = \frac{1}{T} q^\alpha - \frac{q_\gamma}{eT} P^{\gamma\alpha}. \quad (26)$$

The final form of the dissipation inequality is

$$q^\alpha \partial_\alpha \frac{1}{T} - \frac{1}{T} \left(P^{\alpha\beta} + \frac{q^\beta q^\alpha}{e} - P \Delta^{\alpha\beta} \right) \partial_\alpha u_\beta - P^{\alpha\gamma} \partial_\alpha \frac{q_\gamma}{T e} \geq 0. \tag{27}$$

The last term in this expression with a derivative of one of the constitutive quantities indicates that we cannot give proper thermodynamic fluxes and forces as a solution of the inequality. Another problem appears with (21), because l_α , the spacelike part of the Lagrange multiplier in a local rest frame, was assumed independent of the derivatives of e and u^α . Thus, the Fourier heat conduction is excluded as a possible constitutive function. Both problems indicate that a complete theory may exist only either in an enlarged constitutive space or in an extended basic state space. One possible means of resolution is to introduce higher order derivatives of the basic state space into the constitutive state space, and construct a second-order weakly nonlocal theory. Another possibility is to enlarge the basic state space and construct an extended theory. In both cases, the key that may lead beyond the traditional Müller–Israel–Stewart theory is the new internal energy E .

4. Extended irreversible thermodynamics of relativistic fluids

Motivated by the results of the previous section we calculate the entropy production by a direct substitution of the balance of the energy into the entropy balance. We are to construct an extended theory, introducing q^α as an independent variable, but exploiting the fact that the entropy depends both on the energy and momentum densities in the specific way derived above.

The entropy flux is assumed to have the essentially classical form

$$J^\alpha = \frac{1}{T} q^\alpha. \tag{28}$$

Substituting the energy balance (3) into the entropy balance equation, we arrive at the following entropy production formula:

$$\begin{aligned} \partial_\alpha S^\alpha &= \dot{s}(e^2 + q^\alpha q_\alpha, s) + s \partial_\alpha u^\alpha + \partial_\alpha J^\alpha \\ &= -\frac{1}{T} (e \partial_\alpha u^\alpha + \partial_\alpha q^\alpha + q^\alpha \dot{u}_\alpha + P^{\alpha\beta} \partial_\beta u_\alpha) + \frac{q^\alpha}{T e} \dot{q}_\alpha + s \partial_\alpha u^\alpha + \partial_\alpha \left(\frac{1}{T} q^\alpha \right) \\ &= -\frac{1}{T} \left(P^{\alpha\beta} - (-e + sT) \Delta^{\alpha\beta} \right) \partial_\alpha u_\beta + q^\alpha \left(\partial_\alpha \frac{1}{T} - \frac{\dot{u}^\alpha}{T} - \frac{\dot{q}^\alpha}{eT} \right) \geq 0. \end{aligned} \tag{29}$$

In isotropic continua, the above entropy production results in constitutive functions assuming a linear relationship between the thermodynamic fluxes and forces. The thermodynamic fluxes are the *viscous stress* $\Pi^{\alpha\beta} = (P^{\alpha\beta} - (sT - e) \Delta^{\alpha\beta})$, and the energy flux q^α . For these, we get

$$\Pi^{\alpha\beta} = P^{\alpha\beta} - \Delta^{\alpha\beta} \left(p - \frac{q^\beta q_\beta}{e} \right) = -2\eta (\Delta^{\alpha\gamma} \Delta^{\beta\mu} \partial_\gamma u_\mu)^{s0} - \eta_v \partial_\gamma u^\gamma \Delta^{\alpha\beta}, \tag{30}$$

$$q^\alpha = -\lambda \frac{1}{T^2} \Delta^{\alpha\gamma} \left(\partial_\gamma T + T \dot{u}^\alpha + \frac{T \dot{q}^\alpha}{e} \right), \tag{31}$$

where s0 denotes the symmetric traceless part of the corresponding second order tensor, for example

$$(A^{ij})^{s0} = \frac{1}{2} (A^{ij} + A^{ji}) - \frac{1}{3} A^l{}^l \delta^{ij},$$

and we have introduced the scalar thermostatic pressure according to (24), making $p \neq P_\alpha^\alpha/3$. Equations (30) and (31) are the relativistic generalizations of the Newtonian viscous stress function and the Fourier law of heat conduction. The shear and bulk viscosity coefficients, η and η_v , and the heat conduction coefficient, λ , are nonnegative according to the inequality of the entropy production (29).

Equations (3) and (4) are the evolution equations of a relativistic, heat conducting ideal fluid, together with the constitutive functions (30) and (31). As special cases we can get the relativistic Navier–Stokes equation by substituting (30) into (4) and assuming $q^\alpha = 0$, or the relativistic heat conduction equation by substituting (31) into (3) and assuming that $\Pi^{\alpha\beta} = 0$. The heat conduction part results in a special extended theory, where only the energy flux appears as an independent variable.

5. Summary and discussion

In the first part of the paper we investigated the local equilibrium theory of special relativistic fluids. We saw that there may be no such theory that could give a complete solution of the entropy inequality with the conditions that there be

- (i) local Lagrange–Farkas multipliers;
- (ii) local entropy (16);
- (iii) no additional term in the entropy flux (19).

The first two assumptions were necessary to get a particular solution of the Liu equations and the dissipation inequality. On the other hand, they are natural in local equilibrium.

We conclude that either an extension of the basic state space or an enlargement of the constitutive state space may give a complete solution. Our investigations indicate a particular dependence of the entropy on the energy and momentum densities, leading to a distinction of internal and total energy densities of relativistic fluids.

The local rest frame energy density $e = u_\alpha T^{\alpha\beta} u_\beta$ is usually interpreted as internal energy in thermodynamic theories. However, the symmetry of the energy-momentum tensor can hide fact that while energy flux is related to dissipation, momentum density is not. This is a property of the relativistic theory, and not apparent in the nonrelativistic case because the nonrelativistic limit results in asymmetric energy-momentum. According to the previous investigations, the total energy density e (minus the time-timelike part of the energy-momentum tensor) is not a suitable internal energy, and the entropy density should be a function of the absolute value of the energy vector $E^\alpha = -u_\beta T^{\alpha\beta}$, the timelike part of the energy momentum.

To compare our proposal to the traditional Müller–Israel–Stewart theory [Israel 1976; Israel and Stewart 1980], it is instructive to expand the internal energy into the series, assuming that $e^2 > q^\alpha q_\alpha$:

$$E = \sqrt{|e^2 - q^\alpha q_\alpha|} \approx e - \frac{q^2}{2e} + \dots \quad (32)$$

The last, quadratic term in the above expression is what appears in the Müller–Israel–Stewart theory. However, in our case the corresponding relaxation time is fixed $\tau = 1/e$; the quadratic term is only the first approximation; and only the energy flux is introduced as an independent variable in our extended theory, with no need for viscous stress.

The series expansion is an instructive comparison to nonrelativistic hydrodynamics. Therein, the internal energy is the difference of the total energy and the relative kinetic energy. In (32) the quadratic expression is what one could consider as a kind of energy of the flow, considering only the local rest frame momentum density without any connection to an external observer. In a sense, our expression shows that by introducing E as internal energy, we declared that the momentum of the flow does not make a dissipative contribution.

The extension of the present calculations considering the balance of particle number is straightforward. Moreover, one can show that the above system of equations gives a stable homogeneous equilibrium in linear stability investigations, contrary to the theory of Eckart [Ván and Bíró 2008], and can therefore be considered as a minimal viable extension of the local equilibrium theory. The advantages of our approach over the Müller–Israel–Stewart one are that there are no additional material parameters compared to the Eckart theory and the stability of the homogeneous equilibrium does not require additional assumptions beyond the inequalities of thermodynamic stability.

Acknowledgment

We gratefully acknowledge enlightening discussions with Professor László Csernai.

References

- [Eckart 1940a] C. Eckart, “The thermodynamics of irreversible processes, I: The simple fluid”, *Phys. Rev.* **58**:3 (1940), 267–269.
- [Eckart 1940b] C. Eckart, “The thermodynamics of irreversible processes, III: Relativistic theory of the simple fluid”, *Phys. Rev.* **58**:10 (1940), 919–924.
- [Geroch 1995] R. Geroch, “Relativistic theories of dissipative fluids”, *J. Math. Phys.* **36**:8 (1995), 4226–4241.
- [Groot and Mazur 1962] S. R. Groot and P. Mazur, *Non-equilibrium thermodynamics*, North-Holland Publishing, Amsterdam, 1962.
- [Gyarmati 1970] I. Gyarmati, *Non-equilibrium thermodynamics/Field theory and variational principles*, Springer, Berlin, 1970.
- [Hiscock and Lindblom 1985] W. A. Hiscock and L. Lindblom, “Generic instabilities in first-order dissipative relativistic fluid theories”, *Phys. Rev. D* **31**:4 (1985), 725–733.
- [Hiscock and Lindblom 1987] W. A. Hiscock and L. Lindblom, “Linear plane waves in dissipative relativistic fluids”, *Phys. Rev. D* **35**:12 (1987), 3723–3732.
- [Israel 1976] W. Israel, “Nonstationary irreversible thermodynamics: a causal relativistic theory”, *Ann. Phys. New York* **100**:1–2 (1976), 310–331.
- [Israel and Stewart 1980] W. Israel and J. M. Stewart, “Progress in relativistic thermodynamics and electrodynamics of continuous media”, Chapter 13, pp. 491–525 in *General relativity and gravitation: one hundred years after the birth of Albert Einstein*, vol. 2, edited by A. Helde, Plenum Press, New York, 1980.
- [Lindblom 1996] L. Lindblom, “The relaxation effect in dissipative relativistic fluid theories”, *Ann. Phys. New York* **247**:1 (1996), 1–18.
- [Liu 1972] I.-S. Liu, “Method of Lagrange multipliers for exploitation of the entropy principle”, *Arch. Ration. Mech. An.* **46**:2 (1972), 131–148.
- [Müller 1967] I. Müller, “On the entropy inequality”, *Arch. Ration. Mech. An.* **26**:2 (1967), 118–141.
- [Ván 2003] P. Ván, “Weakly nonlocal irreversible thermodynamics”, *Ann. Phys. Leipzig* **12**:3 (2003), 146–173.
- [Ván and Bíró 2008] P. Ván and T. S. Bíró, “Relativistic hydrodynamics - causality and stability”, *Eur. Phys. J.* **155**:1 (2008), 201–212. arXiv:0704.2039v2.

Received 7 Feb 2008. Accepted 25 Mar 2008.

PÉTER VÁN: vp@rmki.kfki.hu

KFKI Research Institute for Particle and Nuclear Physics, Konkoly Thege Miklós út 29-33, H-1121 Budapest, Hungary

and

Bergen Center for Computational Science, Høyteknologisenteret, Thormøhlensgate 55, N-5008 Bergen, Norway
<http://newton.phy.bme.hu/~van>

A CONTINUOUS MODEL FOR AN ARTERIAL TISSUE, INCORPORATING REMODELING AND VOLUMETRIC GROWTH

FONS VAN DE VEN AND IHOR MACHYSHYN

A continuum-mechanics approach for the derivation of a model for the behavior, that is, the growth and remodeling, of an arterial tissue under a mechanical load is presented. This behavior exhibits an interplay between two phenomena: continuum mechanics and biology. The tissue is modeled as a continuous mixture of two components: elastin and collagen. Both components are incompressible, but the tissue as a whole can show volumetric growth due to the creation of collagen. Collagen is a fibrous structure, having a strain-induced preferred orientation. Remodeling of the tissue incorporates degradation of elastin and strain-induced creation and degradation of collagen fibers. Both elastin and collagen are considered to be nonlinear elastic media; elastin as a neo-Hookean material and collagen fibers behaving according to an exponential law. The modeling is based on the classical balance laws of mass and momentum.

1. Introduction

An aneurysm is a localized dilatation or ballooning of blood vessels. The size of an aneurysm was considered to be a critical indicator of the rupture potential and need for medical intervention. However, size is no longer considered to be an accurate parameter as there have been incidents of small aneurysms rupturing and large ones remaining intact. It is now believed that aneurysms rupture when the hemodynamically induced wall stress exceeds the wall strength. This necessitates a mechanical analysis of the biological tissue.

In modeling aneurysms and other cardiovascular pathologies, we will encounter the interplay of two phenomena: continuum mechanics and biology. Whereas traditional engineering materials passively respond to a change in their environment, biological tissues adapt to their environment by changing their configuration and material properties.

In this paper (originally presented at the TRECOP'07 conference on continuum physics) we will not aim at a physiological justification of our tissue model, but when needed we will use partial results from existing models in the literature. In contrast to many of these models, we will base our model strictly on the basic principles of continuum mechanics. Moreover, we refrain from giving an extensive literature review; for this we refer to the forthcoming [Machyshyn 2008]. Here, we only mention [Humphrey and Rajagopal 2002; Kroon and Holzapfel 2007; Baek et al. 2005; 2006].

We will present a continuous model for a tissue based on the basic laws of continuum mechanics coupled with considerations on the biological behavior of arterial vessels. A tissue of an arterial vessel is mainly built up of two components: elastin and collagen. Elastin behaves as an isotropic nonlinear elastic solid medium, and has as a special feature that it degrades (vanishes) during the formation of an aneurysm.

Keywords: arterial tissue, volumetric growth, strain-induced orientation, elastin, collagen.

Collagen has an anisotropic fibrous structure that can take up stresses in a nonlinear elastic way. Collagen remodels in two ways. On one hand collagen fibers can weaken, in that they elongate or disappear. On the other, new collagen can be laid down or passive fibers can become active, strengthening the collagen as a whole. We will propose a continuous mixture model for an arterial tissue in which remodeling is modeled by taking into account degradation of elastin, local changes of mass of collagen and elastin – resulting in volumetric growth of the tissue – and stress- or strain-induced preferred directions for the lay-down of collagen fibers. In order to more basically incorporate the idea of a distributed lay-down of fibers, Muschik et al. [2000] introduced the concept of mesoscopic continuum physics. This is a very elegant concept that also accounts for thermodynamical effects. However, these effects are not considered in this paper.

2. Basic model of a tissue

Our basic model for an arterial tissue is a three-dimensional continuous mixture of two components: *elastin* and *collagen*. These two components are both intrinsically incompressible, but the mixture as a whole can show volumetric growth caused by mass production. This is due to the *degradation* of elastin, modeled as vanishing of elastin particles, and the continuous *creation* (or lay-down) of new collagen fibers and *degradation* (removal) of old ones. By these processes, the total amount, or mass, of elastin and collagen continuously changes in time, which can result in growth or shrinkage of the tissue.

Two important state variables for the analysis to come are the *volumetric fractions*, n_e and n_c , of elastin and collagen, respectively. They are defined as the relative amount of elastin or collagen in the mixture; they are dimensionless and they sum up to one, so

$$n_e + n_c = 1. \quad (1)$$

The elastin is modeled as an isotropic nonlinear elastic solid, and its elastic constitutive behavior is described by an incompressible neo-Hookean model. As elastin can only degrade, the amount of elastin is monotone decreasing once degradation has started.

On the other hand, collagen is an anisotropic fibrous medium. The elastic fibers can only take up stresses in their fiber direction. As constitutive equation for these elastic stresses we will adapt a nonlinear exponential law. Important fiber properties are their orientation (direction) and prestretch. At each moment in time, and thus at each configuration of the tissue, the fiber directions are described by a distribution function for the fiber orientations. This distribution function changes continuously in time, governed by the state of stretch of the tissue. A specific choice for this distribution function (see Section 6), which was first introduced by Baek et al. [2005; 2006], will be given further on.

Initially in an unloaded state, the collagen fibers are crimped, in which state they do not contribute to the strength of the tissue. When the tissue is loaded, the elastin will be stretched, and there will come a state in which the collagen fibers become uncrimped; the tissue stretch in this state in the direction of a collagen fiber is called the *recruitment stretch*. Here, we will consider the recruitment stretch as a state variable, which in some sense governs the adaptation of the newly created collagen fibers to the state of stretch of the tissue. This adaptation is modeled such that a newly laid-down collagen fiber is always in the same state of preferred stretch, called the *attachment stretch*. In contrast to the variable recruitment stretch, the attachment stretch is a constant material parameter in our model.

Before degradation of elastin starts, the tissue is in its healthy state. This is a loaded equilibrium state, in which the tissue is stretched and in which the collagen is always stretched to its attachment stretch λ_a . The total amount of elastin (no degradation) and collagen do not change, and thus there is no mass production or volumetric growth in this state. However, also in this state there is a continuous turnover (creation and degradation) of collagen, but in such a way that the amount of degraded collagen is always equal to that of newly created collagen, thus keeping the total mass (and volume) of collagen constant.

Finally, for later use, we define the *metabolic equilibrium state* as the state in which the stretch in each collagen fiber is equal to the attachment stretch λ_a .

3. Basics of volumetric growth for a one-component medium

In this section, we try to explain the peculiar behavior of a medium with internal mass production and volumetric growth by considering, as an example, a simple or single-component medium (not a mixture, as this case will be dealt with in the remainder of this paper). In so doing, we follow the approach of Kuhl et al. [2007].

To introduce volumetric growth due to mass production, we consider a one-component intrinsic incompressible medium having as reference configuration: G_r with reference position vector \mathbf{X} , and as deformed current configuration: $G = \mathcal{G}(t)$ with current (at time t) position vector $\mathbf{x} = \mathbf{x}(\mathbf{X}, t)$. The density ρ of the medium is constant and uniform. The deformation gradient is $\mathcal{F}(\mathbf{X}, t) = \partial \mathbf{x} / \partial \mathbf{X}$, and the associated Jacobian is $J = \det \mathcal{F} = J(\mathbf{X}, t)$.

A material partial volume b with configuration $g = g(t)$ at the current time t , and reference configuration g_r , is defined as a part of the whole body across the boundary of which no mass flux takes place. However, inside b , mass sources can be active, causing changes of the total mass contained in b .

The volume of b is

$$V(t) = \int_{g(t)} dv = \int_{g_r} J(\mathbf{X}, t) dv_r, \tag{2}$$

and its mass is

$$M(t) = \int_{g(t)} \rho dv = \rho \int_{g_r} J(\mathbf{X}, t) dv_r. \tag{3}$$

Since this mass $M = M(t)$ is *not* constant, the balance of mass yields

$$\begin{aligned} \frac{d}{dt} M(t) &= \frac{d}{dt} \left[\rho \int_{g_r} J(\mathbf{X}, t) dv_r \right] \\ &= \rho \int_{g_r} \dot{J}(\mathbf{X}, t) dv_r = \rho \int_{g(t)} \frac{\dot{J}}{J} dv = \int_{g(t)} \dot{m} dv, \end{aligned} \tag{4}$$

where $\dot{m} = \dot{m}(\mathbf{X}, t)$ is the mass source, the rate of mass production per unit of current volume (in kg/m³sec). This leads to the local mass equation

$$\rho \frac{dJ}{dt} = J \dot{m}. \tag{5}$$

The balance of momentum for a medium with volumetric growth reads

$$\frac{d}{dt} \int_{g(t)} \rho \mathbf{v} dv = \int_{\partial g(t)} \mathbf{t} dS + \int_{g(t)} \rho \mathbf{b} dv, \tag{6}$$

where now, however, the total body force must be split up into a purely mechanical part, $\rho \mathbf{b}_m$, (the external body force) and a part due to the growth of mass, according to

$$\rho \mathbf{b} = \rho \mathbf{b}_m + \dot{m} \mathbf{v} , \tag{7}$$

where \mathbf{v} is the velocity.

Using successively the equalities

$$\frac{d}{dt} \int_{g(t)} \rho \mathbf{v} dv = \frac{d}{dt} \int_{g_r} \rho \mathbf{v} J dv_r = \int_{g_r} \rho (\dot{\mathbf{v}} J + \mathbf{v} \dot{J}) dv_r = \int_{g(t)} (\rho \dot{\mathbf{v}} + \dot{m} \mathbf{v}) dv , \tag{8}$$

Cauchy's stress law

$$\mathbf{t} = \mathcal{T} \mathbf{n} , \tag{9}$$

and (7), we obtain the local momentum balance

$$\rho \dot{\mathbf{v}} + \dot{m} \mathbf{v} = \text{div} \mathcal{T} + \rho \mathbf{b}_m + \dot{m} \mathbf{v} , \tag{10}$$

or

$$\rho \dot{\mathbf{v}} = \text{div} \mathcal{T} + \rho \mathbf{b}_m , \tag{11}$$

revealing that the effect of mass production in the local momentum balance has disappeared, and that the local momentum equation takes its classical form.

In (9), \mathbf{t} is the stress vector, or traction, \mathcal{T} is the stress tensor, and \mathbf{n} is the unit outward normal vector on the boundary ∂g of g .

4. Configurations and deformations

In this section, we consider the four different configurations depicted in Figure 1:

- (1) The unloaded state $G_{r,0}$: in this state both the elastin and the collagen are unloaded, but it is assumed that the collagen is not crimped, meaning that $\lambda_{\text{rec},0} = 1$.
- (2) The healthy state G_r : this state is an equilibrium state under a given external load; equilibrium implies here that the collagen stretch is equal to the attachment stretch λ_a ; this healthy state is assumed to be known, and this state is in our further analysis considered as *the* reference state (note

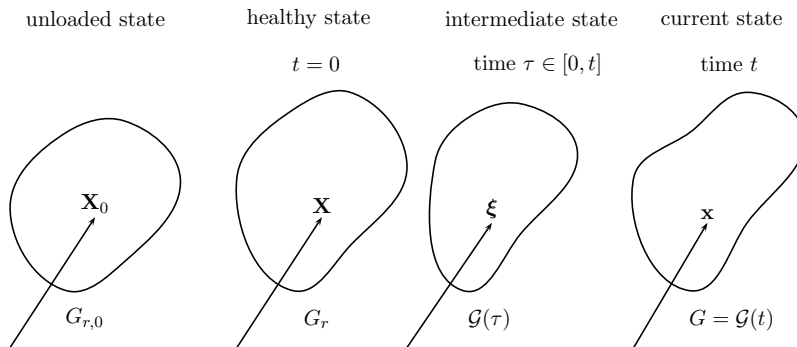


Figure 1. Configurations of tissue body \mathcal{B} .

that this is not an undeformed or stress-free state). At the initial time $t = 0$, the tissue is in its healthy state and then the degradation followed by remodeling and volumetric growth starts.

- (3) The intermediate state $\mathcal{G}(\tau)$: the intermediate time τ ranges from $t = 0$ to the current time t , and at each τ new collagen fibers are laid down.
- (4) The current state $G = \mathcal{G}(t)$: this is the final deformed state we wish to determine.

To describe the deformation of the tissue \mathcal{B} , we consider an infinitesimal material volume element containing the material point \mathcal{P} . The position of \mathcal{P} in $G_{r,0}$ is given by its position vector \mathbf{X}_0 , and further by \mathbf{X} in G_r , by ξ in $\mathcal{G}(\tau)$, and by \mathbf{x} in G . Here, we consider ξ and \mathbf{x} as functions of \mathbf{X} and τ , and of \mathbf{X} and t , respectively,

$$\xi = \xi(\mathbf{X}, t) , \quad \mathbf{x} = \mathbf{x}(\mathbf{X}, t) . \tag{12}$$

Recalling that the total deformation gradient of the tissue, or the elastin, from $G_{r,0}$ to G is \mathcal{F}_{tot} , then

$$\mathcal{F}_{\text{tot}} = \frac{\partial \mathbf{x}}{\partial \mathbf{X}_0} = \frac{\partial \mathbf{x}}{\partial \mathbf{X}} \frac{\partial \mathbf{X}}{\partial \mathbf{X}_0} = \mathcal{F} \mathcal{F}_0 , \tag{13}$$

where $\mathcal{F} = \mathcal{F}(\mathbf{X}, t)$.

The partial deformation from ξ to \mathbf{x} is described by

$$\hat{\mathcal{F}}(\mathbf{X}, t, \tau) = \frac{\partial \mathbf{x}}{\partial \xi} = \frac{\partial \mathbf{x}}{\partial \mathbf{X}} \frac{\partial \mathbf{X}}{\partial \xi} = \mathcal{F}(\mathbf{X}, t) \mathcal{F}^{-1}(\mathbf{X}, \tau) , \tag{14}$$

or

$$\mathcal{F}(\mathbf{X}, t) = \hat{\mathcal{F}}(\mathbf{X}, t, \tau) \mathcal{F}(\mathbf{X}, \tau) . \tag{15}$$

Consider a collagen fiber created at time τ in direction γ with initial stretch λ_a , having the initial direction vector

$$\mathbf{e}_c^{(0)}(\mathbf{X}, \tau, \gamma) = \cos \gamma \mathbf{v}_1(\mathbf{X}, \tau) + \sin \gamma \mathbf{v}_2(\mathbf{X}, \tau) , \tag{16}$$

with $\mathbf{v}_{1,2}$ in the principal directions of $\mathcal{F}(\mathbf{X}, \tau)$. How the distribution of $\mathbf{e}_c^{(0)}$ depends on the state of deformation at τ will be explained further on. The unit vectors \mathbf{v}_1 and \mathbf{v}_2 span a surface in which the main stretching takes place; in the third direction there is only shrinking. For instance, for an arterial tissue modeled as a tube under internal pressure and axial stretch, \mathbf{v}_1 and \mathbf{v}_2 are in the azimuthal and axial direction, while the radial direction is the third direction in which compression takes place.

Let $\mathbf{e}_{c,0}$ be the direction vector representing $\mathbf{e}_c^{(0)}$ in the unloaded state $G_{r,0}$, then

$$\mathbf{e}_{c,0}(\mathbf{X}, \tau, \gamma) = \frac{\mathcal{F}_{\text{tot}}^{-1}(\mathbf{X}, \tau) \mathbf{e}_c^{(0)}(\mathbf{X}, \tau, \gamma)}{\|\mathcal{F}_{\text{tot}}^{-1}(\mathbf{X}, \tau) \mathbf{e}_c^{(0)}(\mathbf{X}, \tau, \gamma)\|} . \tag{17}$$

The elastin stretch λ at time τ in the direction $\mathbf{e}_c^{(0)}$ is

$$\lambda(\mathbf{X}, \tau, \gamma) = \|\mathcal{F}_{\text{tot}}(\mathbf{X}, \tau) \mathbf{e}_{c,0}(\mathbf{X}, \tau, \gamma)\| = \frac{1}{\|\mathcal{F}_{\text{tot}}^{-1}(\mathbf{X}, \tau) \mathbf{e}_c^{(0)}(\mathbf{X}, \tau, \gamma)\|} , \tag{18}$$

where in the latter step we have used (17).

Since the collagen stretch λ_c at the moment it is laid down is equal to λ_a , we obtain for the recruitment stretch

$$\lambda_{\text{rec}}(\mathbf{X}, \tau, \gamma) = \frac{\lambda(\mathbf{X}, \tau, \gamma)}{\lambda_a} = \frac{1}{\lambda_a \|\mathcal{F}_{\text{tot}}^{-1}(\mathbf{X}, \tau) \mathbf{e}_c^{(0)}(\mathbf{X}, \tau, \gamma)\|}. \tag{19}$$

Hence, λ_{rec} is not a function of the current time t , and we will use the above relation to eliminate λ_{rec} from our further calculations.

The collagen stretch $\lambda_c(\mathbf{X}, t, \tau, \gamma)$ at the current time t of the fiber laid down at time τ in the direction $\mathbf{e}_c^{(0)}$ is thus

$$\lambda_c(\mathbf{X}, t, \tau, \gamma) = \frac{\lambda(\mathbf{X}, t, \gamma)}{\lambda_{\text{rec}}(\mathbf{X}, \tau, \gamma)} = \lambda_a \frac{\|\mathcal{F}_{\text{tot}}^{-1}(\mathbf{X}, \tau) \mathbf{e}_c^{(0)}(\mathbf{X}, \tau, \gamma)\|}{\|\mathcal{F}_{\text{tot}}^{-1}(\mathbf{X}, t) \mathbf{e}_c^{(0)}(\mathbf{X}, \tau, \gamma)\|}. \tag{20}$$

Let the initial direction at τ , $\mathbf{e}_c^{(0)}(\mathbf{X}, \tau, \gamma)$, deform to the current direction vector \mathbf{e}_c at time t , then

$$\mathbf{e}_c(\mathbf{X}, t, \tau, \gamma) = \frac{\hat{\mathcal{F}}(\mathbf{X}, t, \tau) \mathbf{e}_c^{(0)}(\mathbf{X}, \tau, \gamma)}{\|\hat{\mathcal{F}}(\mathbf{X}, t, \tau) \mathbf{e}_c^{(0)}(\mathbf{X}, \tau, \gamma)\|}. \tag{21}$$

5. Mass balances

The tissue is here considered as a mixture of two components: elastin and collagen. Let b be a material partial volume of \mathcal{B} containing both elastin and collagen particles. In a material volume there is no mass flux across the boundaries of the volume, but due to the degradation and production of elastin and collagen, the mass of b is not necessarily conserved. Moreover, although both elastin and collagen are modeled as intrinsically incompressible, the volume of b is not conserved: there is a volumetric growth due to the mass production. This volumetric growth is represented by the value of the Jacobian $J = \det \mathcal{F}$, which is greater than one in case of positive volumetric growth, and less than one in case of tissue resorption. Because J is related to the volumetric growth, we replace J by $J_g = J_g(\mathbf{X}, t)$. Since no volumetric growth takes place in the healthy phase, $J_0 = \det \mathcal{F}_0 = 1$.

Let $g = g(t)$ be the configuration of b at time t , with g_r its reference configuration in G_r . The volume of b is given by

$$V(t) = \int_{g(t)} dv = \int_{g_r} J_g(\mathbf{X}, t) dv_r, \tag{22}$$

which is comparable to Section 3.

The total mass of b consists of the mass of elastin, M_e , and that of collagen, M_c . With ρ_e and ρ_c the constant intrinsic densities of elastin and collagen, respectively, and n_e and n_c their volume fractions, we have for the total mass of b

$$M(t) = M_e(t) + M_c(t), \tag{23}$$

where

$$M_e(t) = \int_{g(t)} \rho_e n_e(\mathbf{X}, t) dv = \rho_e \int_{g_r} n_e(\mathbf{X}, t) J_g(\mathbf{X}, t) dv_r, \tag{24}$$

and

$$M_c(t) = \int_{g(t)} \rho_c n_c(\mathbf{X}, t) dv = \rho_c \int_{g_r} n_c(\mathbf{X}, t) J_g(\mathbf{X}, t) dv_r. \tag{25}$$

We denote the rates of mass production per unit of current volume for elastin and collagen by \dot{m}_e and \dot{m}_c (kg/m³sec), respectively. The change of elastin mass is only due to degradation, meaning that \dot{m}_e is negative, and is given by

$$\dot{M}_e(t) = \int_{g(t)} \dot{m}_e(\mathbf{X}, t) dv = \int_{g_r} \dot{m}_e(\mathbf{X}, t) J_g(\mathbf{X}, t) dv_r . \tag{26}$$

For collagen, the situation is somewhat more complex: here, we have collagen production at every time τ from $t = 0$ to the current time t , but meanwhile the collagen produced at τ is monotone decreasing during the period from τ to t , which is described by the monotone decreasing degradation function of collagen $q_c = q_c(t)$. Here, we have assumed that the degradation function q_c is uniform over \mathcal{B} .

Let us introduce a new *rate of production of volume fraction of collagen* $v_c = v_c(\mathbf{X}, t, \tau)$, such that $v_c(\mathbf{X}, t, \tau) d\tau$ is the volume fraction of collagen in $V(t)$ at t produced from τ to $\tau + d\tau$ in $V(\tau)$ and still surviving at t . Thus, equating the rate of change of the collagen in $V(t)$ due to the production in $V(\tau)$ from τ to $\tau + d\tau$ multiplied by the collagen degradation function from τ to t , we obtain

$$\begin{aligned} \rho_c \int_{g(t)} v_c(\mathbf{X}, t, \tau) dv \, d\tau &= \rho_c \int_{g_r} v_c(\mathbf{X}, t, \tau) J_g(\mathbf{X}, t) dv_r \, d\tau \\ &= \int_{g(\tau)} \dot{m}_c(\mathbf{X}, \tau) dv(\tau) \, d\tau \, q_c(t - \tau) \\ &= \int_{g_r} \dot{m}_c(\mathbf{X}, \tau) J_g(\mathbf{X}, \tau) dv_r \, q_c(t - \tau) \, d\tau , \end{aligned} \tag{27}$$

which, after localization, yields

$$v_c(\mathbf{X}, t, \tau) = \frac{\dot{m}_c(\mathbf{X}, \tau) J_g(\mathbf{X}, \tau)}{\rho_c J_g(\mathbf{X}, t)} q_c(t - \tau) . \tag{28}$$

The latter relation implies that the total collagen mass of b at the current time t is given by

$$\begin{aligned} M_c(t) &= M_{c,r} + \int_0^t \rho_c \int_{g(t)} v_c(\mathbf{X}, t, \tau) dv \, d\tau \\ &= M_{c,r} + \int_0^t \int_{g_r} \dot{m}_c(\mathbf{X}, \tau) q_c(t - \tau) J_g(\mathbf{X}, \tau) dv_r \, d\tau , \end{aligned} \tag{29}$$

where $M_{c,r}$ is the collagen mass in b in the healthy state G_r .

Differentiating this relation with respect to t and using that, by normalization, $q(0) = 1$, we find that the change of the collagen mass in b from $t = 0$ to the current time t is given by

$$\dot{M}_c(t) = \int_{g_r} \dot{m}_c(\mathbf{X}, t) J_g(\mathbf{X}, t) dv_r + \int_0^t \int_{g_r} \dot{m}_c(\mathbf{X}, \tau) \dot{q}_c(t - \tau) J_g(\mathbf{X}, \tau) dv_r \, d\tau . \tag{30}$$

Taking the time derivatives of $M_e(t)$ and $M_c(t)$ according to (26) and (30) in terms of the integrals over g_r , equating the results to (25) and (26), respectively, and realizing that these results hold for arbitrary b , we arrive at the local mass balance equations

$$\rho_e \frac{d}{dt} (J_g n_e) = J_g \dot{m}_e , \tag{31}$$

for elastin, and

$$\rho_c \frac{d}{dt} (J_g n_c) = J_g \dot{m}_c + \int_0^t \dot{m}_c(\mathbf{X}, \tau) \dot{q}_c(t - \tau) J_g(\mathbf{X}, \tau) d\tau, \tag{32}$$

for collagen. Note that d/dt stands for the material time derivative, so

$$\frac{d}{dt} f = \frac{\partial f(\mathbf{X}, t)}{\partial t}, \tag{33}$$

where f is arbitrary.

The initial conditions for (31) and (32) are $n_e(\mathbf{X}, 0) = n_{e,r}$ and $n_c(\mathbf{X}, 0) = n_{c,r}$. Dividing (31) by ρ_e and (32) by ρ_c , adding them together and using the trivial relation

$$n_e(\mathbf{X}, t) + n_c(\mathbf{X}, t) = 1, \tag{34}$$

we obtain the integro-differential equation for J_g :

$$\dot{J}_g = \frac{1}{\rho_e} J_g \dot{m}_e + \frac{1}{\rho_c} J_g \dot{m}_c + \frac{1}{\rho_c} \int_0^t \dot{m}_c(\mathbf{X}, \tau) \dot{q}_c(t - \tau) J_g(\mathbf{X}, \tau) d\tau, \tag{35}$$

with the initial condition $J_g(\mathbf{X}, 0) = 1$.

At this point, we have derived four equations for the four unknowns J_g , n_e , n_c , and v_c , successively (35), (31), (32), and (28), under the momentary assumption that the production rates \dot{m}_e and \dot{m}_c are given. Inspection, especially with use of (30), shows us that

$$n_c(\mathbf{X}, t) = n_{c,r} + \int_0^t v_c(\mathbf{X}, t, \tau) d\tau. \tag{36}$$

However, in contrast to what we said above, the production rates \dot{m}_e and \dot{m}_c are not explicitly given; we need constitutive equations for these quantities. We will not derive these constitutive equations herein, but rather use constitutive equations found in the literature; see specifically [Driessen 2006; Baek et al. 2005; 2006].

The elastin rate we choose here is constant and uniform, that is,

$$\dot{m}_e(\mathbf{X}, t) = -\mu_e, \tag{37}$$

for t running from $t = 0$ to the final time $t = t_f$; before $t = 0$ and after t_f there is no degradation of elastin. Here, μ_e is a given constant material parameter.

The collagen rate we split into two parts as

$$\dot{m}_c(\mathbf{X}, t) = \dot{m}_c^h(\mathbf{X}, t) + \dot{m}_c^e(\mathbf{X}, t), \tag{38}$$

where the superindices ‘ h ’ and ‘ e ’ stand for ‘healthy’ and ‘extra’, respectively.

For the first term we take

$$\dot{m}_c^h(\mathbf{X}, t) = \frac{\rho_c}{Q_c} n_c(\mathbf{X}, t), \quad Q_c = \int_{-\infty}^t q_c(t - \tau) d\tau = \int_0^\infty q_c(\tau) d\tau. \tag{39}$$

This term is chosen in such a way that the net collagen mass production in the healthy state is zero.

The ‘extra’ production term can be related to either the state of stress or stretch of the collagen. Baek et al. [2005, Eq. (16)] use a stress-induced growth-rate relation, while the same authors discuss [2006]

three possible cases, the last of which is a stretch-induced growth-rate relation. In this study, we opt for the latter, and take for this the specific relation

$$\dot{m}_c^e(\mathbf{X}, t) = K_g(\bar{\lambda}_c(\mathbf{X}, t) - \lambda_a), \tag{40}$$

where $\bar{\lambda}_c$ is a kind of averaged collagen stretch, averaged over the set of collagen fibers in the current state $G = \mathcal{G}(t)$ and defined as

$$\bar{\lambda}_c(\mathbf{X}, t) - \lambda_a = \frac{1}{\pi n_c(\mathbf{X}, t)} \int_0^t v_c(\mathbf{X}, t, \tau) \int_{-\pi/2}^{\pi/2} \lambda_c(\mathbf{X}, t, \tau, \gamma) \, d\gamma \, d\tau . \tag{41}$$

We see that the constitutive equation contains the unknown collagen stretch λ_c , which is in turn related to the unknown deformation gradient \mathcal{F} according to (20). For the determination of \mathcal{F} , we need the momentum equation as derived in Section 3. However, we will first discuss how to model the distribution of the collagen fibers over their different directions.

Finally, we make the following choice for the collagen degradation function q_c :

$$q_c(t) = e^{-t/T}, \tag{42}$$

where T (in sec) is a time constant that is characteristic for the rate of degradation of the collagen. We note that the time scale t_f for the elastin degradation is much larger than that of remodeling, so $T \ll t_f$.

For this choice, the coefficient Q_c becomes

$$Q_c = \int_0^\infty e^{-\tau/T} \, d\tau = T. \tag{43}$$

6. Distribution of collagen fibers

At each intermediate time τ a new generation of collagen fibers is continuously created. These fibers are laid down in a plane spanned by the two unit vectors \mathbf{v}_1 and \mathbf{v}_2 , the principal directions of the deformation gradient $\mathcal{F} = \mathcal{F}(\mathbf{X}, \tau)$ (see Equation (16)), such that for $\lambda \in \mathbb{R}$,

$$\mathcal{F}\mathbf{v} = \lambda\mathbf{v}. \tag{44}$$

The direction of each individual fiber is given by γ , the angle between the fiber direction and the \mathbf{v}_1 -axis. The distribution of these directions is assumed to be governed by a kind of double normal distribution $D(\mathbf{X}, \tau, \gamma)$ defined as

$$D(\mathbf{X}, \tau, \gamma) = e^{-1/\sigma} \left(\exp \frac{\cos[2(\gamma - \mu)]}{\sigma} + \exp \frac{\cos[2(\gamma + \mu)]}{\sigma} \right), \tag{45}$$

where $\pm\mu = \pm\mu(\mathbf{X}, \tau)$ are the mean fiber directions, and $\sigma = \sigma(\mathbf{X}, \tau)$ is the width of the distribution. The value of γ runs from $-\pi/2$ to $\pi/2$; $\gamma = 0$ corresponds with the \mathbf{v}_1 -direction, and $\gamma = \pm\pi/2$ with the $\pm\mathbf{v}_2$ -direction. A plot of a specific distribution function of the type (45) is shown in Figure 2.

Let $N_c(\mathbf{X}, t, \tau, \gamma)d\tau$ denote the volume fraction of collagen at time t that is created at time τ , from τ to $\tau + d\tau$, having the direction γ and surviving at t (hence, N_c is not so much the volume fraction, but

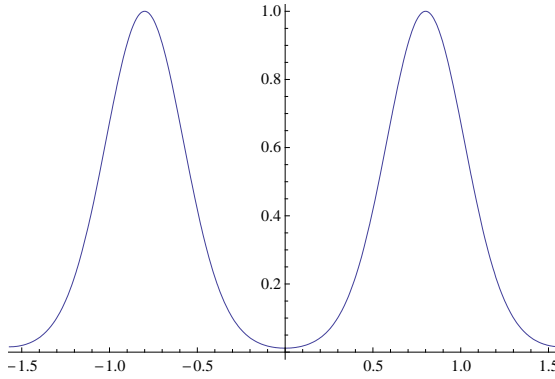


Figure 2. Distribution function D as function of γ for $\mu = 0.8$ and $\sigma = 0.2$.

rather the rate of change thereof). Then, clearly,

$$v_c(\mathbf{X}, t, \tau) = \int_{-\pi/2}^{\pi/2} N_c(\mathbf{X}, t, \tau, \gamma) \, d\gamma . \tag{46}$$

Since the distribution of N_c is governed by D , the latter relation implies that

$$N_c(\mathbf{X}, t, \tau, \gamma) = \bar{D}(\mathbf{X}, \tau, \gamma) v_c(\mathbf{X}, t, \tau) , \tag{47}$$

with

$$\bar{D}(\mathbf{X}, \tau, \gamma) = \frac{D(\mathbf{X}, \tau, \gamma)}{\int_{-\pi/2}^{\pi/2} D(\mathbf{X}, \tau, \gamma) \, d\gamma} . \tag{48}$$

The mean μ and width σ are related to the principal stretches of $\mathcal{F}(\mathbf{X}, \tau)$ in the state $\mathcal{G}(\tau)$. The larger principle stretch $\lambda_1 = \lambda_1(\mathbf{X}, \tau)$ corresponds to the first principle direction $\mathbf{v}_1 = \mathbf{v}_1(\mathbf{X}, \tau)$, while smaller one, λ_2 , corresponds to \mathbf{v}_2 . Moreover, since we only consider tissues that are principally stretched, we always have $\lambda_1 > 1$. Following [Driessen 2006, Sect. 8.2.2], we take

$$\mu(\mathbf{X}, \tau) = \arctan\left(\frac{g_2}{g_1}\right), \quad \sigma(\mathbf{X}, \tau) = \frac{k}{g_1/g_2 - 1} , \tag{49}$$

where the so-called stimulus functions g_1 and g_2 are related to their corresponding principle stretches as

$$g_1(\mathbf{X}, \tau) = \lambda_1(\mathbf{X}, \tau) - 1, \quad \text{and} \quad g_2 = \begin{cases} \lambda_2(\mathbf{X}, \tau) - 1, & \lambda_2 > 1, \\ 0, & \lambda_2 < 1. \end{cases} \tag{50}$$

The volume fraction due to the distribution N_c , as given in (47), will turn up in a constitutive equation for the stress given in the next section.

7. Momentum equation and stresses

Following Humphrey and Rajagopal [2002, p. 421] and many others in this field, we assume that we may consider the mixture of elastin and collagen as a constrained mixture that is homogenized with regard to the stresses. This implies that we only need to satisfy the overall momentum law for the mixture as a whole, and not the two partial momentum laws for the components separately. As we have shown in

Section 3, this relation keeps its classical form; see (11). In the following, we shall neglect inertia terms (the deformations we consider are extremely slow) and we exclude external body forces, by which the local momentum equation reduces to the simple equilibrium equation

$$\operatorname{div} \mathcal{T} = 0. \tag{51}$$

We now need a constitutive equation for the stress tensor \mathcal{T} . For the constrained mixture we consider here, we may adapt a *rule-of-mixture* relation for the stress, stating that the partial stresses due to elastin or collagen are proportional to their volumetric fractions n_e or n_c , respectively. Accordingly, we assume that the total stress in the tissue in the current configuration at time t is built up of elastin stress and collagen stress according to

$$\mathcal{T}(\mathbf{X}, t) = -p(\mathbf{X}, t)\mathcal{I} + \mathcal{T}_e(\mathbf{X}, t) + \mathcal{T}_c(\mathbf{X}, t), \tag{52}$$

where p is a pressure term, needed to account for the incompressibility of elastin and collagen, and \mathcal{I} is the unit tensor. The elastin is modeled as an incompressible isotropic neo-Hookean material with

$$\mathcal{T}_e(\mathbf{X}, t) = c_e(\mathcal{B}(\mathbf{X}, t) - \mathcal{I}), \tag{53}$$

where c_e is the elastin shear modulus and $\mathcal{B} = \mathcal{F}\mathcal{F}^T$ is the left Cauchy–Green tensor.

For the collagen stress, we follow van Oijen [2003, Sect. 3.2.4]. The collagen fibers can only take up tensile stress in their fiber direction, and the nonlinear stress-strain behavior of the collagen fibers is captured by an exponential form for the fiber stress. This leads to the formulation

$$\mathcal{T}_c(\mathbf{X}, t) = \int_0^t \int_{-\pi/2}^{\pi/2} \{N_c[\tau_f(\lambda_c) - \mathbf{e}_c \cdot \mathcal{T}_e \mathbf{e}_c] \mathbf{e}_c \otimes \mathbf{e}_c\}(\mathbf{X}, t, \tau, \gamma) \, d\gamma \, d\tau, \tag{54}$$

where

$$\tau_f(\lambda_c) = 2k_1\lambda_c^2(\lambda_c^2 - 1) \exp[k_2(\lambda_c^2 - 1)^2], \tag{55}$$

with k_1 and k_2 as material constants and $\lambda_c = \lambda_c(\mathbf{X}, t, \tau, \gamma)$ given by (20). For the \mathcal{T}_e in the integral in (54) one must read $\mathcal{T}_e(\mathbf{X}, \tau)$.

In (52)–(54), the contribution of $n_e\mathcal{T}_e$ is split into \mathcal{T}_e and $-n_c\mathcal{T}_e$, with the latter taken up in (54). However, in (54) this is only done in the fiber direction and not in the transverse direction. The reason for this is that the stress perpendicular to the fiber direction is uncoupled from the fiber fraction, which would mean that the transversal properties of the tissue are not affected by the fibers. This is not logical, as then the tissue would become unnaturally weak in the transverse direction leaving only the elastin to contribute to its stiffness. Oijen [2003] compensated for this by taking in the transverse direction the full \mathcal{T}_e , and not the partial $n_e\mathcal{T}_e$. Mechanically, this means that he gives the collagen fibers a transverse stiffness that is equal to that of the elastin. The stress perpendicular to the fiber direction is uncoupled from the fiber fraction, meaning that the transversal properties of the tissue are not affected by the fibers.

8. One-dimensional example

We consider as a first example a one-dimensional problem for a slender circular rod loaded by a fixed uniaxial tensile stress. Let \mathbf{e}_3 be the axial direction of the rod, then the axial normal stress $T_{33} = S$ is given, while all other stresses are zero, that is, $T_{ij} = 0$, $(i, j) \neq (3, 3)$. All collagen fibers are in the \mathbf{e}_3 -direction, so the distribution of the fibers does not play a role here.

In the unloaded state G_0 the tissue is unstretched, whereas in the healthy state the rod is loaded and stretched such that the collagen stretch $\lambda_{c,r}$ is equal to its attachment stretch λ_a . By the (not very relevant) assumption that $\lambda_{rec} = 1$ in the healthy state, we see that the stretch of the tissue, and the elastin, in the \mathbf{e}_3 -direction is equal to λ_a . Since there is no volumetric growth in the healthy state, $\det \mathcal{F}_0 = 1$ and thus the matrix of \mathcal{F}_0 is of the form (also accounting for rotational symmetry of the problem)

$$\mathcal{F}_0 = \begin{pmatrix} \lambda_a^{-1/2} & 0 & 0 \\ 0 & \lambda_a^{-1/2} & 0 \\ 0 & 0 & \lambda_a \end{pmatrix}. \tag{56}$$

We consider next the current state $G = \mathcal{G}(t)$. This state is here a homogeneous state, so there is no dependence on \mathbf{X} in this example. The total deformation gradient is $\mathcal{F}_{tot}(t) = \mathcal{F}(t)\mathcal{F}_0$, implying that the tissue stretch in the \mathbf{e}_3 -direction is

$$\lambda(t) = \|\mathcal{F}_{tot}(t)\mathbf{e}_3\| = \|\mathcal{F}(t)\mathcal{F}_0\mathbf{e}_3\| = \|\mathcal{F}(t)\lambda_a\mathbf{e}_3\| = \lambda_a F_{33}. \tag{57}$$

Due to the rotational symmetry: $F_{11} = F_{22}$, and thus the matrix of $\mathcal{F}(t)$ is

$$\mathcal{F}(t) = \begin{pmatrix} F_{11}(t) & 0 & 0 \\ 0 & F_{11}(t) & 0 \\ 0 & 0 & \lambda(t)/\lambda_a \end{pmatrix}. \tag{58}$$

Since $\det \mathcal{F}_0 = 1$, the Jacobian in G is equal to

$$J_g(t) = \det \mathcal{F}(t) = \frac{\lambda(t)}{\lambda_a} F_{11}^2(t), \tag{59}$$

yielding

$$F_{11}(t) = \sqrt{\frac{\lambda_a}{\lambda(t)} J_g(t)}. \tag{60}$$

In the intermediate state $\mathcal{G}(\tau)$ we have

$$\hat{\mathcal{F}}(t, \tau) = \mathcal{F}(t)\mathcal{F}^{-1}(\tau) = \begin{pmatrix} F_{11}(t)/F_{11}(\tau) & 0 & 0 \\ 0 & F_{11}(t)/F_{11}(\tau) & 0 \\ 0 & 0 & \lambda(t)/\lambda(\tau) \end{pmatrix}. \tag{61}$$

Moreover, the collagen stretch of a fiber created at time τ is

$$\lambda_c(t, \tau) = \lambda_a \frac{\lambda(t)}{\lambda(\tau)}. \tag{62}$$

From (35), we obtain with $\dot{m}_e(t) = -\mu_e$ and $\dot{m}_c(t) = \dot{m}_c^h(t) + \dot{m}_c^e(t)$, where $\dot{m}_c^h(t) = \rho_c n_c(t)/T$, and $\dot{m}_c^e(t) = K_g(\bar{\lambda}_c(t) - \lambda_a)$. The ordinary differential equation for $J_g(t)$ is

$$\begin{aligned} \dot{J}_g(t) &= -\frac{\mu_e}{\rho_e} J_g(t) + \frac{1}{T} J_g(t) n_c(t) + \frac{K_g}{\rho_c} (\bar{\lambda}_c(t) - \lambda_a) J_g(t) - \frac{1}{T} J_g(t) n_c(t) \\ &= \left[-\frac{\mu_e}{\rho_e} + \frac{K_g}{\rho_c} (\bar{\lambda}_c(t) - \lambda_a) \right] J_g(t). \end{aligned} \tag{63}$$

For this one-dimensional problem, $\bar{\lambda}_c$ follows from (41) as

$$\bar{\lambda}_c(t) - \lambda_a = \frac{1}{n_c(t)} \int_0^t v_c(t, \tau) \lambda_c(t, \tau) \, d\tau, \tag{64}$$

where, according to (28)

$$v_c(t, \tau) = \frac{J_g(\tau)}{\rho_c J_g(t)} \left[\frac{\rho_c}{T} n_c(\tau) + K_g(\bar{\lambda}_c(\tau) - \lambda_a) \right] e^{-(t-\tau)/T}. \tag{65}$$

Substituting (65) and (62) into (64), we obtain the following integral equation for $\bar{\lambda}_c(t)$:

$$\bar{\lambda}_c(t) - \lambda_a = \frac{\lambda_a \lambda(t)}{\rho_c J_g(t) n_c(t)} \int_0^t \left[\frac{\rho_c}{T} n_c(\tau) + K_g(\bar{\lambda}_c(\tau) - \lambda_a) \right] \frac{J_g(\tau)}{\lambda(\tau)} e^{-(t-\tau)/T} \, d\tau. \tag{66}$$

Further, we find from (36) that

$$n_c(t) = n_{c,r} + \frac{1}{\rho_c J_g(t)} \int_0^t \left[\frac{\rho_c}{T} n_c(\tau) + K_g(\bar{\lambda}_c(\tau) - \lambda_a) \right] J_g(\tau) e^{-(t-\tau)/T} \, d\tau. \tag{67}$$

At this point, we have with (63), (66) and (67) three equations for the four unknowns $\dot{J}_g(t)$, $\bar{\lambda}_c(t)$, $n_c(t)$ and $\lambda(t)$. The missing equation for $\lambda(t)$ will follow from the equations for the stresses. Since we have here a homogeneous stress situation, the equilibrium equations are trivially satisfied. The pressure p will follow from the condition that $T_{11} = T_{22} = 0$, while the remaining equation $T_{33} = S$ will yield the equation for $\lambda(t)$ we are looking for.

The stresses T_{11} and T_{22} do not contain a collagen part, and they are give by

$$T_{11} = T_{22} = -p(t) + c_e(F_{11}^2(t) - 1) = -p(t) + c_e \left(\frac{\lambda_a}{\lambda(t)} J_g(t) - 1 \right), \tag{68}$$

Hence, $T_{11} = T_{22} = 0$ yields

$$p(t) = c_e \left(\frac{\lambda_a}{\lambda(t)} J_g(t) - 1 \right). \tag{69}$$

Next, T_{33} follows from (52)–(54) as

$$\begin{aligned} T_{33}(t) &= -p(t) + c_e(F_{33}^2(t) - 1) + \int_0^t v_c(t, \tau) [\tau_f(\lambda_c) - T_{e,33}](t, \tau) \, d\tau \\ &= c_e \left[\frac{\lambda^2(t)}{\lambda_a^2} - \frac{\lambda_a}{\lambda(t)} J_g(t) \right] + \int_0^t v_c(t, \tau) [\tau_f(\lambda_c(t, \tau)) - \tau_e(\tau)] \, d\tau, \end{aligned} \tag{70}$$

with v_c as given by (65), $\tau_f(\lambda_c)$ by (55), and λ_c by (62), while τ_e stands for

$$\tau_e(\tau) = T_{e,33}(t) = c_e \left(\frac{\lambda^2(\tau)}{\lambda_a^2} - 1 \right). \tag{71}$$

The missing equation for $\lambda(t)$ is the simple one

$$T_{33}(t) = S. \tag{72}$$

Hence, we now have three equations for our three fundamental unknowns: $J_g(t)$, $n_c(t)$ and $\lambda(t)$; the auxiliary variables $v_c(t, \tau)$, $\lambda_c(t, \tau)$ and $\bar{\lambda}_c(t)$ are determined by (65), (62), and (66), respectively.

However, even for this most simple example this set of equations is already very complex and cannot be solved analytically. Therefore, this set, which has only one independent variable, the time t , must be solved by numerical integration. At this stage, we refrain from doing this; it remains an option for further research.

9. Discussion and perspectives

In this paper, we have constructed a model for remodeling and volumetric growth in an arterial tissue, considered as a constrained mixture of elastin and collagen and based on a continuum-mechanics approach. This is in contrast to several other approaches, for example, [Machyshyn 2008] and [Driessen 2006], who built their models in a more discrete way, both in time and space, directly aiming at a finite element implementation. As far as we could compare the present continuous model with the discrete model developed in [Machyshyn 2008], we found complete correspondence.

We established a complete system for the four essential unknowns in the problem of a loaded tissue: the volumetric fraction of collagen, the Jacobian of the deformation (characteristic for the volumetric growth), the stretch of the collagen fibers, and the stretch of the tissue. The derivation is based on the classical balance laws of mass and momentum. Our model incorporates mass production, volumetric growth, degradation of elastin, strain-induced preferred fiber orientation and collagen creation, isotropic nonlinear (neo-Hookean) elastic behavior of elastin, and anisotropic (fibrous) nonlinear (exponential) elastic behavior of collagen.

In this paper, we gave the general derivation of the continuous model, but only applied it to a simple one-dimensional example. We did not perform explicit numerical calculations. This, together with a treatment of more complex examples, was beyond the scope of this article. In the near future, we hope to apply this model to more complex (tube-like) structures, and to do the necessary numerical calculations, with the ultimate goal of an adequate model for the growth of aneurysms in cerebral blood vessels.

References

- [Baek et al. 2005] S. Baek, K. R. Rajagopal, and J. D. Humphrey, “Competition between radial expansion and thickening in the enlargement of an intracranial saccular aneurysm”, *J. Elasticity* **80** (2005), 13–31.
- [Baek et al. 2006] S. Baek, K. R. Rajagopal, and J. D. Humphrey, “A theoretical model of enlarging intracranial fusiform aneurysms”, *J. Biomech. Eng.* **128** (2006), 142–149.
- [Driessen 2006] N. Driessen, *Modeling and remodeling of the collagen structure of cardiovascular tissues*, PhD-thesis, Technische Universiteit Eindhoven, The Netherlands, 2006.
- [Humphrey and Rajagopal 2002] J. D. Humphrey and K. R. Rajagopal, “A constrained mixture model for growth and remodeling of soft tissues”, *Math. Mod. Meth. Appl. S.* **12** (2002), 407–430.
- [Kroon and Holzapfel 2007] M. Kroon and G. A. Holzapfel, “A model for saccular cerebral aneurysm growth by collagen fibre remodelling”, *J. Theor. Biol.* **247** (2007), 775–787.
- [Kuhl et al. 2007] E. Kuhl, R. Maas, G. Himpel, and A. Menzel, “Computational modeling of arterial wall growth”, *Biomechan. Model. Mechanobiol.* **6** (2007), 321–331.
- [Machyshyn 2008] I. Machyshyn, *A model for growth and remodeling of cerebral aneurysms*, Ph.D. thesis, Technische Universiteit Eindhoven, The Netherlands, 2008.
- [Muschik et al. 2000] W. Muschik, H. Ehrentraut, and C. Papenfuss, “Concepts of mesoscopic continuum physics with application to biaxial liquid crystals”, *J. Non-Equilib. Thermodyn.* **25** (2000), 179–197.

[van Oijen 2003] C. H. G. A. van Oijen, *Mechanics and design of fiber-reinforced vascular prostheses*, PhD-thesis, Technische Universiteit Eindhoven, The Netherlands, 2003.

Received 7 Feb 2008. Accepted 25 Mar 2008.

FONS VAN DE VEN: a.a.f.v.d.ven@tue.nl

Eindhoven University of Technology, Department of Mathematics and Computing Science, P.O.Box 513, 5600 MB Eindhoven, The Netherlands

<http://www.win.tue.nl/casa/aboutus/permstaff/37.html>

IHOR MACHYSHYN: i.machyshyn@tue.nl

Eindhoven University of Technology, Biomedical Engineering, Materials Technology, P.O. Box 513, 5600 MB Eindhoven, The Netherlands

SUBMISSION GUIDELINES

ORIGINALITY

Authors may submit manuscripts in PDF format on-line. Submission of a manuscript acknowledges that the manuscript is *original and has neither previously, nor simultaneously, in whole or in part, been submitted elsewhere*. Information regarding the preparation of manuscripts is provided below. Correspondence by email is requested for convenience and speed. For further information, write to:

Marie-Louise Steele
Division of Mechanics and Computation
Durand Building, Room 262
Stanford University
Stanford CA 94305

LANGUAGE

Manuscripts must be in English. A brief abstract of about 150 words or less must be included. The abstract should be self-contained and not make any reference to the bibliography. Also required are keywords and subject classification for the article, and, for each author, postal address, affiliation (if appropriate), and email address if available. A home-page URL is optional.

FORMAT

Authors are encouraged to use L^AT_EX and the standard article class, but submissions in other varieties of T_EX, and, exceptionally in other formats, are acceptable. Electronic submissions are strongly encouraged in PDF format only; after the refereeing process we will ask you to submit all source material.

REFERENCES

Bibliographical references should be listed alphabetically at the end of the paper and include the title of the article. All references in the bibliography should be cited in the text. The use of B^IB_TE_X is preferred but not required. Tags will be converted to the house format (see a current issue for examples), however, in the manuscript, the citation should be by first author's last name and year of publication, e.g. "as shown by Kramer, et al. (1994)". Links will be provided to all literature with known web locations and authors are encouraged to provide their own links on top of the ones provided by the editorial process.

FIGURES

Figures prepared electronically should be submitted in Encapsulated PostScript (EPS) or in a form that can be converted to EPS, such as GnuPlot, Maple, or Mathematica. Many drawing tools such as Adobe Illustrator and Aldus FreeHand can produce EPS output. Figures containing bitmaps should be generated at the highest possible resolution. If there is doubt whether a particular figure is in an acceptable format, the authors should check with production by sending an email to:

production@mathscipub.org

Each figure should be captioned and numbered so that it can float. Small figures occupying no more than three lines of vertical space can be kept in the text ("the curve looks like this:"). It is acceptable to submit a manuscript with all figures at the end, if their placement is specified in the text by means of comments such as "Place Figure 1 here". The same considerations apply to tables.

WHITE SPACE

Forced line breaks or page breaks should not be inserted in the document. There is no point in your trying to optimize line and page breaks in the original manuscript. The manuscript will be reformatted to use the journal's preferred fonts and layout.

PROOFS

Page proofs will be made available to authors (or to the designated corresponding author) at a web site in PDF format. Failure to acknowledge the receipt of proofs or to return corrections within the requested deadline may cause publication to be postponed.

Journal of Mechanics of Materials and Structures

Volume 3, N^o 6 June 2008

Preface	BOGDAN T. MARUSZEWSKI, WOLFGANG MUSCHIK AND KRZYSZTOF W. WOJCIECHOWSKI	1033
An introduction of the local displacements of mass and electric charge phenomena into the model of the mechanics of polarized electromagnetic solids	YAROSLAV BURAK, VASYL KONDRAT AND OLHA HRYTSYNA	1037
New conception of the FEM base functions applied to solving an inverse heat transfer problem	ANDRZEJ FRĄCKOWIAK, JENS VON WOLFERSDORF AND MICHAŁ CIAŁKOWSKI	1047
Dynamics of a rope as a rigid multibody system	PAWEŁ FRITZKOWSKI AND HENRYK KAMINSKI	1059
The optimal shape parameter of multiquadric collocation method for solution of nonlinear steady-state heat conduction in multilayered plate	JAN ADAM KOŁODZIEJ AND MAGDALENA MIERZWICZAK	1077
The application of the method of fundamental solutions to a simulation of the two-dimensional sloshing phenomenon	JAN ADAM KOŁODZIEJ AND MAGDALENA MIERZWICZAK	1087
Propagation of a surface wave in a vortex array along a superconducting heterostructure	BOGDAN T. MARUSZEWSKI, ANDRZEJ DRZEWIECKI AND ROMAN STAROSTA	1097
On nonlinear kinetic effects in the vortex array in superconductors	BOGDAN T. MARUSZEWSKI	1105
Thermodynamics of inhomogeneous ferroelectrics	GERARD A. MAUGIN AND LILIANA RESTUCCIA	1113
Exploitation of the dissipation inequality, if some balances are missing	WOLFGANG MUSCHIK, VITA TRIANI AND CHRISTINA PAPENFUSS	1125
Variational principles for heat conduction in dissipative continua	STANISŁAW SIENIUTYCZ	1135
Non-Newtonian fluid flow in a porous medium	ANITA USCIŁOWSKA	1151
Internal energy in dissipative relativistic fluids	PÉTER VÁN	1161
A continuous model for an arterial tissue, incorporating remodeling and volumetric growth	FONS VAN DE VEN AND IHOR MACHYSHYN	1171



1559-3959(200806)3:6;1-3